View metadata, citation and similar papers at core.ac.uk
brought to you by CORE
provided by Institutionelles Repositorium der Leibniz Universität Hannover

Mathematical modelling and numerical simulations in physical geodesy

Von der Fakultät für Mathematik und Physik
der Gottfried Wilhelm Leibniz Universität Hannover
zur Erlangung des Grades
Doktor der Naturwissenschaften
Dr. rer. nat.

genehmigte Dissertation

von

Dipl.-Math. Adrian Costea

geboren am 29.06.1980 in Brasov

2012

Referent:	Prof. Dr. Ernst P. Stephan, Leibniz Universität Hannover
Korreferenten:	Prof. Dr. Than Tran, University of New South Wales Sydney
	PD Dr. Matthias Maischak, Brunel University, Uxbridge, UK
Tag der Promotion:	19.07.2012

Abstract

The present dissertation discusses the theoretical and numerical analysis of the nonlinear Molodensky problem. We discuss on Hörmander's treatment of the nonlinear Molodensky problem [19] and derive convergence rates for the Nash-Hörmander method, which are missing in [19]. We also show estimates proving convergence of the Nash-Hörmander method with restart for the Molodensky problem.
The main focus of this work is the development of an implementable algorithm (with and without smoother) for the Molodensky problem, based on the Nash-Hörmander method.
We analyse two different approaches to solve the linearized Molodensky problem. The first is based on solving the linearized Molodensky problem with the boundary element method by solving pseudodifferential equations on a sequence of new surfaces with the Galerkin method. We apply this approach to the Nash-Hörmander method for the Molodensky problem with surface update. We analyse the evaluation of the Hessian matrix, which is a key point in the Nash-Hörmander algorithm in all its versions and is needed for the update of the surfaces. Furthermore, we show that the heat kernel can be used as a smoother in the Nash-Hörmander algorithm.
The second approach to solve the linearized Molodensky problem is based on the use of meshless methods. To get a first insight on the use of these methods, we first consider the Neumann problem for the Laplacian exterior to an oblate spheroid, which gives a better approximation of the true earth surface than the sphere. We use spherical radial basis functions in the solution of the boundary integral equations arising from the Dirichlet-to-Neumann map. This approach is particularly suitable for handling scattered satellite data. Furthermore, we use spherical radial basis functions on the unit sphere to approximate the solution of the linearized Molodensky problem.

Key words: nonlinear Molodensky problem, boundary element method, heat kernel smoothing, spherical radial basis functions

Zusammenfassung

In der vorliegenden Dissertation wird das nichtlineare Molodensky-Problem sowohl theoretisch wie auch numerisch analysiert. Wir stellen Hörmander's Behandlung des nichtlinearen Molodensky-Problems vor und leiten in [19] fehlende Konvergenzraten für die Nash-Hörmander Methode her. Des Weiteren geben wir Abschätzungen an, die die Konvergenz der Nash-Hörmander Methode mit Neustart für das Molodensky Problem zeigen.

Das Hauptaugenmerk dieser Arbeit ruht auf der Entwicklung eines implementierbaren Algorithmus (mit und ohne Glätter), basierend auf der Nash-Hörmander Methode, für das Molodensky Problem.

Insbesondere werden zwei unterschiedliche Ansätze zur Lösung des linearisierten Problems vorgestellt. Der Erste basiert auf das Lösen des linearisierten Molodensky-Problems mit der Randelementmethode durch das Lösen von Pseudodifferentialgleichungen auf einer Folge von neuen Oberflächen mit der Galerkin Methode. Wir wenden diesen Ansatz auf die Nash-Hörmander Methode für das Molodensky Problem mit Oberflächenupdate an. Wir analysieren die Berechnung der Hessematrix, was ein wesentlicher Punkt im Nash-Hörmander Algorithmus in all seinen Versionen ist, und für die Oberflächenupdates notwendig ist. Des Weiteren zeigen wir, dass Glättung mit dem Wärmeleitungskern für den Nash-Hörmander Algorithmus verwendet werden kann.

Der zweite Ansatz zur Lösung des linearisierten Molodensky Problems basiert auf der Verwendung sogenannter gitterfreien Methoden. Um einen ersten Einblick über den Einsatz dieser Methoden zu bekommen, betrachten wir als Erstes ein Neumann-Problem im Außenraum zum abgeplatteten Ellipsoid. Wir verwenden sphärische radiale Basisfunktionen in der Lösung der Randintegralgleichungen, die durch die Dirichlet-zu-Neumann Abbildung entstehen. Dieser Ansatz ist besonders geeignet für die Handhabung von Satellitendaten. Des Weiteren, verwenden wir sphärische radiale Basisfunktionen auf der Einheitskugel, um die Lösung des linearisierten Molodensky Problems zu approximieren.

Schlagworte: nichtlineares Molodensky Problem, Randelementmethode, Glättung mit Wärmeleitungskern, sphärische radiale Basisfunktionen

Acknowledgments

First of all, I would like to express my gratitude to my supervisor Prof. Dr. E.P. Stephan who helped me with choosing the topic for this thesis and who supported me with his knowledge and experience during the last 4 years.

I have furthermore to thank my co-referees Dr. M. Maischak and Prof. Dr. T. Tran for their readiness to examine the present thesis.

I would also like to show my appreciation to Lothar Banz, Dr. Quoc Thong Le Gia and Dr. Heiko Gimperlein for their valuable hints, the fruitful discussions and the collaboration over the last years. Additionally, I would like to thank Florian Leydecker for his careful proofreading.

Particularly, I would like to give my special thanks to my parents Magda and Adrian Costea and to my fiancée Paula Moldovan for their patience and mental support during my studies and my work on this thesis.

We thank the cluster of excellence QUEST for financial support.

Hannover, den 15. Mai 2012 Adrian Costea

Contents

1. Introduction **1**

2. An Abstract Framework for the Discrete Nash-Hörmander Method **5**

2.1. The Implicit Function Theorem and Smoothing 5
2.2. The Discrete Nash-Hörmander Method 9
2.3. Discrete Nash-Hörmander Method with Restart 11
2.4. Abstract Uniqueness Result for the Implicit Function Theorem 18

3. The Molodensky Problem **21**

3.1. The Linearized Molodensky Problem 23
3.2. The Non-Linear Molodensky Problem 31

4. The Discrete Nash-Hörmander Method for the Molodensky Problem **41**

4.1. Boundary Element Solutions 41
4.2. Nash-Hörmander Algorithm without Smoother 52
4.3. Nash-Hörmander Algorithm with Smoother 54
4.4. Heat Equation and Smoothing 59

5. Numerical Results Based on Boundary Elements **65**

5.1. Numerical Experiments 65
5.2. Computation of the Gravity Gradient to the Discrete BEM-Solution . . 76
5.2.1. Numerical Experiments 78

A. **85**

A.1. Proof of Hörmanders Existence Theorem 85
A.2. Hörmander Appendix 91
A.3. Boundary Integral Operators 93
A.4. Proofs of Lemma 4.3 and Proposition 4.4 95

6. A Meshless Method for an Exterior Neumann Boundary Value Problem on an Oblate Spheroid **99**

6.1. Preliminary Results 99
6.2. Weak Boundary Integral Formulation 101
6.3. Galerkin Approximation Using SRBFs 102
6.4. A Priori Estimate for the Galerkin Approximation of the Exact Solution 105
6.5. Implementation of the Approximation Method 108
6.6. Numerical Experiments 111

7. A First Application of Meshless Methods to the Linearized Molodensky Problem 119
7.1. Boundary Integral Equation 119
7.2. Meshless Galerkin Method with Boundary Integral Equations 122
7.3. Numerical Example 124

B. 131
B.1. A Short Introduction to Spherical Radial Basis Functions 131
B.1.1. Basic Definitions and Notations 131
B.1.2. Spherical Radial Basis Functions 132

8. Conclusion 135

List of Figures

4.1. Nash-Hörmander method 51
4.2. The curve $\gamma_{r,\eta}$ 61

5.1. Mean Radius-Error in the l_2-norm without smoother 69
5.2. Mean Radius-Error in the l_2-norm with smoother 70
5.3. Mean Gravity Vector Error in the l_2-norm with smoother 70
5.4. Pointwise Error $\|u_N(\vec{q}) - u(\vec{q})\|_{l_2}$ computed in a set of 10242 exterior points for the linearized Molodensky problem with smoother 70
5.5. Mean Radius-Error in the l_2-norm with smoother and restart 71
5.6. Mean Gravity Vector Error in the l_2-norm with smoother and restart . . 71
5.7. $N = 2$ and $N = 3$ icosahedron refinements without smoother 73
5.8. $N = 2$ and $N = 3$ icosahedron refinements with smoother, $\theta_0 = 3.8, \kappa = 2$ 74
5.9. $N = 2$ and $N = 3$ icosahedron refinements with smoother, $\theta_0 = 2.6, \kappa = 6$ 75
5.10. BEM-Error $\|\mu_h - \mu_\infty\|_V$ in the energy norm for the 2d case 78
5.11. Error of the Hessian approximation for a point outside of Γ 79
5.12. Error of the Hessian approximation for a point close to Γ_h 80
5.13. Error of the Hessian approximation for a point on Γ_h 81
5.14. BEM-Error $\|\mu_h - \mu_\infty\|_V$ in the energy norm for the 3d case on the cube 82
5.15. Error of the Hessian approximation 3d case 82
5.16. Error of the Hessian approximation 3d case sphere for a point outside Γ 83
5.17. Error of the Hessian approximation 3d case sphere for a point on Γ . . . 83

6.1. $F(N)$ computed for $N^* = 80$ 106
6.2. $F(N)$ computed for $N^* = 100$ 106
6.3. $F(N)$ computed for $N^* = 120$ 106
6.4. Log-log plot for $\mathcal{H}^{1/2}(\Gamma_0)$ errors using Wendland RBFs $\rho_m(r)$ 115
6.5. Log-log plot for $\mathcal{H}^{1/2}(\Gamma_0)$ errors using Matern RBFs $\nu_m(r)$ 115
6.6. Image of Saff points on the oblate spheroid 118
6.7. Image of satellite points on the oblate spheroid 118

7.1. Uniformly distributed Saff points on $\mathbb{S}^2$ ($N = 1000$ Saff points), c.f. [15] 128
7.2. Boundary element mesh consisting of triangles with vertices at $N = 1000$ Saff points 128
7.3. Pointwise error $|(u_N(\boldsymbol{q}) - u(\boldsymbol{q}))|$ with $\tilde{\mu}_N$ computed with radial basis functions ($m = 0, 1, 2$) and piecewise constants in the Saff points in Fig 7.1 and Fig 7.2. 129

7.4. Pointwise error $|(u_N(\boldsymbol{q}) - u(\boldsymbol{q}))|$ for $\tilde{\mu}_N$ computed on N=3458 scattered points with scaled radial basis functions or piecewise constants 129

List of Tables

5.1. Pointwise Errors for the linearized Molodensky problem with smoother . 72
5.2. Values of the smoothing parameter $\frac{1}{\theta_m}$ 72

6.1. Matérn's RBFs 110
6.2. Wendland's RBFs 111
6.3. Errors with Saff points and $\rho_m(r)$ 114
6.4. Errors with Saff points and $\nu_m(r)$ 114
6.5. Errors on grided points, with $\rho_m(r)$, using conjugate gradient method for $N_{max} = 120, N_{truncate} = 80$ 116
6.6. Errors on grided points, with $\rho_m(r)$, using conjugate gradient method for $N_{max} = 120, N_{truncate} = 100$ 116
6.7. Errors on grided points, with $\rho_m(r)$, using conjugate gradient method for $N_{max} = 120, N_{truncate} = 120$ 117
6.8. Errors with scattered points from MAGSAT, using conjugate gradient method for $N_{max} = 120, N_{truncate} = 100$ and $\rho_0(r)$ 117
6.9. Errors with scattered points from MAGSAT, for overlapping additive Schwarz preconditioner for $N_{max} = 120, N_{truncate} = 100$ and $\rho_0(r)$ 117

7.1. Meshless Galerkin approximation u_N of gravity potential u; single layer density computed by spherical radial basis functions centered at N Saff points 126
7.2. Standard BEM Galerkin approximation u_N of gravity potential u; single layer density computed by pw. constants on triangles with N Saff points 126
7.3. Meshless Galerkin approximation with spherical radial basis functions at scattered points on $\mathbb{S}^2$ 127
7.4. BEM Galerkin approximation with pw. constants on triangles with vertices at scattered points 127

1. Introduction

The determination of the shape of the earth and its gravity field, from measured data, is a problem of high importance in geodesy. Molodensky proposed in 1945 the direct gravimetric determination of the surface of the earth [29, 30]. The problem of Molodensky is an exterior (geodetic) boundary value problem with given data on the earth surface. A precise mathematical description of this problem was first given by L. Hörmander [19]. Hörmander's treatment of the nonlinear Molodensky problem is based on the continuous implicit function theorem and its discrete version which is based on the method of Nash [35]. We will refer to this method as the Nash-Hörmander method. Hörmander applied the implicit function theorem to the Molodensky problem and proved that Molodensky's problem complies with the conditions of the implicit function theorem. His mathematical procedure involves an appropriate smoothing. The convergence of the abstract Nash-Hörmander iteration procedure is proved in [19] by using different Hölder norms and estimates for the linearized problem as well as for the nonlinearity. The main result of Hörmander's work is a theorem on the existence and uniqueness of Molodensky's problem.
In this thesis we derive convergences rates for the Nash-Hörmander method (Theorem 2.2) which are missing in the original work of Hörmander. We show estimates proving convergence of the Nash-Hörmander algorithm with restart for the Molodensky problem. Furthermore, we develop implementable algorithms for the Molodensky problem based on the Nash-Hörmander method and on our method with restart - using the boundary element method and discuss the numerical difficulties arising in the implementation.
There are many different approaches to solve the linearized Molodensky problem [12, 21, 48]. One of the methods to solve the linearized Molodensky problem is the standard boundary element method as presented in [21] (for radial basis functions see [48]). In this thesis, we also convert the linearized Molodensky problem to a pseudodifferential equation (boundary integral equation) by making a single layer potential ansatz for the gravitational potential u. By adding additional side conditions involving the first order spherical harmonics, we obtain a well posed problem. Thus, we look for the density of the single layer potential and the expansion coefficients of the spherical harmonics as unknowns in the integral equation. Hence, we obtain approximate solutions via the boundary element Galerkin scheme by approximating the density either by standard piecewise polynomials, here quadratic in Section 4.1 or by spherical radial basis functions in Section 7.1.

In this thesis we solve approximately the nonlinear Molodensky problem, which means that we reconstruct the shape of the earth by using given data of the gravitational potential. We solve the linearized Molodensky problem (4.2) with the boundary element method by solving pseudodifferential equations on a sequence of new surfaces with the Galerkin method. Here, the new surfaces are obtained by updates which themselves are obtained by solving a further exterior Dirichlet problem (4.5) for harmonic functions with the single layer potential ansatz and computing the Hessian of this potential. As mentioned above, an appropriate smoothing is necessary for the Nash-Hörmander iteration procedure. For this purpose, we apply a heat kernel smoothing using Laplace-Beltrami eigenfunctions and use the algorithm by Seo and Chung [44]. We show that the heat kernel can be used as smoother in the Nash-Hörmander algorithm (Theorem 4.1). Originally, Hörmander used smoothing with a suitable mollifier together with Fourrier transformation (Theorem A.10 in [19]).

Another approach to treat the linearized Molodensky problem is based on the use of meshless methods. First in Section 6.1 we consider the Neumann problem for the Laplacian exterior to an oblate spheroid, which is a better approximation of the true earth surface than the sphere. We use the Galerkin method with spherical radial basis functions in the solution of the boundary integral equation arising from the Dirichlet-to-Neumann map, which converts the boundary value problem into a pseudodifferential equation on the oblate spheroid. This meshless approach with radial basis functions is particularly suitable for handling scattered satellite data. In Section 7.1 we use spherical radial basis functions on the unit sphere to approximate the solution of the linearized Molodensky problem.

The principal gain of this work is the development of an implementable algorithm (with/without smoother) for the Molodensky problem. For a good update of the surface it is crucial to obtain good approximations for the Hessian of the gravity potential. The accuracy of the evaluation of the Hessian matrix strongly influences the approximate solution of the boundary integral equations resulting from the linearized Molodensky problem and the auxiliary Dirichlet problem, which are solved on the updated surface. We believe that our solution procedure by solving an appropriate sequence (of firstly linearized Molodensky problems, then exterior Dirichlet problems and computation of Hessian and finally, surface update and starting again with the linearized Molodensky problem with the updated surfaces and so on) is suitable to approximate the solution of the nonlinear Molodensky problem. Our numerical results show that it is necessary to start with a fine mesh to get good, practicable results, because the dimension of the approximation scheme (Galerkin BEM) remains the same as the triangulation on the new surfaces are obtained as images of the vertices of the first mesh under the computed surface update. We perform an extensive analysis on the numerical evaluation of the Hessian. Furthermore, we present in Chapter 7 a meshless method for the solution of the linearized Molodensky problem as an alternative solution procedure. Some results of this meshless method have already been published in [7, 48]

This thesis is organized as follows:

In Chapter 2 we first introduce, following Hörmander [19], the abstract Nash-Hörmander method for the continuous and discrete implicit function theorem. Then, we state Hörmander's results on existence and convergence (Theorem 2.1) and uniqueness (Theorem 2.3). Our main result of Chapter 2 is Theorem 2.2 where we prove the convergence of the discrete Nash-Hörmander method with smoother -with and without restart - together with an a priori error estimate ((2.43) and Proposition (2.1)).

Chapter 3 is dedicated to the Molodensky problem. Following again Hörmander [19], we introduce the linearized and nonlinear Molodensky problems. We present in detail Hörmanders existence and uniqueness proof of the nonlinear Molodensky problem Theorem 3.2. We work out numerous details which are omitted in [19].

In Chapter 4 we first present a boundary element method to convert the linearized Molodensky problem and the additional Dirichlet problem into boundary integral equations, using a single layer potential ansatz. We also analyse the convergence of the boundary element approximation for these problems. Secondly, we identify the Nash-Hörmander algorithm for the particular case of the Molodensky problem and present different versions: without and with smoother and furthermore with restart and smoother. Finally, we show that heat kernel smoothing is suitable for the Nash-Hörmander method.

Chapter 5 is devoted to numerical experiments for these three different versions of the Nash-Hörmander algorithm based on boundary element approximations. For a sufficiently fine approximation of the initial surface our numerical simulations show that the Nash-Hörmander algorithm with restart and heat equation smoother gives good results for a final surface which belongs to the measured gravity field. Here, detailed numerical experiments for the computation of the Hessian in the 2d and 3d case are presented. The computation of the Hessian is a crucial item in the Nash-Hörmander algorithm. Therefore we had to take here special care and thus we have exploited various ways to compute the Hessian.

In Chapter 6 we discuss on the use of meshless methods in geophysical applications; we solve the Neumann problem for the Laplacian exterior to an oblate spheroid by solving the Dirichlet-to-Neumann map, which gives a pseudodifferential equation on the spheroid.

In Chapter 7 we apply meshless methods to get Galerkin approximations to the solution of the linearized Molodensky problem on the unit sphere by solving a Fredholm boundary integral equation of the second kind. In case of the unit sphere, the pseudodifferential equation for the linearized Molodensky problem from Chapter 4 (4.8) coincides with this boundary integral equation.

Further, the thesis contains 2 appendices. In Appendix A we list results from Hörmanders paper [19] and work out various details. Furthermore, we list some basic results on boundary integral operators. In Appendix B we give a short introduction into spherical radial basis functions.

2. An Abstract Framework for the Discrete Nash-Hörmander Method

In this chapter we introduce the abstract framework for the discrete Nash-Hörmander method. Following Hörmander [19], we analyse the continuous implicit function theorem and then its discrete version, which is based on the method of Nash [35]. In doing so, we will work out some of the important assertions and mention this at the appropriate position. For some very technical details we refer to [19]. We also state Hörmander's results on existence, convergence and uniqueness. This analysis is fundamental for the analysis of the nonlinear Molodensky problem given in Chapter 3. Furthermore, we derive with Theorem 2.2 convergence rates for the Nash-Hörmander method, which are missing in the original work of Hörmander and show a priori estimates proving the convergence of the Nash-Hörmander algorithm with restart for the Molodensky problem (Proposition 2.1).

2.1. The Implicit Function Theorem and Smoothing

Let M be a given C^∞ manifold. The problem under consideration reads:
Let $\Phi : C^\infty(M, \mathbb{R}^N) \to C^\infty(M, \mathbb{R}^{N'})$ and a smooth u_0 be given, find u close to u_0 such that

$$\Phi(u) = \Phi(u_0) + f \tag{2.1}$$

for small f, provided that $\Phi'(u)$ has a right inverse $\Psi(u)$ for u close to u_0.
Following Hörmander [19], we first sketch a continuous parameter version of the proof of the usual implicit function theorem [43]. Given u_0 for small f, find $u(\theta)$, $\theta \in [0, \infty)$, such that $u(0) = u_0, f_0 := \Phi(u_0)$ and $f_0 + f = \lim_{\theta \to \infty} \Phi(u(\theta))$. This requires that $d\Phi/d\theta = \Phi'(u(\theta))\dot{u}(\theta) = f$, where $\dot{u} = \frac{du}{d\theta}$. This holds if

$$\dot{u}(\theta) = \Psi(u(\theta))f,$$

where $\Psi(u)$ denotes the right inverse of $\Phi'(u)$. Now, integrating this equation with initial condition $u(0) = u_0$, gives a solution $u = \lim_{\theta \to \infty} u(\theta)$ of $\Phi(u) = f_0 + f$.
More generally Hörmander [19] takes $h \in C^\infty$ with

$$h(\theta) = \begin{cases} 0 & \text{in} \quad (-\infty, 1/3) \\ 1 & \text{in} \quad (2/3, \infty) \end{cases}$$

with $\Phi(u(\theta)) = f_0 + h(\theta)f$ for

$$\dot{u}(\theta) = h(\theta)\Psi(u(\theta))f.$$

Here is a difficulty: If $\Psi(u)f$ is less regular than u, then we may get an unsolvable Cauchy problem. We will explain this "effect" for the case of the Molodensky problem in Chapter 3. In order to overcome this difficulty, Hörmander follows the ideas of Nash to apply smoothing [35]. He denotes by S_θ a smoothing operator, which has the properties listed in Theorem A.10 given in Appendix A.2 and by setting $v = S_\theta u$ he replaces $\Psi(u)$ by $\Psi(v)$. Concerning S_θ, he demands that this may not be defined for small θ and he lets θ run from some large value θ_0 to ∞ and remarks that the map $u \to \Psi(S_\theta u)$ has nice properties under mild regularity conditions on Ψ (see below).
The Cauchy problem reads

$$\dot{u}(\theta) = \Psi(v(\theta))g(\theta), \quad v(\theta) = S_\theta u(\theta), \quad u(\theta_0) = u_0, \tag{2.2}$$

where g has to be prescribed so that u solves

$$\frac{d}{d\theta}\Phi(u(\theta)) = \Phi'(u(\theta))\dot{u}(\theta) = \Phi'(u(\theta))\Psi(v(\theta))g(\theta) = g(\theta) + e(\theta). \tag{2.3}$$

Here we define the error e as

$$e(\theta) := (\Phi'(u(\theta)) - \Phi'(v(\theta)))\dot{u}(\theta). \tag{2.4}$$

This equation is a consequence of the following simple calculation

$$\frac{d}{d\theta}\Phi(u(\theta)) = g(\theta) + \Phi'(u(\theta))\dot{u}(\theta) - g(\theta) = g(\theta) + \Phi'(u(\theta))\dot{u}(\theta) - \Phi'(v(\theta))\dot{u}(\theta).$$

By integrating (2.3) with $u(\theta) \to u(\infty)$ for $\theta \to \infty$ we have

$$\Phi(u(\infty)) - \Phi(u_0) = \int_{\theta_0}^{\infty} g(\theta)d\theta + \int_{\theta_0}^{\infty} e(\theta)d\theta.$$

Because we want this to be equal to f, we define

$$\int_{\theta_0}^{\theta} g(\bar{\theta})d\bar{\theta} := h(\theta - \theta_0)S_\theta f - S_\theta E(\theta), \tag{2.5}$$

where

$$E(\theta) := \int_{\theta_0}^{\theta} e(\bar{\theta})h(\theta - \bar{\theta})d\bar{\theta} \tag{2.6}$$

is the accumulated error up to $\theta - 1/3$. Now, the function g is determined by the solution up to $\theta - 1/3$ and thus, g can be considered as known in (2.2). Following Hörmander this is the reason why the integration of (2.2) has to be extended to $\theta = \infty$. The error due to the regularization operators S_θ has to be corrected after $\theta + 1/3$, the new error after $\theta + 2/3$, and so on.

In order to avoid regularity conditions on Ψ, Hörmander proposes to work with a difference approximation to the differential equations of Nash. He introduces this in

such a way that *one stays very close to the differential equations.* We present this method in Section 2.2.
Now, using (2.4) and Taylor's theorem, the norm of

$$e(\theta) = (\Phi'(u(\theta)) - \Phi'(v(\theta)))\dot{u}(\theta)$$

is dominated up to a constant by the norm of $\langle \Phi''(w, v(\theta) - u(\theta)), \dot{u}(\theta) \rangle$ where $w = \eta u(\theta) + (1-\eta)v(\theta)$ for some $\eta \in [0,1]$. Thus, the error e is essentially the second differential of Φ acting on $(v(\theta) - u(\theta))$ and $\dot{u}(\theta)$, which are small for large θ, such that the error e should be very small.

In order to analyse the continuity properties that we have to assume for Φ'', we follow Hörmander [19, Section 2.1] and first consider a typical case where Φ is a partial differential operator acting on functions u in a convex bounded set $\Omega \subset \mathbb{R}^n$.
Let $F(x, U)$ be smooth in $x \in \bar{\Omega}$ and in $U = \{u_\alpha\}_{|\alpha| \le m}$, where $u_\alpha \in \mathbb{R}$, $\alpha = (\alpha_1, ..., \alpha_n) \in \mathbb{Z}_+^n$. We set

$$\Phi(u) = F(x, \{\partial^\alpha u(x)\}), \quad \partial^\alpha = \left(\frac{\partial}{\partial x_1}\right)^{\alpha_1} \cdots \left(\frac{\partial}{\partial x_n}\right)^{\alpha_n}.$$

Now, let F_α be the partial derivative of F with respect to u_α. We have then for the second differential of Φ

$$\Phi''(u; v, w) = \sum_{|\alpha|,|\beta| \le m} F_{\alpha\beta}(x, \{\partial^\gamma u\}_{|\gamma| \le m}) \partial^\alpha v \partial^\beta w.$$

We first introduce the Hölder spaces.

Definition 2.1 (Definition A.3 [19]). *Let $k \in \mathbb{N}_0, k < a \le k+1$ and $B \subseteq \mathbb{R}^n$ compact, convex such that $\mathring{B} \neq \emptyset$.*
Define

$$\mathscr{H}^a(B) := \{u \in C^k(B) : \|u\|_0 = \sup_{x \in B} |u(x)| < \infty \quad \textit{and} \\ |u|_a := \sum_{|\alpha|=k} \sup_{x \neq y \in B} \frac{|\partial^\alpha u(x) - \partial^\alpha u(y)|}{|x-y|^{a-k}} < \infty\}.$$

We also set $\mathscr{H}^0(B) := C(B)$. Then $\mathscr{H}^a$ with the norm $\|\cdot\|_a := \|\cdot\|_0 + |\cdot|_a$ is a Banach space.

Hörmander claims that if a bound M is prescribed for $\|\partial^\alpha u\|_0$, $|\alpha| \le m$, Theorems A.7 and A.8 yield for $a \ge 0$

$$\|\Phi''(u; v, w)\|_a \le C_{a,M}(\|v\|_{m+a}\|w\|_m + \|v\|_m\|w\|_{m+a} + \|v\|_m\|w\|_m\|u\|_{m+a}). \tag{2.7}$$

Next, we want to prove (2.7). Applying Theorem A.7, we deduce

$$\begin{aligned}\|\Phi''(u;v,w)\|_a &= \|\sum_{|\alpha|\le m}\sum_{|\beta|\le m} F_{\alpha\beta}(x,\{\partial^\gamma u\})\partial^\alpha v\,\partial^\beta w\|_a \\ &\le C\sum_{|\alpha|\le m}\sum_{|\beta|\le m}\{\|F_{\alpha\beta}(x,\{\partial^\gamma u\})\|_a\|\partial^\alpha v\|_0\|\partial^\beta w\|_0 \\ &\qquad + \|F_{\alpha\beta}(x,\{\partial^\gamma u\})\|_0\|\partial^\alpha v\|_a\|\partial^\beta w\|_0 \\ &\qquad + \|F_{\alpha\beta}(x,\{\partial^\gamma u\})\|_0\|\partial^\alpha v\|_0\|\partial^\beta w\|_a\}.\end{aligned}$$

Now by taking the $\max_{\alpha,\beta}$ and noting that

$$\|\partial^\alpha v\|_0 \le \|v\|_m, \quad \|\partial^\alpha v\|_a \le \|v\|_{m+a}$$

and that the same type of estimates hold for w, using $\|\partial^\alpha u\|_0 \le M$, we obtain

$$\|\Phi''(u;v,w)\|_a \le C_M\{\max_{\alpha,\beta}\|F_{\alpha\beta}(x,\{\partial^\gamma u\})\|_a\|v\|_m\|w\|_m + \|v\|_{m+a}\|w\|_m + \|v\|_m\|w\|_{m+a}\}. \tag{2.8}$$

Now, applying Theorem A.8 for $\|F_{\alpha\beta}(x,\{\partial^\gamma u\})\|_a$, we have two cases:

$$\|F_{\alpha\beta}(x,\cdot)\circ\partial^\gamma u\|_a \le \begin{cases}\|F_{\alpha\beta}(x,\cdot)\|_1\|\partial^\gamma u\|_a + \|F_{\alpha\beta}(x,\cdot)\|_0, & 0\le a\le 1\\ C(\|F_{\alpha\beta}(x,\cdot)\|_1\|\partial^\gamma u\|_1^a + \|F_{\alpha\beta}(x,\cdot)\|_a\|\partial^\gamma u\|_a + \|F_{\alpha\beta}(x,\cdot)\|_0), & a\ge 1.\end{cases}$$

Choosing now $|\gamma|\le m$, the first case gives

$$\max_{\alpha,\beta}\|F_{\alpha\beta}(x,\{\partial^\gamma u\})\|_a \le C_M\|u\|_{m+a}.$$

For the second case we have for $\|\partial^\gamma u\|_1^a$ by using Theorem A.5 and $\gamma \le m$

$$\|\partial^\gamma u\|_1^a \le \|u\|_{m+1}^a \le C_a\|u\|_{m+a}$$

and we obtain

$$\max_{\alpha,\beta}\|F_{\alpha\beta}(x,\{\partial^\gamma u\})\|_a \le C_{a,M}\|u\|_{m+a}.$$

Combining now the last two estimates with (2.8) we have proved (2.7).

This estimate is similar to the estimate for the operator in the Molodensky problem given in (3.56). Increasing a in (2.7), the order of differentiability increases in only one of the factors in the summation terms of the right hand side of (2.7) and there it increases like a. More generally, Hörmander [19, (2.1.5)] allows estimates of the form

$$\begin{aligned}\|\Phi''(u;v,w)\|_{\lambda_0+a} \le C\{&\|v\|_{m_1+a}\|w\|_{m_2} + \|v\|_{m_2}\|w\|_{m_1+a} + \\ &(\|v\|_{m_3}\|w\|_{m_4} + \|v\|_{m_4}\|w\|_{m_3})\|u\|_{m_5+a}, \quad 0\le a\le a_\Phi,\end{aligned} \tag{2.9}$$

where $\lambda_0, m_1, ..., m_5$ are non-negative numbers. (λ_0 indicates that the norm refers to the range space of Φ, m and μ will be used for norms in the domain of Φ). Furthermore, (2.9) is only valid if u has a fixed bound in a suitable Hölder class. He also assumes concerning Ψ that [19, (2.1.6)]

$$\|\Psi(v)g\|_{\mu_1+a} \leq C(\|g\|_{\lambda_1+a} + \|g\|_{\lambda_2}\|v\|_{\mu_2+a}), \qquad 0 \leq a \leq a_\Psi \tag{2.10}$$

when v is bounded in a suitable Hölder class. This estimate is similar to (3.16) given there for the Molodensky problem. Using the estimates (2.9) and (2.10), Hörmander [19, Theorem 2.2.2] shows the existence of a solution $u \in \mathscr{H}^{\alpha+\lambda_1}$ of the equation $\Phi(u) = f$ with $f \in \mathscr{H}^{\alpha+\lambda_1}$. α, a_Φ and a_Ψ are large enough compared to the constants $(m_1, \dots)$ in (2.9), (2.10). We will analyse this in Appendix A.1.

2.2. The Discrete Nash-Hörmander Method

In this section we introduce Hörmander's difference approximation to the system (2.2)-(2.6) of Nash. Let θ_0, κ large, and set for $k = 0, 1, 2, \dots$

$$\theta_k = (\theta_0^\kappa + k)^{1/\kappa} \ , \quad \triangle_k = \theta_{k+1} - \theta_k \ .$$

Following the notation of Hörmander, we set

$$u_{k+1} = u_k + \triangle_k \dot{u}_k, \quad \dot{u}_k = \psi(v_k) g_k, \quad v_k = S_{\theta_k} u_k. \tag{2.11}$$

where $\dot{u}_k$ is just a notation, which does not indicate differentiation. We form

$$\begin{aligned} \Phi(u_{k+1}) - \Phi(u_k) &= \Phi(u_k + \triangle_k \dot{u}_k) - \Phi(u_k) - \Phi'(u_k)\triangle_k \dot{u}_k \\ &\quad + (\Phi'(u_k) - \Phi'(v_k))\triangle_k \dot{u}_k + \triangle_k g_k = \triangle_k (g_k + e_k), \end{aligned} \tag{2.12}$$

where

$$\begin{aligned} &e_k = e_k' + e_k'' \\ &e_k' = (\Phi'(u_k) - \Phi'(v_k))\dot{u}_k, \quad e_k'' = (\Phi(u_k + \triangle_k \dot{u}_k) - \Phi(u_k) - \Phi'(u_k)\triangle_k \dot{u}_k)/\triangle_k. \end{aligned} \tag{2.13}$$

Summing up from 0 to k, we obtain

$$\Phi(u_{k+1}) - \Phi(u_0) = \sum_{j=0}^{k} \triangle_j (g_j + e_j).$$

Since the limit as $k \to \infty$ must be equal to f, we set

$$\sum_{j=0}^{k} \triangle_j g_j + S_{\theta_k} E_k = S_{\theta_k} f, \tag{2.14}$$

where $\quad E_k = \sum_{j=0}^{k-1} \triangle_j e_j$ is the sum of all preceding errors.
Hence,

$$\triangle_0 g_0 = S_{\theta_0} f, \quad g_k = \triangle_k^{-1}((S_{\theta_k} - S_{\theta_{k-1}})(f - E_{k-1}) - S_{\theta_k}\triangle_{k-1} e_{k-1}), \quad k > 0. \tag{2.15}$$

This can be seen as follows:
With $E_0 = 0$ we have $\triangle_0 g_0 = S_{\theta_0} f$. Next, we can rewrite (2.14) as

$$\sum_{j=0}^{k} \triangle_j g_j = S_{\theta_k}(f - E_k)$$

so that

$$\begin{aligned}\triangle_k g_k &= S_{\theta_k}(f - E_k) - \sum_{j=0}^{k-1} \triangle_j g_j = S_{\theta_k}(f - E_k) - S_{\theta_{k-1}}(f - E_{k-1}) \\ &= (S_{\theta_k} - S_{\theta_{k-1}})f - S_{\theta_k} E_k + S_{\theta_{k-1}} E_{k-1}.\end{aligned}$$

Hence, noting that

$$E_k = \sum_{j=0}^{k-1} \triangle_j e_j = \triangle_{k-1} e_{k-1} + E_{k-1} \tag{2.16}$$

we obtain

$$\begin{aligned}\triangle_k g_k &= (S_{\theta_k} - S_{\theta_{k-1}})f - S_{\theta_k}(\triangle_{k-1} e_{k-1} + E_{k-1}) + S_{\theta_{k-1}} E_{k-1} \\ &= (S_{\theta_k} - S_{\theta_{k-1}})(f - E_{k-1}) - S_{\theta_k} \triangle_{k-1} e_{k-1}.\end{aligned}$$

Next, we follow again Hörmander and present the precise hypothesis under which Hörmander derives a convergence result for the above method, which gives in the limit $k \to \infty$ the solution of the implicit function theorem.

Following the notations of Hörmander, let M be a given compact C^∞ manifold, $u_0 \in C^\infty(M, \mathbb{R}^N)$. He assumes that for a certain $\mu \geq 0$ the map Φ is defined for all $u \in C^\infty(M, \mathbb{R}^N)$ in a convex $\mathscr{H}^\mu$ neighborhood V_0 of u_0 and that $\Phi(u) \in C^\infty(M, \mathbb{R}^{N'})$. He also assumes that if $u \in V_0$ and $u_1, u_2 \in C^\infty(M, \mathbb{R}^N)$, then $\Phi(u + t_1 u_1 + t_2 u_2)$ is a C^2 function of t_1, t_2 with values in $C^\infty(M, \mathbb{R}^{N'})$ for t_1, t_2 close to 0. Furthermore, he assumes that the estimate (2.9) holds for the mixed second order derivative $\Phi''(u; u_1, u_2)$ at $t_1 = t_2 = 0$. Finally, he assumes that $\Psi(u)$ is defined for $u \in C^\infty(M, \mathbb{R}^N) \cap V_0$ and that $\Psi(u) : C^\infty(M, \mathbb{R}^{N'}) \to C^\infty(M, \mathbb{R}^N)$ such that estimate (2.10) holds.
Now we take $f \in \mathscr{H}^{\alpha+\lambda_1}$ to be small. A certain set of conditions on α and the other constants in (2.9) and (2.10), which are given by [19, (2.2.28)], guarantees that for large enough κ and θ_0 an infinite sequence $\{u_k\}$ can be defined by (2.11) – (2.16) and that it converges to $u \in \mathscr{H}^{\alpha+\mu_1}$ in the $\mathscr{H}^a$ topology, for every $a < \alpha + \mu_1$ while $\Phi(u_k) \to \Phi(u_0) + f$. If for some $a < \alpha + \mu_1$, Φ has a continuous extension from $\mathscr{H}^a$ to $\mathscr{H}^0$, it follows that $\Phi(u) = \Phi(u_0) + f$.
Now we first state Hörmander's convergence theorem. In the Appendix A.1 we give a summary of the several steps that are needed in the proof and also present some details which are omitted in Hörmander's version.

Theorem 2.1 (Theorem 2.2.2 [19])**.** *Let M be a compact C^∞ manifold, Φ a map from $C^\infty(M,\mathbb{R}^N)$ to $C^\infty(M,\mathbb{R}^{N'})$, defined in a $\mathscr{H}^\mu$ neighborhood V of u_0, which has a second differential satisfying (2.9) for $u \in V \cap C^\infty$. Assume that the first differential has a right inverse Ψ satisfying (2.10) for $v \in V$, that a certain set of necessary conditions on α and the other constants are fulfilled and that $\alpha + \mu_1$ is not an integer. Then there is a neighborhood V_1 of 0 in $\mathscr{H}^{\alpha+\lambda_1}$ and large constants θ_0 and κ such that*

(i) *the Nash iteration scheme (2.11) - (2.15) has solutions $u_k \in V \cap C^\infty$ for every $f \in V_1, k = 1, 2, ...$*

(ii) *u_k converges when $k \to \infty$ to a limit $u(f) \in \mathscr{H}^{\alpha+\mu_1}$ in the $\mathscr{H}^a$ topology for every $a < \alpha + \mu_1$ and is bounded in $\mathscr{H}^{\alpha+\mu_1}$.*

(iii) *$\Phi(u_k) \to \Phi(u_0) + f$ in $\mathscr{H}^a$ for every $a < \alpha + \lambda_1$ and is bounded in $\mathscr{H}^{\alpha+\lambda_1}$.*

(iv) *$\|u(f) - u_0\|_{\alpha+\mu_1} \to 0$ if $f \to 0$ in $\mathscr{H}^{\alpha+\lambda_1}$.*

(v) *If $f \in \mathscr{H}^{\beta+\lambda_1}$ for some $\beta \geq \alpha$ such that the necessary conditions [19, (2.2.24)] are fulfilled with α replaced by β, then $u(f) \in \mathscr{H}^{\beta+\mu_1}$ if $\beta + \mu_1$ is not an integer, and moreover $u_k \to u(f)$ in $\mathscr{H}^a$ when $a < \beta + \mu_1$,*

$$\Phi(u_k) \to \Phi(u_0) + f \quad in \quad \mathscr{H}^a \quad when \quad a < \beta + \lambda_1.$$

2.3. Discrete Nash-Hörmander Method with Restart

We will compute with the above algorithm with restart numerical simulations for the Molodensky problem (see Section 5.1). Therefore, we use a corresponding set of constants cf. [19, Example 2]. The constants provided with an index are those which occur in [19], for example $C_{A.10.iii}$ means the constant in Theorem A.10, property (*iii*) in Hörmander's appendix. We start by refining Hörmander's estimates for the error after k steps. In the notation of Hörmander [19, page 20] we have, by using [19, page 25 Example 2], the following lemma (see [19, Lemma 2.2.1]).

Lemma 2.1. *Let $\epsilon > 0$, $\alpha + \epsilon \notin \mathbb{N}$, $-\epsilon \leq \alpha_- \leq \alpha \leq \alpha_+$.*
Assume that for some $k \geq 0$

$$\|\dot{u}_j\|_{a+\epsilon} \leq \delta\theta_j^{a-\alpha-1} \tag{2.17}$$

for $a \in [\alpha_-, \alpha_+]$.
It follows that

$$U = \sum_{j=0}^{k} \triangle_j \dot{u}_j \in \mathscr{H}^{\alpha+\epsilon}, \quad \|U\|_a \leq C_{A.11}\delta \quad if \quad a \leq \alpha + \epsilon \tag{2.18}$$

and for some fixed a_0 we have

$$\|U - S_{\theta_{k+1}}U\|_a \leq C_{2.2.6}\delta\theta_{k+1}^{a-\alpha-\epsilon} \quad \forall\, 0 \leq a \leq \alpha_+ + \epsilon \tag{2.19}$$

$$\|S_{\theta_{k+1}}U\|_a \leq \widetilde{C}_{2.2.6}\delta\theta_{k+1}^{(a-\alpha-\epsilon)_+} \quad \forall\, 0 \leq a \leq a_0. \tag{2.20}$$

Corollary 2.1. *Let* $\epsilon_j > 0$, $\epsilon_1 + \epsilon_2 \le \epsilon_0$, $\mu \le \alpha + \epsilon$, a, δ *as above.*
We define

$$V_0 := \{u \in C^\infty : \|u - u_0\|_\mu \le \epsilon_0\}$$
$$V_1 := \{u \in C^\infty : \|u - u_0\|_\mu \le \epsilon_1\}$$
$$V_2 := \{u \in C^\infty : \|u\|_\mu \le \epsilon_2\}.$$

Assume that

$$\theta \ge \theta_0 = \left(\frac{\epsilon_1}{C_{A.10.iii}\|u_0\|_a}\right)^{\frac{1}{a-\mu}}.$$

Then $S_\theta u_0 \in V_1$ *and if* $a = \mu \le \alpha + \epsilon$ *and*

$$\delta \le \frac{\epsilon_2}{C_{A.10.i} \cdot C_{11}},$$

we have $U, S_\theta U \in V_2$*. In this case, also* $u_{k+1} = u_0 + U \in V_1 + V_2 \subseteq V_0$ *and* $S_{\theta_{k+1}} u_{k+1} \in V_1 + V_2 \subseteq V_0$*.*

Next we derive convergence rates for the Nash-Hörmander method. Now, setting $v_k := S_{\theta_k} u_k$, we obtain $\forall\, a \le \alpha + \epsilon$ and $\forall\, b \ge a$, such that A.10.iii is valid

$$\begin{aligned} \|u_j - v_j\|_a &= \|u_0 + U - S_{\theta_j}(u_0 + U)\|_a \\ &\le \|u_0 - S_{\theta_j} u_0\|_a + \|U - S_{\theta_j} U\|_a \\ &\le C_{A.10.iii}\|u_0\|_b \theta_j^{a-b} + C_{2.2.6}\delta\theta_j^{a-\alpha-\epsilon}. \end{aligned} \tag{2.21}$$

In the special case $b = \alpha + \epsilon$ we have

$$\|u_j - v_j\|_a = (C_{A.10.iii}\|u_0\|_{\alpha+\epsilon} + C_{2.2.6}\delta)\theta_j^{a-\alpha-\epsilon}. \tag{2.22}$$

Similarly, we deduce for all $a \le a_0$ and all b, such that A.10.i is valid

$$\begin{aligned} \|v_j\|_a &\le \|S_{\theta_j} u\|_a + \|S_{\theta_j} U\|_a \\ &\le C_{A.10.i}\theta_j^{a-b}\|u_0\|_b + \widetilde{C}_{2.2.6}\delta\theta_j^{(a-\alpha-\epsilon)_+} \\ &\le (C_{A.10.i}\|u_0\|_{\alpha+\epsilon} + \widetilde{C}_{2.2.6}\delta)\theta_j^{(a-\alpha-\epsilon)_+}, \end{aligned} \tag{2.23}$$

where the last inequality is again for the special case $b = \alpha + \epsilon$.
In the following, we consider a quantitative estimate for δ in (2.17). We are going to use (2.21), (2.23) and

$$\|u_j\|_a \le \underbrace{\max\big(C_{A.11}, \sum_{j=0}^{\infty} \triangle_j \theta_j^{-1}\big)}_{=:\mathfrak{C}_{11}} \delta\theta_{j+1}^{(a-\alpha-\epsilon)_+} + \|u_0\|_a \tag{2.24}$$

to estimate the smoothing error e'_j. By using ([19, (2.1.5)$'$ Hörmander]), we deduce

$$\begin{aligned}
\|e'_j\|_{2\epsilon+a} \leq\ & C_2\{\|u_j - v_j\|_{2+3\epsilon+a}\|\dot{u}_j\|_0 \\
& + \|u_j - v_j\|_0\|\dot{u}_j\|_{2+3\epsilon+a} \\
& + 2\|u_j - v_j\|_0\|\dot{u}_j\|_0(\|u_j\|_{3+2\epsilon+a} + \|v_j\|_{3+2\epsilon+a}) \\
\leq\ & C_2\{(C_{A.10.iii}\|u_0\|_b\theta_j^{2+3\epsilon+a-b} + C_{2.2.6}\delta\theta_j^{2+2\epsilon+a-\alpha})\delta\theta_j^{-\alpha-1} \\
& (C_{A.10.iii}\|u_0\|_{c_1}\theta_j^{-c_1} + C_{2.2.6}\delta\theta_j^{-\alpha-\epsilon})\delta\theta_j^{1+2\epsilon+a-\alpha} \\
& + 2(C_{A.10.iii}\|u_0\|_{c_2}\theta_j^{-c_2} + C_{2.2.6}\delta\theta_j^{-\alpha-\epsilon})\delta\theta_j^{-\alpha-1}\cdot \\
& \cdot((1 + C_{A.10.i})\|u_0\|_{3+2\epsilon+a} + (\mathfrak{C}_{11} + \widetilde{C}_{2.2.6})\delta\theta_j^{(a-\alpha-\epsilon)_+}\}
\end{aligned} \tag{2.25}$$

for b, such that A.10.iii is true for $(2 + 3\epsilon + a, b)$ and c_j such that A.10.iii is true for $(0, c_1), (0, c_2)$.
Similarly, for the linearization error e''_j ([19, (2.1.5)$''$ Hörmander]) we obtain

$$\begin{aligned}
\|e''_j\|_{2\epsilon+a} \leq\ & C_2\triangle_j\{\|\dot{u}_j\|_{2+3\epsilon+a}\|\dot{u}_j\|_0 \\
& + \|\dot{u}_j\|_0^2(\|u_j\|_{3+2\epsilon+a} + \|\dot{u}_j\|_{3+2\epsilon+a})\} \\
\leq\ & C_2\triangle_j\{\delta\theta_j^{1+3\epsilon+a-\alpha}\delta\theta_j^{-\alpha-1} \\
& + (\delta\theta_j^{-\alpha-1})^2(\mathfrak{C}_{11}\delta\theta_{j+1}^{(3+2\epsilon+a-\alpha)_+} + \|u_0\|_{3+2\epsilon+a} \\
& + \delta\theta_j^{2+2\epsilon+a-\alpha}\} \\
\leq\ & C_2\triangle_j\delta^2\{\theta_j^{3\epsilon+a-2\alpha} \\
& + 2\mathfrak{C}_{11}(\delta\theta_{j+1}^{(3+2\epsilon+a-\alpha)_+} + \|u_0\|_{3+2\epsilon+a})\theta_j^{-2\alpha-2}\}.
\end{aligned} \tag{2.26}$$

Let $e_j = e'_j + e''_j$ and $E_k = \sum_{j=0}^{k-1}\triangle_j e_j$. By [19, page 22 Hörmander] we have

$$g_{k+1} = \widetilde{S}_k(f - E_k) - \frac{\triangle_k}{\triangle_{k+1}}S_{\theta_{k+1}}e_k$$

and the following estimates

$$\|S_{\theta_{k+1}}e_k\|_{\widetilde{a}} \leq C_{A.10.ii}\theta_k^{-(b-\widetilde{a})_+}\|e_k\|_b \tag{2.27}$$

$$\begin{aligned}
\|\widetilde{S}_k E_k\|_{\widetilde{a}} &\leq C_{A.10.iv}\theta_k^{\widetilde{a}-b-1}\|E_k\|_b \\
&\leq C_{A.10.iv}\theta_k^{\widetilde{a}-b-1}\sum_{j=0}^{k-1}\triangle_j\|e_j\|_b.
\end{aligned} \tag{2.28}$$

In order to keep the formulas manageable, we write (2.25) and (2.26) in the schematic form

$$\|e'_j\|_{2\epsilon+a} \leq \sum_{n=1}^{N}\mathfrak{C}_n\delta\{\|u_0\|_{A_n}, \delta, \delta^2, \|u_0\|_{B_n}\delta, \|u_0\|_{c_n}\|u_0\|_{c'_n}\}\theta_j^{-d_n} \tag{2.29}$$

$$\|e''_j\|_{2\epsilon+a} \leq \sum_{n=1}^{N}\widetilde{\mathfrak{C}}_n\triangle_j\delta^2\{1, \delta, \|u_0\|_{3+2\epsilon+a}\}\theta_j^{-\widetilde{d}_n}. \tag{2.30}$$

Note that (2.27) immediately leads to an explicit estimate for $S_{\theta_{k+1}} e_k$.
To estimate $\widetilde{S}_k E_k$, we consider the terms $(1, \triangle_j)(\dots)\theta_j^{-d_n}$ on the right hand side of (2.29) and (2.30) separately. Explicit expressions will be used later in (2.35). For the right hand side of (2.29) there are 3 alternatives:
If $d_n < 1$ we have $\forall\, \tau > 0$ small

$$\begin{aligned}
&\sum_{j=0}^{k-1} \triangle_j \Big(\sum_{n=1}^{N} \mathfrak{C}_n \delta\{\|u_0\|_{A_n}, \delta, \delta^2, \|u_0\|_{B_n}\delta, \|u_0\|_{c_n}\|u_0\|_{c'_n}\}\Big)\theta_j^{-d_n} \\
&\leq \theta_k^{-d_n+1+\tau}\Big(\sum_{n=1}^{N} \mathfrak{C}_n \delta\{\|u_0\|_{A_n}, \delta, \delta^2, \|u_0\|_{B_n}\delta, \|u_0\|_{c_n}\|u_0\|_{c'_n}\}\Big) \sum_{j=0}^{k-1} \triangle_j \theta_j^{-1-\tau} \\
&\leq C_\tau \theta_k^{-d_n+1+\tau}\Big(\sum_{n=1}^{N} \mathfrak{C}_n \delta\{\|u_0\|_{A_n}, \delta, \delta^2, \|u_0\|_{B_n}\delta, \|u_0\|_{c_n}\|u_0\|_{c'_n}\}\Big).
\end{aligned}$$

Here we have used

$$\triangle_j \theta_j^{-1-\tau} \leq C\kappa^{-1}\theta_j^{1-\kappa-1-\tau} = C\kappa^{-1}(\theta_0^\kappa + j)^{-1-\frac{\tau}{\kappa}}, \tag{2.31}$$

where

$$\infty > C_\tau \geq \sum_{j=0}^{\infty} C\kappa^{-1}(\theta_0^\kappa + j)^{-1-\frac{\tau}{\kappa}}$$

is independent of $\theta_0 \geq \theta_0^{\min} > 0$ and $\kappa > 0$.

Remark 2.1. *This is only necessary if we want to vary k with the step, otherwise we can just work with the summands*

$$\triangle_j \Big(\sum_{n=1}^{N} \mathfrak{C}_n \delta\{\|u_0\|_{A_n}, \delta, \delta^2, \|u_0\|_{B_n}\delta, \|u_0\|_{c_n}\|u_0\|_{c'_n}\}\Big)\theta_j^{-d_n}$$

separately.

If $d_n > 1$ we have $\forall\, \tau > 0$ small

$$\begin{aligned}
&\sum_{j=0}^{k-1} \triangle_j \Big(\sum_{n=1}^{N} \mathfrak{C}_n \delta\{\|u_0\|_{A_n}, \delta, \delta^2, \|u_0\|_{B_n}\delta, \|u_0\|_{c_n}\|u_0\|_{c'_n}\}\Big)\theta_j^{-d_n} \\
&\leq \theta_0^{-d_n+1+\tau}\Big(\sum_{n=1}^{N} \mathfrak{C}_n \delta\{\|u_0\|_{A_n}, \delta, \delta^2, \|u_0\|_{B_n}\delta, \|u_0\|_{c_n}\|u_0\|_{c'_n}\}\Big) \sum_{j=0}^{k-1} \triangle_j \theta_j^{-1-\tau} \\
&\leq C_\tau \theta_0^{-d_n+1+\tau}\Big(\sum_{n=1}^{N} \mathfrak{C}_n \delta\{\|u_0\|_{A_n}, \delta, \delta^2, \|u_0\|_{B_n}\delta, \|u_0\|_{c_n}\|u_0\|_{c'_n}\}\Big).
\end{aligned}$$

and if $d_n = 1$ we have $\forall\, \tau > 0$ small

$$\sum_{j=0}^{k-1} \triangle_j \Big(\sum_{n=1}^{N} \mathfrak{C}_n \delta\{\|u_0\|_{A_n}, \delta, \delta^2, \|u_0\|_{B_n}\delta, \|u_0\|_{c_n}\|u_0\|_{c'_n}\}\Big)\theta_j^{-d_n} \tag{2.32}$$

$$\leq C_\tau \theta_k^{\tau}\Big(\sum_{n=1}^{N} \mathfrak{C}_n \delta\{\|u_0\|_{A_n}, \delta, \delta^2, \|u_0\|_{B_n}\delta, \|u_0\|_{c_n}\|u_0\|_{c'_n}\}\Big). \tag{2.33}$$

Finally, for the estimate of the right hand side in (2.30) we have

$$\sum_{j=0}^{k-1} \triangle_j^2 (\sum_{n=1}^{N} \widetilde{\mathfrak{C}}_n \delta^2 \{1, \delta, \|u_0\|_{3+2\epsilon+a}\} \theta_j^{-\widetilde{d}_n}) \le C_\tau \kappa^{-1} \theta_0^{2-\widetilde{d}_n-\kappa-\tau} (\sum_{n=1}^{N} \widetilde{\mathfrak{C}}_n \delta^2 \{1, \delta, \|u_0\|_{3+2\epsilon+a}\}).$$

Choosing κ large, this is arbitrarily small. Concluding, the right hand side in (2.28) is estimated, for any $\tau > 0$ small and any $k > 0$, by terms $C_{A.10.iv} \theta_k^{\widetilde{a}-b-1}$ times

$$\begin{cases} C_\tau \theta_k^{-d_n+1+\tau} (\mathfrak{C}_n \delta \{\|u_0\|_{A_n}, \delta, \delta^2, \|u_0\|_{B_n} \delta, \|u_0\|_{c_n} \|u_0\|_{c'_n}\}) \text{ if } d_n < 1 \\ C_\tau \theta_0^{-d_n+1+\tau} (\mathfrak{C}_n \delta \{\|u_0\|_{A_n}, \delta, \delta^2, \|u_0\|_{B_n} \delta, \|u_0\|_{c_n} \|u_0\|_{c'_n}\}) \text{ if } d_n > 1 \\ C_\tau \theta_k^{\tau} (\mathfrak{C}_n \delta \{\|u_0\|_{A_n}, \delta, \delta^2, \|u_0\|_{B_n} \delta, \|u_0\|_{c_n} \|u_0\|_{c'_n}\}) \text{ if } d_n = 1 \\ C_\tau \kappa^{-1} \theta_0^{2-\widetilde{d}_n-\kappa+\tau} (\widetilde{\mathfrak{C}}_n \delta^2 \{1, \delta, \|u_0\|_{3+2\epsilon+a}\}) \text{ for } e''_j. \end{cases}$$

Now, the final step in our analysis is to combine the estimates above with

$$\begin{aligned} \|\dot{u}_{k+1}\|_{a+\epsilon} &\le C(\|g_{k+1}\|_{a+\epsilon} + \|g_{k+1}\|_\epsilon \theta_{k+1}^{(2+a-\alpha)_+}) \\ g_{k+1} &= \widetilde{S}_k (f - E_k) - \frac{\triangle_k}{\triangle_{k+1}} S_{\theta_{k+1}} e_k \end{aligned}$$

and

$$\|\tilde{S}_k f\|_b \le C_{A.10.iv} \theta^{b-c-1} \|f\|_c.$$

By using

$$\|S_{\theta_{k+1}} e_k\|_b \le C_{A.10.ii} \theta_{k+1}^{b-\widetilde{c}} \|e'_k\|_{\widetilde{c}} + C_{A.10.ii} \theta_{k+1}^{b-\widetilde{\widetilde{c}}} \|e'_k\|_{\widetilde{\widetilde{c}}}$$

and $\frac{\triangle_k}{\triangle_{k+1}} < C$, under the assumption that $\widetilde{c}, \widetilde{\widetilde{c}} \gg b$, we have explicitly

$$\begin{aligned} \|g_{k+1}\|_b \le{}& C_{A.10.iv} \theta_{k+1}^{b-c-1} \|f\|_c + \|\widetilde{S}_k E_k\|_b + \frac{\triangle_k}{\triangle_{k+1}} \|S_{\theta_{k+1}} e_k\|_b \\ \le{}& C_{A.10.iv} \theta_{k+1}^{b-c-1} \|f\|_c \\ &+ C C_{A.10.ii} \theta_{k+1}^{b-\tilde{c}} \sum_{n=1}^{N} \mathfrak{C}_n \delta \theta_k^{-d_n} \{\|u_0\|_{\widetilde{A}_n}, \delta, \delta^2, \|u_0\|_{\widetilde{B}_n} \delta, \|u_0\|_{\widetilde{c}_n} \|u_0\|_{\widetilde{c}'_n}\} \\ &+ C C_{A.10.ii} \theta_{k+1}^{b-\widetilde{\widetilde{c}}} \sum_{n=1}^{N} \widetilde{\mathfrak{C}}_n \triangle_k \delta^2 \theta_k^{-\widetilde{d}_n} \{1, \delta, \|u_0\|_{3+\widetilde{\widetilde{c}}}\} \\ &+ C_\tau C_{A.10.iv} \theta_k^{b-\gamma-1} \Bigg\{ \sum_{\substack{n=1 \\ \underline{d}_n<1}}^{N} \theta_k^{-\underline{d}_n+1+\tau} \mathfrak{C}_n \delta \{\|u_0\|_{\underline{A}_n}, \delta, \delta^2, \|u_0\|_{\underline{B}_n} \delta, \|u_0\|_{\underline{c}_n} \|u_0\|_{\underline{c}'_n}\} \\ &+ \sum_{\substack{n=1 \\ \underline{d}_n>1}}^{N} \theta_0^{-\underline{d}_n+1+\tau} \mathfrak{C}_n \delta \{\|u_0\|_{\underline{A}_n}, \delta, \delta^2, \|u_0\|_{\underline{B}_n} \delta, \|u_0\|_{\underline{c}_n} \|u_0\|_{\underline{c}'_n}\} \\ &+ \sum_{\substack{n=1 \\ \underline{d}_n=1}}^{N} \theta_k^{\tau} \mathfrak{C}_n \delta \{\|u_0\|_{\underline{A}_n}, \delta, \delta^2, \|u_0\|_{\underline{B}_n} \delta, \|u_0\|_{\underline{c}_n} \|u_0\|_{\underline{c}'_n}\} \\ &+ \kappa^{-1} \delta^2 \sum_{n=1}^{N} \widetilde{\mathfrak{C}}_n \theta_0^{2-\widetilde{\underline{d}}_n-\kappa+\tau} \{1, \delta, \|u_0\|_{3+\gamma}\} \Bigg\} \end{aligned}$$

where $d_n, \widetilde{A}_n, \widetilde{B}_n, \widetilde{c}_n, \widetilde{c}'_n$ are the indices in (2.29) when we set $\widetilde{c} = 2\epsilon + a$, $\widetilde{d}_n$ are the exponents in (2.30) when we set $\widetilde{\widetilde{c}} = 2\epsilon + a$ and $\underline{d}_n, \underline{A}_n, \underline{B}_n, \underline{c}_n, \underline{c}'_n, \widetilde{\underline{d}_n}$ the indices in (2.29) and (2.30) when we set $\gamma = 2\epsilon + a$.
The estimate for $\dot{u}_{k+1}$ is given by ([19, 2.2.13 Hörmander])

$$\|\dot{u}_{k+1}\|_{a+\epsilon} \leq C_{2.1.6}(\|g_{k+1}\|_{a+\epsilon} + \|g_{k+1}\|_{\epsilon}\theta_{k+1}^{(2-a-\alpha)_+}). \tag{2.34}$$

Using $b = a + \epsilon$ and $b = \epsilon$ in the estimate for $\|g_{k+1}\|_b$, by recalling (2.25) and (2.26), we identify the terms in (2.29) and (2.30) involving

$$\begin{aligned}
d_1 : &\quad \mathfrak{C}_1(\delta\|u_0\|_\beta\theta_k^{1+\widetilde{c}+\epsilon-\beta-\alpha} + \delta\|u_0\|_{\widetilde{\beta}}\theta_k^{-\widetilde{\beta}+1+\widetilde{c}-\alpha}) \\
d_2 : &\quad \mathfrak{C}_2\delta^2(\theta_k^{1+\widetilde{c}-2\alpha+\tau} + \theta_k^{1+\widetilde{c}-2\alpha-\epsilon}) \\
d_3 : &\quad \mathfrak{C}_3\delta^2(\|u_0\|_{\widetilde{\widetilde{\beta}}}\theta_k^{-\widetilde{\widetilde{\beta}}+\tau-\alpha-1+(\widetilde{c}-\alpha-3\epsilon)_+} + \|u_0\|_{3+\widetilde{c}}\theta_k^{\tau-2\alpha-\epsilon-1}) \\
d_4 : &\quad \mathfrak{C}_4\delta\|u_0\|_{\widetilde{\widetilde{\beta}}}\theta_k^{-\widetilde{\widetilde{\beta}}+\tau-\alpha-1}\|u_0\|_{3+\widetilde{c}} \\
d_5 : &\quad \mathfrak{C}_5\delta^3\theta_k^{\tau-2\alpha-1-\epsilon+(\widetilde{c}-\alpha-3\epsilon)_+} \\
\widetilde{d}_1 : &\quad \widetilde{\mathfrak{C}}_1\delta^2\triangle_k\theta_k^{-2\tau+\epsilon-2\alpha+\widetilde{\widetilde{c}}} \\
\widetilde{d}_2 : &\quad \widetilde{\mathfrak{C}}_2\delta^3\triangle_k\theta_k^{(3+\widetilde{\widetilde{c}}-\alpha)_+}\theta_k^{-2\tau-2\alpha-2} \\
\widetilde{d}_3 : &\quad \widetilde{\mathfrak{C}}_3\delta^2\triangle_k\|u_0\|_{3+\widetilde{\widetilde{c}}}\theta_k^{-2\tau-2\alpha-2}
\end{aligned} \tag{2.35}$$

where β is such that A.10.iii is true for $(2 + \epsilon + \widetilde{c}, \beta)$, $\widetilde{\beta}$ such that A.10.iii is true for $(0, \widetilde{\beta})$ and $\widetilde{\widetilde{\beta}}$ such that A.10.iii is true for $(0, \widetilde{\widetilde{\beta}})$.
Now, to simplify the estimates crudely we choose $c = \alpha + \epsilon$. For $\beta, \widetilde{\beta}, \widetilde{\widetilde{\beta}}$ sufficiently large, we note that the f-term in the estimate has the highest exponent of θ_k and we denote this exponent by $E := a - \alpha - 1$.
We can write all the other terms $\theta_k^{(\cdots)}$ as $\theta_k^E\theta_k^{(\cdots)-E}$ where $(\cdots) - E < 0$. For given $u_0, \beta, \widetilde{\beta}, \widetilde{\widetilde{\beta}}, \widetilde{c}, \widetilde{\widetilde{c}}$ we can thus choose for a $\sigma > 0$ small, $\theta_0 = \theta_0(\sigma)$ large enough such that

$$\begin{aligned}
&\theta_0^{(\cdots)-E}(1 + \|u_0\|_X + \|u_0\|_0\|u_0\|_X) \\
&< \frac{\sigma}{20}\{C_{2.1.6} \cdot C_{A.6}\max\{C_{A.10.ii}, C_{A.10.iv}\}\max\{\mathfrak{C}_n, \widetilde{\mathfrak{C}}_n\}\max\{C, C_\tau\}\}^{-1}
\end{aligned} \tag{2.36}$$

where $X = \max\{3 + \widetilde{c} + \widetilde{\widetilde{\beta}}, \beta, \widetilde{\beta}\}$ and $\|u_0\|_0 > 0$.
From this we deduce

$$\|\dot{u}_{k+1}\|_{a+\epsilon} \leq \theta_{k+1}^E(2 \cdot C_{2.1.6}C_{A.10.iv}\|f\|_{\alpha+\epsilon} + \delta\sigma(1 + \delta + \delta^2)). \tag{2.37}$$

So given δ, let $\sigma := \frac{1}{2}\frac{1}{1+\delta+\delta^2}$.
Then for all f in the ball $\{u : \|u\|_{\alpha+\epsilon} < \frac{\delta}{4C_{2.1.6}C_{A.10.iv}}\}$ we have

$$\|\dot{u}_{k+1}\|_{a+\epsilon} \leq \delta\theta_{k+1}^E. \tag{2.38}$$

We also note that $4 \cdot C_{2.1.6}C_{A.10.iv}\|f\|_{\alpha+\epsilon} < \delta$.
On the other hand, we have using $\triangle_0 g_0 = S_{\theta_0}f$, $v_0 = S_{\theta_0}u_0$ and $\dot{u}_0 = \Psi(v_0)g_0$, the

solution of the linearized problem $\dot{u}_0$,

$$\begin{aligned}
\|\dot{u}_0\|_{a+\epsilon} &= \left\| \frac{\Psi(S_{\theta_0}u_0)}{\triangle_0} S_{\theta_0} f \right\|_{a+\epsilon} \\
&\le \frac{C_{2.1.6}}{\triangle_0} (\|S_{\theta_0} f\|_{a+\epsilon} + \|S_{\theta_0} f\|_\epsilon \|S_{\theta_0} u_0\|_{2+\epsilon+a}) \\
&\le \theta_0 \frac{C_{2.1.6}}{\triangle_0} (C_{A.10.ii}\theta_0^{a-\alpha-1}\|f\|_{\alpha+\epsilon} + C_{A.10.ii}^2 \theta_0^{-\alpha-1}\|f\|_{\alpha+\epsilon}\|u_0\|_{2+\epsilon+a}) \\
&\le 2\frac{\theta_0}{\triangle_0} C_{2.1.6}C_{A.10.ii}(1 + C_{A.10.ii}\theta_0^{-a}\|u_0\|_{2+\epsilon+a})\|f\|_{\alpha+\epsilon}\theta_0^{a-\alpha-1}.
\end{aligned}$$

Let

$$\mathfrak{C} = \max\{2\frac{\theta_0}{\triangle_0} C_{2.1.6}C_{A.10.ii}(1 + C_{A.10.ii}\theta_0^{-a}\|u_0\|_{2+\epsilon+a}), 4 \cdot C_{216}C_{A.10.iv}\}. \tag{2.39}$$

We set

$$\begin{aligned}
\delta &= \max\{2\frac{\theta_0}{\triangle_0} C_{2.1.6}C_{A.10.ii}(1 + C_{A.10.ii}\theta_0^{-a}\|u_0\|_{2+\epsilon+a}), 4 \cdot C_{2.1.6}C_{A.10.iv}\}\|f\|_{\alpha+\epsilon} \\
&= \mathfrak{C}\|f\|_{\alpha+\epsilon}.
\end{aligned}$$

Note that for this δ (2.38) is fulfilled and by induction we deduce

$$\|\dot{u}_{k+1}\|_{a+\epsilon} \le \mathfrak{C}\|f\|_{\alpha+\epsilon}\theta_{k+1}^E \quad \forall\, k \ge 0. \tag{2.40}$$

Alltogether we have proven the following quantitative version of Hörmander's theorem (Theorem 2.1).

Theorem 2.2. *Let f be given as in* (2.1). *Under the assumptions of Lemma 2.1 and with $\delta = \mathfrak{C}\|f\|_{\alpha+\epsilon}$, for $\mathfrak{C}$ the constant in* (2.39), *given θ_0 as in (2.36) we have with the Nash-Hörmander iterates $u_{k+1} = u_k + \triangle_k \dot{u}_k$ in* (2.11)

$$\|\dot{u}_k\|_{a+\epsilon} \le \mathfrak{C}\|f\|_{\alpha+\epsilon}\theta_k^E, \quad \forall\, k \ge 0, E = a - \alpha - 1, a \le \alpha + \epsilon, \epsilon > 0. \tag{2.41}$$

In particular, $\{u_k\}_{k=1}^\infty$ converges in $\mathscr{H}^{a+\epsilon}$ towards the solution u of (2.1).

Let us consider the following modification of the algorithm (see Algorithm 4.3) :

(0) Choose an approximate solution u_0 and θ_0.

(1) Using u_0 do k steps of Hörmander's method leading to u_k.

(2) Set $u_0 = u_k$, a corresponding θ_0 and go to (1).

We denote the approximate solution after l iterations of (1) by $u^{(l)}$ and the corresponding θ_0 by $\theta_0^{(l)}$. To analyse this algorithm, we consider the result of the usual algorithm after the k-th step. Let $u = u_0 + \sum_{j=0}^\infty \triangle_j \dot{u}_j$ be the exact solution. Using Theorem 2.2 above and the same argument as in (2.31) we have

$$\begin{aligned}
\|u - u_k\|_{a+\epsilon} &\le \sum_{j=k+1}^\infty \triangle_j \|\dot{u}_j\|_{a+\epsilon} \le \mathfrak{C}\|f\|_{\alpha+\epsilon} \sum_{j=k+1}^\infty \triangle_j \theta_j^E \\
&\le C_\tau \mathfrak{C}\|f\|_{\alpha+\epsilon}\theta_k^{E+1+\tau}
\end{aligned}$$

for all $\tau > 0$ small such that $E + 1 + \tau < 0$ i.e.

$$\|u - u_k\|_{a+\epsilon} \leq \widetilde{C}_\tau \|\Phi(u) - \Phi(u_0)\|_{\alpha+\epsilon} \theta_k^{E+1+\tau}. \tag{2.42}$$

We now assume that Φ has a locally Hölder-continuous extension $\Phi : \mathscr{H}^{s+3}_{loc} \to \mathscr{H}^{s}_{loc}$ with Hölder exponent ν for every (sufficiently large) $s \geq \alpha + \epsilon$. (As is true for the Molodensky problem by Hörmander's analysis).
Then

$$\|\Phi(u) - \Phi(u_0)\|_{\alpha+\epsilon} \leq C_\Phi^K \|u - u_0\|^\nu_{\alpha+\epsilon+3}$$

for $\|u - u_0\|_{\alpha+\epsilon+3} \leq K$ bounded and hence

$$\|u - u_k\|_{a+\epsilon} \leq \widetilde{C}_\tau C_\Phi^K \theta_k^{E+1+\tau} \|u - u_0\|^\nu_{\alpha+\epsilon+3} \quad \forall\, \tau > 0 \tag{2.43}$$

where $E < -1$ and τ is sufficiently small such that $E + 1 + \tau < 0$.
Iterating this yields that the sequence of iterates $u^{(l)}$ of the restarted algorithm converges to u, if we choose a sufficiently rapidly increasing sequence of θ_0's corresponding to the size of the Hölder norms of $u - u^{(l)}$.

Proposition 2.1. *Assume in addition Φ is Lipschitz continuous i.e $\nu = 1$ then for any sufficiently rapidly increasing sequence $\theta_0^{(l)}$ and $\mathscr{C}(j) := C_\tau^{(j)} (C_\Phi^k)^{(j)} (\theta_k^{E+1+\tau})^{(j)}$ we have*

$$\|u - u_k^{(l)}\|_{a+\epsilon} \leq \big(\prod_{j=0}^{l-1} \mathscr{C}(j)\big) \|u - u_0\|_{l(\alpha-a+3)+a+\epsilon}.$$

2.4. Abstract Uniqueness Result for the Implicit Function Theorem

Here we report on the uniqueness result given by Hörmander in [19, Section 2.3]. For the ease of the reader we use Hörmander's notation again and present the key steps of his derivation. First, he assumes that there is a left inverse $\Psi(u)$ of $\Phi'(u)$ and furthermore, he requires that the crucial estimates (2.9) and (2.10) still hold for $u, v \in C^\infty \cap V$, where V is a convex $\mathscr{H}^\mu$ neighborhood of u_0. He assumes $u_k, v_k \in V \cap C^\infty$ with

$$u_k \to u, \quad v_k \to v \qquad \text{in} \quad \mathscr{H}^{\alpha+\mu_1} \tag{2.44}$$

$$\Phi(u_k) \to \Phi(u_0) + f, \quad \Phi(v_k) \to \Phi(u_0) + f \quad \text{in} \quad \mathscr{H}^{\beta+\lambda_1}. \tag{2.45}$$

Hörmander's aim is to show under certain conditions on α, β that either u or v are far apart or else $u = v$. Setting

$$R_k := \Phi(v_k) - \Phi(u_k) - \Phi(u_k)'(v_k - u_k), \quad T_k := \Phi(u_k) - \Phi(v_k) \tag{2.46}$$

and adding up these equations yields

$$R_k + T_k = -\Phi(u_k)'(v_k - u_k). \tag{2.47}$$

Multiplication with $\Psi(u_k)$, gives

$$u_k - v_k = \Psi(u_k)(R_k + T_k).$$

Now using (2.9), (2.10) there holds

$$\|R_k\|_{\lambda_0+a} \leq C\{\|u_k - v_k\|_{m1+a}\|u_k - v_k\|_{m2} + \|u_k - v_k\|_{m3}\|u_k - v_k\|_{m4}(\|u_k\|_{m5+a} + \|v_k\|_{m1+a})\}, \quad 0 \leq a \leq a_\Phi \tag{2.48}$$

$$\|u_k - v_k\|_{\mu_1+a_0} \leq C(\|R_k + T_k\|_{\lambda_1+a_0} + \|R_k + T_k\|_{\lambda_2}\|u_k\|_{\mu_2+a_0}), \quad 0 \leq a_0 \leq a_\Psi. \tag{2.49}$$

First, consider the contributions from T_k. By using (2.44), (2.45) and letting $k \to \infty$, Hörmander shows that these tend to 0. This is achieved by imposing the following conditions

$$\mu_2 + a_0 \leq \mu_1 + \alpha, \quad \lambda_1 + a_0 \leq \lambda_1 + \beta, \quad \lambda_2 \leq \lambda_1 + \beta.$$

Using the notations

$$M = \mu_2 - \mu_1, \quad \Lambda_j = \lambda_j - \lambda_{j-1},$$

we finally deduce

$$a_0 + M \leq \alpha, \quad a_0 \leq \beta, \quad \Lambda_2 \leq \beta, \quad 0 \leq a_0 \leq a_\Psi. \tag{2.50}$$

Now, consider the contributions of R_k in (2.49). For this purpose one first notes that $u_k - v_k$ occurs quadratically in the right hand side of (2.48). If one could get a power higher than 1 of $\|u_k - v_k\|_{\mu_1+a_0}$ in the right hand side of (2.49), one would be able to use the fact that if $\delta \leq C\delta^\gamma$ with $\gamma > 1$, then either $\delta = 0$ or else $\delta \geq C^{1/(1-\gamma)}$. Setting $\delta_k = \|u_k - v_k\|_{\mu_1+a_0}$ and using Theorem A.5 one gets

$$\|u_k - v_k\|_{\mu_1+a} \leq C\delta_k^{(\alpha-a)/(\alpha-a_0)}, \quad a_0 \leq a \leq \alpha$$

from which Hörmander deduces

$$\|u_k - v_k\|_a \leq C\delta_k^{(\alpha+\mu_1-a)/(\alpha-a_0)}, \quad a_0 + \mu_1 \leq a \leq \alpha + \mu_1.$$

By using the fact that δ_k is positive and as small as needed and imposing that $0 \leq a \leq a_0 + \mu_1$ one has

$$\|u_k - v_k\|_a \leq C\delta_k.$$

This estimate can be used with (2.48), which gives

$$\|R_k\|_{\lambda_0+a} \leq C\delta_k^\gamma, \quad \text{for} \quad \gamma > 1 \quad \text{and} \quad a \geq 0, \tag{2.51}$$

if a certain set of conditions (see [19, (2.3.8)]) is fulfilled. Setting $\lambda_0 + a = \lambda_2$ or $\lambda_0 + a = \lambda_1 + a_0$ or $a = 0$ the contributions of R_k in the right hand side of (2.49) can be estimated by $C\delta_k^\gamma$ and one obtains

$$\delta < C\delta^\gamma, \quad \delta = \|v - u\|_{\mu_1+a_0}, \quad \text{for} \quad \gamma > 1 \tag{2.52}$$

where C depends only on $\|u\|_{\alpha+\mu_1} + \|v\|_{\alpha+\mu_1}$.
Denote by $\Phi^{-1}_{\alpha,\beta}(f)$ the set of all $u \in \mathscr{H}^{\alpha+\mu_1}$ such that for some sequence $u_k \in V \cap C^\infty$, where V is a convex $\mathscr{H}^\mu$ neighborhood of u_0

$$u_k \to u \quad \text{in} \quad \mathscr{H}^{\alpha+\mu_1}, \quad \Phi(u_k) \to \Phi(u_0) + f \quad \text{in} \quad \mathscr{H}^{\beta+\lambda_1}$$

leads to the following uniqueness result.

Theorem 2.3 (Theorem 2.3.1 [19])**.** *Assume that $\Phi'(u)$ when $u \in V \cap C^\infty$ has a left inverse $\Psi(u)$ and that (2.44), (2.45) are valid when $u \in V \cap C^\infty$ and $v \in V \cap C^\infty$. Also assume that a set of necessary conditions is fulfilled. For every bounded set B in $\mathscr{H}^{\alpha+\mu_1}$ one can find a constant N such that $\Phi^{-1}_{\alpha,\beta}(f) \cap B$ never has more than N elements and $\|u - v\|_0 > \frac{1}{N}$ for any two different elements.*

Proof. By (2.52) there is a constant C depending on B, such that if $u, v \in B \cap \Phi^{-1}_{\alpha,\beta}(f)$ are different elements, we have

$$\|v - u\|_{\mu_1+a_0} \geq c > 0.$$

Using Theorem A.5 and a fixed bound for $\|v - u\|_{\mu_1+\alpha}$ we have

$$0 < c \leq \|v - u\|_{\mu_1+a_0} \leq C\|v - u\|_0^\lambda \|v - u\|_{\mu_1+\alpha}^{1-\lambda} \leq \widetilde{C}\|v - u\|_0^\lambda$$

and by noting that

$$\|v - u\|_0 \geq \left(\frac{c}{\widetilde{C}}\right)^{1/\lambda} =: \delta$$

there is a fixed lower bound δ for $\|u - v\|_0$.
Now, $B \subset \mathscr{H}^{\alpha+\mu_1}$ is precompact in $\mathscr{H}^0$ and we can cover $\overline{B}$ by a finite number of balls N

$$\overline{B} \subseteq \bigcup_{j=1}^{N} \{u : \|u - u_j\|_0 < \delta/3\}.$$

In each of the balls $\{u : \|u - u_j\|_0 < \delta/3\}$ we have at most one solution. It is then clear that $B \cap \Phi^{-1}_{\alpha,\beta}(f)$ cannot contain more than N elements. □

3. The Molodensky Problem

Molodensky proposed in 1945 the direct gravimetric determination of the surface of the earth [29, 30]. The problem of Molodensky is an exterior (geodetic) boundary value problem with given data on the earth surface. Following Moritz [17, 31], the Molodensky problem can be formulated briefly as follows: given, at all points of the earth's surface φ, the gravitational potential W and the gravity vector G determine the surface φ.
The potential W can be determined by levelling combined with gravity measurements; this gives the potential apart from an additive constant. The length $|G|$ of the gravity vector is measured by gravimetry and the direction of G, which is the plumb line, is obtained by astronomical measurements of the latitude ϕ and longitude λ. It is assumed that these measurements are corrected for luni-solar tidal effects and other temporal variations, so that our problem is independent of time. We further suppose that the very small effect of the atmosphere has been taken into account by an appropriate reduction.
Now, following Hörmander [19], the earth is assumed to be a rigid body, which rotates with a constant and known angular velocity ω around a fixed axis, which passes through the earth's center of mass, whose surface is diffeomorphic to the sphere under a map $\varphi : \mathbb{S}^2 \to \mathbb{R}^3$, with $\mathbb{S}^2 = \{x \in \mathbb{R}^3; x_1^2 + x_2^2 + x_3^2 = 1\}$. This center of mass will be taken as the origin 0 of a cartesian coordinate system, the x_3 axis coinciding with the axis of rotation.
The measured data W and G may then be considered as functions on $\mathbb{S}^2$

$$W : \mathbb{S}^2 \to \mathbb{R}, \quad G : \mathbb{S}^2 \to \mathbb{R}^3.$$

We want to find a differentiable embedding $\varphi : \mathbb{S}^2 \to \mathbb{R}^3$ such that

$$W = w \circ \varphi \ , \quad G = \nabla w \circ \varphi = g \circ \varphi \quad \text{on} \quad \mathbb{S}^2, \tag{3.1}$$

where $w : \varphi(\mathbb{S}^2) \to \mathbb{R}$ denotes the gravity potential, $g = \nabla w : \varphi(\mathbb{S}^2) \to \mathbb{R}^3$ the gravity and $\circ$ the composition.
The static gravitational potential v is harmonic in the exterior of the earth with boundary values

$$w(x) = v(x) + \frac{\omega^2}{2}(x_1^2 + x_2^2) \quad \text{on} \quad \varphi(\mathbb{S}^2) \tag{3.2}$$

where ω is the angular velocity.
At infinity, v satisfies the radiation condition

$$v(x) = \frac{M}{|x|} + \mathcal{O}(|x|^{-3}) \quad \text{for} \quad x \to \infty \tag{3.3}$$

where (in suitable units) M is the unknown mass of the earth and the absence of $|x|^{-2}$–terms fixes the center of mass to 0.
Furthermore, the absence of first degree harmonics $x_j/|x|^3$ in (3.3) means that for known φ, W must satisfy three linear independent conditions. This will be explained in detail in the next section. Given W and the surface of the earth φ, G is recovered by solving the exterior Dirichlet problem for v and computing the gradient.
Hörmander gives in [19, Chapter III] a procedure to obtain φ as a functional of G and W. In the following we present his approach.
The first step in finding φ is to examine the linearized equations. To do so we consider in the following one parameter families of functions φ, W, G, w, v, g which depend differentiably on the parameter θ. We denote the derivatives with respect to θ by a dot.
We obtain from (3.2) and (3.3) that $\dot{w} = \dot{v}$ is harmonic and has no first degree harmonic component at infinity. With $W = w(\theta, \varphi(\theta, x, y, z)) = w(\theta, (\tilde{x}, \tilde{y}, \tilde{z}))$ applying the chain rule we have

$$\begin{aligned}\dot{W} = \frac{dw}{d\theta} =&(\nabla_\theta w)(\theta, \varphi(\theta, x, y, z)) + (\nabla_{\tilde{x}} w)(\theta, \varphi(\theta, x, y, z))\frac{\partial \tilde{x}}{\partial \theta}\\ &+ (\nabla_{\tilde{y}} w)(\theta, \varphi(\theta, x, y, z))\frac{\partial \tilde{y}}{\partial \theta} + (\nabla_{\tilde{z}} w)(\theta, \varphi(\theta, x, y, z))\frac{\partial \tilde{z}}{\partial \theta}.\end{aligned}$$

With $\tilde{x} = \varphi_1(\theta, x, y, z)$ we have

$$\frac{\partial \tilde{x}}{\partial \theta} = \frac{\partial \varphi_1}{\partial \theta}(\theta, x, y, z) = \dot{\varphi}_1$$

and analogously $\frac{\partial \tilde{y}}{\partial \theta} = \dot{\varphi}_2, \frac{\partial \tilde{z}}{\partial \theta} = \dot{\varphi}_3$.
With $\partial_\theta w = \dot{w}$ and $\langle\ ,\ \rangle$ denoting the scalar product we finally obtain

$$\begin{aligned}\dot{W} &= \dot{w}(\theta, \varphi(\theta, x, y, z)) + \langle(\nabla w)(\theta, \varphi(\theta, x, y, z)), \dot{\varphi}(\theta, \varphi(\theta, x, y, z))\rangle\\ &= \dot{w} \circ \varphi + \langle(\nabla w) \circ \varphi, \dot{\varphi}\rangle\\ &= \dot{v} \circ \varphi + \langle G, \dot{\varphi}\rangle.\end{aligned} \tag{3.4}$$

In the same way we obtain

$$\begin{aligned}\dot{G} &= \dot{g}(\theta, \varphi(\theta, x, y, z)) + \langle(\nabla g)(\theta, \varphi(\theta, x, y, z)), \dot{\varphi}(\theta, \varphi(\theta, x, y, z))\rangle\\ &= \dot{g} \circ \varphi + \langle(\nabla g) \circ \varphi, \dot{\varphi}\rangle\\ &= \dot{v}' \circ \varphi + \langle g' \circ \varphi, \dot{\varphi}\rangle.\end{aligned} \tag{3.5}$$

These are the linearized equations for $\dot{W}$ and $\dot{G}$.
Now, in order to solve (3.5) for $\dot{\varphi}$, we assume that the so called Marussi condition [22] is fulfilled, i.e.

$$\det g'(x) \neq 0, \quad x \in \varphi(\mathbb{S}^2). \tag{3.6}$$

Now, using (3.5) we deduce

$$\dot{\varphi} = (\nabla g \circ \varphi)^{-1}(\dot{G} - \nabla \dot{v} \circ \varphi) \quad \text{on} \quad \mathbb{S}^2 \tag{3.7}$$

and inserting this in (3.4) we must form the scalar product with G. Following Hörmander, g' is a symmetric matrix and we are interested in the vector h defined by

$$h = -{g'}^{-1} g, \quad \text{such that} \quad g = -g' h \tag{3.8}$$

where h is the tangent of the curve along which g has a fixed direction and changes in length, so that we have

$$g(x + \varepsilon h) = g(x)(1 - \varepsilon) + O(\varepsilon^2), \quad \epsilon \to 0.$$

Hörmander also assumes that the "isozenithal" vector field h is never tangential to $\varphi(\mathbb{S}^2)$.
Now, by inserting (3.7) into (3.4) with $h = -g'^{-1}g$ and $G = g \circ \varphi$ we have

$$\begin{aligned}\dot{W} &= \dot{v} \circ \varphi + \langle g \circ \varphi, (g' \circ \varphi)^{-1}\dot{G}\rangle - \langle g \circ \varphi, (g' \circ \varphi)^{-1}\mathrm{grad}\,\dot{v} \circ \varphi\rangle \\ &= \dot{v} \circ \varphi - \langle \dot{G}, h \circ \varphi\rangle + \langle \mathrm{grad}\,\dot{v} \circ \varphi, h \circ \varphi\rangle,\end{aligned}$$

and thus

$$(\dot{v} + \langle \mathrm{grad}\,\dot{v}, h\rangle) \circ \varphi = \dot{W} + \langle \dot{G}, h \circ \varphi\rangle \quad \text{on} \quad \mathbb{S}^2. \tag{3.9}$$

In order to solve (3.5) for $\dot{\varphi}$, assuming that $\dot{W}$ and $\dot{G}$ are given, we have to find a harmonic function $\dot{v}$ outside $\varphi(\mathbb{S}^2)$ which is regular and has no first degree harmonic component at infinity. Then $\dot{v}$ satisfies (3.9) and we obtain $\dot{\varphi}$ from (3.7).
Before concluding this section, we want to explain the reason for introducing a smoothing in Molodensky's problem. Following [31] it is a well known difficulty with many higher order solutions that the higher order terms are getting rougher and rougher. This is the case if an iteration involves differentiation: the derivative is almost always less smooth than the original function. A similar effect, due to differentiation, occurs in the iterative solution of the nonlinear Molodensky problem: the functions involved get rougher and rougher and the iteration is likely to "blow up". Assume that we have some approximate solution for which φ has k derivatives. The isozenithal vector field h, as given by (3.8), involves twice differentiating the gravity potential w. Thus, h can only be expected to have $k-2$ derivatives and therefore, one cannot hope for more than $k-2$ derivatives for $\dot{\varphi}$. This *loss of derivatives* of two orders in each step of iteration is the reason why the Fréchet derivative, given by the linearized Molodensky problem, does not have a bounded inverse in the Banach spaces used for studying the nonlinear Molodensky problem. Therefore, we have to counteract this "roughening effect" by a suitable smoothing, taking care, that the degree of smoothing is successively reduced so as, in the limit, to obtain the right result.

3.1. The Linearized Molodensky Problem

Assume that φ_0 is a C^∞ embedding of the unit sphere $\mathbb{S}^2$ in $\mathbb{R}^3$. Following Hörmander, let $W_0 : \mathbb{S}^2 \to \mathbb{R}$ and $G_0 : \mathbb{S}^2 \to \mathbb{R}^3$ be C^∞ functions such that for a harmonic function v_0 outside $\varphi_0(\mathbb{S}^2)$, (3.1), (3.2) and (3.3) are fulfilled. Furthermore, let g_0 satisfy (3.6), h_0 be never tangential to $\varphi_0(\mathbb{S}^2)$ and we require injectivity of the linearization, which means there is no trivial harmonic function in the exterior of $\varphi_0(\mathbb{S}^2)$ satisfying (3.3) and the homogeneous boundary condition

$$(u + \langle \mathrm{grad}\,u, h_0\rangle) \circ \varphi_0 = 0 \quad \text{on} \quad \mathbb{S}^2. \tag{3.10}$$

These conditions are fulfilled if $\varphi_0(\mathbb{S}^2)$ is the unit sphere and W_0, G_0 are close to the gravitational potential respectively field of a spherical earth.
The condition (3.10) guarantees a unique solution for inhomogenous boundary conditions

$$(u + \langle \operatorname{grad} u, h_0 \rangle) \circ \varphi = f \quad \text{on} \quad \mathbb{S}^2$$

for f outside a subspace of $C^\infty(\partial\Omega)$ of codimension 3. For the sphere, the subspace is spanned by the spherical harmonics $\{Y_{1,-1}, Y_{1,0}, Y_{1,1}\}$ of degree 1. In general, we may use the restrictions to $\varphi_0(\mathbb{S}^2)$ of linearly independent homogeneous harmonic functions. We can fix some basis $\{A_j\}_{j=1}^3$ of this three–dimensional subspace such that if $u_j^{\varphi_0}$ is a harmonic function in the exterior of $\varphi_0(\mathbb{S}^2)$ with $u_j^{\varphi_0}|_{\varphi_0(\mathbb{S}^2)} = A_j$ and $u_j^{\varphi_0}(x) \to 0$ for $|x| \to \infty$, then the first degree harmonics of $\{u_j^{\varphi_0}\}_{j=1}^3$ in the multipole expansion at infinity are linearly independent.
In the following let $\epsilon > 0$. We want to show that if we choose W and G sufficiently close to W_0 and G_0 in $\mathscr{H}^{2+\epsilon}(\mathbb{S}^2)$, then there exists an embedding φ close to φ_0 in $\mathscr{H}^{2+\epsilon}$ and small constants a_1, a_2, a_3, such that for some harmonic function v outside $\varphi(\mathbb{S}^2)$ there holds

$$W = w \circ \varphi + \sum_{j=1}^{3} a_j A_j, \quad G = w' \circ \varphi = g \circ \varphi \tag{3.11}$$

with

$$w(x) = v(x) + \omega^2(x_1^2 + x_2^2)/2 \tag{3.12}$$

$$v(x) = \frac{c}{|x|} + O(|x|^{-3}), \quad x \to \infty. \tag{3.13}$$

Thus, when W and G are close to W_0 and G_0 there is a unique way of modifying W by a linear combination of A_1, A_2, A_3 so that the Molodensky problem becomes solvable with a solution φ close to φ_0. By using the reformulation (3.11) - (3.13) we have the advantage that G is now a well defined function of W and φ, for all W and φ close to W_0, φ_0. The exterior Dirichlet problem

$$\Delta u = 0, \quad u \to 0 \quad \text{at} \quad \infty, \quad u \circ \varphi = W - \omega^2(\varphi_1^2 + \varphi_2^2)/2$$

has a unique solution, and it can be split uniquely into a sum

$$u = v + \sum_{j=1}^{3} a_j u_j^{\varphi}$$

where v has no first degree harmonic component at ∞ and

$$\Delta u_j^{\varphi} = 0 \quad \text{outside} \quad \varphi_0(\mathbb{S}^2), \quad u_j^{\varphi} \circ \varphi = A_j \quad \text{on} \quad \mathbb{S}^2, \quad u_j \to 0 \quad \text{at} \quad \infty. \tag{3.14}$$

Defining w by (3.12) and v from above, then

$$w \circ \varphi + \sum_{j=1}^{3} a_j A_j = \omega^2(\varphi_1^2 + \varphi_2^2)/2 + v \circ \varphi + \sum_{j=1}^{3} a_j u_j^{\varphi} \circ \varphi = W,$$

G being defined by the second term in (3.11). From now on we write $G =: \Gamma(W, \varphi)$. The linearization of the reformulated equations (3.11) - (3.13) is done as in the introduction, having an additional sum $\sum_{j=1}^{3} \dot{a}_j A_j$ so that we obtain

$$(\dot{v} + \langle \operatorname{grad} \dot{v}, h \rangle) \circ \varphi = \dot{W} + \langle \dot{G}, h \circ \varphi \rangle - \sum_{i=1}^{3} \dot{a}_j A_j. \tag{3.15}$$

Choosing A_1, A_2, A_3 properly guarantees that for given $\dot{W}, \dot{G}$ there are unique constants $(\dot{a}_1, \dot{a}_2, \dot{a}_3)$ such that there exists a harmonic function $\dot{v}$ satisfying (3.13) and (3.15). The corresponding $\dot{\varphi}$ obtained by using (3.7) gives the inverse of the differential to be estimated before we can apply the method of Nash. In order to apply the method of Nash, a careful study of the second differential of the map Γ is also required. We do this in Section 3.2.

We examine the Dirichlet problem for the Laplacian in the exterior of $\varphi(\mathbb{S}^2)$ and estimate the solution of this problem. The main result of this section is the following theorem.

Theorem 3.1 (Theorem 3.3.2, [19]). *Assume that φ and W are in small neighborhoods of φ_0 and W_0 in $\mathscr{H}^{2+\epsilon}$ and that φ, W as well as $\dot{G}, \dot{W}$ are smooth. Then there is a unique harmonic function outside $\varphi(\mathbb{S}^2)$ satisfying (3.13) and (3.15) for some $\dot{a}_j \in \mathbb{R}$. For the corresponding perturbation $\dot{\varphi}$ given by (3.7), the estimate*

$$\|\dot{\varphi}\|_a \leq C_a\{\|\dot{W}\|_a + \|\dot{G}\|_a + (\|\dot{W}\|_\epsilon + \|\dot{G}\|_\epsilon)(\|W\|_{2+a} + \|\varphi\|_{2+a}) \tag{3.16}$$

is valid.

In the following we give the proof of this theorem.
Throughout this section, following [19], we denote by φ a C^∞ map $\mathbb{S}^2 \to \mathbb{R}^3$, which for $\epsilon > 0$, is in a small $\mathscr{H}^{2+\epsilon}$ neighborhood of φ_0. Note that by an inversion with respect to an interior point of $\varphi_0(\mathbb{S}^2)$, the exterior Dirichlet problem can be reduced to an interior Dirichlet problem and then, by the maximum principle the coefficients of the spherical harmonics expansion at infinity are continuous linear functions of the Dirichlet data in the maximum norm. Following Hörmander, we choose a C^∞ map $T : \mathbb{S}^2 \to \mathbb{R}^3$ such that $T(x)$ points to the exterior of $\varphi_0(\mathbb{S}^2)$ at $\varphi_0(x)$. Then one can find a small constant $\gamma > 0$ such that the map $\widetilde{\varphi}$ defined by

$$\mathbb{S}^2 \times [0,1] \ni (x,t) \to \varphi(x) + \gamma t T(x) \in \mathbb{R}^3 \tag{3.17}$$

is a diffeomorphism for all φ close to φ_0 in $\mathscr{H}^{2+\epsilon}$. In order to work with the Riemannian metric, Hörmander identifies $\mathbb{S}^2 \times [0,1]$ with $\Omega = \{x \in \mathbb{R}^3; 1 \leq |x| \leq 2\}$ by means of the map $(x,t) \to (1+t)x$, and uses (3.17) to pull back the Euclidean metric in $\mathbb{R}^3$ to the Riemannian metric

$$\langle d\varphi + \gamma(T dt + t dT), d\varphi + \gamma(T dt + t dT) \rangle \quad \text{in} \quad \Omega.$$

More generally, for each φ we can find a $T(\varphi)$ and we can estimate the metric tensor (g_{ij}) using Theorem A.7 by

$$\|g_{ij}\|_a \leq C_a \|\varphi\|_{1+a}. \tag{3.18}$$

Here, an uniform upper bound has been imposed on φ' and $\|\varphi\|_0$ has a fixed lower bound. We now consider the exterior Dirichlet problem

$$\Delta u = 0 \quad \text{outside} \quad \varphi(\mathbb{S}^2), \quad u \to 0 \quad \text{at} \quad \infty, \quad u \circ \varphi = U_0 \quad \text{on} \quad \mathbb{S}^2.$$

For this problem we know that a solution exists and is bounded by $\|U_0\|_0$ everywhere. Hence, all derivatives can be estimated by a constant times $\|U_0\|_0$ on compact subsets of the exterior of $\varphi(\mathbb{S}^2)$. With this Hörmander obtains for the pullback U of u to Ω using Theorem A.8 and writing $\Sigma = \{x; |x| = 2\}$,

$$\|U\|_a^\Sigma \leq C_a \|U_0\|_0 \|\varphi\|_a.$$

Here $\|U\|_a^\Sigma$ denotes the Hölder norm on Σ as explained in the appendix. U satisfies the Laplace-Beltrami equation with respect to the metric (g_{ij}), which is of the form considered in Theorem A.14 with the coefficient matrix $A = |\det g|^{1/2} g^{-1}$. Using Theorem A.8 and (3.18) we have

$$\|A\|_a \leq C_a \|\varphi\|_{1+a}. \tag{3.19}$$

Applying Theorem A.14 for $a > 0$ and not an integer, we deduce

$$\|U\|_{1+a}^\Omega \leq C_a (\|U_0\|_{1+a}^{\mathbb{S}^2} + \|U_0\|_{1+\epsilon}^{\mathbb{S}^2} \|\varphi\|_{1+a}^{\mathbb{S}^2}). \tag{3.20}$$

If $|\alpha| < 1 + a$, we deduce

$$\|(\partial^\alpha u) \circ \varphi\|_{1+a-|\alpha|} \leq C_a (\|U_0\|_{1+a} + \|U_0\|_{1+\epsilon} \|\varphi\|_{1+a}). \tag{3.21}$$

Our aim is now to verify (3.21). To do so, we note that $(\partial^\alpha u) \circ \varphi$ is the restriction of $\delta^\alpha U$ to $\mathbb{S}^2$ and Theorem A.8 gives

$$\delta^\alpha = \delta_1^{\alpha_1}, \ldots, \delta_k^{\alpha_k}, \quad \delta_j = \sum_{j=1}^{3} c_{jk} \partial / \partial x_k, \quad c = ({}^t \tilde{\varphi}')^{-1}, \quad \|c\|_a \leq C_a \|\varphi\|_{a+1}.$$

Hörmander claims that for $b > 0$, the following estimate holds [19, (3.2.6)]

$$\|\delta^\alpha U\|_b \leq C_b (\|U\|_{b+|\alpha|} + \|\varphi\|_{b+|\alpha|} \|U\|_1). \tag{3.22}$$

In the following, we derive in detail various estimates [19, (3.2.5), (3.2.6)] of Hörmander's proof. Now, by setting $b = 1 + a - |\alpha|$ and inserting (3.20) into (3.22)

$$\begin{aligned}
\|\delta^\alpha U\|_{1+a-|\alpha|} &\leq C_a (\|U\|_{1+a} + \|\varphi\|_{1+a} \|U\|_{1+\epsilon}) \\
&\leq C_a (\|U_0\|_{1+a} + \|\varphi\|_{1+a} \|U_0\|_{1+\epsilon} \\
&\quad + \|\varphi\|_{1+a} (\|U_0\|_{1+\epsilon} + \|U_0\|_{1+\epsilon} \|\varphi\|_{1+a})) \\
&\leq C_a (\|U_0\|_{1+a} + \|U_0\|_{1+\epsilon} \|\varphi\|_{1+a}),
\end{aligned}$$

we obtain (3.21).

When $|\alpha| = 1$, by using Theorem A.7 we obtain the estimate (3.22) in the following way

$$\begin{aligned}\|\sum_1^3 c_{jk}\partial_k U\|_b &\le \sum_1^3 \|c_{jk}\|_b\|\partial_k U\|_0 + \sum_1^3 \|c_{jk}\|_0\|\partial_k U\|_b \\ &= \|c\|_b\|\partial_k U\|_0 + \|c\|_0\|\partial_k U\|_b \\ &\le C_b\|\varphi\|_{1+b}\|U\|_1 + C_b \underbrace{\|\varphi\|_1}_{\le C}\|U\|_{1+b} \\ &\le C_b(\|U\|_{1+b} + \|\varphi\|_{1+b}\|U\|_1).\end{aligned}$$

Assuming that $|\alpha| = k+1$ and that (3.22) is already proved for $|\alpha| = k$, we obtain for some j

$$\|\delta^\alpha U\|_b = \|\delta^{\alpha-1}(\delta U)\|_b \le C(\|\delta_j U\|_{b+|\alpha|-1} + \|\varphi\|_{b+|\alpha|-1}\|\delta_j U\|_1).$$

By setting $k = |\alpha| - 1$ we have

$$\|\delta^\alpha U\|_b \le C(\|\delta_j U\|_{b+k} + \|\varphi\|_{b+k}\|\delta_j U\|_1).$$

Using now (3.22) with b replaced by $b+k$ or 1 and $|\alpha| = 1$ we deduce

$$\begin{aligned}\|\delta_j U\|_{b+k} &\le C(\|U\|_{b+k+1} + \|\varphi\|_{b+k+1}\|U\|_1) \\ \|\delta_j U\|_1 &\le C(\|U\|_2 + \|\varphi\|_2\|U\|_1)\end{aligned}$$

and we have the following estimate

$$\|\delta^\alpha U\|_b \le C(\|U\|_{b+k+1} + \|\varphi\|_{b+k+1}\|U\|_1 + \|\varphi\|_{b+k}(\|U\|_2 + \|\varphi\|_2\|U\|_1)). \tag{3.23}$$

Applying now Corollary A.6, Hörmander deduces

$$\|\varphi\|_{b+k}\|U\|_2 \le C(\|\varphi\|_1\|U\|_{b+k+1} + \|\varphi\|_{b+k+1}\|U\|_1\|) \tag{3.24}$$

which we show now:
By Corollary A.6 we have

$$\|u\|_\alpha\|u\|_\beta \le C\sum_j \|u\|_{\alpha_j}\|u\|_{\beta_j}$$

if $(\alpha,\beta) \in \text{conv}\,\{(\alpha_j,\beta_j) = \sum_{j=1}^2 \lambda_j(\alpha_j,\beta_j) \quad \text{with} \quad \sum_{j=1}^2 \lambda_j = 1, \lambda_j \ge 1\}$.
In (3.24) we set $\alpha = b+k, \beta = 2$, $\alpha_1 = \beta_2 = 1$ and $\alpha_2 = \beta_1 = b+k+1$.
Now, using $(\alpha,\beta) = \lambda(\alpha_1,\beta_1) + (1-\lambda)(\alpha_2,\beta_2)$, we have the following system of equations:

$$\begin{pmatrix} b+k \\ 2 \end{pmatrix} = \lambda \begin{pmatrix} 1 \\ b+k+1 \end{pmatrix} + (1-\lambda)\begin{pmatrix} b+k+1 \\ 1 \end{pmatrix}$$

which implies

$$\lambda = \frac{1}{b+k}, \qquad 2 = \lambda(b+k+1) + (1-\lambda)$$

which means that we found a λ satisfying both equations. Furthermore, with this λ we can write α and β as a convex combination of (α_j, β_j) and by Corollary A.6 (3.24) holds. Using this estimate in (3.23) and noting that $\|\varphi\|_2$ is bounded, we have proved (3.22).

Now we are in the position to derive the desired estimate (3.16) for $\dot{\varphi}$ with the help of the above estimates. Later on, following Hörmander, we will use this result on $\dot{\varphi}$ (Theorem 3.1) to derive estimates of the map

$$\Gamma : (W, \varphi) \mapsto G.$$

Following [19], we assume that W and φ are smooth and use just the bounds indicated explicitly and a small uniform bound for $\|\varphi - \varphi_0\|_{2+\epsilon}$.
Using (3.21) and the triangle inequality, we have the following estimate for the solution u of the exterior Dirichlet problem with data $U_0 = W - \omega^2(\varphi_1^2 + \varphi_2^2)$

$$\begin{aligned}
\|(\partial^\alpha u) \circ \varphi\|_{1+a-|\alpha|} &\leq C_a\{\|W - \omega^2(\varphi_1^2 + \varphi_2^2)\|_{1+a} + \|W - \omega^2(\varphi_1^2 + \varphi_2^2)\|_{1+\epsilon}\|\varphi\|_{1+a}\} \\
&\leq C_a\{\|W\|_{1+a} + \omega^2 \underbrace{\|(\varphi_1^2 + \varphi_2^2)\|_{1+a}}_{\leq C\|\varphi\|_{1+a}} \\
&\quad + (\|W\|_{1+\epsilon} + \omega^2 \underbrace{\|(\varphi_1^2 + \varphi_2^2)\|_{1+\epsilon}}_{\leq C})\|\varphi\|_{1+a}) \\
&\leq C_a\{\|W\|_{1+a} + (\|W\|_{1+\epsilon} + \omega^2)\|\varphi\|_{1+a}\}, \quad |\alpha| < 1 + a.
\end{aligned}$$

Moreover, we have for the solution u_j^φ of (3.14) with Dirichlet data A_j

$$\|(\partial^\alpha u_j^\varphi) \circ \varphi\|_{1+a-|\alpha|} \leq C_a\|\varphi\|_{1+a}.$$

If $\|\varphi\|$ is close to $\|\varphi_0\|$, the first degree harmonics in the expansion of u_j^φ at ∞ are close to those of u_j and so they span all first degree harmonics. Because the coefficients in the spherical harmonics expansion of u at ∞ can be bounded by $\|W\|_0 + \omega^2$, we have for v (defined as on page 24)

$$\|(\partial^\alpha v) \circ \varphi\|_{1+a-|\alpha|} \leq C_a\{\|W\|_{1+a} + (\|W\|_{1+\epsilon} + \omega^2)\|\varphi\|_{1+a}\}, \quad \text{if} \quad a > \max(0, |\alpha| - 1).$$

By taking $|\alpha| = 1$ we obtain the following estimate for the gravity $\Gamma(W, \varphi) = G = v' \circ \varphi + \omega^2(\varphi_1, \varphi_2, 0)$

$$\|G\|_a \leq C(\|W\|_{1+a} + (\|W\|_{1+\epsilon} + \omega^2)\|\varphi\|_{1+a}). \tag{3.25}$$

If φ and W are close to φ_0 and W_0 in $\mathscr{H}^{2+\epsilon}$, the Marussi condition is uniformly satisfied. If we fix now ω, (3.25) gives

$$\begin{aligned}
\|g' \circ \varphi\|_a = \|G\|_{a+1} &\leq C(\|W\|_{2+a} + \underbrace{(\|W\|_{2+\epsilon} + \omega^2)}_{\leq C}\|\varphi\|_{2+a}) \\
&\leq C_a(\|W\|_{2+a} + \|\varphi\|_{2+a})
\end{aligned} \tag{3.26}$$

and we have an uniform bound for the right hand side when $a = \epsilon$. The uniform validity of the Marussi condition and the fact that by Theorem A.8 inverse functions have essentially the same Hölder norms, gives

$$\|g'^{-1} \circ \varphi\|_a \leq C_a(\|W\|_{2+a} + \|\varphi\|_{2+a}). \tag{3.27}$$

Again, the right hand side is bounded when $a = \epsilon$. We now apply Theorem A.7 to find a bound for the isozenithal vector field $h = -g'^{-1}g$

$$\begin{aligned} \|h \circ \varphi\| &= \|(g'^{-1} \circ \varphi)(g \circ \varphi)\|_a \\ &\leq C(\|g'^{-1} \circ \varphi\|_a \underbrace{\|g \circ \varphi\|_0}_{\leq C} + \underbrace{\|g'^{-1} \circ \varphi\|_0}_{\leq C} \|g \circ \varphi\|_a) \\ &\leq C(\|g'^{-1} \circ \varphi\|_a + \|g \circ \varphi\|_a) \\ &\leq C(\|W\|_{2+a} + \|\varphi\|_{2+a}). \end{aligned} \tag{3.28}$$

By Theorems A.7 and A.8 the same estimate is valid for the transform $(\tilde{\varphi}')^{-1}(h \circ \varphi)$ of h as a vector field. To complete the proof of Theorem 3.1 Hörmander applies the following lemma, which estimates the harmonic function outside $\varphi(\mathbb{S}^2)$ which satisfies (3.13) and (3.15), where we write the right hand side as $F = \dot{W} + \langle \dot{G}, h \circ \varphi \rangle$.

Lemma 3.1 (Lemma 3.2.1 [19]). *If φ is sufficiently close to φ_0 in $\mathscr{H}^{2+\epsilon}$, and $\dot{v}$ is a harmonic function in $\mathscr{H}^{1+\epsilon}$ outside $\varphi(\mathbb{S}^2)$ which satisfies (3.13) and*

$$(\dot{v} + \langle grad\, \dot{v}, h \rangle) \circ \varphi = F + \sum_{j=1}^{3} \alpha_j A_j \tag{3.29}$$

then

$$\|\dot{v} \circ \varphi\|_{1+\epsilon} + \sum_{j=1}^{3} |\alpha_j| \leq C\|F\|_\epsilon. \tag{3.30}$$

Proof. Proof by contradiction, see [19, page 33]. □

Setting $B\dot{v} := (\dot{v} + \langle \mathrm{grad}\, \dot{v}, h \rangle) \circ \varphi$, Hörmander [18, p. 265] says that $LHS := dim\{\dot{v} : \Delta\dot{v} = 0, B\dot{v} = 0\} = codim\{(\widetilde{F}, F) \in C^\infty(\mathbb{R}^3 \setminus \overline{\Omega}) \times C^\infty(\mathbb{S}^2) : \Delta\dot{v} = \widetilde{F}, B\dot{v} = F \quad \text{has a solution}\} =: RHS$. By (3.13) the range of B has codimension 3, or $RHS \geq 3$, so also $LHS \geq 3$. On the other hand, (3.30) with $F = 0$ says that any solution to $\Delta u = 0, Bu = 0$, which satisfies (3.13), is 0. Therefore, $LHS \leq 3$, hence $LHS = RHS = 3$. Furthermore, (3.30) also says that A_1, A_2, A_3 are 3 linearly independent functions complementing the range of the boundary condition B. Therefore, for every $F \in C^\infty$ there exist solutions $\dot{v}, \alpha_j$ as postulated in Lemma 3.1. The argument for $F \in \mathscr{H}^\epsilon$ is identical.
Returning now to (3.15), we have found that there is a unique solution $\dot{v}$ and that

$$\|\dot{v} \circ \varphi\|_{1+\epsilon} + \sum_{j=1}^{3} |\dot{a}_j| \leq C\|\dot{W} + \langle \dot{G}, h \circ \varphi \rangle\|_\epsilon. \tag{3.31}$$

In the following, we again work out in detail the sketchy arguments in Hörmanders proof. In order to apply Theorem A.14 we identify

$$\dot{v}\circ\varphi = u = g_0 \quad \text{on} \quad \mathbb{S}^2 := \Sigma_1 \quad \text{and}$$

$$Bu = \sum_1^n B_j \frac{\partial u}{\partial x_j} + B_0 u = g_1 = \dot{W} + \langle \dot{G}, h\circ\varphi\rangle - \sum_{i=1}^3 \dot{a}_j A_j \quad \text{on} \quad \mathbb{S}^2 := \Sigma_1$$

and obtain

$$\begin{aligned}\|\dot{v}\circ\varphi\|_{1+a} \leq C\{&\|\dot{W} + \langle \dot{G}, h\circ\varphi\rangle - \sum_{i=1}^3 \dot{a}_j A_j\|_a + \|\dot{v}\circ\varphi\|_0 \\ &+ (\|\dot{W} + \langle \dot{G}, h\circ\varphi\rangle - \sum_{i=1}^3 \dot{a}_j A_j\|_\epsilon + \|\dot{v}\circ\varphi\|_0(\|h\circ\varphi\|_a + \|A\|_a)\}.\end{aligned}$$

Using the estimates for $\|h\circ\varphi\|_a$ and $\|A\|_a$ and estimating $\|\dot{v}\circ\varphi\|_0$ by $\|\dot{v}\circ\varphi\|_{1+\epsilon}$, we obtain applying the triangle inequality

$$\begin{aligned}\|\dot{v}\circ\varphi\|_{1+a} \leq & C\{\|\dot{W}\|_a + \|\langle \dot{G}, h\circ\varphi\rangle\|_a + \|\sum_{j=1}^3 \dot{a}_j A_j\|_a + \|\dot{v}\circ\varphi\|_{1+\epsilon} \\ &+(\|\dot{W}\|_\epsilon + \|\langle \dot{G}, h\circ\varphi\rangle\|_\epsilon + \|\sum_{j=1}^3 \dot{a}_j A_j\|_\epsilon + \|\dot{v}\circ\varphi\|_{1+\epsilon})(\|W\|_{2+a} + \|\varphi\|\|_{2+a})\}.\end{aligned}$$

Now, by using Theorem A.7 and for the terms involving h (3.28) we have

$$\begin{aligned}\|\langle \dot{G}, h\circ\varphi\rangle\|_a &\leq C\{\|\dot{G}\|_a \|h\circ\varphi\|_0 + \|\dot{G}\|_0 \|h\circ\varphi\|_a\} \\ &\leq C\{\|\dot{G}\|_a + \|\dot{G}\|_\epsilon(\|W\|_{2+a} + \|\varphi\|_{2+a})\}\end{aligned}$$

and

$$\|\langle \dot{G}, h\circ\varphi\rangle\|_\epsilon \leq C\|\dot{G}\|_\epsilon.$$

We finally obtain with (3.31)

$$\|\dot{v}\circ\varphi\|_{1+a} \leq C\{\|\dot{W}\|_a + \|\dot{G}\|_a + (\|\dot{W}\|_\epsilon + \|\dot{G}\|_\epsilon)(\|W\|_{2+a} + \|\varphi\|_{2+a}).$$

By (3.22), the same estimate is valid for $\|\mathrm{grad}\,\dot{v}\circ\varphi\|_a$.
We now estimate the corresponding perturbation $\dot{\varphi}$ given by

$$\dot{\varphi} = (g'\circ\varphi)^{-1}(\dot{G} - \mathrm{grad}\,\dot{v}\circ\varphi).$$

We already observed in the proof of (3.28) that

$$\|(g'\circ\varphi)^{-1}\|_a \leq C(\|W\|_{2+a} + \|\varphi\|_{2+a}). \tag{3.32}$$

Hence, Theorem A.7 and the triangle inequality give

$$\begin{aligned}\|\dot{\varphi}\|_a &\leq \|(g'\circ\varphi)^{-1}\dot{G}\|_a + \|(g'\circ\varphi)^{-1}\mathrm{grad}\ \dot{v}\circ\varphi\|_a \\ &\leq C\{\|(g'\circ\varphi)^{-1}\|_a\|\dot{G}\|_0 + \|(g'\circ\varphi)^{-1}\|_0\|\dot{G}\|_a \\ &\qquad + \|(g'\circ\varphi)^{-1}\|_a\|\mathrm{grad}\ \dot{v}\circ\varphi\|_0 + \|(g'\circ\varphi)^{-1}\|_0\|\mathrm{grad}\ \dot{v}\circ\varphi\|_a\} \\ &\leq C\{\|(g'\circ\varphi)^{-1}\|_a\|\dot{G}\|_0 + \underbrace{\|(g'\circ\varphi)^{-1}\|_0}_{\leq C}\|\dot{G}\|_a\ \}.\end{aligned}$$

Now for $\|\dot{G}\|_0$ and $\|\dot{G}\|_1$ we have the following estimates

$$\|\dot{G}\|_0 \leq \|\dot{G}\|_{1+\epsilon} = \|\dot{v} \circ \varphi\|_{1+\epsilon} \leq C\{\|\dot{W}\|_\epsilon + \|\dot{G}\|_\epsilon\}$$
$$\|\dot{G}\|_a = \|\dot{v} \circ \varphi\|_{1+a} \leq C\{\|\dot{W}\|_a + \|\dot{G}\|_a + (\|\dot{W}\|_\epsilon + \|\dot{G}\|_\epsilon)(\|W\|_{2+a} + \|\varphi\|_{2+a})\}.$$

Combing these estimates with (3.32), we finally obtain (3.16).□

3.2. The Non-Linear Molodensky Problem

In this subsection we give estimates for the second differential of the map Γ namely $\Gamma''_{W,\varphi}, \Gamma''_{\varphi,\varphi}$. Because $\Gamma(W,\varphi)$ is affinely linear in W, we have $\Gamma''_{WW} = 0$ and we can restrict ourselves to the study of the second differential of Γ with respect to φ and the mixed second differential, which due to the affine linearity is essentially the same as the first differential with respect to φ.
Throughout this section, following [19], we denote by φ a C^∞ map $\mathbb{S}^2 \to \mathbb{R}^3$, which for $\epsilon > 0$, is in a small $\mathscr{H}^{2+\epsilon}$ neighborhood of φ_0, defined as in Section 3.1.
In the following assume that φ and W are smooth and that φ vary smoothly with a parameter θ. Then $G = \Gamma(\varphi, W)$ varies smoothly with θ. For the derivative $\dot{G}$ with respect to θ we then have

$$\dot{G} = \dot{v}' \circ \varphi + (g' \circ \varphi)\dot{\varphi} \tag{3.33}$$

with $\dot{v}$ the harmonic function outside $\varphi(\mathbb{S}^2)$ which satisfies the radiation condition (3.13) and

$$0 = \dot{v} \circ \varphi + \langle G, \dot{\varphi} \rangle + \sum_1^3 \dot{a}_j A_j. \tag{3.34}$$

Hörmander claims that if we subtract the corresponding equations with $W = 0$, then the mixed second differential with respect to φ and W can be interpreted as the bilinear map $(\dot{\varphi}, W) \mapsto \dot{G}$.
In order to show this we define

$$F(W) := \dot{G} = \Gamma_\varphi(W, \varphi) \tag{3.35}$$

where the lower index φ denotes differentiation with respect to φ. Using the fact that $\Gamma(W,\varphi)$ is linear in W, the derivative of $F(W)$ with respect to W in direction z is given by

$$F'(W)z = F(z) - F(0) = \frac{d}{d\varphi}(\Gamma(z,\varphi) - \Gamma(0,\varphi)).$$

We first analyse $\Gamma(z,\varphi) - \Gamma(0,\varphi)$ which is the derivative of Γ with respect to W.
Choosing accordingly to (3.11) - (3.13)

$$z := \left(\frac{\omega^2}{2}(x_1^2 + x_2^2) + v\right) \circ \varphi + \sum_{j=1}^3 a_j A_j$$
$$0 = \left(\frac{\omega^2}{2}(x_1^2 + x_2^2) + v_0\right) \circ \varphi + \sum_{j=1}^3 a_j A_j$$

we deduce

$$\begin{aligned}\Gamma(z,\varphi)-\Gamma(0,\varphi) &= G(z,\varphi)-G(0,\varphi)\\ &= \left(\frac{\omega^2}{2}(x_1^2+x_2^2)+v-\frac{\omega^2}{2}(x_1^2+x_2^2)-v_0\right)'\circ\varphi\\ &= (v-v_0)'\circ\varphi.\end{aligned}$$

Now, by using $W=0$ and the fact that w and $\sum_{j=1}^{3} a_j A_j$ are linear independent we have $v_0=0$ and conclude for $\omega=0$

$$\Gamma_W\,(W,\varphi)=\Gamma(z,\varphi)-\Gamma(0,\varphi)=v'\circ\varphi=G.$$

Finally, by taking the derivative with respect to φ and recalling (3.35), we conclude

$$\Gamma_{W\varphi}(W,\varphi)=\dot{G}=\Gamma_\varphi(W,\varphi). \tag{3.36}$$

In the following we assume no a priori bound for W.
Recalling (3.21)

$$\|(\partial^\alpha u)\circ\varphi\|_{1+a-|\alpha|}\le C_a(\|U_0\|_{1+a}+\|U_0\|_{1+\epsilon}\|\varphi\|_{1+a})$$

we have for the solution u of the Dirichlet problem in the exterior of $\varphi(\mathbb{S}^2)$ with boundary data $-\langle G,\dot\varphi\rangle := U_0$ when a is positive but not an integer, by using Theorem A.7

$$\begin{aligned}\|u\circ\varphi\|_{1+a}+\|u'\circ\varphi\|_a &\le C_a(\|\langle G,\dot\varphi\rangle\|_{1+a}+\|\langle G,\dot\varphi\rangle\|_{1+\epsilon}\|\varphi\|_{1+a})\\ &\le C_a\{\|G\|_{1+a}\|\dot\varphi\|_0+\|G\|_0\|\dot\varphi\|_{1+a}\\ &\qquad+(\|G\|_{1+\epsilon}\|\dot\varphi\|_0+\|G\|_0\|\dot\varphi\|_{1+\epsilon})\|\varphi\|_{1+a}\}.\end{aligned}$$

Because the numbers $\dot a_j$ in (3.34) can be estimated by $\|\langle G,\dot\varphi\rangle\|_0$, this estimate is also valid if we replace u by $\dot v$. With $\omega=0$ we have from (3.25) the following bound for G

$$\|G\|_a\le C(\|W\|_{1+a}+\|W\|_{1+\epsilon}\|\varphi\|_{1+a})$$

and we deduce

$$\begin{aligned}\|G\|_{1+a}\|\dot\varphi\|_0 &\le C(\|W\|_{2+a}+\|W\|_{1+\epsilon}\|\varphi\|_{2+a})\|\dot\varphi\|_0\\ \|G\|_0\|\dot\varphi\|_{1+a}\le\|G\|_\epsilon\|\dot\varphi\|_{1+a} &\le C\|W\|_{1+\epsilon}\|\dot\varphi\|_{1+a}\\ \|G\|_0\|\dot\varphi\|_{1+\epsilon} &\le C\|W\|_{1+\epsilon}\|\dot\varphi\|_{1+\epsilon}\\ \|G\|_{1+\epsilon}\|\dot\varphi\|_0 &\le C(\|W\|_{2+\epsilon}+\|W\|_{1+\epsilon}\|\varphi_{2+a}\|)\|\dot\varphi\|_0.\end{aligned}$$

Combining all these estimates we obtain

$$\begin{aligned}\|\mathrm{grad}\,\dot v\circ\varphi\|_a\le C_a\{&(\|W\|_{2+a}+\|W\|_{1+\epsilon}\|\varphi\|_{2+a})\|\dot\varphi\|_0+\|W\|_{1+\epsilon}\|\dot\varphi\|_{1+a}\\ &+(\|W\|_{2+\epsilon}\|\dot\varphi\|_0+\|W\|_{1+\epsilon}\|\dot\varphi\|_{1+\epsilon})\|\varphi\|_{1+a}\}.\end{aligned}$$

Now we want to find an estimate for $\|(g'\circ\varphi)\dot\varphi\|$. Theorem A.7 gives

$$\|(g'\circ\varphi)\dot\varphi\|_a\le C(\|g'\circ\varphi\|_a\|\dot\varphi\|_0+\|g'\circ\varphi\|_0\|\dot\varphi\|_a). \tag{3.37}$$

Using the estimate (3.25) with $\omega = 0$ we have

$$\begin{aligned} \|g' \circ \varphi\|_a &\le C(\|W\|_{2+a} + \|W\|_{1+\epsilon}\|\varphi\|_{2+a}) \\ \|g' \circ \varphi\|_0 &\le \|g' \circ \varphi\|_\epsilon \le C\|W\|_{2+\epsilon}, \end{aligned}$$

and we obtain

$$\|(g' \circ \varphi)\dot{\varphi}\|_a \le C\{(\|W\|_{2+a} + \|W\|_{1+\epsilon}\|\varphi\|_{2+a})\|\dot{\varphi}\|_0) + \|W\|_{2+\epsilon}\|\dot{\varphi}\|_a\}. \tag{3.38}$$

Now, with these estimates, recalling (3.34) and using Corollary A.6, Hörmander proves, when $a \ge \epsilon$ is not an integer, the following estimate for the mixed second differential

$$\begin{aligned} \|\Gamma''_{W\varphi}(\varphi; W, \dot{\varphi})\|_a = \|\dot{G}\|_a &\le \|v' \circ \varphi\|_a + \|(g' \circ \varphi)\dot{\varphi}\|_a \\ &\le C_a\{(\|W\|_{2+a}\|\dot{\varphi}\|_\epsilon + \|W\|_{1+\epsilon}\|\dot{\varphi}\|_{1+a}) \\ &\quad + \|\varphi\|_{2+a}\|W\|_{1+\epsilon}\|\dot{\varphi}\|_0 \\ &\quad + \|\varphi\|_{1+a}(\|W\|_{2+\epsilon}\|\dot{\varphi}\|_0 + \|W\|_{1+\epsilon}\|\dot{\varphi}\|_{1+\epsilon})\}. \end{aligned} \tag{3.39}$$

We have to estimate now the second differential of $\Gamma(W, \varphi)$ with respect to φ. We have again $\omega \ne 0$, while W is now close to W_0 in $\mathscr{H}^{2+\epsilon}$. Let $X, Y : \mathbb{S}^2 \to \mathbb{R}^3$ be two smooth maps. We differentiate $G = \Gamma(W, \varphi + sX + tY)$ with respect to s and t, putting $s = t = 0$ afterwards.
We denote by ${}^{X}G$ the derivative of G with respect to s and rewrite (3.33) and (3.34) for the first derivatives as follows

$${}^{X}G = {}^{X}v' \circ\varphi + (g' \circ \varphi)X \tag{3.40}$$

$$0 = {}^{X}v + \langle G, X\rangle + \sum_{j=1}^{3} {}^{X}a_j\, A_j \tag{3.41}$$

where ${}^{X}v$ is harmonic outside $(\varphi + tY)(\mathbb{S}^2)$ and satisfies (3.13).
Differentiation with respect to t gives, with $s = t = 0$,

$$\Gamma''_{\varphi\varphi}(W, \varphi; X, Y) = {}^{XY}G = {}^{XY}v' \circ\varphi + ({}^{X}v'' \circ\varphi)Y + ({}^{Y}v'' \circ\varphi)X + (v''' \circ \varphi)(X, Y) \tag{3.42}$$

where ${}^{XY}v$ is harmonic outside $\varphi(\mathbb{S}^2)$ and satisfies (3.13). The Dirichlet data are given by

$$0 = {}^{XY}v \circ\varphi + \langle({}^{X}v' \circ\varphi), Y\rangle + \langle({}^{Y}v' \circ\varphi), X\rangle + (g' \circ \varphi)(X, Y) + \sum_{1}^{3} {}^{XY}a_j\, A_j \tag{3.43}$$

We obtain this equation by differentiating (3.41) and using (3.40). From now on, we take $s = t = 0$ in (3.40) and (3.41).
In order to estimate $\Gamma''_{\varphi\varphi}$ we have to use the estimates that we stated above and take φ and W in a small $\mathscr{H}^{2+\epsilon}$ neighborhood of φ_0 and W_0.
If we replace ω^2 and $\|W\|_{1+\epsilon}$ by a constant, (3.25) gives an estimate for G

$$\|G\|_a \le C_a(\|W\|_{1+a} + \|\varphi\|_{1+a}).$$

Using Theorem A.7 we have the following estimate for $\|\langle G, X\rangle\|_a$

$$
\begin{aligned}
\|\langle G, X\rangle\|_a &\leq C_a\{(\|G\|_a\|X\|_0 + \|G\|_0\|X\|_a\} \\
&\leq C_a\{(\|W\|_{1+a} + \|\varphi\|_{1+a})\|X\|_0 + \|X\|_a\}
\end{aligned}
$$

when $a > 0$ is not an integer. We can estimate the constants ${}^{X}a_j$ in (3.41) by $\|\langle G, X\rangle\|_0$, hence by $\|X\|_0$ and this implies

$$
\begin{aligned}
\| {}^{X}v \circ\varphi\|_a &\leq \|\langle G, X\rangle\|_a + \|\sum_{j=1}^{3} {}^{X}a_j\, A_j\|_a \\
&\leq C_a\{(\|W\|_{1+a} + \|\varphi\|_{1+a})\|X\|_0 + \|X\|_a\} + \sum_{j=1}^{3} \underbrace{\|A_j\|_a}_{\leq C} \underbrace{|\,{}^{X}a_j\,|}_{\leq\|X\|_0} \\
&\leq C_a\{(\|W\|_{1+a} + \|\varphi\|_{1+a})\|X\|_0 + \|X\|_a\}.
\end{aligned}
$$

Note hat the right hand side is bounded by $C\|X\|_{1+\epsilon}$, when $a = 1 + \epsilon$ and we deduce from (3.21)

$$
\| {}^{X}v' \circ\varphi\|_a \leq C_a\{(\|W\|_{2+a} + \|\varphi\|_{2+a})\|X\|_0 + \|X\|_{1+a} + \|X\|_{1+\epsilon}\|\varphi\|_{1+a}\}.
$$

If $a = \epsilon$, then the right hand side in the estimate above is bounded by $C\|X\|_{1+\epsilon}$ and we have by using Theorem A.7

$$
\begin{aligned}
\|\langle({}^{X}v' \circ \varphi), Y\rangle\|_a &\leq C_a\{[(\|W\|_{2+a} + \|\varphi\|_{2+a})\|X\|_0 + \|X\|_{1+a} \\
&\quad + \|X\|_{1+\epsilon}\|\varphi\|_{1+a}]\|Y\|_0 + \underbrace{\| {}^{X}v' \circ \varphi\|_\epsilon}_{\leq C\|X\|_{1+\epsilon}} \|Y\|_a\} \\
&\leq C_a\{[(\|W\|_{2+a} + \|\varphi\|_{2+a})\|X\|_0 + \|X\|_{1+a} \\
&\quad + \|X\|_{1+\epsilon}\|\varphi\|_{1+a}]\|Y\|_0 + \|X\|_{1+\epsilon}\|Y\|_a\}.
\end{aligned}
\tag{3.44}
$$

Using the same proof as for the estimate above we deduce

$$
\begin{aligned}
\|({}^{X}v'' \circ\varphi)Y\|_a \leq C_a\{&[(\|W\|_{3+a} + \|\varphi\|_{3+a})\|X\|_0 + \|X\|_{2+a} \\
&+ \|X\|_{1+\epsilon}\|\varphi\|_{2+a}]\|Y\|_0 \\
&+ [(\|W\|_{3+\epsilon} + \|\varphi\|_{3+\epsilon})\|X\|_0 + \|X\|_{2+\epsilon}]\|Y\|_a\}.
\end{aligned}
\tag{3.45}
$$

By interchanging $X$and Y we also have

$$
\begin{aligned}
\|({}^{Y}v'' \circ\varphi)X\|_a \leq C_a\{&[(\|W\|_{3+a} + \|\varphi\|_{3+a})\|Y\|_0 + \|Y\|_{2+a} \\
&+ \|Y\|_{1+\epsilon}\|\varphi\|_{2+a}]\|X\|_0 \\
&+ [(\|W\|_{3+\epsilon} + \|\varphi\|_{3+\epsilon})\|Y\|_0 + \|Y\|_{2+\epsilon}]\|X\|_a\}.
\end{aligned}
\tag{3.46}
$$

Now we know by (3.26) that

$$
\|(g' \circ \varphi)\|_a \leq C_a(\|W\|_{2+a} + \|\varphi\|_{2+a}).
$$

When $a = \epsilon$, the right hand side is bounded and by applying twice Theorem A.7 we obtain

$$\begin{aligned}\|(g' \circ \varphi)(X,Y)\|_a &\le C(\|g' \circ \varphi\|_a \|(X,Y)\|_0 + \|g' \circ \varphi\|_0)\|(X,Y)\|_a) \\ &\le C(\|g' \circ \varphi\|_a \|X\|_0 \|Y\|_0 \\ &\quad + \|g' \circ \varphi\|_0(\|X\|_a\|Y\|_0 + \|X\|_0\|Y\|_a)) \\ &\le C\{(\|W\|_{2+a} + \|\varphi\|_{2+a})\|X\|_0\|Y\|_0 + \|X\|_a\|Y\|_0 + \|X\|_0\|Y\|_a\}.\end{aligned} \tag{3.47}$$

The coefficients ${}^{XY}a_j$ in the last term in (3.43) can be estimated for example by the maximum norm of the preceding three terms. By combining the estimates (3.44) and (3.47) we conclude

$$\begin{aligned}\| {}^{XY}v \circ \varphi\|_a \le C_a\{&(\|W\|_{2+a} + \|\varphi\|_{2+a})\|X\|_0\|Y\|_0 \\ &+ \|\varphi\|_{1+a}(\|X\|_{1+\epsilon}\|Y\|_0 + \|X\|_0\|Y\|_{1+\epsilon}) \\ &+ \|X\|_{1+a}\|Y\|_0 + \|X\|_{1+\epsilon}\|Y\|_a + \|Y\|_{1+a}\|X\|_0 \\ &+ \|Y\|_{1+\epsilon}\|X\|_a + \|X\|_a\|Y\|_0 + \|X\|_0\|Y\|_a\} \\ \le C_a\{&(\|W\|_{2+a} + \|\varphi\|_{2+a})\|X\|_0\|Y\|_0 \\ &+ \|\varphi\|_{1+a}(\|X\|_{1+\epsilon}\|Y\|_0 + \|X\|_0\|Y\|_{1+\epsilon}) \\ &+ \|X\|_{1+a+\epsilon}\|Y\|_0 + \|X\|_0\|Y\|_{1+a+\epsilon}\}.\end{aligned} \tag{3.48}$$

To obtain the last estimate we use the fact that

$$\begin{aligned}&\|X\|_{a+1}\|Y\|_0 + \|X\|_a\|Y\|_0 \le C\|X\|_{a+1}\|Y\|_0 \le C\|X\|_{1+a+\epsilon}\|Y\|_0 \\ &\|Y\|_{a+1}\|X\|_0 + \|X\|_0\|Y\|_a \le C\|Y\|_{1+a+\epsilon}\|X\|_0\end{aligned}$$

and that by Corollary A.6 the following estimates hold

$$\begin{aligned}\|X\|_a\|Y\|_{1+\epsilon} &\le C(\|X\|_{1+a+\epsilon}\|Y\|_0 + \|X\|_0\|Y\|_{1+a+\epsilon}) \\ \|Y\|_a\|X\|_{1+\epsilon} &\le C(\|Y\|_{1+a+\epsilon}\|X\|_0 + \|Y\|_0\|X\|_{1+a+\epsilon}).\end{aligned}$$

Using the assumption that φ and W are in a small $\mathscr{H}^{2+\epsilon}$ neighborhood of φ_0 and W_0, we have in particular

$$\begin{aligned}\| {}^{XY}v \circ \varphi\|_{1+\epsilon} \le C\{&(\|W\|_{3+\epsilon} + \|\varphi\|_{3+\epsilon})\|X\|_0\|Y\|_0 \\ &+ \underbrace{\|\varphi\|_{2+\epsilon}}_{\le C}(\|X\|_{2+2\epsilon}\|Y\|_0 + \|X\|_0\|Y\|_{2+2\epsilon}) \\ &+ \|X\|_{2+2\epsilon}\|Y\|_0 + \|X\|_0\|Y\|_{2+2\epsilon}\} \\ \le C\{&(\|W\|_{3+\epsilon} + \|\varphi\|_{3+\epsilon})\|X\|_0\|Y\|_0 \\ &+ \|X\|_{2+2\epsilon}\|Y\|_0 + \|X\|_0\|Y\|_{2+2\epsilon}\}.\end{aligned}$$

In order to give an estimate for $\| {}^{XY}v' \circ \varphi\|_a$ we have to apply (3.21). For this we need the following estimate given by using Corollary A.6

$$\|\varphi\|_{1+a}(\|\varphi\|_{3+\epsilon} + \|W\|_{3+\epsilon}) \le C(\|\varphi\|_{3+a} + \|W\|_{3+a}) \tag{3.49}$$

because there is a bound for $\|\varphi\|_{1+\epsilon}$ and $\|W\|_{1+\epsilon}$. Now recalling (3.21) by setting $\alpha = 1$ we have

$$\|\partial u \circ \varphi\|_a \leq C_a(\|U_0\|_{1+a} + \|U_0\|_{1+\epsilon}\|\varphi\|_{1+a}).$$

Setting $U_0 = {}^{XY}v \circ\varphi$ we deduce

$$\begin{aligned}\| {}^{XY}v' \circ\varphi\|_a \leq C_a\{&(\|W\|_{3+a} + \|\varphi\|_{3+a})\|X\|_0\|Y\|_0 \\ &+ \|\varphi\|_{2+a}(\|X\|_{1+\epsilon}\|Y\|_0 + \|X\|_0\ |Y\|_{1+\epsilon}) \\ &+ \|X\|_{2+a+\epsilon}\|Y\|_0 + \|X\|_0\|Y\|_{2+a+\epsilon} \\ &+ \|\varphi\|_{1+a}((\|W\|_{3+\epsilon} + \|\varphi\|_{3+\epsilon})\|X\|_0\|Y\|_0 \\ &+ \|X\|_{2+2\epsilon}\|Y\|_0 + \|X\|_0\|Y\|_{2+2\epsilon})\}.\end{aligned}$$

By using (3.49), we finally obtain the following estimate as given by Hörmander

$$\begin{aligned}\| {}^{XY}v' \circ\varphi\|_a \leq C_a\{&(\|W\|_{3+a} + \|\varphi\|_{3+a})\|X\|_0\|Y\|_0 \\ &+ \|\varphi\|_{1+a}(\|X\|_{2+2\epsilon}\|Y\|_0 + \|X\|_0\|Y\|_{2+2\epsilon}) \\ &+ \|\varphi\|_{2+a}(\|X\|_{1+\epsilon}\|Y\|_0 + \|X\|_0\ |Y\|_{1+\epsilon}) \\ &+ \|X\|_{2+a+\epsilon}\|Y\|_0 + \|X\|_0\|Y\|_{2+a+\epsilon}\}.\end{aligned}$$

By the same argument that we have used to get (3.28) we deduce

$$\|(v''' \circ \varphi)\|_a \leq C(\|W\|_{3+a} + \|\varphi\|_{3+a}).$$

Now we are ready to estimate the last term in (3.42). Using twice Theorem A.7 and noting that $\|(v''' \circ \varphi)\|_0 \leq \|(v''' \circ \varphi)\|_\epsilon$

$$\begin{aligned}\|(v''' \circ \varphi)(X, Y)\|_a &\leq C(\|(v''' \circ \varphi)\|_a(\|X\|_0\|Y\|_0 + \|X\|_0\|Y\|_0) \\ &\quad + \|(v''' \circ \varphi)\|_0(\|X\|_a\|Y\|_0 + \|X\|_0\|Y\|_a)) \\ &\leq C_a\{(\|W\|_{3+a} + \|\varphi\|_{3+a})\|X\|_0\|Y\|_0 \\ &\quad + \|(v''' \circ \varphi)\|_\epsilon(\|X\|_a\|Y\|_0 + \|X\|_0\|Y\|_a)\} \\ &\leq C_a\{|W\|_{3+a} + \|\varphi\|_{3+a})\|X\|_0\|Y\|_0 \\ &\quad + (\|W\|_{3+\epsilon} + \|\varphi\|_{3+\epsilon})(\|X\|_a\|Y\|_0 + \|X\|_0\|Y\|_a)\}.\end{aligned} \tag{3.50}$$

Having all these estimates we are ready to estimate the second differential with respect to φ given by (3.42). We obtain, when $a > 0$ is not an integer,

$$\begin{aligned}\|\Gamma''_{\varphi\varphi}(W, \varphi; X, Y)\|_a \leq C_a\{&(\|W\|_{3+a} + \|\varphi\|_{3+a})\|X\|_0\|Y\|_0 \\ &+ \|\varphi\|_{2+a}(\|X\|_{1+\epsilon}\|Y\|_0 + \|X\|_0\ |Y\|_{1+\epsilon}) \\ &+ \|\varphi\|_{1+a}(\|X\|_{2+2\epsilon}\|Y\|_0 + \|X\|_0\|Y\|_{2+2\epsilon}) \\ &+ (\|W\|_{3+\epsilon} + \|\varphi\|_{3+\epsilon})(\|X\|_a\|Y\|_0 + \|X\|_0\|Y\|_a) \\ &+ \|X\|_{2+a+\epsilon}\|Y\|_0 + \|X\|_0\|Y\|_{2+a+\epsilon} \\ &+ \|X\|_{2+a}\|Y\|_0 + \|X\|_{2+\epsilon}\|Y\|_a \\ &+ \|Y\|_{2+a}\|X\|_0 + \|Y\|_{2+\epsilon}\|X\|_a\}.\end{aligned} \tag{3.51}$$

In order to simplify the bound and obtain the same estimate as stated by Hörmander, we first note that

$$\begin{aligned}\|X\|_{2+a}\|Y\|_0 &\leq \|X\|_{2+a+\epsilon}\|Y\|_0\\ \|Y\|_{2+a}\|X\|_0 &\leq \|Y\|_{2+a+\epsilon}\|X\|_0.\end{aligned}$$

Now we use Corollary A.6 to find a bound for $\|X\|_{2+\epsilon}\|Y\|_a$. We claim

$$\|Y\|_a\|X\|_{2+\epsilon} \leq C\{\|Y\|_{2+a+\epsilon}\|X\|_0 + \|Y\|_0\|X\|_{2+a+\epsilon}\}. \tag{3.52}$$

By Corollary A.6 we have

$$\|u\|_\alpha\|u\|_\beta \leq C\sum_j \|u\|_{\alpha_j}\|u\|_{\beta_j}$$

if $(\alpha,\beta) \in \text{conv}\ \{(\alpha_j,\beta_j) = \sum_{j=1}^2 \lambda_j(\alpha_j,\beta_j) \quad \text{with} \quad \sum_{j=1}^2 \lambda_j = 1, \lambda_j \geq 1\}$.
In (3.52), we set $\alpha = a, \beta = 2+\epsilon$, $\alpha_1 = \beta_2 = 2+a+\epsilon$ and $\alpha_2 = \beta_1 = 0$. Now using $(\alpha,\beta) = \lambda(\alpha_1,\beta_1) + (1-\lambda)(\alpha_2,\beta_2)$ we have the following system of equations:

$$\begin{pmatrix} a \\ 2+\epsilon \end{pmatrix} = \lambda \begin{pmatrix} 2+a+\epsilon \\ 0 \end{pmatrix} + (1-\lambda)\begin{pmatrix} 0 \\ 2+a+\epsilon \end{pmatrix}$$

which implies

$$\lambda = \frac{a}{2+a+\epsilon}, \qquad 1-\lambda = \frac{2+\epsilon}{2+a+\epsilon}$$

which means that we have found a λ satisfying both equations. Furthermore, with this λ we can write α and β as a convex combination of (α_j,β_j) and by Corollary A.6 (3.52) holds.
By the same proof we obtain:

$$\|Y\|_{2+\epsilon}\|X\|_a \leq C\{\|X\|_{2+a+\epsilon}\|Y\|_0 + \|X\|_0\|Y\|_{2+a+\epsilon}\}.$$

Using now (3.51) we finally obtain when $a > 0$ is not an integer,

$$\begin{aligned}\|\Gamma''_{\varphi\varphi}(W,\varphi;X,Y)\|_a \leq C_a\{&(\|W\|_{3+a} + \|\varphi\|_{3+a})\|X\|_0\|Y\|_0\\ &+ \|\varphi\|_{2+a}(\|X\|_{1+\epsilon}\|Y\|_0 + \|X\|_0\ |Y\|_{1+\epsilon})\\ &+ \|\varphi\|_{1+a}(\|X\|_{2+2\epsilon}\|Y\|_0 + \|X\|_0\|Y\|_{2+2\epsilon})\\ &+ (\|W\|_{3+\epsilon} + \|\varphi\|_{3+\epsilon})(\|X\|_a\|Y\|_0 + \|X\|_0\|Y\|_a)\\ &+ (\|X\|_{2+a+\epsilon}\|Y\|_0 + \|X\|_0\|Y\|_{2+a+\epsilon})\}.\end{aligned} \tag{3.53}$$

We want to further simplify this bound by means of Corollary A.6. We may imagine in the last term the bounded factor $\|W\|_{2+\epsilon} + \|\varphi\|_{2+\epsilon}$ present. We also notice that in the first three terms a drop of differentiation on φ with one unit is accompanied by a rise of differentiation of X or Y with $1+\epsilon$ units.
Now let us take a look at $\|W\|_{3+\epsilon}\|Y\|_a$. We claim that

$$\|W\|_{3+\epsilon}\|Y\|_a \leq C\{\|Y\|_{2+a+\epsilon}\|W\|_{2+\epsilon} + \|W\|_{3+a}\|Y\|_0\}. \tag{3.54}$$

To prove this estimate we use again Corollary A.6. In (3.54) we set $\alpha = 3+\epsilon, \beta = a$, $\alpha_1 = 2+\epsilon, \alpha_2 = 3+a, \beta_1 = 2+a+\epsilon, \beta_2 = 0$. Using again $(\alpha,\beta) = \lambda(\alpha_1,\beta_1)+(1-\lambda)(\alpha_2,\beta_2)$ we have

$$\begin{aligned}(3+\epsilon) &\leq \lambda(2+\epsilon)+(1-\lambda)(3+a)\\ a &= \lambda(2+a+\epsilon)\end{aligned}$$

which implies

$$\lambda = \frac{a}{a+2+\epsilon}, \quad 2\epsilon+\epsilon^2 \leq a+\epsilon a$$

and we deduce that for $\epsilon > 0$ small enough

$$2\epsilon \leq a.$$

With this condition we have found a λ satisfying both equations and by Corollary A.6 (3.54) holds.
By the same proof we also have the following estimates

$$\begin{aligned}\|W\|_{3+\epsilon}\|X\|_a &\leq C\{\|X\|_{2+a+\epsilon}\|W\|_{2+\epsilon}+\|W\|_{3+a}\|Y\|_0\}\\ \|\varphi\|_{3+\epsilon}\|Y\|_a &\leq C\{\|Y\|_{2+a+\epsilon}\|\varphi\|_{2+\epsilon}+\|\varphi\|_{3+a}\|Y\|_0\}\\ \|\varphi\|_{3+\epsilon}\|X\|_a &\leq C\{\|X\|_{2+a+\epsilon}\|\varphi\|_{2+\epsilon}+\|\varphi\|_{3+a}\|X\|_0\}.\end{aligned}$$

With these estimates we can drop the fourth term in (3.53). If we want to drop the second and third terms in (3.53), we have to look at terms of the form $\|\varphi\|_{2+a}\|X\|_{1+\epsilon}$. We prove the estimate for one of these terms, while the other estimates can be proved in the same way. We claim that:

$$\|\varphi\|_{2+a}\|X\|_{1+\epsilon} \leq C\{\|\varphi\|_{3+a}\|X\|_0+\|X\|_{2+a+\epsilon}\|\varphi\|_{2+\epsilon}\}. \tag{3.55}$$

To prove this estimate we use again Corollary A.6. In (3.55) we set $\alpha = 2+a, \beta = 1+\epsilon$, $\alpha_1 = 3+a, \alpha_2 = 2+\epsilon, \beta_1 = 0, \beta_2 = 2+a+\epsilon$. With $(\alpha,\beta) = \lambda(\alpha_1,\beta_1)+(1-\lambda)(\alpha_2,\beta_2)$ we have

$$\begin{aligned}(2+a) &\leq \lambda(3+a)+(1-\lambda)(2+\epsilon)\\ (1+\epsilon) &= (1-\lambda)(2+a+\epsilon)\end{aligned}$$

which implies

$$\lambda = \frac{a+1}{2+a+\epsilon}, \quad \epsilon a \leq 1+\epsilon+\epsilon^2$$

and with the condition

$$a \leq (1+\epsilon+\epsilon^2)/\epsilon$$

we have found a λ satisfying both equations and by Corollary A.6 (3.55) holds.
In conclusion, we can drop the second, third and fourth terms, provided that

$$2\epsilon < a < (1+\epsilon+\epsilon^2)/\epsilon$$

for a in any finite interval if ϵ is small enough. Note that this is the same condition as given by Hörmander. We finally obtain under this hypothesis

$$\|\Gamma''_{\varphi\varphi}(W,\varphi;X,Y)\|_a \leq C_a\{(\|W\|_{3+a} + \|\varphi\|_{3+a})\|X\|_0\|Y\|_0 + \|X\|_{2+a+\epsilon}\|Y\|_0 + \|X\|_0\|Y\|_{2+a+\epsilon}\}. \tag{3.56}$$

Assume that $\varphi_0, W_0, G_0, A_1, A_2, A_3$ have the properties given in the introduction. We set for smooth φ and W that are close to φ_0 and W_0 in $\mathscr{H}^{2+\epsilon}$

$$\Gamma(W,\varphi) = G \tag{3.57}$$

with G defined by (3.11) - (3.13). We consider now the map

$$\Phi(W,\varphi) = (\Gamma(W,\varphi), W). \tag{3.58}$$

Summing up, we have shown estimates (3.39) and (3.56) for Γ' and Γ'', as well as the invertibility of $\Phi'(W,\varphi)$ and an estimate (3.16) for the φ and (trivially) W-component of its inverse. Therefore, all the assumptions in Theorem 2.1 and Theorem 2.3 are satisfied and Hörmander obtains the following existence and uniqueness theorem.

Theorem 3.2 (Theorem 3.4.1 [19])**.** *For all W, G in a $\mathscr{H}^{2+\epsilon}$ neighborhood of W_0, G_0,$\epsilon > 0$ arbitrary the modified Molodensky problem (3.11) - (3.13) has a solution φ close to φ_0 in $\mathscr{H}^{2+\epsilon}$ and (a_1, a_2, a_3) close to 0 in $\mathbb{R}^3$. If W, G are in $\mathscr{H}^a$ for some $a > 2+\epsilon$ which is not an integer, then $\varphi \in \mathscr{H}^a$. One can find a $\mathscr{H}^{3+\epsilon}$ neighborhood of φ_0 which cannot contain two solutions of the problem.*

Following now Moritz [31], let us explain the meaning of this theorem. The $\mathscr{H}^{2+\epsilon}$ neighborhood of W_0 contains all functions W with $\|W - W_0\|_{2+\epsilon} < \delta$ for δ sufficiently small. From the smallness of this norm we deduce that not only the maximum deviation of W from W_0 i.e max $|W - W_0|$ is small, but also that max $|DW - DW_0|$ and max $|D^2W - D^2W_0|$ are small, so that additionally to W close to W_0, the first and second derivatives of W must be close of those of W_0.
The first statement of Hörmander's theorem asserts the existence of a solution if a good approximation φ_0 of the earth's surface φ is available. We need a good approximation for the maximum deviation of φ and φ_0, but also for their first and second derivatives and good approximations to the potential W and the gravity G. The second statement reveals that the surface φ is as smooth as the data W and G. This means that if the data W and G are n times differentiable and the n-th derivatives satisfy a Hölder condition, then φ will be n times differentiable and the n-th derivatives satisfy a Hölder condition. Finally by the third statement uniqueness is ensured under a stronger condition $\mathscr{H}^{3+\epsilon}$ (neighborhood) than for the first statement $\mathscr{H}^{2+\epsilon}$ (neighborhood). Here, Hörmander claims that one can replace $\mathscr{H}^{3+\epsilon}$ by $\mathscr{H}^{2+\epsilon}$, so that existence and uniqueness hold under the same condition. We also note that for the second statement ϵ is assumed not to be an integer (because Hölder conditions with $\epsilon \neq 0$ are essential in potential-theoretical considerations) whereas for the first and third statements integer values of ϵ are admitted.

4. The Discrete Nash-Hörmander Method for the Molodensky Problem

4.1. Boundary Element Solutions

In this section we present a new boundary element method on a sequence of surfaces obtained by the Nash-Hörmander method. Here we convert the linearized Molodensky problem and an additional Dirichlet problem into boundary integral equations by making a single layer potential ansatz for the gravitational potential u. Thus, our solution procedure for the Molodensky problem consists in solving sequences of integral equations and computing a correction $\dot{\varphi}_m$ of the map φ_m which describes the new surface. This correction is obtained via the Hessian, the second derivative of the gravity potential and has to be done with care due to the various sources of error for the approximations. We comment on this below. We consider the case of a non-rotating sphere i.e. $\frac{1}{2}\omega^2(x_1^2 + x_2^2) = 0$.
This together with (3.1) implies that

$$v = w \qquad W = v \circ \varphi \qquad G = \nabla v \circ \varphi = g \circ \varphi \tag{4.1}$$

with $v : \varphi(\mathbb{S}^0) \to \mathbb{R}$ and $g = \nabla v : \varphi(\mathbb{S}^0) \to \mathbb{R}^3$, where we define $\mathbb{S}^0 := \{x \in \mathbb{R}^3; x_1^2 + x_2^2 + x_3^2 = 1\}$.
We reformulate the linearized problem (3.15) and set for the ease of presentation $\dot{v} := u$ and $\mathbb{S}^m := \varphi_m(\mathbb{S}^0)$.

In each iteration step m, we compute the linearized problem as follows:
Given $\dot{W}_m : \mathbb{S}^0 \to \mathbb{R}, \dot{G}_m : \mathbb{S}^0 \to \mathbb{R}^3, h_m : \mathbb{S}^m \to \mathbb{R}^3$ and $\varphi_m : \mathbb{S}^0 \subset \mathbb{R}^3 \to \mathbb{S}^m \subset \mathbb{R}^3$.
Find $u_m : \mathbb{S}^m \to \mathbb{R}$ such that

$$\begin{aligned}
&\Delta u_m = 0 \quad \text{in} \quad \mathbb{R}^3 \backslash \bar{\Omega}_m,\ \partial\Omega_m = \mathbb{S}^m \\
&u_m + \nabla u_m \cdot h_m = \dot{W}_m \circ \varphi_m^{-1} + (\dot{G}_m \circ \varphi_m^{-1}) \cdot h_m - \sum_{j=1}^{3} \dot{a}_{j,m} \widetilde{A}_j(x)\big|_{x \in \mathbb{S}^m} \quad \text{on} \quad \mathbb{S}^m \\
&u_m(x) = \frac{c}{|x|} + O(|x|^{-3}) \quad \text{when} \quad |x| \to \infty, \quad c \in \mathbb{R},
\end{aligned} \tag{4.2}$$

for some $\widetilde{A}_j \in C^\infty(\mathbb{S}^m)$ and constants $\dot{a}_{j,m} \in \mathbb{R}$, such that (4.2) becomes well posed. A feasible choice for $\widetilde{A}_j$ is given below.

In order to compute the correction $\dot{\varphi}_m : \mathbb{S}^0 \to \mathbb{R}^3$ given by

$$\dot{\varphi}_m = (\nabla g_m \circ \varphi_m)^{-1}(\dot{G}_m - \nabla u_m \circ \varphi_m) \tag{4.3}$$

we need to compute g_m (with g_m=grad $\overline{v}_m$).

We define $W_{m-1}^{total} : \mathbb{S}^0 \to \mathbb{R}$ for a small stepsize $\triangle_j$ by

$$W_{m-1}^{total} = \begin{cases} v_0 \circ \varphi_0 + \triangle_0 u_0 \circ \varphi_0 + \triangle_1 u_1 \circ \varphi_1 + \cdots + \triangle_{m-1} u_{m-1} \circ \varphi_{m-1}, & \text{for} \quad m \geq 1 \\ v_0 \circ \varphi_0 \quad \text{for} \quad m = 0 \end{cases}$$

which is the accumulated potential up to iteration index $m-1$, where $v_0 = \frac{1}{||x||}$ is the potential of the unit sphere and $w_m^{total} : \mathbb{S}^m \to \mathbb{R}$ is given by

$$w_m^{total} = W_{m-1}^{total} \circ \varphi_m^{-1} + \triangle_m u_m \quad \text{on} \quad \mathbb{S}^m. \tag{4.4}$$

Now we consider the Dirichlet problem:
For given w_m^{total} on $\mathbb{S}^m$, find $\overline{v}_m : \mathbb{S}^m \to \mathbb{R}$ such that

$$\begin{aligned} &\Delta \overline{v}_m = 0 \quad \text{in} \quad \mathbb{R}^3 \backslash \bar{\Omega}_m,\ \partial\Omega_m = \mathbb{S}^m \\ &\overline{v}_{m|\partial\Omega_m} = w_m^{total} - \sum_{j=1}^{3} \dot{a}_{j,m} \widetilde{A}_j(x)\big|_{x \in \mathbb{S}^m} \quad \text{on} \quad \mathbb{S}^m \\ &\overline{v}_m(x) = \frac{c}{|x|} + O(|x|^{-3}) \quad \text{when} \quad |x| \to \infty \end{aligned} \tag{4.5}$$

for some $\widetilde{A}_j$ and constants $\dot{a}_{j,m}$, which are not necessarily the same as in (4.2).
With this we can compute $g_m = \nabla \overline{v}_m$ and $\nabla g_m = \nabla^2 \overline{v}_m$. This yields together with (4.3) the correction $\dot{\varphi}_m$ to the embedding φ_m.

Next, we use a single layer potential ansatz for $u_m = V_m \mu_m$ in (4.2) and satisfy the decaying condition at ∞ in a weak sense.
Let

$$f_m := (\dot{W}_m \circ \varphi_m^{-1} + (\dot{G}_m \circ \varphi_m^{-1}) \cdot h_m) \in L^2(\mathbb{S}^m). \tag{4.6}$$

We obtain with the Fredholm operator S of index zero by

$$S := V + \frac{1}{2} \cos(\measuredangle(\boldsymbol{n}, \boldsymbol{h}))I + K'(\boldsymbol{h}) \tag{4.7}$$

from (4.2) the pseudodifferential equation on the surface $\mathbb{S}^m$

$$S\mu_m = f_m. \tag{4.8}$$

V is the single layer potential and $K'(\boldsymbol{h})$ denotes the directional derivative of the single layer potential in direction $\boldsymbol{h}$. In particular for $\boldsymbol{h} = \boldsymbol{n}$, $K'(\boldsymbol{n})$ is the standard adjoint double layer potential.
Furthermore, let $A_j = \frac{x_j}{|x|^3}$ and $\mathcal{N} := \text{span}\,\{A_j\}_{j=1,\dots,3}$. In particular, if $\mu_m \in L^2(\mathbb{S}^m) \cap \mathcal{N}^\perp$, then $u_m = V_m \mu_m$ satisfies the decaying condition of (4.2). Since $f_m \in L^2(\mathbb{S}^m)$, but not necessarily in $S(L^2(\mathbb{S}^m) \cap \mathcal{N}^\perp)$, it is clear that the $\widetilde{A}_j$ must be chosen such that span $\{\widetilde{A}_j\}_{j=1}^3 + S(L^2(\mathbb{S}^m) \cap \mathcal{N}^\perp) = L^2(\mathbb{S}^m)$ for (4.2) to be well defined. Obviously, $\widetilde{A}_j := SA_j|_{\mathbb{S}^m}$ is a feasible choice and leads directly to the variational formulation of (4.8), with $(\dot{a}_{j,m})_{j=1}^3 = \dot{a}_m$:

Find $(\mu_m, \dot{a}_m) \in (L^2(\mathbb{S}^m) \cap \mathcal{N}^\perp) \times \mathbb{R}^3$, with the L^2-scalar product on $\mathbb{S}^m$ $\langle\cdot,\cdot\rangle_{\mathbb{S}^m}$, such that

$$\langle S\mu_m, \phi\rangle_{\mathbb{S}^m} + \langle S\sum_{j=1}^{3} \dot{a}_{j,m} A_j, \phi\rangle_{\mathbb{S}^m} = \langle f_m, \phi\rangle_{\mathbb{S}^m} \quad \forall \phi \in L^2(\mathbb{S}^m).$$

Furthermore, $\mu_m \in L^2(\mathbb{S}^m) \cap \mathcal{N}^\perp$ is equivalent to $\mu_m \in L^2(\mathbb{S}^m)$ such that

$$\langle \mu_m, A_j\rangle_{\mathbb{S}^m} = 0 \quad j = 1, 2, 3.$$

which yields the mixed formulation:
Find $(\mu_m, \dot{a}_m) \in L^2(\mathbb{S}^m) \times \mathbb{R}^3$ such that

$$\begin{aligned} \langle S\mu_m, \phi\rangle_{\mathbb{S}^m} + \langle S\sum_{j=1}^{3} \dot{a}_{j,m} A_j, \phi\rangle_{\mathbb{S}^m} &= \langle f_m, \phi\rangle_{\mathbb{S}^m} \quad && \forall \phi \in L^2(\mathbb{S}^m) \\ \langle \mu_m, A_k\rangle_{\mathbb{S}^m} &= 0 && k = 1, 2, 3. \end{aligned} \tag{4.9}$$

With the L^2 scalar product $\langle\cdot,\cdot\rangle_{\mathbb{S}_h^m}$ on the approximating surface $\mathbb{S}_h^m$ given by the triangulation $\mathcal{T}_h^m$, the corresponding discrete formulation is given by:
Find $(\mu_{m,h}, \dot{a}_{m,h}) \in S_h(\mathbb{S}_h^m) \times \mathbb{R}^3$ such that

$$\begin{aligned} \langle S\mu_{m,h}, \phi_h\rangle_{\mathbb{S}_h^m} + \langle S\sum_{j=1}^{3} \dot{a}_{j,m,h} A_j, \phi_h\rangle_{\mathbb{S}_h^m} &= \langle f_m, \phi_h\rangle_{\mathbb{S}_h^m} \quad && \forall \phi_h \in S_h(\mathbb{S}_h^m) \\ \langle \mu_{m,h}, A_k\rangle_{\mathbb{S}_h^m} &= 0 && k = 1, 2, 3 \end{aligned} \tag{4.10}$$

where $L^2(\mathbb{S}^m) \supset S_h(\mathbb{S}_h^m) = \{$space of discontinuous p.w. polynomials of degree 2 on a regular partition $\mathcal{T}_h^m$ into triangles approximating $\mathbb{S}^m\} = \operatorname{span}\{b_j\}_{j=1}^N$.
With

$$\dot{a}_{j,m,h} \in \mathbb{R}, \quad j = 1, 2, 3, \quad \mu_{m,h} = \sum_{j=1}^{N} \mu_{j,m} b_j, \quad \phi_{m,h} = \sum_{j=1}^{N} \phi_{j,m} b_j$$

we obtain the following equations:

$$\begin{aligned} \sum_{j=1}^{N} \mu_{j,m} \langle Sb_j, b_k\rangle_{\mathbb{S}_h^m} + \sum_{j=1}^{3} \dot{a}_{j,m} \langle SA_j, b_k\rangle_{\mathbb{S}_h^m} &= \langle f_m, b_k\rangle_{\mathbb{S}_h^m} \quad && 1 \le k \le N \\ \sum_{j=1}^{n} \mu_{j,m} \langle b_j, A_k\rangle_{\mathbb{S}_h^m} &= 0 && k = 1, 2, 3. \end{aligned} \tag{4.11}$$

This yields, in matrix notation, the following system of linear equations, in which the lower index m is omitted for the ease of presentation:

$$\begin{bmatrix} S & \widetilde{S} \\ \Lambda & 0 \end{bmatrix} \begin{bmatrix} \vec{\mu}^h \\ \vec{a}^h \end{bmatrix} = \begin{bmatrix} \vec{f} \\ \vec{0} \end{bmatrix}$$

where $(S_{kj}) = \langle Sb_j, b_k\rangle, (\widetilde{S}_{kj}) = \langle SA_j, b_k\rangle, (\Lambda_{kj}) = \langle b_j, A_k\rangle, (f_k) = \langle f_m, b_k\rangle$ and $\vec{\mu} \in \mathbb{R}^N, \vec{a} \in \mathbb{R}^3$.
For the computation of the Hessian $\nabla\nabla\overline{v}_m|_{\mathbb{S}^m}$, we have to solve approximately problem

(4.5) by the boundary element method. Using the above procedure for the Dirichlet problem (4.5) with $\widetilde{A}_j = VA_j|_{\mathbb{S}^m}$ since span $\{\widetilde{A}_j\}_{j=1}^3 + V_m(H^{-1/2}(\mathbb{S}^m) \cap \mathcal{N}^\perp) = H^{1/2}(\mathbb{S}^m)$ for (4.5) to be well posed we obtain the following weak formulation:
Find $(\tilde{\mu}_m, \dot{\tilde{a}}_m) \in H^{-1/2}(\mathbb{S}^m) \times \mathbb{R}^3$ such that

$$\begin{aligned} \langle V\tilde{\mu}_m, \xi\rangle_{\mathbb{S}^m} + \langle V\sum_{j=1}^{3} \dot{\tilde{a}}_{j,m} A_j, \xi\rangle_{\mathbb{S}^m} &= \langle w_m^{total}, \xi\rangle_{\mathbb{S}^m} \quad \forall \xi \in H^{-1/2}(\mathbb{S}^m) \\ \langle \tilde{\mu}_m, A_k\rangle_{\mathbb{S}^m} &= 0 \qquad\qquad k = 1,2,3. \end{aligned} \tag{4.12}$$

The corresponding discrete formulation is then given by:
Find $(\tilde{\mu}_{m,h}, \dot{\tilde{a}}_{m,h}) \in S_h(\mathbb{S}_h^m) \times \mathbb{R}^3$ such that

$$\begin{aligned} \langle V\tilde{\mu}_{m,h}, \xi_h\rangle_{\mathbb{S}_h^m} + \langle V\sum_{j=1}^{3} \dot{\tilde{a}}_{j,m,h} A_j, \xi_h\rangle_{\mathbb{S}_h^m} &= \langle w_m^{total}, \xi_h\rangle_{\mathbb{S}_h^m} \quad \forall \xi_h \in S_h(\mathbb{S}_h^m) \\ \langle \tilde{\mu}_{m,h}, A_k\rangle_{\mathbb{S}_h^m} &= 0 \qquad\qquad k = 1,2,3 \end{aligned} \tag{4.13}$$

where $H^{-1/2}(\mathbb{S}^m) \supset S_h(\mathbb{S}_h^m) = \{$space of discontinuous p.w. polynomials of degree 2 on a regular partition $\mathcal{T}_h^m$ into triangles approximating $\mathbb{S}^m\}$.
Analogously we obtain with

$$\dot{\tilde{a}}_{j,m,h} \in \mathbb{R}, \quad j = 1,2,3, \quad \tilde{\mu}_{m,h} = \sum_{j=1}^{N} \tilde{\mu}_{j,m}\eta_j, \quad \zeta_i \in \text{span}\{\eta_i\}$$

the following equations with $\widetilde{f}_m = w_m^{total}$:

$$\begin{aligned} \sum_{j=1}^{N} \widetilde{\mu}_{j,m}\langle V\eta_j, \zeta_k\rangle_{\mathbb{S}_h^m} + \sum_{j=1}^{3} \dot{\tilde{a}}_{j,m}\langle VA_j, \zeta_k\rangle_{\mathbb{S}_h^m} &= \langle \widetilde{f}_m, \zeta_k\rangle_{\mathbb{S}_h^m} \quad 1 \le k \le N \\ \sum_{j=1}^{n} \widetilde{\mu}_{j,m}\langle \eta_j, A_k\rangle_{\mathbb{S}_h^m} &= 0 \qquad\qquad k = 1,2,3. \end{aligned} \tag{4.14}$$

Rewritten in short

$$\begin{bmatrix} V & \widetilde{V} \\ \Lambda & 0 \end{bmatrix} \begin{bmatrix} \vec{\widetilde{\mu}}^h \\ \vec{\widetilde{a}}^h \end{bmatrix} = \begin{bmatrix} \vec{f} \\ \vec{0} \end{bmatrix}.$$

Let us take a look at the right hand side of this equation:

$$\langle \widetilde{f}_m, \xi\rangle_{\mathbb{S}^m} = \langle w_m^{total}, \xi\rangle_{\mathbb{S}^m} \quad \forall \xi \in S_h(\mathbb{S}^m)$$

Using (4.4) and the ansatz $u_i = V_i\mu_i$ we have

$$\begin{aligned}\langle w_m^{total}, \xi\rangle_{\mathbb{S}^m} =&\langle W_{m-1}^{total} \circ \varphi_m^{-1}, \xi\rangle_{\mathbb{S}^m} + \triangle_m \langle u_m, \xi\rangle_{\mathbb{S}^m}\\ =&\langle (v_0 \circ \varphi_0) \circ \varphi_m^{-1}, \xi\rangle_{\mathbb{S}^m} + \sum_{i=0}^{m-1} \triangle_i \langle (u_i \circ \varphi_i) \circ \varphi_m^{-1}, \xi\rangle_{\mathbb{S}^m}\\ &+ \triangle_m \langle V_m\mu_m, \xi\rangle_{\mathbb{S}^m} \qquad (4.15)\\ =&\langle (v_0 \circ \varphi_0) \circ \varphi_m^{-1}, \xi\rangle_{\mathbb{S}^m} + \sum_{i=0}^{m-1} \triangle_i \langle (V_i\mu_i \circ \varphi_i) \circ \varphi_m^{-1}, \xi\rangle_{\mathbb{S}^m}\\ &+ \triangle_m \langle V_m\mu_m, \xi\rangle_{\mathbb{S}^m}.\end{aligned}$$

To simplify our analysis here we do not consider the errors resulting from approximations of the surfaces. There holds the following a priori error estimate for the Galerkin solution of the linearized problem (4.9). To get started, we first assume that there are no perturbations in the right hand side of the Galerkin equations. Later on we will also regard perturbations in the right hand side (Proposition 4.3, Proposition 4.5).

Proposition 4.1. *Let $\mu_m, \psi_m = \sum_{j=1}^{3} \dot{a}_{j,m} A_j$ be the exact solution of* (4.9) *and $\mu_{m,h}, \psi_{m,h}$ be the Galerkin solution of* (4.10). *Then there exists a constant C independent of h but depending on m (m fixed) such that there holds*

$$\|\mu_m - \mu_{m,h}\|_{L^2(\mathbb{S}^m)} + \|\psi_m - \psi_{m,h}\|_{L^2(\mathbb{S}^m)} \le C \inf_{v\in S_h} \|\mu_m - v\|_{L^2(\mathbb{S}^m)} \le C h^{3/2-\epsilon} \|u\|_{H^{3/2-\epsilon}(\mathbb{S}^m)}. \qquad (4.16)$$

The proof follows directly from the following considerations.

For the ease of presentation we rewrite the system of equations (4.9) as:
Find $(\mu_m, \psi_m) \in L^2(\mathbb{S}^m) \times \mathcal{N}$ such that with $f = f_m$

$$\begin{aligned}\langle S\mu_m, \phi\rangle + \langle S\psi_m, \phi\rangle &= \langle f, v\rangle \quad \forall\, \phi \in L^2(\mathbb{S}^m)\\ \langle \mu_m, A_k\rangle &= 0 \qquad\quad \forall\, A_k \in \mathcal{N}\end{aligned} \qquad (4.17)$$

and the discrete formulation (4.10) to:
Find $(\mu_{m,h}, \psi_{m,h}) \in S_h(\mathbb{S}_h^m) \times \mathcal{N}$ such that

$$\begin{aligned}\langle S\mu_{m,h}, \phi_h\rangle + \langle S\psi_{m,h}, \phi_h\rangle &= \langle f, \phi_h\rangle \quad \forall\, \phi_h \in S_h(\mathbb{S}_h^m)\\ \langle \mu_{m,h}, A_k\rangle &= 0 \qquad\quad \forall\, A_k \in \mathcal{N}.\end{aligned} \qquad (4.18)$$

We know from [28] that S satisfies a Gårding inequality: there exists $\gamma > 0$ and a compact operator $\mathcal{C}$ on $L^2(\mathbb{S}^m)$ such that

$$\forall\, v \in L^2(\mathbb{S}^m): \quad Re\langle v, (S + \mathcal{C})v\rangle \ge \gamma \|v\|_{L^2(\mathbb{S}^m)}^2. \qquad (4.19)$$

For the ease of presentation we set in the following $\mathcal{M} := L^2(\mathbb{S}^m), \mathcal{M}_N := S_h(\mathbb{S}_h^m)$ and $u_N := \mu_{m,h}, p_N := \psi_{m,h}, v_N := \phi_h, q := A_k$.

Lemma 4.1 (Lemma 1 [21]). *Let $S : \mathcal{M} \to \mathcal{M}$ be bounded, injective and assume that (4.19) holds. Let $\{\mathcal{M}_N\}_N$ be a dense sequence of subspaces of $\mathcal{M}$. Then there exist $N_0 \in \mathbb{N}, \gamma_0 > 0$ such that for every $N \geq N_0$ holds the discrete inf-sup condition*

$$\inf_{0 \neq u_N \in \mathcal{M}_N} \sup_{0 \neq v_N \in \mathcal{M}_N} \frac{|\langle Su_N, v_N \rangle|}{\|u_N\|_{\mathcal{M}} \|v_N\|_{\mathcal{M}}} \geq \gamma_0. \tag{4.20}$$

For the analysis of (4.17) and (4.18) we define the bilinear form $B : (\mathcal{M}, \mathcal{N}) \times (\mathcal{M}, \mathcal{N}) \to \mathbb{R}$ by

$$B(u, p; v, q) := \langle Su, v \rangle + \langle Sp, v \rangle + \langle u, q \rangle. \tag{4.21}$$

From the inf-sup condition for B follows the unique solvability of (4.17) and (4.18) and the quasi optimal convergence of u_N, p_N in (4.18) to u, p.
For $(u, p) \in (\mathcal{M}, \mathcal{N})$ we define $|||(u, p)||| := (\|u\|^2_{\mathcal{M}} + \|p\|^2_{\mathcal{M}})^{1/2}$. For the continuous version of the inf-sup condition for B we have the following lemma.

Lemma 4.2. *The bilinear form B satisfies the inf-sup condition on $(\mathcal{M}, \mathcal{N}) \times (\mathcal{M}, \mathcal{N})$ i.e.*

$$\inf_{\substack{0 \neq u \in \mathcal{M} \\ p \in \mathcal{N}}} \sup_{\substack{0 \neq v \in \mathcal{M} \\ q \in \mathcal{N}}} \frac{|B(u, p; v, q)|}{\|(u, p)\|_{\mathcal{M}} \|(v, q)\|_{\mathcal{M}}} \geq \gamma_0. \tag{4.22}$$

Furthermore, we need the discrete inf-sup condition for the form B.

Proposition 4.2 (Proposition 1 [21]). *Let $\{\mathcal{M}_N\}_N$ be dense in $\mathcal{M}$ and $\mathcal{N} \subset \mathcal{M}$ be finite dimensional. Define*

$$\eta(N) := \sup_{p \in \mathcal{N}} \inf_{p_N \in \mathcal{M}_N} \frac{\|p - p_N\|_{\mathcal{M}}}{\|p\|_{\mathcal{M}}}. \tag{4.23}$$

Then there holds $\forall\, N \geq N_0$

$$\inf_{\substack{u_N \in \mathcal{M}_N \\ p \in \mathcal{N}}} \sup_{\substack{v_N \in \mathcal{M}_N \\ q \in \mathcal{N}}} \frac{|B(u_N, p; v_N, q)|}{|||(u_N, p)|||\, |||(v_N, q)|||} \geq \gamma_0 > 0. \tag{4.24}$$

provided N_0 is such that $\eta(N_0)$ is sufficiently small.

Now, observation shows that the integral operator S and the spaces $\mathcal{M}_N$ and their discrete counter parts satisfy the assumptions in the foregoing Lemma 4.2 and in Proposition 4.2. Hence application of these results yield immediately the result of our proposition. Next, let us consider the case of a perturbed right hand side in (4.10).

Denoting after the first Nash-Hörmander step the perturbed data by an upper g, we have from (4.18) the following problem:
Find $(u^g_N, p^g_N) \in \mathcal{M}_N \times \mathcal{N}$ such that

$$\begin{aligned} \langle Su^g_N, v_N \rangle + \langle Sp^g_N, v_N \rangle &= \langle f^g, v_N \rangle \quad && \forall\, v_N \in \mathcal{M}_N \\ \langle u^g_N, q \rangle &= 0 && \forall\, q \in \mathcal{N} \end{aligned} \tag{4.25}$$

where we abbreviate $f^g = \dot{G}_m^g \circ (\varphi_m^{-1})^g \cdot h^g$ for $f = \dot{G}_m \circ (\varphi_m^{-1}) \cdot h$.
Now, by subtracting (4.25) from (4.18), we deduce

$$\langle S(u_N - u_N^g), v_N\rangle + \langle S(p_N - p_N^g), v_N\rangle + \langle u_N - u_N^g, q\rangle = \langle f - f^g, v_N\rangle$$

$\forall\, v_N \in \mathcal{M}_N, q \in \mathcal{N}$ and using the definition of the bilinear form B we conclude

$$B(u_N - u_N^g, p_N - p_N^g; v_N, q) = \langle f - f^g, v_N\rangle. \tag{4.26}$$

Applying the discrete inf-sup condition (4.24), (4.26) and Cauchy Schwarz inequality yields

$$\begin{aligned}
\gamma_0 |||(u_N - u_N^g, p_N - p_N^g)||| &\le \sup_{\substack{v_N \in \mathcal{M}_N \\ q \in \mathcal{N}}} \frac{B(u_N - u_N^g, p_N - p_N^g; v_N, q)}{|||(v_N, q)|||} \\
&= \sup_{\substack{v_N \in \mathcal{M}_N \\ q \in \mathcal{N}}} \frac{\langle f - f^g, v_N\rangle}{|||(v, q)|||} \\
&\underset{\text{C.S.}}{\le} \sup_{\substack{v_N \in \mathcal{M}_N \\ q \in \mathcal{N}}} \frac{\|f - f^g\|_{\mathcal{M}} \|v_N\|_{\mathcal{M}}}{(\|v_N\|_{\mathcal{M}}^2 + \|q\|_{\mathcal{M}}^2)^{1/2}} \\
&\le \sup_{v_N \in \mathcal{M}_N} \frac{\|f - f^g\|_{\mathcal{M}} \|v_N\|_{\mathcal{M}}}{\|v_N\|_{\mathcal{M}}} = \|f - f^g\|_{\mathcal{M}}.
\end{aligned}$$

Now, by combining this estimate with (4.16) we obtain with

$$\begin{aligned}
\|u - u_N^g\|_{\mathcal{M}} + \|p - p_N^g\|_{\mathcal{M}} \le \|u - u_N\|_{\mathcal{M}} + \|u_N - u_N^g\|_{\mathcal{M}} \\
+ \|p - p_N\|_{\mathcal{M}} + \|p_N - p_N^g\|_{\mathcal{M}}
\end{aligned}$$

the following result

Proposition 4.3. *Let f^g be a perturbation of f, let u, p be the exact solution of* (4.9) *and u_N^g, p_N^g the Galerkin solution of the perturbed problem* (4.25)*. Then there holds the following quasi optimal error estimate with a constant C independent of h*

$$\|u - u_N^g\|_{\mathcal{M}} + \|p - p_N^g\|_{\mathcal{M}} \le C \inf_{v \in \mathcal{M}_N} \|u - v\|_{\mathcal{M}} + \frac{1}{\gamma_0} \|f - f^g\|_{\mathcal{M}}.$$

It would be optimal if the perturbation in the right hand side f, is at least of the same order as the discretization error $\inf_{v \in \mathcal{M}_N} \|u - v\|_{\mathcal{M}}$.

Next, we analyse the convergence of the boundary element approximation for the auxiliary problem (4.5). We first analyse the case of a non perturbed right hand side. Let us recall the discrete formulation for the Dirichlet problem. For the ease of presentation we rewrite problem (4.12) as follows:
Find$(u, p) \in H^{-1/2}(\mathbb{S}^m) \times \mathcal{N}$ such that

$$\begin{aligned}
\langle Vu, v\rangle + \langle Vp, v\rangle &= \langle f, v\rangle \quad \forall\, v \in H^{-1/2}(\mathbb{S}^m) \\
\langle u, q\rangle &= 0 \qquad\quad \forall\, q \in \mathcal{N}.
\end{aligned} \tag{4.27}$$

The discrete formulation to (4.13) reads as:
Find $(u_N, p_N) \in S_h(\mathbb{S}_h^m) \times \mathcal{N}$ such that

$$\begin{aligned} \langle Vu_N, v_N\rangle + \langle Vp_N, v_N\rangle &= \langle f, v_N\rangle \quad \forall\, v_N \in S_h(\mathbb{S}_h^m) =: Q_N \\ \langle u_N, q\rangle &= 0 \qquad\qquad \forall\, q \in \mathcal{N}. \end{aligned} \tag{4.28}$$

The coercivity of the single layer potential V implies

$$\exists \alpha > 0 \quad \forall\, u \in H^{-1/2}(\mathbb{S}^m) : \langle Vu, u\rangle \geq \alpha \|u\|^2_{H^{-1/2}(\mathbb{S}^m)}.$$

Having this, the discrete inf-sup condition holds, i.e.

$$\sup_{v_N \in Q_N} \frac{|\langle Vu_N, v_N\rangle|}{\|v_N\|_{H^{-1/2}(\mathbb{S}^m)}} \geq \frac{|\langle Vu_N, u_N\rangle|}{\|u_N\|_{H^{-1/2}(\mathbb{S}^m)}} \geq \alpha_0 \|u_N\|_{H^{-1/2}(\mathbb{S}^m)}.$$

With the bilinear form $B : (H^{-1/2}(\mathbb{S}^m), \mathcal{N}) \times (H^{-1/2}(\mathbb{S}^m), \mathcal{N}) \to \mathbb{R}$ given by

$$B(u, p; v, q) := \langle Vu, v\rangle + \langle Vp, v\rangle + \langle u, q\rangle \tag{4.29}$$

for $(u, p) \in (H^{-1/2}(\mathbb{S}^m), \mathcal{N})$ and

$$|||(u, p)||| := (\|u\|^2_{H^{-1/2}(\mathbb{S}^m)} + \|p\|^2_{H^{-1/2}(\mathbb{S}^m)})^{1/2},$$

we can derive analogously the following results. The respective proofs are listed in Appendix A.4.

Lemma 4.3. *The bilinear form B satisfies the inf-sup condition on $(H^{-1/2}(\mathbb{S}^m), \mathcal{N}) \times (H^{-1/2}(\mathbb{S}^m), \mathcal{N})$, i.e.*

$$\exists \alpha_0 > 0 : \inf_{\substack{u \in H^{-1/2}(\mathbb{S}^m) \\ p \in \mathcal{N}}} \sup_{\substack{v \in H^{-1/2}(\mathbb{S}^m) \\ q \in \mathcal{N}}} \frac{|B(u, p; v, q)|}{|||(u, p)|||\, |||(v, q)|||} \geq \alpha_0 \tag{4.30}$$

Proposition 4.4. *Let $\{Q_N\}_N$ be dense in $H^{-1/2}(\mathbb{S}^m)$ and $\mathcal{N} \subset H^{-1/2}(\mathbb{S}^m)$ be finite dimensional. We define*

$$\eta(N) := \sup_{p \in \mathcal{N}} \inf_{p_N \in Q_N} \frac{\|p - p_N\|_{H^{-1/2}(\mathbb{S}^m)}}{\|p\|_{H^{-1/2}(\mathbb{S}^m)}}. \tag{4.31}$$

Then there holds for all $N \geq N_0$

$$\inf_{\substack{u_N \in Q_N \\ p \in \mathcal{N}}} \sup_{\substack{v_N \in Q_N \\ q \in \mathcal{N}}} \frac{|B(u_N, p; v_N, q)|}{|||(u_N, p)|||\, |||(v_N, p)|||} \geq \alpha_0 > 0, \tag{4.32}$$

provided that N_0 is such that $\eta(N_0)$ is sufficiently small.

By [47] we know that (4.32) implies quasi-optimal convergence i.e.

$$\|u - u_N\|_{H^{-1/2}(\mathbb{S}^m)} + \|p - p_N\|_{H^{-1/2}(\mathbb{S}^m)} \leq C \inf_{v \in Q_N, q \in \mathcal{N}} \{\|u - v\|_{H^{-1/2}(\mathbb{S}^m)} + \|p - q\|_{H^{-1/2}(\mathbb{S}^m)}\}.$$

Since $\arg \inf_{q\in\mathcal{N}}(\inf_{v\in Q_N}\{\|u-v\|_{H^{-1/2}(\mathbb{S}^m)} + \|p-q\|_{H^{-1/2}(\mathbb{S}^m)}\}) = p$, we conclude

$$\|u-u_N\|_{H^{-1/2}(\mathbb{S}^m)} + \|p-p_N\|_{H^{-1/2}(\mathbb{S}^m)} \leq C \inf_{v\in Q_N} \|u-v\|_{H^{-1/2}(\mathbb{S}^m)} \leq Ch^2\|u\|_{H^{3/2-\epsilon}(\mathbb{S}^m)}. \tag{4.33}$$

In the following, let us consider again the case of a perturbed right hand side.
First, we recall the discrete formulation:
Find $(u_N, p_N) \in Q_N \times \mathcal{N}$ such that

$$\begin{aligned} \langle Vu_N, v_N\rangle + \langle Vp_N, v_N\rangle &= \langle f, v_N\rangle \quad \forall\, v_N \in Q_N \\ \langle u_N, q\rangle &= 0 \qquad\quad \forall\, q \in \mathcal{N}. \end{aligned} \tag{4.34}$$

Denoting the perturbed data by an upper g we have the following problem:
Find $(u_N^g, p_N^g) \in Q_N \times \mathcal{N}$ such that

$$\begin{aligned} \langle Vu_N^g, v_N\rangle + \langle Vp_N^g, v_N\rangle &= \langle f^g, v_N\rangle \quad \forall\, v_N \in Q_N \\ \langle u_N^g, q\rangle &= 0 \qquad\quad \forall\, q \in \mathcal{N}. \end{aligned} \tag{4.35}$$

Now, by subtracting (4.35) from (4.34), we deduce

$$\langle V(u_N-u_N^g), v_N\rangle + \langle V(p_N-p_N^g), v_N\rangle + \langle u_N-u_N^g, q\rangle = \langle f-f^g, v_N\rangle, \forall v_N \in Q_N, q \in \mathcal{N}$$

and using the definition of the bilinear form B, we conclude

$$B(u_N-u_N^g, p_N-p_N^g; v_N, q) = \langle f-f^g, v_N\rangle. \tag{4.36}$$

Applying the discrete inf-sup condition (4.32), (4.36) and Cauchy Schwarz inequality yields

$$\begin{aligned} \alpha_0|||(u_N-u_N^g, p_N-p_N^g)||| &\leq \sup_{\substack{v_N\in Q_N\\ q\in\mathcal{N}}} \frac{B(u_N-u_N^g, p_N-p_N^g; v_N, q)}{|||(v_N, q)|||} \\ &= \sup_{\substack{v_N\in Q_N\\ q\in\mathcal{N}}} \frac{\langle f-f^g, v_N\rangle}{|||(v,q)|||} \\ &\underset{\text{C.S.}}{\leq} \sup_{\substack{v_N\in Q_N\\ q\in\mathcal{N}}} \frac{\|f-f^g\|_{H^{-1/2}(\mathbb{S}^m)}\|v_N\|_{H^{-1/2}(\mathbb{S}^m)}}{(\|v_N\|^2_{H^{-1/2}(\mathbb{S}^m)} + \|q\|^2_{H^{-1/2}(\mathbb{S}^m)})^{1/2}} \\ &\leq \sup_{v_N\in Q_N} \frac{\|f-f^g\|_{H^{-1/2}(\mathbb{S}^m)}\|v_N\|_{H^{-1/2}(\mathbb{S}^m)}}{\|v_N\|_{H^{-1/2}(\mathbb{S}^m)}} \\ &= \|f-f^g\|_{H^{-1/2}(\mathbb{S}^m)}. \end{aligned}$$

Now, by combining this estimate with (4.33), we obtain with

$$\begin{aligned} \|u-u_N^g\|_{H^{-1/2}(\mathbb{S}^m)} + \|p-p_N^g\|_{H^{-1/2}(\mathbb{S}^m)} &\leq \|u-u_N\|_{H^{-1/2}(\mathbb{S}^m)} + \|u_N-u_N^g\|_{H^{-1/2}(\mathbb{S}^m)} \\ &\quad + \|p-p_N\|_{H^{-1/2}(\mathbb{S}^m)} + \|p_N-p_N^g\|_{H^{-1/2}(\mathbb{S}^m)} \\ &\leq C\inf_{v\in Q_N}\|u-v\|_{H^{-1/2}(\mathbb{S}^m)} + \frac{1}{\alpha_0}\|f-f^g\|_{H^{-1/2}(\mathbb{S}^m)} \end{aligned}$$

the following result.

Proposition 4.5. *Let f^g be a perturbation of f, let u, p be the exact solution of* (4.12) *and u_N^g, p_N^g the Galerkin solution of the perturbed problem* (4.35)*. Then there holds the following quasi optimal error estimate with a constant C independent of h*

$$\|u - u_N^g\|_{H^{-1/2}(\mathbb{S}^m)} + \|p - p_N^g\|_{H^{-1/2}(\mathbb{S}^m)} \leq C \inf_{v \in Q_N} \|u - v\|_{H^{-1/2}(\mathbb{S}^m)} + \frac{1}{\gamma_0} \|f - f^g\|_{H^{-1/2}(\mathbb{S}^m)}.$$

Again, it would be optimal if the perturbation in the right hand side f is at least of the same order as the discretization error $\inf_{v \in Q_N} \|u - v\|_{H^{-1/2}(\mathbb{S}^m)}$.

Remark 4.1. *From Nédélec [36] it is well known, that finite elements to approximate the surface should be one order higher than the finite elements to approximate the solution of the integral equation with the single layer potential. In our numerical experiments in Chapter 5 we have used second degree polynomials on triangles to approximate the Galerkin solution of the first kind integral equation with the single layer, but approximated the surface only by triangles (i.e. piecewise linears). We needed to take second degree polynomials to be able to compute the Hessian from the single layer potential to get reasonable numerical results (see Section 5.2). Of course, in view of Nédélec's result we therefore should take higher order elements to approximate the surface updates in the Nash-Hörmander algorithm. But this will require further software development which is topic of future research. Instead, we have taken a sufficiently fine initial mesh, hence fine approximation of the starting surface by triangles and applied heat kernel smoothing to obtain a running implementation.*

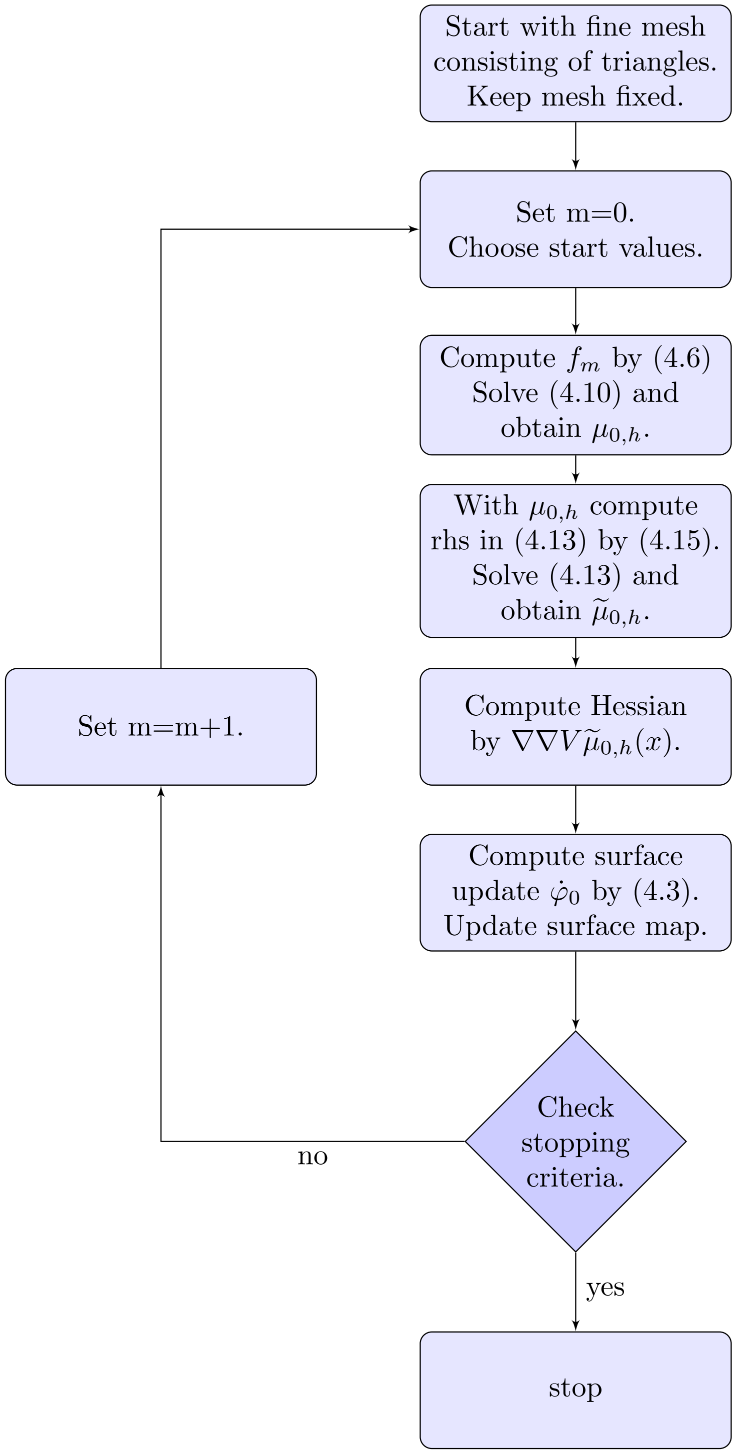

Figure 4.1.: Nash-Hörmander method

4.2. Nash-Hörmander Algorithm without Smoother

In this section we identify the Nash-Hörmander algorithm for the Molodensky problem.

Let us recall the abstract Nash-Hörmander method. As in Section 2.2 we set for some large θ_0, κ

$$\theta_k = (\theta_0^\kappa + k)^{1/\kappa}, \quad \triangle_k = \theta_{k+1} - \theta_k. \tag{4.37}$$

Now, we want to analyse the algorithm for the case without smoother. Thus, by setting $S_\theta = id$, where S_θ denotes the smoothing operator which has the properties listed in Theorem A.10, by noting that $v_k = u_k$ we deduce from (2.11)

$$u_{k+1} = u_k + \triangle_k \dot{u}_k, \quad \dot{u}_k = \Psi(u_k) g_k. \tag{4.38}$$

We also note that (2.12) can be replaced by

$$\begin{aligned} \Phi(u_{k+1}) - \Phi(u_k) &= \Phi(u_k + \triangle_k \dot{u}_k) - \Phi(u_k) - \Phi'(u_k)\triangle_k \dot{u}_k + \triangle_k g_k \\ &= \triangle_k (g_k + e_k). \end{aligned} \tag{4.39}$$

The absence of smoothing implies that $e_k' = 0$ in (2.13), which means that the error e_k in (2.13) is just given by the linearization error e_k'' defined as

$$e_k'' = (\Phi(u_k + \triangle_k \dot{u}_k) - \Phi(u_k) - \Phi'(u_k)\triangle_k \dot{u}_k)/\triangle_k. \tag{4.40}$$

Now, let us rewrite the abstract algorithm for the particular case of the Molodensky problem.
We define $u := [W, \varphi] : \mathbb{S}^2 \to \mathbb{R} \times \mathbb{R}^3$ and set $\dot{u} = [\dot{W}, \dot{\varphi}], \dot{u}_k = [\dot{W}_k, \dot{\varphi}_k]$. Using now (4.38) we have

$$W_{k+1} = W_k + \triangle_k \dot{W}_k, \quad \varphi_{k+1} = \varphi_k + \triangle_k \dot{\varphi}_k \quad \text{and} \quad (\dot{W}_k, \dot{\varphi}_k) = \Psi(W_k, \varphi_k) g_k. \tag{4.41}$$

From (4.39) we deduce

$$\begin{aligned} \Phi(W_{k+1}, \varphi_{k+1}) - \Phi(W_k, \varphi_k) &= \Phi(W_k + \triangle_k \dot{W}_k, \varphi_k + \triangle_k \dot{\varphi}_k) - \Phi(W_k, \varphi_k) \\ &\quad - \Phi'(W_k, \varphi_k)\triangle_k \begin{pmatrix} \dot{W}_k \\ \dot{\varphi}_k \end{pmatrix} + \triangle_k g_k = \triangle_k (g_k + e_k) \end{aligned}$$

where we have defined

$$\triangle_k e_k := \Phi(W_k + \triangle_k \dot{W}_k, \varphi_k + \triangle \dot{\varphi}_k) - \Phi(W_k, \varphi_k) - \Phi'(W_k, \varphi_k)\triangle_k \begin{pmatrix} \dot{W}_k \\ \dot{\varphi}_k \end{pmatrix}. \tag{4.42}$$

We set accordingly to (3.57) and (3.58) $\Phi(W, \varphi) = \begin{pmatrix} \Gamma(W, \varphi) \\ W \end{pmatrix}$ and $\Gamma(W, \varphi) = G$.

Thus, we deduce from (4.42)

$$\begin{aligned}
\triangle_k e_k &= \Phi(W_k + \triangle_k \dot{W}_k, \varphi_k + \triangle \dot{\varphi}_k) - \Phi(W_k, \varphi_k) - \Phi'(W_k, \varphi_k)\triangle_k \begin{pmatrix} \dot{W}_k \\ \dot{\varphi}_k \end{pmatrix} \\
&= \begin{pmatrix} \Gamma(W_k + \triangle_k \dot{W}_k, \varphi_k + \triangle_k \dot{\varphi}_k) \\ W_k + \triangle_k \dot{W}_k \end{pmatrix} - \begin{pmatrix} \Gamma(W_k, \varphi_k) \\ W_k \end{pmatrix} - \begin{pmatrix} \Gamma'(W_k, \varphi_k)\triangle_k \begin{pmatrix} \dot{W}_k \\ \dot{\varphi}_k \end{pmatrix} \\ \triangle_k \dot{W}_k \end{pmatrix} \\
&= \begin{pmatrix} \Gamma(W_k + \triangle_k \dot{W}_k, \varphi_k + \triangle_k \dot{\varphi}_k) - \Gamma(W_k, \varphi_k) - \Gamma'(W_k, \varphi_k)\triangle_k \begin{pmatrix} \dot{W}_k \\ \dot{\varphi}_k \end{pmatrix} \\ 0 \end{pmatrix} \\
&= \begin{pmatrix} G_{k+1} - G_k - \triangle_k g_k^1 \\ 0 \end{pmatrix}.
\end{aligned}$$

Here we have used (4.41) and the fact that $\Psi(W_k, \varphi_k)$ has a right inverse $\Phi'(W_k, \varphi_k)$ and therefore we have

$$\triangle_k \Phi'(W_k, \varphi_k) \begin{pmatrix} \dot{W}_k \\ \dot{\varphi}_k \end{pmatrix} = \begin{pmatrix} \Gamma'(W_k, \varphi_k)\triangle_k \begin{pmatrix} \dot{W}_k \\ \dot{\varphi}_k \end{pmatrix} \\ \triangle_k \dot{W}_k \end{pmatrix} = \triangle_k g_k := \triangle_k \begin{pmatrix} g_k^1 \\ g_k^2 \end{pmatrix}.$$

In conclusion we have

$$\triangle_k e_k = \begin{pmatrix} G_{k+1} - G_k - \triangle_k g_k^1 \\ 0 \end{pmatrix}. \tag{4.43}$$

Now, recalling (2.15) by setting $S_\theta = id$ and denoting by W_{meas} the given values for the gravity potential and by G_{meas} the given values for the gravity vector we have

$$\triangle_0 g_0 = f = \begin{pmatrix} G_{meas} - G_0 \\ W_{meas} - W_0 \end{pmatrix} \tag{4.44}$$

$$\triangle_k g_k = (-\triangle_{k-1} e_{k-1}). \tag{4.45}$$

Using (4.44) and noting that $\triangle_0 g_0^1 = G_{meas} - G_0$ we obtain from (4.45)

$$\begin{aligned}
\triangle_1 g_1 = -\triangle_0 e_0 &= \begin{pmatrix} -(G_1 - G_0 - \triangle_0 g_0^1) \\ 0 \end{pmatrix} = \begin{pmatrix} G_{meas} - G_1 \\ 0 \end{pmatrix} \\
\triangle_2 g_2 = -\triangle_1 e_1 &= \begin{pmatrix} -(G_2 - G_1 - \triangle_0 g_1^1) \\ 0 \end{pmatrix} = \begin{pmatrix} G_{meas} - G_2 \\ 0 \end{pmatrix}
\end{aligned}$$

and summarising we have

$$\triangle_k g_k = \begin{pmatrix} G_{meas} - G_k \\ 0 \end{pmatrix}.$$

Algorithm 4.1. *(Nash-Hörmander Algorithm without Smoother)*

---

1. *For given measured data* W_{meas}, G_{meas} *choose* $W_0, G_0, h_0, \varphi_0, \theta_0 \gg 1, \kappa \gg 1$
2. *For* $m = 0, 1, 2, \ldots$ *do*
   a) *Compute* $\theta_m = (\theta_0^\kappa + m)^{1/\kappa}, \triangle_m = \theta_{m+1} - \theta_m$ *and*
   $$\dot{G}_m = \frac{G_{meas} - G_m}{\triangle_m}$$
   b) *Compute*
   $$\dot{W}_m = \begin{cases} \frac{W_{meas} - W_0}{\triangle_0}, & for \quad m = 0 \\ 0, & for \quad m \geq 1 \end{cases}$$
   c) *Find* u_m *by solving the linearized problem (4.2)*
   d) *Find* $\overline{v}_m$ *by solving (4.5) with* w_m^{total} *as defined in (4.4)*
   e) *Compute* $g_m = \nabla \overline{v}_m$ *and* $\nabla g_m = \nabla^2 \overline{v}_m$
   f) *Compute the surface increment* $\dot{\varphi}_m$ *by*
   $$\dot{\varphi}_m = (\nabla g_m \circ \varphi_m)^{-1} (\dot{G}_m - \nabla u_m \circ \varphi_m)$$
   and update surface map by $\varphi_{m+1} = \varphi_m + \triangle_m \dot{\varphi}_m$
   g) *Update direction vector and gravity potential by*
   $$h_{m+1} = ((-(\nabla g_m)^{-1} g_m) \circ \varphi_m) \circ (\varphi_{m+1})^{-1}$$
   $$G_{m+1} = g_m \circ \varphi_m$$
   h) *Stop if* $\|g_m \circ \varphi_m - G_{meas}\| < tol$

Alltogether, this algorithm gives us a strategy how to compute the right hand side terms in (4.2) and the update $\dot{\varphi}_m$ via $\dot{W}_m, \dot{G}_m$ and hence, f_m in the Galerkin scheme (4.9).

4.3. Nash-Hörmander Algorithm with Smoother

As already shown by Hörmander [19], his algorithm needs a smoother- without it does not converge. In the following, we describe how the abstract Nash-Hörmander algorithm with smoother can be applied to the Molodensky problem. As in subsection (4.2) we set for some large θ_0, κ

$$\theta_k = (\theta_0^\kappa + k)^{1/\kappa}, \quad \triangle_k = \theta_{k+1} - \theta_k.$$

We want to analyse now the algorithm with smoother. We denote by S_θ the smoothing operator which has the properties listed in Theorem A.10. Now we recall (2.11), i.e.

$$u_{k+1} = u_k + \triangle_k \dot{u}_k, \quad \dot{u}_k = \psi(v_k) g_k, \quad v_k = S_{\theta_k} u_k. \tag{4.46}$$

We define again for the case of the Molodensky problem $u := [W, \varphi] : \mathbb{S}^2 \to \mathbb{R} \times \mathbb{R}^3$ and set $\dot{u} = [\dot{W}, \dot{\varphi}]$, $\dot{u}_k = [\dot{W}_k, \dot{\varphi}_k]$.
From (4.46) we deduce

$$\begin{aligned} W_{k+1} &= W_k + \triangle_k \dot{W}_k & \varphi_{k+1} &= \varphi_k + \triangle_k \dot{\varphi}_k \\ (\dot{W}_k, \dot{\varphi}_k) &= \Psi(\widetilde{W}_k, \widetilde{\varphi}_k) g_k & (\widetilde{W}_k, \widetilde{\varphi}_k) &= S_{\theta_k}(W_k, \varphi_k). \end{aligned} \tag{4.47}$$

Now, by recalling (2.12) we have

$$\begin{aligned} \Phi(W_{k+1}, \varphi_{k+1}) - \Phi(W_k, \varphi_k) &= \Phi(W_k + \triangle_k \dot{W}_k, \varphi_k + \triangle_k \dot{\varphi}_k) - \Phi(W_k, \varphi_k) \\ &\quad - \Phi'(W_k, \varphi_k) \triangle_k \begin{pmatrix} \dot{W}_k \\ \dot{\varphi}_k \end{pmatrix} \\ &\quad + (\Phi'(W_k, \varphi_k) - \Phi'(\widetilde{W}_k, \widetilde{\varphi}_k)) \triangle_k \begin{pmatrix} \dot{W}_k \\ \dot{\varphi}_k \end{pmatrix} \\ &\quad + \triangle_k g_k = \triangle_k (g_k + e_k) \end{aligned}$$

where we defined

$$\begin{aligned} e_k &:= e_k' + e_k'', \quad e_k' := (\Phi'(W_k, \varphi_k) - \Phi'(\widetilde{W}_k, \widetilde{\varphi}_k)) \begin{pmatrix} \dot{W}_k \\ \dot{\varphi}_k \end{pmatrix} \\ e_k'' &:= (\Phi(W_k + \triangle_k \dot{W}_k, \varphi_k + \triangle_k \dot{\varphi}_k) - \Phi(W_k, \varphi_k) \\ &\quad - \Phi'(W_k, \varphi_k) \triangle_k \begin{pmatrix} \dot{W}_k \\ \dot{\varphi}_k \end{pmatrix})/\triangle_k. \end{aligned} \tag{4.48}$$

We set accordingly to (3.57) and (3.58) $\Phi(W, \varphi) = \begin{pmatrix} \Gamma(W, \varphi) \\ W \end{pmatrix}$ and $\Gamma(W, \varphi) = G$ and define

$$\dot{G} := \Gamma'(W, \varphi) \begin{pmatrix} \dot{W} \\ \dot{\varphi} \end{pmatrix} \tag{4.49}$$

the Fréchet derivative of Γ in (W, φ) in the direction $(\dot{W}, \dot{\varphi})$. Now let us first analyse the smoothing error e'_k. We have

$$
\begin{aligned}
e'_k &= \Phi'(W_k, \varphi_k)\begin{pmatrix}\dot{W}_k\\ \dot{\varphi}_k\end{pmatrix} - \Phi'(\tilde{W}_k, \tilde{\varphi}_k)\begin{pmatrix}\dot{W}_k\\ \dot{\varphi}_k\end{pmatrix}\\
&= \begin{pmatrix}\Gamma'(W_k,\varphi_k)\begin{pmatrix}\dot{W}^k\\ \dot{\varphi}^k\end{pmatrix}\\ (\mathbb{I},0)\begin{pmatrix}\dot{W}^k\\ \dot{\varphi}^k\end{pmatrix}\end{pmatrix} - \begin{pmatrix}\Gamma'(\widetilde{W}_k,\widetilde{\varphi}_k)\begin{pmatrix}\dot{W}^k\\ \dot{\varphi}^k\end{pmatrix}\\ (\mathbb{I},0)\begin{pmatrix}\dot{W}^k\\ \dot{\varphi}^k\end{pmatrix}\end{pmatrix}\\
&= \begin{pmatrix}\Gamma'(W_k,\varphi_k)\begin{pmatrix}\dot{W}^k\\ \dot{\varphi}^k\end{pmatrix} - \Gamma'(\widetilde{W}_k,\widetilde{\varphi}_k)\begin{pmatrix}\dot{W}^k\\ \dot{\varphi}^k\end{pmatrix}\\ 0\end{pmatrix} = \begin{pmatrix}\dot{G}_k - g_k^1\\ 0\end{pmatrix}
\end{aligned}
$$

where we have used (4.47) and the fact that $\Psi(W_k, \varphi_k)$ has a right inverse $\Phi'(W_k, \varphi_k)$. Now we consider the linearization error e''_k:

$$
\begin{aligned}
\triangle_k e''_k &= \Phi(W_k + \triangle_k \dot{W}_k, \varphi_k + \triangle\dot{\varphi}_k) - \Phi(W_k,\varphi_k) - \Phi'(W_k,\varphi_k)\triangle_k\begin{pmatrix}\dot{W}_k\\ \dot{\varphi}_k\end{pmatrix}\\
&= \begin{pmatrix}\Gamma(W_k + \triangle_k\dot{W}_k, \varphi_k + \triangle_k\dot{\varphi}_k)\\ W_k + \triangle_k\dot{W}_k\end{pmatrix} - \begin{pmatrix}\Gamma(W_k,\varphi_k)\\ W_k\end{pmatrix} - \begin{pmatrix}\Gamma'(W_k,\varphi_k)\triangle_k\begin{pmatrix}\dot{W}_k\\ \dot{\varphi}_k\end{pmatrix}\\ \dot{W}_k\end{pmatrix}\\
&= \begin{pmatrix}\Gamma(W_k + \triangle_k\dot{W}_k, \varphi_k + \triangle_k\dot{\varphi}_k) - \Gamma(W_k,\varphi_k) - \Gamma'(W_k,\varphi_k)\triangle_k\begin{pmatrix}\dot{W}_k\\ \dot{\varphi}_k\end{pmatrix}\\ 0\end{pmatrix}\\
&= \begin{pmatrix}G_{k+1} - G_k - \triangle_k\dot{G}_k\\ 0\end{pmatrix}.
\end{aligned}
$$

Now, the first equation in (2.15) gives

$$
\triangle_0 g_0 = S_{\theta_0} f = S_{\theta_0}\begin{pmatrix}G_{meas} - G_0\\ W_{meas} - W_0\end{pmatrix}. \tag{4.50}
$$

Furthermore, the second equation in (2.15) is

$$
\triangle_k g_k = (S_{\theta_k} - S_{\theta_{k-1}})(f - E_{k-1}) - S_{\theta_k}\triangle_{k-1}e_{k-1} \tag{4.51}
$$

with $E_k = \sum_0^{k-1}\triangle_j e_j$ and thus $E_0 = 0$.
First we analyse the first component of g_k which we denote by g_k^1. From (4.50) we have $\triangle_0 g_0^1 = S_{\theta_0}(G_{meas} - G_0)$ and we deduce using (4.51)

$$
\begin{aligned}
\triangle_1 g_1^1 &= (S_{\theta_1} - S_{\theta_0})(G_{meas} - G_0) - \triangle_0 S_{\theta_1}(\dot{G}_0 - g_0^1) - S_{\theta_1}(G_1 - G_0 - \triangle_0\dot{G}_0)\\
&= (S_{\theta_1} - S_{\theta_0})(G_{meas} - G_0) - \triangle_0 S_{\theta_1}(\dot{G}_0 - g_0^1 + \frac{G_1 - G_0}{\triangle_0} - \dot{G}_0)\\
&= S_{\theta_1}(G_{meas} - G_0 + \triangle_0 g_0^1 - G_1 + G_0) - S_{\theta_0}(G_{meas} - G_0)\\
&= S_{\theta_1}(G_{meas} - G_1 + \triangle_0 g_0^1) - S_{\theta_0}(G_{meas} - G_0).
\end{aligned}
$$

By noting that $E_1 = \begin{pmatrix} \triangle_0 e_0^1 \\ 0 \end{pmatrix} = \triangle_0 \begin{pmatrix} (e_0')^1 + (e_0'')^1 \\ 0 \end{pmatrix}$ we have

$$\triangle_0 e_0^1 = G_1 - G_0 - \triangle_0 g_0^1 \tag{4.52}$$

and we deduce

$$\begin{aligned}\triangle_2 g_2^1 &= (S_{\theta_2} - S_{\theta_1})(G_{meas} - G_0 - \triangle_0 e_0) - \triangle_1 S_{\theta_2} e_1^1 \\ &= S_{\theta_2}(G_{meas} - G_2 + \triangle_0 g_0^1 + \triangle_1 g_1^1) - S_{\theta_1}(G_{meas} - G_1 + \triangle_0 g_0^1).\end{aligned}$$

In summary, we have

$$\begin{aligned}\triangle_0 g_0^1 &= S_{\theta_0}(G_{meas} - G_0), \\ \triangle_1 g_1^1 &= S_{\theta_1}(G_{meas} - G_1 + \triangle_0 g_0^1) - S_{\theta_0}(G_{meas} - G_0), \\ \triangle_2 g_2^1 &= S_{\theta_2}(G_{meas} - G_2 + \triangle_0 g_0^1 + \triangle_1 g_1^1) - S_{\theta_1}(G_{meas} - G_1 + \triangle_0 g_0^1), \\ &\vdots \\ \triangle_k g_k^1 &= S_{\theta_k}(G_{meas} - G_k + \sum_{j=0}^{k-1} \triangle_j g_j^1) - S_{\theta_{k-1}}(G_{meas} - G_{k-1} + \sum_{j=0}^{k-2} \triangle_j g_j^1).\end{aligned}$$

Since the second component of e_k' and e_k'' is zero, we have for g_k in total

$$\triangle_k g_k = S_{\theta_k} \begin{pmatrix} G_{meas} - G_k + \sum_{j=0}^{k-1} \triangle_j g_j^1 \\ W_{meas} - W_0 \end{pmatrix} - S_{\theta_{k-1}} \begin{pmatrix} G_{meas} - G_{k-1} + \sum_{j=0}^{k-2} \triangle_j g_j^1 \\ W_{meas} - W_0 \end{pmatrix}.$$

Remark 4.2. *In the special case that both, the initial and final surface are spheres, W_{meas} and W are both constants. Therefore, its apparent that $S_{\theta_k}(W_{meas} - W_0) = W_{meas} - W_0$. Hence, the second component in g_k is always zero except for g_0.*

Algorithm 4.2. *(Nash-Hörmander Algorithm with Smoother)*

---

1. *For given measured data W_{meas}, G_{meas} choose $W_0, G_0, h_0, \varphi_0, \theta_0 \gg 1, \kappa \gg 1$*
2. *For $m = 0, 1, 2, \dots$ do*
   a) *Compute*
   $$\theta_m = (\theta_0^\kappa + m)^{1/\kappa}, \quad \triangle_m = \theta_{m+1} - \theta_m \tag{4.53}$$
   b) *Compute*
   $$\dot{W}_m = \begin{cases} \frac{W_{meas} - W_0}{\triangle_0}, & \textit{for} \quad m = 0 \\ 0, & \textit{for} \quad m \geq 1 \end{cases}$$

c) *Compute*

$$\dot{\tilde{G}}_0 := S_{\theta_0}\dot{G}_0 = S_{\theta_0}\big(\frac{G_{meas} - G_0}{\triangle_0}\big)$$

$$\dot{\tilde{G}}_m := \frac{1}{\triangle_k}\big(S_{\theta_k}(G_{meas} - G_m + \sum_{j=0}^{m-1}\triangle_j\dot{\tilde{G}}_j) - S_{\theta_{k-1}}(G_{meas} - G_{m-1} + \sum_{j=0}^{m-2}\triangle_j\dot{\tilde{G}}_j)\big) \tag{4.54}$$

d) *Find u_m by solving the linearized problem (4.2) with $\dot{G}_m$ replaced by $\dot{\tilde{G}}_m$*

e) *Find $\overline{v}_m$ by solving (4.5) with w_m^{total} as defined in (4.4)*

f) *Compute $g_m = \nabla\overline{v}_m$ and $\nabla g_m = \nabla^2\overline{v}_m$*

g) *Compute the surface increment $\dot{\varphi}_m$ by*

$$\dot{\varphi}_m = (\nabla g_m \circ \varphi_m)^{-1}(\dot{\tilde{G}}_m - \nabla u_m \circ \varphi_m)$$

and update surface map by $\varphi_{m+1} = \varphi_m + \triangle_m\dot{\varphi}_m$

h) *Update direction vector and gravity potential by*

$$h_{m+1} = ((-(\nabla g_m)^{-1}g_m)\circ\varphi_m)\circ(\varphi_{m+1})^{-1}$$
$$G_{m+1} = g_m \circ \varphi_m$$

i) *Stop if $\|g_m \circ \varphi_m - G_{meas}\| < tol$*

Algorithm 4.3. *(Nash-Hörmander Algorithm with Smoother and Restart)*

---

1. *For given measured data W_{meas}, G_{meas} choose $W_0, G_0, h_0, \varphi_0, \theta_0 \gg 1, \kappa \gg 1$*
2. *For $l = 0, 1, 2, \dots$ do*
3. *For $m = 0, 1, 2, \dots$ do*

a) *Compute $\theta_m = (\theta_0^\kappa + m)^{1/\kappa}, \triangle_m = \theta_{m+1} - \theta_m$*

b) *Compute*

$$\dot{W}_m = \begin{cases} \frac{W_{meas}-W_0}{\triangle_0}, & \text{for} \quad m = 0 \\ 0, & \text{for} \quad m \geq 1 \end{cases}$$

c) *Compute*

$$\dot{\tilde{G}}_0 := S_{\theta_0}\dot{G}_0 = S_{\theta_0}\big(\frac{G_{meas} - G_0}{\triangle_0}\big)$$

$$\dot{\tilde{G}}_m := \frac{1}{\triangle_k}\big(S_{\theta_k}(G_{meas} - G_m + \sum_{j=0}^{m-1}\triangle_j\dot{\tilde{G}}_j) - S_{\theta_{k-1}}(G_{meas} - G_{m-1} + \sum_{j=0}^{m-2}\triangle_j\dot{\tilde{G}}_j)\big)$$

d) Find u_m by solving the linearized problem (4.2) with $\dot{G}_m$ replaced by $\dot{\tilde{G}}_m$

e) Find $\overline{v}_m$ by solving (4.5) with w_m^{total} as defined in (4.4)

f) Compute $g_m = \nabla \overline{v}_m$ and $\nabla g_m = \nabla^2 \overline{v}_m$

g) Compute the surface increment $\dot{\varphi}_m$ by

$$\dot{\varphi}_m = (\nabla g_m \circ \varphi_m)^{-1}(\dot{\tilde{G}}_m - \nabla u_m \circ \varphi_m)$$

and update surface map by $\varphi_{m+1} = \varphi_m + \triangle_m \dot{\varphi}_m$

h) Update direction vector and gravity potential by

$$\begin{aligned} h_{m+1} &= ((-(\nabla g_m)^{-1} g_m) \circ \varphi_m) \circ (\varphi_{m+1})^{-1} \\ G_{m+1} &= g_m \circ \varphi_m \end{aligned}$$

i) Stop if $\|g_m \circ \varphi_m - G_{meas}\| < tol$

4. Set $G_0 = G_m, h_0 = h_m, \varphi_0 = \varphi_m, \theta_0 = \theta_m$, chose κ, compute W_0 and go to 2

Remark 4.3. *In the notation of this section, using Proposition 2.1, we have*

$$\begin{aligned} \|(W,\varphi) - (W_k^{(l)}, \varphi_k^{(l)})\|_{a+\epsilon} \leq & \Big(\prod_{j=1}^{l-1} \mathscr{C}(j)\Big)(C_\tau \mathfrak{C}(\theta_k^{E+1+\tau})^{(0)}) \\ & \cdot \|(W_{meas} - W_0, G_{meas} - G_0)\|_{(l-1)(\alpha-a+3)+\alpha+\epsilon}. \end{aligned}$$

4.4. Heat Equation and Smoothing

We first recall the standard smoothing operators used to prove the Inverse Function Theorem for suitable Fréchet spaces of functions. Let $\phi \in C_0^\infty(\mathbb{R})$, then

$$S_\theta^{th} u := \phi(\frac{1}{\theta}\nabla)u.$$

They have the following properties ([19, Theorem A.10])

Properties 4.1. *For all $u \in C^\infty(\varphi(\mathbb{S}^2))$ we have*

(0) $\|S_\theta u - u\|_a \stackrel{\theta\to\infty}{\longrightarrow} 0$;

(i) $\|S_\theta u\|_b \leq C\|u\|_a, \quad b \leq a$;

(ii) $\|S_\theta u\|_b \leq C\theta^{b-a}\|u\|_a, \quad a \leq b$;

(iii) $\|u - S_\theta u\|_b \leq C\theta^{b-a}\|u\|_a, \quad b \leq a$;

(iv) $\left\| \frac{d}{d\theta} S_\theta u \right\|_b \leq C\theta^{b-a-1} \|u\|_a$.

However, the corresponding oscillatory integral kernels cannot be stably implemented. Instead, smoothing using the heat equation is frequently used in practice, see e.g [10, Jerome].
More generally than the heat equation, we endow the submanifold $\varphi(\mathbb{S}^2) \subseteq \mathbb{R}^3$ with the metric induced from $\mathbb{R}^3$ and consider the smoothing operator associated to $\phi(x) = e^{-|x|^{2k}}$. I.e. we consider the time $-1/\theta^{2k}$ solution

$$S_\theta u = e^{\frac{1}{\theta^{2k}} A} u = \phi(\frac{1}{\theta}\nabla) u$$

of the higher heat equation

$$\begin{aligned} \frac{d}{dt} v(x,t) - Av(x,t) = 0 \qquad &\text{in} \quad \varphi_m(\mathbb{S}^2) \times (0,\infty) \\ v(x,0) = u(x) \;\; &\text{in} \quad \varphi_m(\mathbb{S}^2) \end{aligned}$$

with the Laplace Beltrami operator Δ, where $A := (-1)^k \Delta^k$ and $u \in \mathscr{H}^a$. Considering $A : \mathscr{H}^{a+2k} \subset \mathscr{H}^a \to \mathscr{H}^a$ as an unbounded operator on the Hölder spaces ($a > 0, a \notin \mathbb{N}$) we have the following theorem.

Theorem 4.1. *A generates an analytic semigroup e^{tA} on $\mathscr{H}^a$ and the operator $S_\theta := e^{\frac{1}{\theta^{2k}} A}$ satisfies the properties (0), (i), (ii), (iv) and in addition*

$$(iii') \qquad \|u - S_\theta u\|_b \leq C\theta^{b-a} \|u\|_a, \quad \forall\, 0 \leq b - a < 2k.$$

We are briefly going to outline the functional-analytic background of these results.
As above, we consider the operator A as an unbounded operator on the Hölder space $\mathscr{H}^a$ with domain $D(A) = \mathscr{H}^{a+2}$ (if $a \notin \mathbb{N}_0$). Using [45, Shubin, Theorem 9.3], we see that $A - \lambda$ is invertible for $\lambda \in \mathcal{S}_{\theta,0} = \{\lambda \in \mathbb{C} : \|\arg(\lambda) < \theta\|\}$, $\theta \in (\pi/2, \pi)$, and that $(A-\lambda)^{-1}$ is a pseudodifferential operator, depending on the parameter λ, whose symbol decays as $\frac{C}{|\lambda|}$. The mapping properties [50, Taylor, Proposition 8.6] of such operators in Hölder spaces, which are analogous to those for Sobolev spaces, therefore imply

$$\|(A-\lambda)^{-1} u\|_{\mathscr{H}^a} \leq \frac{C}{|\lambda|} \|u\|_{\mathscr{H}^a}, \quad \forall\, \lambda \in S_{\theta,0}. \tag{4.55}$$

The theory of analytic semigroups is based on the more general notion of a sectorial operator on a complex Banach space $(X, \|\cdot\|)$.

Definition 4.1. *A is said to be sectorial if there are constants $\omega \in \mathbb{R}, \theta \in]\pi/2, \pi[, C > 0$ such that*

$$\begin{cases} (i) \quad \sigma(A) \supset \mathcal{S}_{\theta,\omega} = \{\lambda \in \mathbb{C} : \lambda \neq \omega, |arg(\lambda - \omega)| < \theta\}, \\ (ii) \quad \|(A-\lambda)^{-1} u\|_X \leq \frac{C}{|\lambda - \omega|} \|u\|_X, \quad \forall\, \lambda \in \mathcal{S}_{\theta,\omega}. \end{cases} \tag{4.56}$$

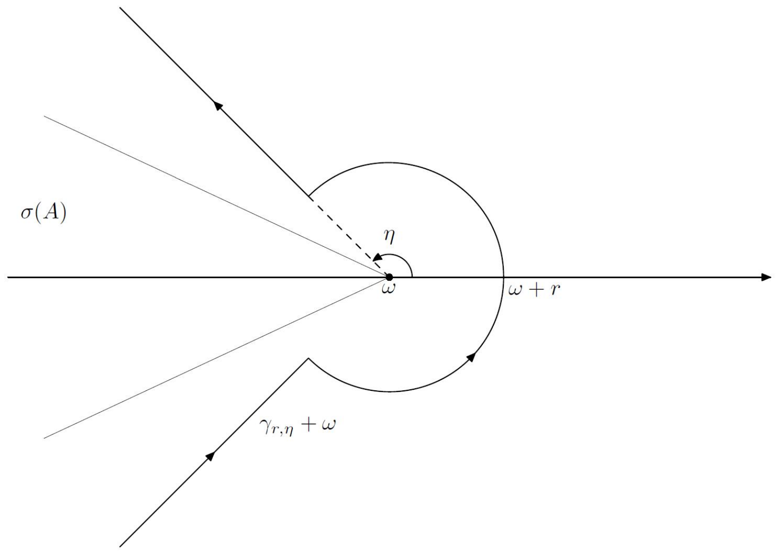

Figure 4.2.: The curve $\gamma_{r,\eta}$

If A is sectorial, we define

$$e^{tA}u := \frac{1}{2\pi i}\int_{\omega+\gamma_{r,\eta}} e^{t\lambda}(A-\lambda)^{-1}u\,d\lambda, \quad t>0, \tag{4.57}$$

the analytic semigroup generated by A, where $r>0, \eta \in]\pi/2, \theta[$ and $\gamma_{r,\eta}$ is the curve $\{\lambda \in \mathbb{C} : |\arg\lambda| = \eta, |\lambda| \geq r\} \cap \{\lambda \in \mathbb{C} : |\arg\lambda| \leq \eta, |\lambda| = r\}$, oriented counterclockwise (see Figure 4.2).

e^{tA} has the following properties:

Proposition 4.6 (Proposition 2.1.1, [23]). *(i)* $\|e^{tA}u\|_X \leq C_0 e^{\omega t}\|u\|_X, \quad \forall t \geq 0.$

(ii) $e^{tA}e^{sA} = e^{(t+s)A}, \quad \forall\, t,s \geq 0.$

(iii) $\lim_{t\to 0^+} \|e^{tA}u - u\|_X = 0, \quad \forall\, u \in \overline{D(A)}.$

(iv) There are constants $C_0, C_1, C_2, \ldots,$ such that

$$\|t^l(A-\omega I)^l e^{tA}u\|_X \leq C_k e^{\omega t}\|u\|_X, \quad t>0. \tag{4.58}$$

(v) $t \mapsto e^{tA}$ is a real-analytic function from $(0,\infty)$ to the Banach space of bounded linear operators on X (with norm given by the operator norm) and

$$\frac{d^l}{dt^l}e^{tA} = A^l e^{tA}, \quad t>0. \tag{4.59}$$

Let us now outline the proof of Theorem 4.1 recalling that by (4.55) $\omega = 0$. First, let us prove Property 4.1(i). Using Proposition 4.6(i) and the fact that $S_\theta = e^{tA}$ is a continuous operator on $\mathscr{H}^b$ we have

$$\|e^{tA}u\|_b \leq C\|u\|_b \leq C\|u\|_a, \quad \forall\, b \leq a$$

and thus, Property 4.1(i).
In order to prove Property 4.1(ii), we first note that by Proposition 4.6(iv) with $\omega = 0$

$$\|t^l A^l e^{tA} u\|_a \leq C_k \|u\|_a, \quad 0 < t \leq 1.$$

Using the fact that $(A-\lambda)^{-1} : \mathscr{H}^a \to \mathscr{H}^{a+2k}$ is continuous, with $\|(A-\lambda)^{-1}u\|_{\mathscr{H}^{a+2k}} \leq C\|u\|_{\mathscr{H}^a}$ independent of λ, we have

$$\|v\|_{a+2k} \leq C\|(A-\lambda)v\|_a \leq C\|Av\|_a + C|\lambda|\|v\|_a.$$

We first set $l = 1$ and $v = te^{tA}u$ and deduce

$$\frac{1}{\tilde{C}}\|te^{tA}u\|_{a+2k} \leq \frac{C}{\tilde{C}}\|(A-\lambda)te^{tA}u\|_a \leq \|tAe^{tA}u\|_a + |\lambda|\|te^{tA}u\|_a \tag{4.60}$$

and by using Proposition 4.6(i) and Proposition 4.6(iv) we have

$$|\lambda|\|te^{tA}u\|_a \leq |\lambda|\|e^{tA}u\|_a \leq C_0|\lambda|\|u\|_a, \quad 0 < t \leq 1,$$
$$\|tAe^{tA}u\|_a \leq C_1\|u\|_a$$

and finally by (4.60) we obtain

$$\|te^{tA}u\|_{a+2k} \leq \bar{C}\|u\|_a.$$

By iterating this argument l-times using

$$\|t^l e^{tA}u\|_{a+2kl} = l^l \|\frac{t}{l}e^{t/l}A \cdot_{\dots} \cdot \frac{t}{l}e^{t/l}Au\|_{a+2kl}$$

we have

$$\|t^l e^{tA}u\|_{a+2kl} \leq \tilde{\bar{C}}\|u\|_a$$

and setting $b = a + 2kl$, Property 4.1(ii) holds for this specific b.
For an arbitrary b, $\tilde{b} := a + 2kl \geq b$, write $b = \lambda a + (1-\lambda)\tilde{b}$. We then have by Theorem A.5

$$\|e^{tA}u\|_b \leq \|e^{tA}u\|_a^{\lambda}\|e^{tA}u\|_{\tilde{b}}^{1-\lambda} \leq Ct^{-l(1-\lambda)}\|u\|_a^{\lambda}\ \|u\|_a^{1-\lambda}$$

and we deduce

$$\|e^{tA}u\|_b \leq Ct^{-(1-\lambda)l}\|u\|_a = Ct^{-(b-a)/2k}\|u\|_a.$$

Setting now $S_\theta := e^{tA}$ with $t = \theta^{-2k}$ we have proved

$$\|S_\theta u\|_b \leq C\theta^{b-a}\|u\|_a$$

and thus, Property 4.1(ii) holds.
For Property 4.1(iv) we first need the following easy computation where we use $t = \theta^{-2k}$

$$\frac{d}{d\theta}e^{tA} = \frac{dt}{d\theta}\frac{d}{dt}e^{tA} = -2kt^{1/2k}(tAe^{tA}) = -\frac{2k}{\theta}tAe^{tA}$$

where by Proposition 4.6(v) we have

$$\frac{d}{dt}e^{tA} = Ae^{tA}$$

and we deduce by the same proof as for Property 4.1(ii) by setting $S_\theta = e^{tA}$

$$\left\|\frac{d}{d\theta}S_\theta u\right\|_b \leq \frac{2k}{\theta}\|tAe^{tA}u\|_b \leq \frac{2k}{\theta}C\theta^{b-a}\|u\|_a = \tilde{C}\theta^{b-a-1}\|u\|_a.$$

Finally, by using Proposition 4.6(iii) and setting again $S_\theta = e^{tA}$ and $t = \theta^{-2k}$ we have

$$\lim_{\theta\to\infty} S_\theta u = u, \quad \forall u \in \overline{\mathscr{H}^{2+a}} \tag{4.61}$$

and thus, Property 4.1(0) holds.
Concerning Theorem 4.1(iii') using a partition of the unity, it suffices to prove the result for a Laplace type operator on $\mathbb{R}^n$. However, for such operators one may use the discussion of Example 3.4 in [53, Trebels-Westphal], which also applies to Hölder spaces. Details will be discussed elsewhere.
For the Laplace operator on $\mathbb{S}^1$, an explicit proof may be found in Butzer-Berens [3, Theorem 2.4.17].

5. Numerical Results Based on Boundary Elements

5.1. Numerical Experiments

For the numerical experiments we set $\varphi : \mathbb{S}^2 \to \mathbb{R}^3$ to be $\varphi(x) = 1.1x$. This means that the sought surface is a sphere of radius 1.1. For such a sphere, the gravity potential $W_{meas} = \frac{1}{1.1}$ and the gravity vector $G_{meas} = -\frac{1}{1.1^2}\frac{x}{|x|}$, both defined on $\mathbb{S}^2$. The initial approximation φ_0 is the unit sphere $\mathbb{S}^2$. Therefore, $W_0 = 1$, $G_0 = -\frac{x}{|x|}$ and $h_0 = \frac{x}{2}$.

An approximation of the Nash-Hörmander solution sequence is obtained by Algorithms 4.1, 4.2 and 4.3. The initial sphere $\mathbb{S}^2$ is approximated by a regular, quasi-uniform mesh consisting of triangles such that the nodes of each triangle lie on $\mathbb{S}^2$. More precisely, the mesh defines an icosahedron which is generated by *maiprogs* [25]. This mesh yields a domain approximation error and is kept fixed for the entire Nash-Hörmander algorithm. The main advantage is that only the coordinates of the nodes have to be updated and not the entire mesh itself. This corresponds to a continuous, piecewise linear representation of φ_m, the new surface at the m-th update of the algorithm.

For reasons that are discussed in Section 5.2, the polynomial degree on each triangle is $p = 2$ and h_m is represented by a discontinuous piecewise constant function interpolating the h_m from equation (4.2) in the midpoints of each triangle. Furthermore, G_m is the linear interpolation of $g|_{\varphi_m(\mathbb{S}^2)}$, obtained from equation (4.5), in the nodes. The local basis functions are monomials for both the linearized Molodensky problem and for the auxiliary Dirichlet problem. This allows to use the analytical computation of the single layer potential as described in [24]. Furthermore, since h_m and the normal on each triangle $\mathcal{T}_n$ are piecewise constant, the jump contributions can be easily computed analytically as well. Again, since h_m is piecewise constant, the matrix $K'(h)$ in (4.7) can be computed semi-analytically by computing the action of the dual operator $K(h)$ on the test functions analytically [24] and performing an hp-composite Gauss quadrature [9, 42] for the outer integration. For that, the integration domain is split into 3 disjoint sets, the so called self-element, which contains the 3 edge singularities from inner integration, the near field, which are all the adjacent elements to the self-element and the remaining elements give the far field. In the far field, standard Gauss quadrature with Duffy transformation is used. For the self-element and near field, the current triangle over which is integrated is decomposed by a geometrically graded mesh with $\sigma = 0.17$ towards the singularities. The number of Gauss quadrature points in each direction

x and y increases linearly with the distance to the singularities. $\langle VA_j, \phi\rangle$ in (4.9) is computed analogously.

Since the finite element space is the same for both the linear Molodensky problem and the auxiliary Dirichlet problem, the single layer potential matrix is reused in (4.10). However, the computation of the right hand side for the Dirichlet problem is very CPU time consuming if a direct computation of (4.15) is used. Since the ansatz and test functions live on different surfaces, the computation of one summand in (4.15) is as expensive as a semi-analytic computation of a single layer potential matrix. In particular, the computational time for the right hand side increases drastically with the number of Nash-Hörmander iterations. The last term in (4.15) is obtained by simple matrix-vector multiplication of the analytically computed single layer potential V_m with the corresponding solution vector μ_m.

Since φ_m is piecewise linear, the Gauss quadrature nodes x for the outer integration are always mapped to exactly the same point on $\varphi_i(\mathbb{S}^2)$ under the mapping $\varphi_i \circ \varphi_m^{-1}(x)$ for each Nash-Hörmander iteration step m. Therefore, if enough memory is available, $V_i\mu_i(\varphi_i \circ \varphi_m^{-1}(x))$ must only be computed once and is stored for all the following iterations, keeping the computational time for the right hand side (4.15) constant for all iterations m. This optimization together with the following parallelization of the code leads to a tremendous reduction of computing time.

With the solution of the Dirichlet problem at hand, the update of the surface in the nodes can be performed as defined in equation (4.3) and with $g, \nabla g$ computed as in Section 5.2. The computation of one Nash-Hörmander iteration is very CPU time consuming and therefore, parallelization of the code is crucial. Without parallelization and optimization of the code we need $4+2m$ hours for the m-th iteration. However, with parallelization and optimization we need only 20 minutes for each of the m iterations for $N = 2$ -icosahedron refinements corresponding to 320 triangles whereas we need 3 hours for each of the m iterations for $N = 3$ -icosahedron refinements corresponding to 1280 triangles. The numerical experiments were carried out on a cluster with 5 nodes à 8 cores with 2.93Ghz and 48GB memory, where each core uses two Intel Nehalem X5570 processors.

In the following three different numerical experiments are presented. The first and the second experiment use the classical Nash-Hörmander algorithm without and with smoother. For the third experiment, the restarted algorithm presented in Section 2.3 with smoother is used.

Since the sought surface is also a sphere, we can expect that the sequences of computed surfaces are slightly perturbed spheres as well. The perturbation should be a direct result of the domain approximation, different discretization errors and rounding errors. Figure 5.1 displays the mean "l_2-radius errors" computed by

$$\|e_r\| = \frac{1}{nr.nodes}\Big[\sum_{i=1}^{nr.nodes} (\|nodes(i)\|_2 - 1.1)^2\Big]^{1/2}$$

versus the number of iterations of the Nash-Hörmander Algorithm 4.1 for the case without smoother. It is remarkable that the error increases after the first step, before decreasing again. This may be a result of the fact that from the second step onwards the right hand side in the linearized Molodensky problem is perturbed due to the approximation errors of the previous steps. Especially the update in φ is also perturbed. Contrary to the linearization error e''_j, the discretization error is not taken into account. Therefore, from the fifth iteration step onwards the propagation of the spacial discretization error, for solving the linearized Molodensky problem, the auxiliary Dirichlet problem and computing the Hessian approximatively, becomes dominating. Refining the mesh reduces the non monotonic behaviour of the error between Step 1 and Step 4, before increasing after Step 5.

The computation using $N = 4$ -icosahedron refinements is not possible due to the following consideration. It is well known that the BEM matrices, V and $K'(h)$ are dense, due to the non-local kernel. In particular, the number of non-zero entries are of order $O(6 \cdot h^{-4})$, where the factor 6 results from the polynomial degree 2, i.e. decreasing the mesh size by factor 2 increases the number of non-zero entries by factor 16. This rapid increase is the reason that only $N = 2$ and $N = 3$ could be used in our computations due to the restrictive memory constraints.

As presented in Section 4.4, heat kernel smoothing can be applied to the Nash-Hörmander algorithm since smoothing with the heat kernel fulfills Properties 4.1 which are crucial for Hörmander's method . To smooth an arbitrary function F, the heat equation with the Laplace-Beltrami operator is solved, where F is the initial data.

$$\begin{aligned} \frac{\partial}{\partial t} u(x,t) - \Delta u(x,t) = 0 \qquad & \text{in} \quad \varphi_m(\mathbb{S}^2) \times (0,\infty) \\ u(x,0) = F(x) \quad & \text{in} \quad \varphi_m(\mathbb{S}^2). \end{aligned}$$

The unique solution of this problem is given by

$$u(x,t) = \sum_{j=0}^{\infty} e^{-\lambda_j t} \langle F, \psi_j \rangle \psi_j(x). \tag{5.1}$$

At $t = 0$ we have

$$u(x,0) = \sum_{j=0}^{\infty} \beta_j \psi_j(x) = F(x)$$

where β_j are the Fourier coefficients $\langle F, \psi_j \rangle$. Here $0 = \lambda_0 < \lambda_1 \leq \lambda_2 \leq \ldots$ are the eigenvalues and $\psi_0, \psi_1, \psi_2, \ldots$ the corresponding eigenfunctions for the Laplace-Beltrami operator Δ, i.e. there holds

$$\Delta \psi_j = -\lambda_j \psi_j. \tag{5.2}$$

The eigenfunctions ψ_j form an othonormal basis in $L^2(\varphi(\mathbb{S}^2))$.

Having the discretized surface, (5.2) can be solved approximately using the FEM method with continuous piecewise linear polynomials leading to the generalized eigenvalue problem with the stiffness matrix C and the mass matrix A of the Laplace-Beltrami operator Δ

$$C\psi_h = \lambda_h A\psi_h \tag{5.3}$$

where ψ_h denotes the unknown L^2-orthonormal eigenfunction, evaluated at the mesh vertices. With ψ_h solving (5.3) the heat kernel can be approximated by

$$e^{-t\Delta}(x,y) = \sum_{j=0}^{M} e^{-t\lambda_{j,h}}\psi_{j,h}(x)\psi_{j,h}(y)$$

where M must be sufficiently large. Once we obtained the components $\psi_{j,h}$ of the eigenfunctions ψ_h, we compute the Fourier coefficients $\beta_{j,h}$ as presented in [44, Eqn. (10)]. Therewith,

$$u_h(x,t) = \sum_{j=0}^{M} e^{-\lambda_{j,h}t}\beta_{j,h}\psi_{j,h}(x). \tag{5.4}$$

For implementation details see [44]. For our numerical experiments F is always of the structure $G_{meas} - G_m + \sum_{j=0}^{m-1} \triangle_j \dot{\tilde{G}}_j$ (see (4.54)). We use $u_h(x, \frac{1}{\theta_m})$ where $t = \frac{1}{\theta_m}$ in (5.4) as the smoothed F, where θ_m is computed by (4.53). We have to take care that the amount of smoothing is successively reduced, such that in the limit ($m \to \infty$) the solution of the nonlinear Molodensky problem is obtained. The values for $\frac{1}{\theta_m}$ used in our numerical experiments are listed in Table 5.2.

We have performed several numerical experiments with different parameters θ_0, κ. We observed 3 problems. Firstly, if the amount of data smoothing is to small, then the results are similar to the unsmoothened case. Secondly, if the amount of data smoothing is too large, then essential information on the right hand side in the linearized Molodensky problem is lost and therefore also in its solution. Thirdly, if the amount of smoothing does not decay sufficiently fast, then the right hand side in the linearized Molodensky problem is close to machine precision. This implies that its solution and its gradient are close to 0 and therefore the update of φ will also be close to 0, leading to no visible convergence. Figure 5.2 shows a choice of parameters θ_0, κ for which none of the 3 above mentioned problems occur.

Figure 5.2 clearly displays that the effect of the discretization error propagation cannot be eliminated. However, increasing the amount of smoothing per iteration for a fixed mesh delays the point at which the discretization error propagation becomes dominating. Decreasing the mesh size, leads to a more even error reduction per iteration step. However, the error reduction per iteration step also decreases. It seems impossible to determine a priori up to which iteration point the error decreases before increasing again.

Figure 5.3 shows the mean "l_2-gravity vector errors" computed by

$$\|e_G\| = \frac{1}{nr.nodes}\Big[\sum_{i=1}^{nr.nodes}(G(i) - G_{meas}(i))^2\Big]^{1/2}$$

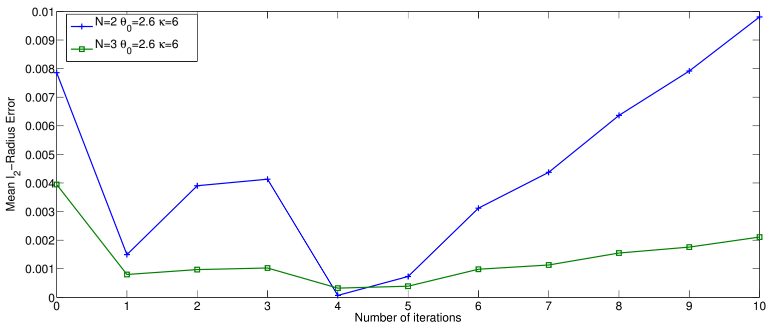

Figure 5.1.: Mean Radius-Error in the l_2-norm without smoother

for the algorithm with smoother. After the first Nash-Hörmander step, the error increases in each iteration step.

Figure 5.4 shows the pointwise error $\|u_N(\vec{q})-u(\vec{q})\|_{l_2}$ computed in a set of 10242 exterior points for the linearized Molodensky problem with smoother ($\theta_0 = 2.6, \kappa = 6$) for the first three Nash-Hörmander iteration steps. Here $u(\vec{q})$ is obtained by extrapolation. All three curves show similar convergence rates, whereas in the higher Nash-Hörmander iteration steps the absolute value of the error increases due to the error propagation in the Nash-Hörmander algorithm. Table 5.1 shows the corresponding convergence rates.

Figure 5.5 displays the l_2-radius errors versus the number of restarts for the restarted algorithm presented in Section 2.3 with smoother. The restart is done after each iteration step. We observe the same structural behaviour as for the other two experiments. Therefore, from the third restart of the algorithm onwards the discretization error propagation becomes dominating. However, refining the mesh, from $N = 2$ to $N = 3$ slightly reduces the error after the second and third restart, before increasing after the third restart.

Figure 5.6 displays the mean "l_2-gravity vector errors" with smoother and restart. Although the values in Figure 5.6 are smaller than in Figure 5.3 and firstly converge up to the fifth iteration step, from this step onwards the method provides uncontrollable surface updates (peaks and undesirable deformations occur). The method is numerically unstable.

Figure 5.7 displays the sequence of obtained surfaces for the case without smoother, while Figures 5.8 and 5.9 display the sequence of obtained surfaces for the case with smoother. The marked point is always the north pole of the sphere, i.e. $x = y = 0$ and only z varies. Interestingly, for each experiment the surface update is almost constant over the mesh points, leading to a sequence of almost spheres.

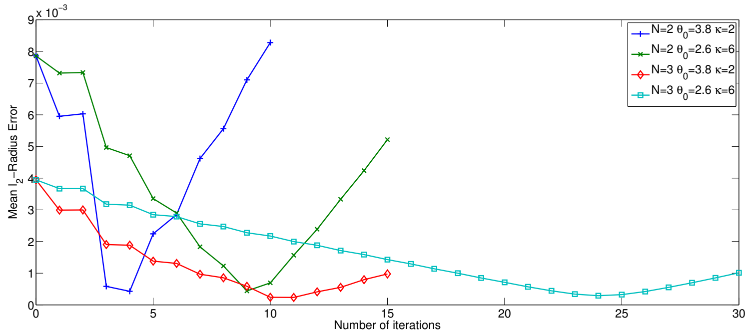

Figure 5.2.: Mean Radius-Error in the l_2-norm with smoother

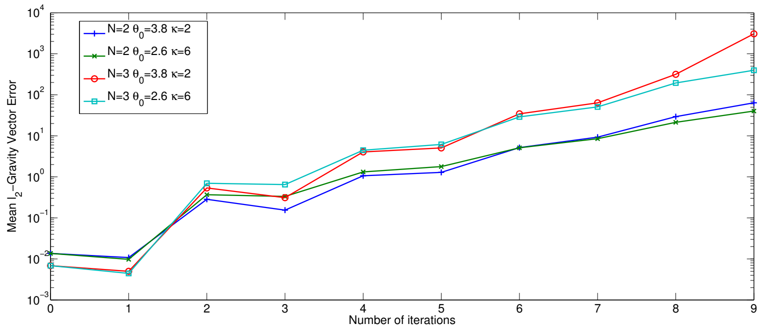

Figure 5.3.: Mean Gravity Vector Error in the l_2-norm with smoother

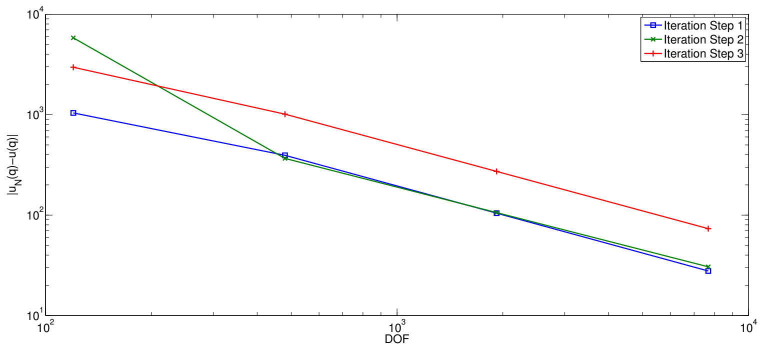

Figure 5.4.: Pointwise Error $\|u_N(\vec{q}) - u(\vec{q})\|_{l_2}$ computed in a set of 10242 exterior points for the linearized Molodensky problem with smoother

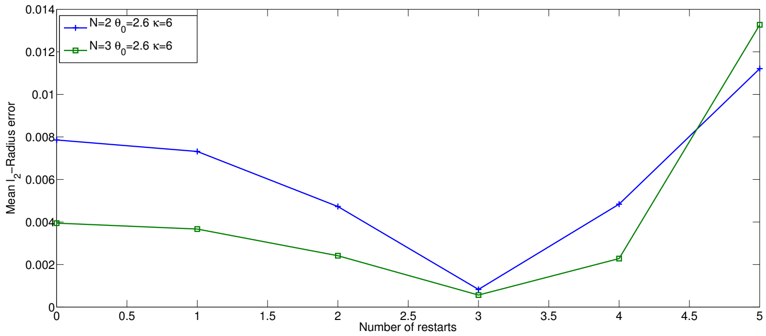

Figure 5.5.: Mean Radius-Error in the l_2-norm with smoother and restart

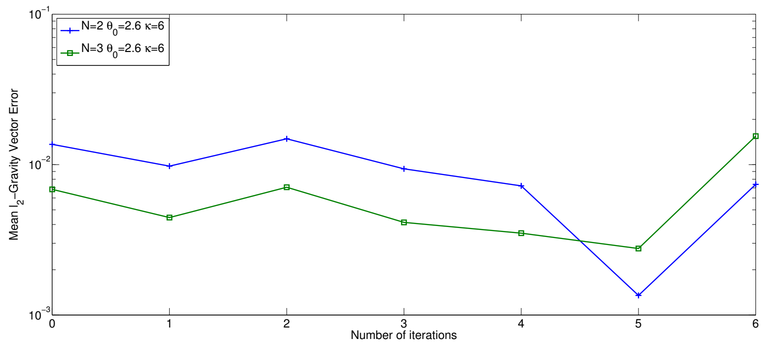

Figure 5.6.: Mean Gravity Vector Error in the l_2-norm with smoother and restart

Iter	DOF	$\lvert(u_N(\boldsymbol{q}) - u(\boldsymbol{q}))\rvert$	EOC
0	120	1.04164e+03	
	480	3.94212e+02	0.70
	1920	1.04676e+02	0.96
	7680	27.79515	0.96
1	120	5.82518e+03	
	480	3.66919e+02	1.99
	1920	1.05925e+02	0.90
	7680	30.57947	0.90
2	120	2.96617e+03	
	480	1.01239e+03	0.77
	1920	2.72407e+02	0.95
	7680	73.29735	0.95

Table 5.1.: Pointwise Errors for the linearized Molodensky problem with smoother

	Iter	$1/\theta_m$
$\theta_0 = 2.6, \kappa = 6$	0	0.38462
	1	0.38441
	$\vdots$	$\vdots$
	5	0.38379
	$\vdots$	$\vdots$
	10	0.38277
$\theta_0 = 3.8, \kappa = 2$	0	0.26315
	1	0.25449
	$\vdots$	$\vdots$
	5	0.23287
	$\vdots$	$\vdots$
	10	0.20654

Table 5.2.: Values of the smoothing parameter $\frac{1}{\theta_m}$

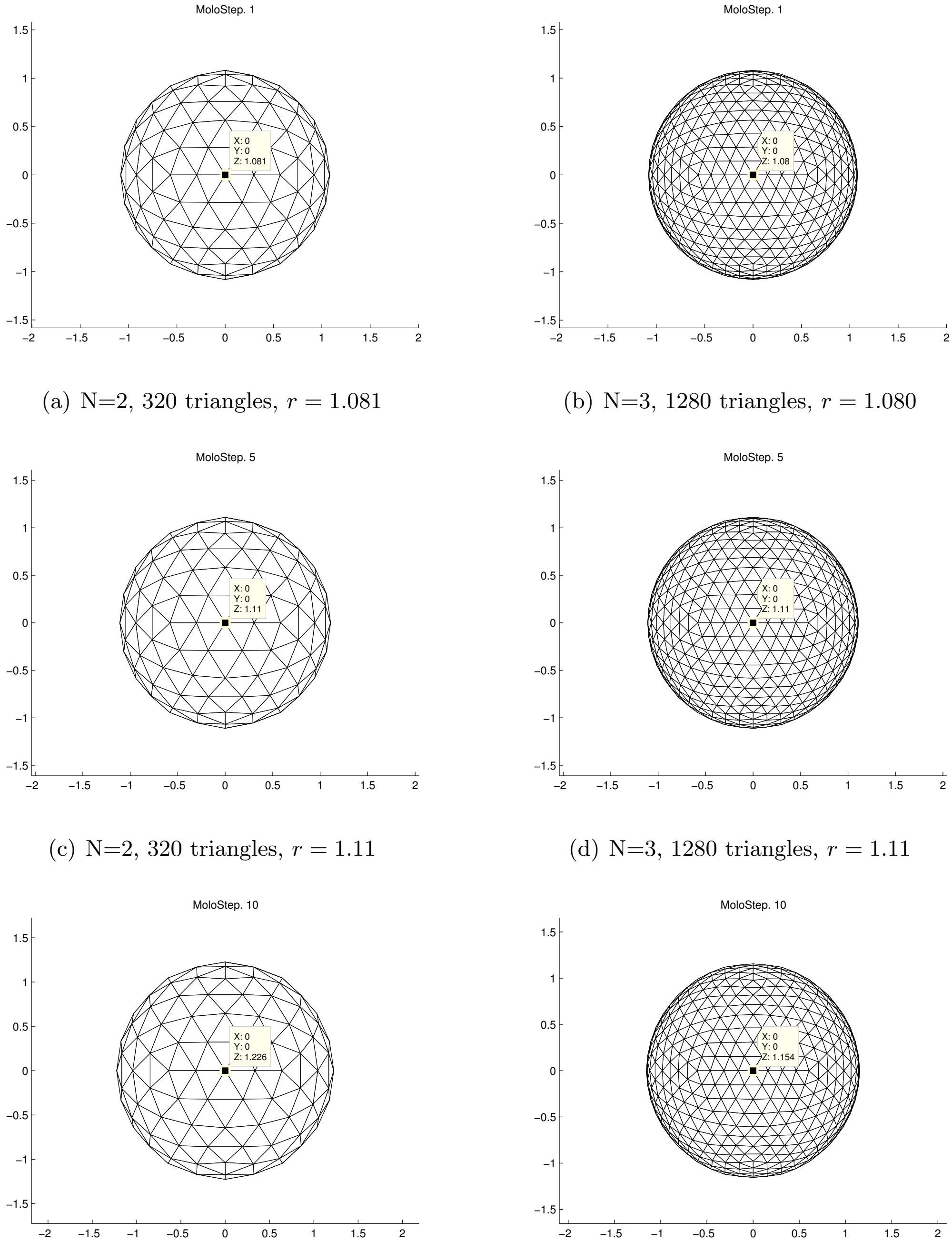

(a) N=2, 320 triangles, $r = 1.081$

(b) N=3, 1280 triangles, $r = 1.080$

(c) N=2, 320 triangles, $r = 1.11$

(d) N=3, 1280 triangles, $r = 1.11$

(e) N=2, 320 triangles, $r = 1.226$

(f) N=3, 1280 triangles, $r = 1.154$

Figure 5.7.: $N = 2$ and $N = 3$ icosahedron refinements without smoother

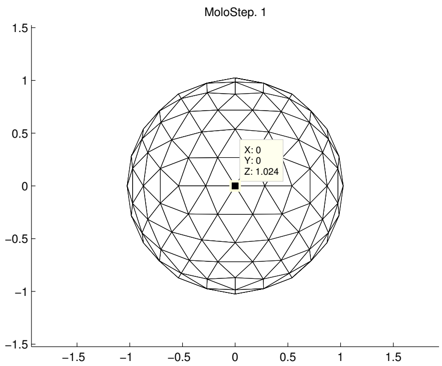

(a) N=2, 320 triangles, $r = 1.024$

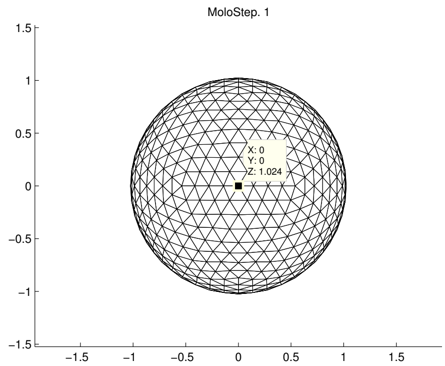

(b) N=3, 1280 triangles, $r = 1.024$

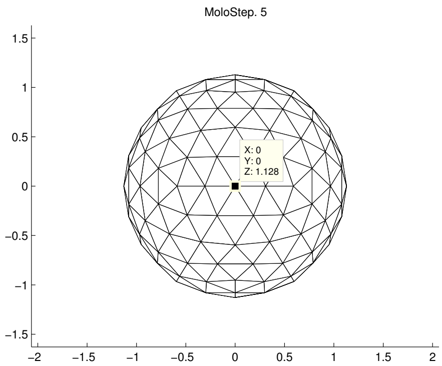

(c) N=2, 320 triangles, $r = 1.128$

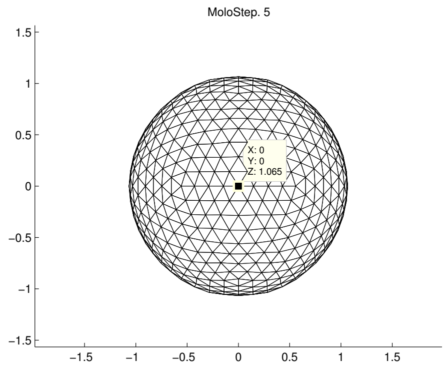

(d) N=3, 1280 triangles, $r = 1.065$

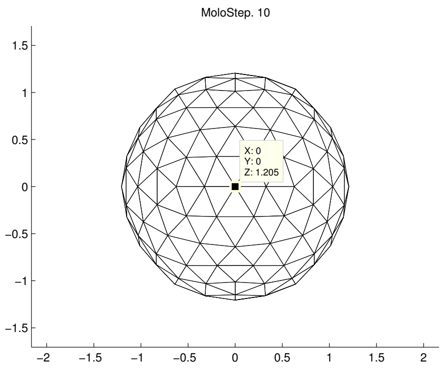

(e) N=2, 320 triangles, $r = 1.205$

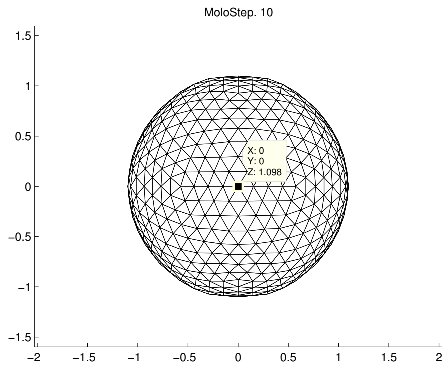

(f) N=3, 1280 triangles, $r = 1.098$

Figure 5.8.: $N = 2$ and $N = 3$ icosahedron refinements with smoother, $\theta_0 = 3.8, \kappa = 2$

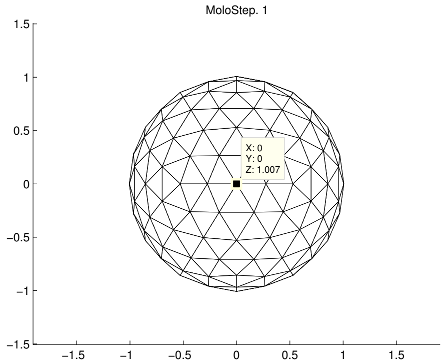

(a) N=2, 320 triangles, $r = 1.007$

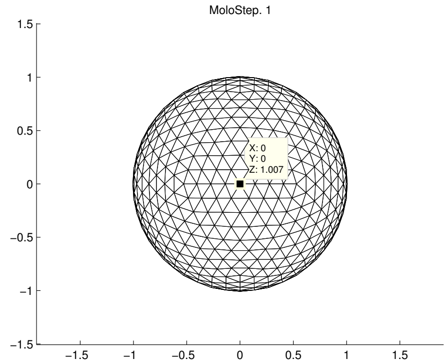

(b) N=3, 1280 triangles, $r = 1.007$

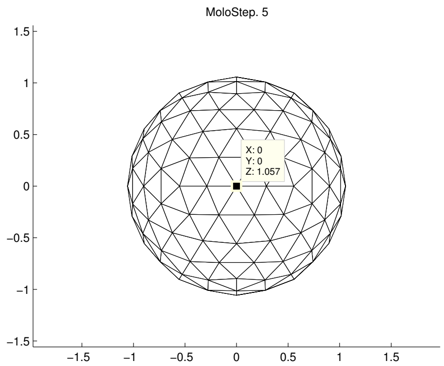

(c) N=2, 320 triangles, $r = 1.057$

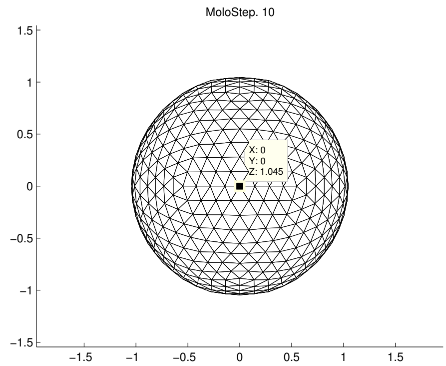

(d) N=3, 1280 triangles, $r = 1.045$

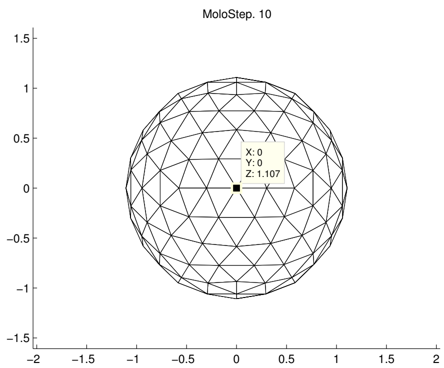

(e) N=2, 320 triangles, $r = 1.107$

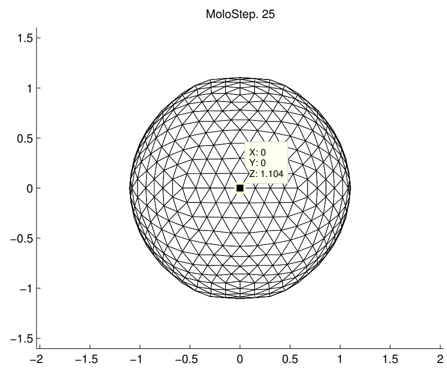

(f) N=3, 1280 triangles, $r = 1.104$

Figure 5.9.: $N = 2$ and $N = 3$ icosahedron refinements with smoother, $\theta_0 = 2.6, \kappa = 6$

5.2. Computation of the Gravity Gradient to the Discrete BEM-Solution

In each iteration step of the Nash-Hörmander algorithm the surface must be updated and for this, the Hessian $\nabla\nabla u|_\Gamma$ has to be computed (see Section 4.1), where u is the solution of the exterior Dirichlet problem

$$-\Delta u = 0 \quad \text{in} \quad \mathbb{R}^d \setminus \overline{\Omega} \tag{5.5a}$$

$$u = g \quad \text{on} \quad \Gamma := \partial\Omega \tag{5.5b}$$

with an appropriate decay condition. The computation of $\nabla\nabla u|_\Gamma$ implicitly assumes $u \in C^2(\mathbb{R}^d \setminus \Omega)$. The exterior Dirichlet problem (5.5) can be solved by a single layer potential ansatz i.e.

$$u(x) = V\mu(x) := \int_\Gamma k(x,y)\mu(y)\, ds_y \tag{5.6}$$

with the kernel

$$k(x,y) = \begin{cases} -\frac{1}{2\pi}\log\|x-y\|, & d=2 \\ \frac{1}{4\pi}\frac{1}{\|x-y\|}, & d=3. \end{cases} \tag{5.7}$$

The solution of the integral equation (5.6) can be approximated by a Galerkin scheme, that is a density $\mu_h \in S_{hp} \subset H^{-\frac{1}{2}}(\Gamma_h)$ is sought such that

$$\langle V\mu_h, \xi\rangle_{\Gamma_h} = \langle g, \xi\rangle_{\Gamma_h} \quad \forall\, \xi \in S_{hp}. \tag{5.8}$$

Here, S_{hp} is the space of piecewise polynomials of degree p to a given h-discretization Γ_h of Γ and $\langle\cdot,\cdot\rangle_{\Gamma_h}$ is the duality pairing between $\widetilde{H}^{\frac{1}{2}}(\Gamma_h)$ and its dual $H^{-\frac{1}{2}}(\Gamma_h)$. To approximate the Hessian we therefore have to compute $(\nabla\nabla V\mu_h)|_{\Gamma_h}$ with

$$\nabla\nabla V\mu_h(x) = \text{p.f.}\int_{\Gamma_h} \nabla_x\nabla_x k(x,y)\mu_h(y)\, ds_y \tag{5.9}$$

for all $x \in \Gamma_h$. The kernel $\nabla_x\nabla_x k(x,y)$ is hypersingular which significantly aggravates the evaluation of this potential. More precisely, the integral only exists as a Hadamard finite-part integral. A complete description of its theory is given in [14] and [26]. Contrary to the Hessian, the normal and tangential derivatives of the single layer potential on the boundary are well analysed [40] and only lead to simpler principle value integrals. Such integrals can be evaluated by a composite Gauss quadrature with geometrical grading towards the singularity [9, 42]. In the case of polynomial ansatz functions, Maischak describes in [24] an analytic evaluation of the single layer and (adjoint) double layer potentials which are used in the forthcoming.

We consider five different approaches to compute the Hessian $\nabla\nabla V\mu_h(x)$ of the discrete solution u_h to (5.6). Note that structurally the computation of $V\mu_h$ is the same as for $V\widetilde{\mu}_h$ in the auxiliary Dirichlet problem (4.12).

1. Using the adjoint double layer potential to compute the gradient with an analytic potential evaluation and using second order accurate finite differences for the second derivatives.
2. As in 1. but with a quadrature rule.
3. Using finite differences for the second order derivatives with an analytic single layer potential evaluation.
4. As in 3. but with a quadrature rule.
5. Using a Hadamard regularization to compute the hypersingular integral (5.9) directly.

In Section 5.2.1 we give numerical examples for these methods in both two and three dimensions. For all approaches which use a quadrature rule, the integration domain is decomposed into the far field, on which a standard Gaussian quadrature rule is applied, the near field and self-element, on which a composite Gaussian quadrature rule with geometrical grading ($\sigma = 0.17$) towards the singularity is applied [9, 42]. In the case of the Hadamard regularization, the value for the self-element is corrected by the term $+\mu_h(x)/|B_\epsilon(x)|$ where $|B_\epsilon(x)|$ is the area of an ϵ-ball around the singularity. We define the self-element as the element in which $\mathcal{P}_{\Gamma_h}(x)$, the closest point projection of the evaluation point x onto Γ_h, lies and we denote by the near field all adjacent elements. All remaining elements give the far field.

Whenever we use finite differences we decompose the Cartesian direction into normal and tangential components. For the tangential components we use the central finite difference scheme, i.e. $u'(x) \approx \frac{u(x+\delta)-u(x-\delta)}{2\delta}$, which is accurate of second order, with δ less than the distance of $\mathcal{P}_{\Gamma_h}(x)$ to the boundary of its linear element. For the normal component we use a combination of the Crank-Nicolson method with the central finite difference scheme, i.e. $u'(x) \approx \frac{4u(x+\delta)-3u(x)-u(x+2\delta)}{2\delta}$, which is second order accurate and is forward oriented.

The methods 1 to 4 are closely related. They compute the Hessian by computing the gradient of the gradient using finite differences and only differ in how the first gradient is obtained. For the first two methods the first differentiation is performed analytically, i.e.

$$\nabla u_h(x) = \nabla V \mu_h(x) = \text{p.v.} \int_{\Gamma_h} \nabla_x k(x,y) \mu_h(y) \, ds_y = K' \mu_h(x) \qquad x \in \mathbb{R}^d \setminus \overline{\Omega}.$$

For the limit $x \to \Gamma_h$ the value has to be corrected by an additional jump term in the normal component [40]. For the computations, the jump term is added whenever the distance of x to Γ_h is less than 10^{-8}. Contrary to (5.9), the adjoint double layer potential K' is only strongly singular which can be integrated by a composite quadrature or evaluated analytically [24].

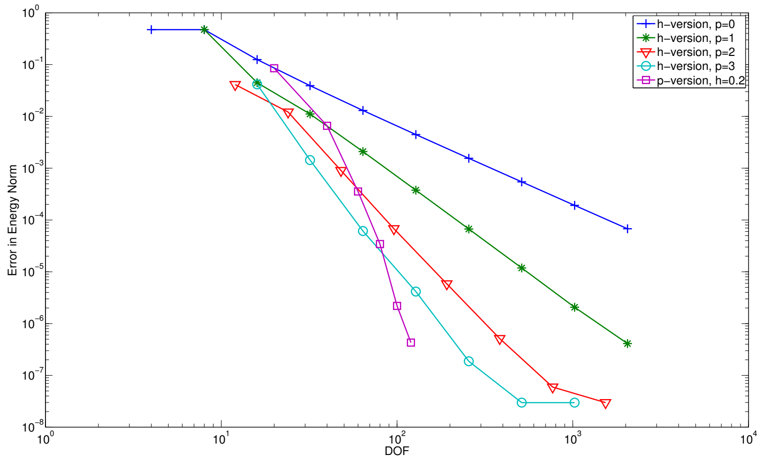

Figure 5.10.: BEM-Error $\|\mu_h - \mu_\infty\|_V$ in the energy norm for the 2d case

5.2.1. Numerical Experiments

In the computations, the finite difference (FD) step size δ is set to 10^{-4} for the normal component and to 10^{-5} for the tangential component when approximating of the second derivative. For the approximation of the first derivative it is set to 10^{-4} for the normal and to 10^{-7} for the tangential component. For the presented numerical experiments the FD-approximation error is of magnitude 10^{-7} if no Galerkin-BEM approximation error (BEM-error) were to occur. In general, also the FD-step size must decrease as the BEM-dofs increase. However, for very small step sizes the finite differences become numerically instable and the BEM-error is dominating anyway.
Let H be the exact Hessian of u and H_h be the approximated Hessian of the approximation u_h. The approximation error of the Hessian is measured in the Frobenius norm for a pointwise evaluation and the BEM-approximation error $\mu - \mu_h$ in the energy norm $\|\mu - \mu_h\|_V^2 := \langle V(\mu - \mu_h), \mu - \mu_h \rangle_{\Gamma_h}$.

A 2d Case Study

Let $\Omega = \left[-\frac{1}{2}, \frac{1}{2}\right]^2$ be the domain and $u = \ln \|x\|$ the exact solution. Then the exact Hessian is $H(x) = \frac{1}{x^2} \begin{pmatrix} 1 - 2x_1^2 & -2x_1x_2 \\ -2x_1x_2 & 1 - 2x_2^2 \end{pmatrix}$. Figure 5.10 displays the BEM-error $\|\mu - \mu_h\|_V$ for four h-versions ($p = 0, 1, 2, 3$) and a p-version ($h = 0.2$). All versions show their characteristic rate of convergence, i.e. 1.5, 2.5, 3.5, 4.5 for the h-versions and exponential for the p-version until the error is about 10^{-8} at which point the quadrature errors for the outer integration in the semi-analytic evaluation of (5.8) dominate the BEM- error with analytic computation of the involved integrals.

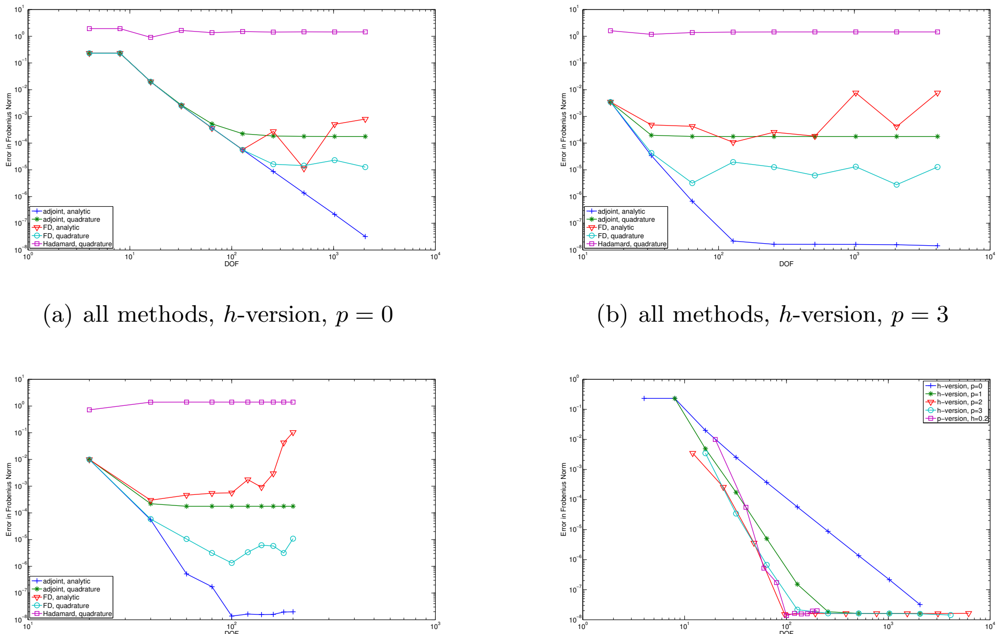

(a) all methods, h-version, $p = 0$

(b) all methods, h-version, $p = 3$

(c) all methods, p-version, $h = 0.2$

(d) all BEM-versions, method 1

Figure 5.11.: Error of the Hessian approximation for a point outside of Γ

A point outside of Γ

The most simplest case is the evaluation for a point x outside of Γ_h, i.e. the integration domain is sufficiently far away from the singularity. The results for the experiment with $x = (1, \frac{1}{3})^T$ are displayed in Figure 5.11. Figures 5.11 (a)-(c) show that the first method is superior to the other methods and that the desired accuracy of $10^{-7} - 10^{-8}$ can be achieved. For the relative error, the values must be divided by $\|H(x)\|_F \approx 1.3310245$. The Hadamard regularization approach is stable but non-converging which is a result from the $\frac{1}{\epsilon}$-scaling of the correction term. Both finite difference methods are instable. Furthermore, for only few dofs, the Hessian error reduces like in the best version, but later stagnates at a high level. Using a quadrature rule to compute the adjoint double layer, in the finite difference scheme the quadrature error blows up to the order of 10^{-4}. This would be even worse for first order accurate schemes like forward Euler, for which δ must be chosen even smaller. Only the method which uses an analytic evaluation of the adjoint double layer converges up to the BEM-approximation error. Figure 5.11 (d) shows that the polynomial degree should be sufficiently large, i.e. $p \geq 2$, for good convergence of the Hessian approximation. The Hadamard regularization method is by far worse than the others and is therefore not suited when approaching the boundary.

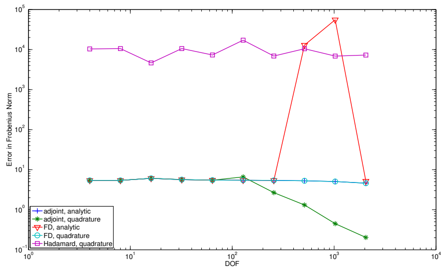

(a) methods 1-4, h-version, $p = 0$

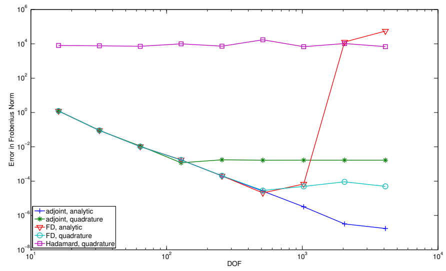

(b) methods 1-4, h-version, $p = 3$

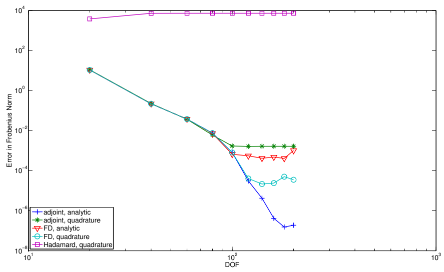

(c) methods 1-4, p-version, $h = 0.2$

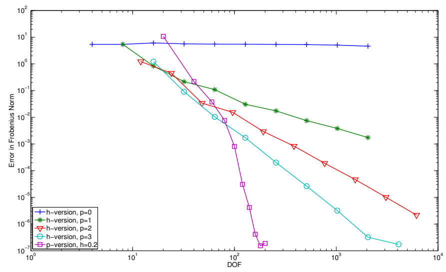

(d) all BEM-versions, method 1

Figure 5.12.: Error of the Hessian approximation for a point close to Γ_h

A point close to Γ_h

Although the evaluation point is not on Γ_h, the closeness of the singularity to the integration domain affects the accuracy of the differentiation schemes. The results for the experiment with $x = (0.5001, \frac{1}{3})^T$, i.e. $dist\,(x, \Gamma) = 10^{-4}$, and $\|H(x)\|_F \approx 4.5240356$ are displayed in Figure 5.12. Figures 5.12 (b)-(c) show the same structural behaviour of the differentiation methods as for the point outside of Γ_h, yet with a slower convergence rate. Rather more, the h-version with $p = 0$ does no longer converge, Figure 5.12 (a). Figure 5.12 (d) shows again the superiority of the p-version and the strong influence of the polynomial degree for the h-versions.

A point directly on Γ_h

The most difficult computation and original task is the computation of the Hessian for x directly on the boundary. The results for the experiment with $x = (\frac{1}{2}, \frac{1}{3})^T$ and $\|H(x)\|_F \approx 4.5254834$ are displayed in Figure 5.13. As in the previous section, the h-version with $p = 0$ does not converge, Figure 5.13 (a), and only the first method is able to achieve the desired high accuracy, Figure 5.13(b)-(c). Again, Figure 5.13 (d) shows the necessity of choosing p sufficiently large or even better to choose the p-version if u is analytic.

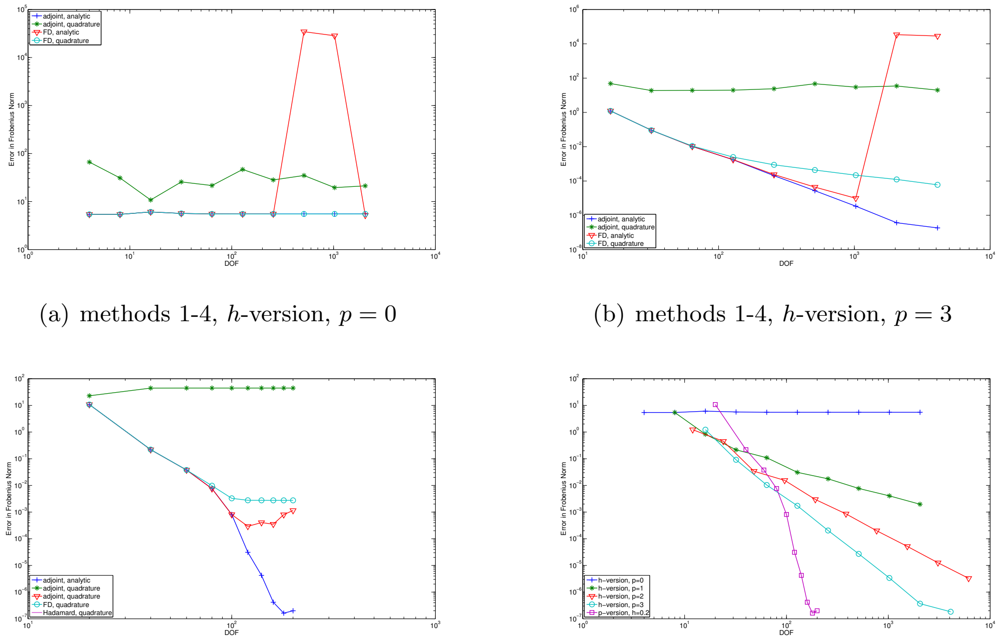

(a) methods 1-4, h-version, $p = 0$

(b) methods 1-4, h-version, $p = 3$

(c) methods 1-4, p-version, $h = 0.2$

(d) all BEM-versions, method 1

Figure 5.13.: Error of the Hessian approximation for a point on Γ_h

A 3d Case Study

Let $\Omega = [-1, 1]^3$ be the domain. For $g \equiv 1$ the exact solution is $u(x) = \frac{1}{\|x\|}$ with the Hessian $H(x) = \frac{3}{\|x\|^5} \begin{pmatrix} x_1^2 & x_1x_2 & x_1x_3 \\ x_1x_2 & x_2^2 & x_2x_3 \\ x_1x_3 & x_2x_3 & x_3^2 \end{pmatrix} - \frac{1}{\|x\|^3} I$. Figure 5.14 displays the BEM-error $\|\mu - \mu_h\|_V$ for three h-versions ($p = 0, 1, 2$). In the 2d-case study we have shown that using the adjoint double layer potential to compute the gradient with an analytic potential evaluation and using second order accurate finite differences for the second derivatives to compute the Hessian provides the best results. In the following we will use this method for our 3d-case analysis. We have carried out again numerical experiments for 3 different types of points. In Figure 5.15 (a) the results for the experiment with $x = (2, \frac{1}{3}, \frac{1}{3})^T$, a point outside the boundary Γ, are displayed. The $h-$ version with $p \geq 1$ converges up to the BEM-approximation error. In Figure 5.15 (b) we display the results for the experiment with $x = (1.0001, \frac{1}{3}, \frac{1}{3})^T$ i.e. $dist\,(x, \Gamma) = 10^{-4}$, a point close to Γ. As in the 2d-case, the $h-$ version with $p = 0$ does not longer converge. It is therefore necessary to choose p sufficiently large i.e. $p \geq 2$ for good convergence of the Hessian approximation. Finally, in Figure 5.15 (c) we display the experiments with $x = (1, \frac{1}{3}, \frac{1}{3})^T$, a point on Γ. Figure 5.15 (c) shows the same structural behaviour as for the point close to Γ. Concluding, we have to choose p sufficiently large i.e. $p \geq 2$, for a good convergence of the Hessian approximation.

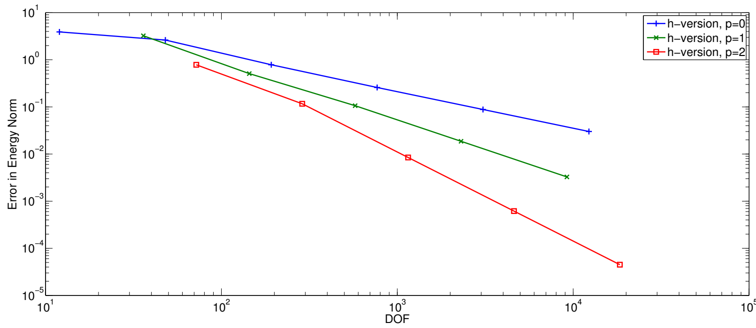

Figure 5.14.: BEM-Error $\|\mu_h - \mu_\infty\|_V$ in the energy norm for the 3d case on the cube

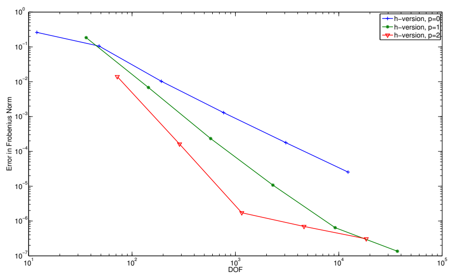

(a) h-versions for a point outside Γ

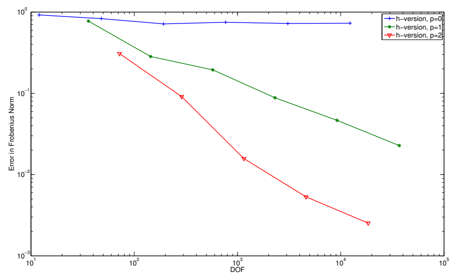

(b) h-versions for a point close to Γ

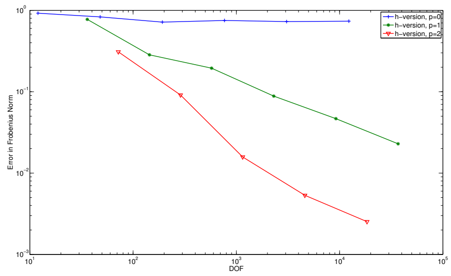

(c) h-versions for a point on Γ

Figure 5.15.: Error of the Hessian approximation 3d case

For the Molodensky problem the domain of interest is a rigid body in $\mathbb{R}^3$ whose surface is diffeomorphic to the sphere under a certain map. Here, the domain is a ball with radius one and center zero corresponding to the first Nash-Hörmander iteration step. We use triangles, i.e. linear elements, to discretize the surface. The exact solution is again $u(x) = \frac{1}{\|x\|}$.

In Figure 5.16 the results for the experiment with $x = c \cdot (1,1,1) + \vec{n}$ and c chosen such that $c \cdot (1,1,1)$ lies on the discretized sphere are displayed. It clearly shows that the uniform h-version with $p = 2$ is superior to the other two h-versions ($p = 0, p = 1$).

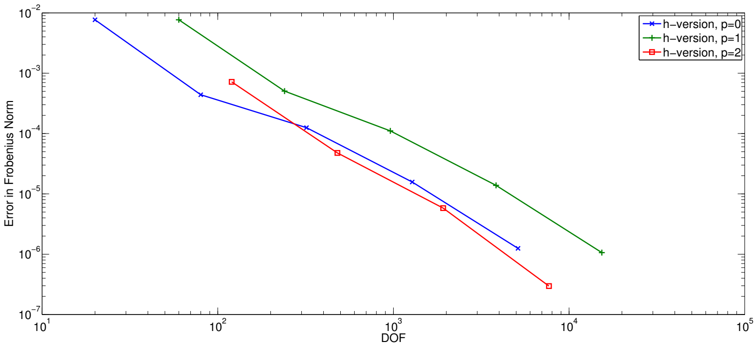

Figure 5.16.: Error of the Hessian approximation 3d case sphere for a point outside Γ

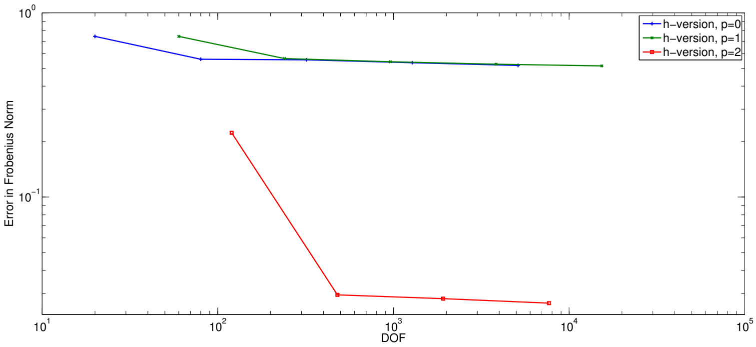

Figure 5.17.: Error of the Hessian approximation 3d case sphere for a point on Γ

Interestingly, all three methods converge with similar rates, contrary to the other 3d-case Figure 5.15(a) for the cube. In Figure 5.17 the results for the experiment with $x = c \cdot (1, 1, 1)$ are displayed. It shows that the h-versions with $p = 0, p = 1$ do not converge and that for $p = 2$ the convergence is very slow. However, even for this few degrees of freedom the absolute error for the $p = 2$ h-version is more than 1 order of magnitude smaller than for the other two h-versions.

A.

A.1. Proof of Hörmanders Existence Theorem

The description of $\mathscr{H}^{\alpha+\mu_1}$ in Theorem A.11 will be important, so we assume that $\alpha+\mu_1$ is not an integer. Assume that $\alpha_- < \alpha < \alpha_+, \alpha_- + \mu_1 \geq 0$. The following Lemma given by Hörmander [19, Lemma 2.2.1] will play an important role in the proof of Theorem 2.1.

Lemma A.1. *If for some integer $k \geq 0$*

$$\|\dot{u}_j\|_{a+\mu_1} \leq \delta\theta_j^{a-\alpha-1}, \quad a \in [\alpha_-, \alpha_+], \quad 0 \leq j \leq k, \tag{A.1}$$

it follows that

$$U = \sum_{j=0}^{k} \triangle_j \dot{u}_j \in \mathscr{H}^{\alpha+\mu_1} \tag{A.2}$$

and that, with the notation $b^+ = max(b, 0)$ and any fixed a_0

$$\begin{aligned} \|U - S_{\theta_{k+1}}U\|_a &\leq C\delta\theta_{k+1}^{a-\alpha-\mu_1}, \qquad 0 \leq a \leq \alpha_+ + \mu_1 \\ \|S_{\theta_{k+1}}U\|_a &\leq C\delta\theta_{k+1}^{(a-\alpha-\mu_1)^+}, \quad 0 \leq a \leq a_0. \end{aligned} \tag{A.3}$$

The constants are independent of θ_0 and κ when θ_0 is large and of course, independent of k.

Proof. With theorem A.11 we have

$$\|U\|_{\alpha+\mu_1} \leq \sum_{j=0}^{k} \triangle_j \|\dot{u}_j\|_{\alpha+\mu_1} \leq \delta \sum_{j=0}^{k} \triangle_j \theta_j^{-1} \leq C\delta$$

and by using (iii) in Theorem A.10, if $a \leq \alpha + \mu_1$ in the first half of (A.3) we deduce

$$\|U - S_{\theta_{k+1}}U\|_a \leq C\theta_{k+1}^{a-\alpha-\mu_1}\|U\|_{\alpha+\mu_1} \leq C\delta\theta_{k+1}^{a-\alpha-\mu_1}.$$

When $a = \alpha_+ + \mu_1$ we obtain from (A.1)

$$\|U\|_a \leq \delta \sum_{j=0}^{k} \triangle_j \theta_j^{\alpha_+-\alpha-1} \leq \delta\theta_{k+1}^{\alpha_+-\alpha} \sum_{j=0}^{k} \triangle_j \theta_j^{-1} \leq C\delta\theta_{k+1}^{\alpha_+-\alpha} \leq C\delta\theta_{k+1}^{(a-\alpha-\mu_1)^+}$$

and (A.3) is valid. By the logarithmic convexity in Theorem A.5 the assertion follows in general. □

Now our aim is to show that (A.1) holds. This will be done by an induction proof. We assume that $\mu \leq \alpha + \mu_1$ and choose the convex neighborhoods V_1 of u_0 in H^μ and V_2 of 0 in H^μ such that $V_1 + V_2 \subset V_0$. For θ_0 large enough, then there holds

$$S_\theta u_0 \in V_1, \quad \theta \geq \theta_0.$$

From (A.3) with δ sufficiently small and $a = \mu \leq \alpha + \mu_1$ it follows that $U \in V_2$ and $S_\theta U \in V_2, \theta \geq \theta_0$. We can apply the estimates above to all values smaller than k. Recalling that $v_k = S_{\theta_k} u_k$ we deduce that (A.3) implies with (A.1) for $j \leq k+1$

$$\begin{aligned} \|u_j - v_j\|_a &\leq C\theta_j^{a-\alpha-\mu_1}, & a &\leq \alpha_+ + \mu_1 \\ \|v_j\|_a &\leq C\theta_j^{(a-\alpha-\mu_1)^+}, & a &\leq a_0. \end{aligned} \tag{A.4}$$

Using (A.1) and (A.4), we first estimate e_j for $j \leq k$, then g_{k+1} and finally $\dot{u}_{k+1}$. If the estimate on $\dot{u}_{k+1}$ comes out as (A.1) for $j = k+1$ and we make sure that (A.1) is valid with $k = 0$, the induction proof of (A.1) will be complete. Furthermore, the proved estimates show that $\Phi(u_k) \to \Phi(u_0) + f$.

Estimate of e'_j

For $u, v, w \in C^\infty(M, \mathbb{R}^N)$ and $u_0 \in V_0$ we assumed that (2.9) is valid. With $u, v \in V_0$ we have that the line segment between them is in V_0 and the derivative of

$$[0,1] \ni t \to (\Phi'(v + t(u-v)) - \Phi'(v)))w$$

is given by $\Phi''(v + t(u-v); u-v, w)$. Now, from (2.9) we deduce by setting $u = v + t(u-v), v = u - v, w = w$ (recalling that $t \in [0,1]$)

$$\begin{aligned} &\|(\Phi'(u) - \Phi'(v))w\|_{\lambda_0+a} \\ &\qquad \leq C\{\|u-v\|_{m_1+a}\|w\|_{m_2} + \|u-v\|_{m_2}\|w\|_{m_1+a} \\ &\qquad\quad + (\|u-v\|_{m_3}\|w\|_{m_4} + \|u-v\|_{m_4}\|w\|_{m_3})(\|u\|_{m_5+a} + \|v\|_{m_5+a})\} \\ &\qquad 0 \leq a \leq a_\Phi. \end{aligned} \tag{A.5}$$

Now e'_j was defined as $e'_j := (\Phi'(u_j) - \Phi'(v_j))\dot{u}_j$. In order to obtain an estimate for e'_j we first set $u = u_j, v = v_j, w = \dot{u}_j$ and deduce

$$\begin{aligned} &\|(\Phi'(u_j) - \Phi'(v_j))\dot{u}_j\|_{\lambda_0+a} \\ &\qquad \leq C\{\|u_j - v_j\|_{m_1+a}\|\dot{u}_j\|_{m_2} + \|u_j - v_j\|_{m_2}\|\dot{u}_j\|_{m_1+a} \\ &\qquad\quad + (\|u_j - v_j\|_{m_3}\|\dot{u}_j\|_{m_4} + \|u_j - v_j\|_{m_4}\|\dot{u}_j\|_{m_3})(\|u_j\|_{m_5+a} + \|v_j\|_{m_5+a})\} \\ &\qquad 0 \leq a \leq a_\Phi. \end{aligned} \tag{A.6}$$

Next we want to show how we can use (A.1) and (A.4) to proof the following estimate stated by Hörmander for e'_j

$$\|e'_j\|_{\lambda_0+a} \leq C\theta_j^{L(\lambda_0+a)-1}. \tag{A.7}$$

From (A.4) we first deduce that

$$0 \le a \le a_\Phi, \quad \max(m_1 + a, m_2, m_3, m_4, m_5 + a) \le \alpha_+ + \mu_1. \tag{A.8}$$

By using now (A.4) and setting $M_1 = m_1 - \mu_1$ we notice that

$$\|u_j - v_j\|_{m_1+a} \le C\theta_j^{a+m_1-\alpha-\mu_1} = C\theta_j^{a+M_1-\alpha}$$

and with $M_j = m_j - \mu_1, \quad j = 2, 3, 4$ we have

$$\|u_j - v_j\|_{m_j} \le C\theta_j^{M_j-\alpha}.$$

Now by setting $M_5 = m_5 - \mu_1$ we deduce

$$\|u_j\|_{m_5+a} \le C\theta_j^{(M_5+a-\alpha)^+}.$$

Note that the same estimate holds for $\|v_j\|_{m_5+a}$. Finally we look at the contributions given by $\dot{u}_j$. By using (A.1) we have

$$\|\dot{u}_j\|_{m_1+a} \le C\theta_j^{M_1+a-\alpha-1} \tag{A.9}$$

and

$$\|\dot{u}_j\|_{m_j} \le C\theta_j^{M_j-\alpha}, \quad \text{for} \quad j = 2, 3, 4. \tag{A.10}$$

If we now use (A.6) with these estimates, we have proved (A.7) if we denote by $L(a+\lambda_0)$ the maximum of the following quantities

$$\begin{aligned} &a + M_1 - \alpha + \max(M_2 - \alpha, \alpha_- - \alpha) \\ &M_2 - \alpha + \max(a + M_1 - \alpha, \alpha_- - \alpha) \\ &M_3 - \alpha + \max(M_4 - \alpha, \alpha_- - \alpha) + (M_5 + a - \alpha)^+ \end{aligned} \tag{A.11}$$

under the assumption that $m_3 \ge m_4$. Assuming that (A.8) is fulfilled for small $a \ge 0$, we note that (A.7) is valid for all $a + \lambda_0 \in [0, \lambda_0]$ if L is defined to be a constant in $[0, \lambda_0]$. We also observe that L is the maximum of a constant and a linear function with slope 1.

Estimate of e''_j

Recalling the definition of e''_j, we have that the first derivative of

$$t \to \Phi(u_j + t\dot{u}_j) - \Phi(u_j) - \Phi'(u_j)t\dot{u}_j$$

vanishes at $t = 0$ and the second derivative is given by $\Phi''(u_j + t\dot{u}_j; \dot{u}_j, \dot{u}_j)$. We already have shown that the line segment between u_j and $u_j + \triangle_j \dot{u}_j$ is in V_0, so that we can now apply (2.9). By setting $u = u_j + t\dot{u}_j, v = w = \dot{u}_j, t = \triangle_j$ we deduce

$$\begin{aligned} \|e''_j\|_{\lambda_0+a} \le C\triangle_j \{&\|\dot{u}_j\|_{m_1+a} \|\dot{u}_j\|_{m_2} \\ &+ \|\dot{u}_j\|_{m_3} \|\dot{u}_j\|_{m_4} (\|u_j\|_{m_5+a} + \|\dot{u}_j\|_{m_5+a})\}. \end{aligned} \tag{A.12}$$

By using (A.1) and the same procedure as for e'_j we obtain the following estimate for e''_j

$$\|e''_j\|_{\lambda_0+a} \leq C\triangle_j \theta_j^{L'(\lambda_0+a)-1} \tag{A.13}$$

with L' independent on the choice of κ and of the same form as L. Using the fact that $\triangle_j \leq \theta_j^{1-\kappa}$ we have

$$\|e''_j\|_{\lambda_0+a} \leq C\theta_j^{L'(\lambda_0+a)-\kappa}$$

and we notice that if κ is so large that $L'(\lambda_0+a)+1-\kappa \leq L(\lambda_0+a)$, the estimate (A.13) will be as good as (A.7). Choosing κ such that this condition is fulfilled and using the fact that $e_j = e'_j + e''_j$, we deduce

$$\|e_j\|_{\lambda_0+a} \leq C\theta_j^{L(\lambda_0+a)-1}. \tag{A.14}$$

Estimate of g_{k+1}

Having this estimate we are ready now to give an estimate on g_{k+1}. Recalling the definition of g_k, we have

$$g_{k+1} = \triangle_{k+1}^{-1}((S_{\theta_{k+1}} - S_{\theta_k})(f - E_k) - \triangle_k S_{\theta_{k+1}} e_k), \quad k > 0. \tag{A.15}$$

Following Hörmander, we reformulate this equation to

$$g_{k+1} = \tilde{S}_k(f - E_k) - \triangle_k/\triangle_{k+1} S_{\theta_{k+1}} e_k \tag{A.16}$$

where the smoothing operator $\tilde{S}_k$ given by

$$\tilde{S}_k = (S_{\theta_{k+1}} - S_{\theta_k})/\triangle_{k+1} = \int_{\theta_k}^{\theta_k+\triangle_k} \dot{S}_\theta d\theta/\triangle_{k+1}$$

has the properties of $dS/d\theta$ in condition (iv) of Theorem A.10.
Using now (A.14) with $a = \lambda_0 + a$ and recalling that by Theorem A.10 (ii)

$$\|S_\theta u\|_a \leq C\theta^{a-b}\|u\|_b, \quad a \leq b$$

we obtain

$$\|S_{\theta_{k+1}} e_k\|_a \leq C\theta_k^{L(a)-1}$$

where a is in any finite interval if L is extended to the right as a continuous function with slope 1.
The next term that we want to estimate is $\tilde{S}_k E_k$. Recalling that $E_k = \sum_{j=0}^{k-1} \triangle_j e_j$, we have to examine two cases.

(i) $L(b) > 0$ if $b = a + \lambda_0$ for the largest value of a satisfying (A.8). Summation of (A.14) gives

$$\|E_k\|_b \leq \sum_{j=0}^{k-1} \triangle_j \|e_j\|_b \leq C \sum_{j=0}^{k-1} \triangle_j \theta_j^{L(b)-1} \leq C\theta_k^{L(b)} \sum_{j=0}^{k-1} \triangle_j \theta_j^{-1} \leq C'\theta_k^{L(b)}.$$

Recalling now (iv) in Theorem A.10 by interchanging a and b we have

$$\|\frac{d}{d\theta}S_\theta u\|_a \leq C\theta^{a-b-1}\|E_k\|_b$$

and we deduce

$$\|\tilde{S}_k E_k\|_a \leq C\theta^{a-b-1}\|E_k\|_b \leq C'\theta^{L(b)+a-b-1} \leq C'\theta^{L(a)-1}$$

where we have used $L(b)+a-b \leq L(a)$.

(ii) If $L(b) \leq 0$, for any $\epsilon > 0$ we have

$$\|E_k\|_b \leq C\sum_0^{k-1} \triangle_j \theta_j^{-1} < C_\epsilon \theta_k^\epsilon$$

and we deduce, using (iv) in Theorem A.10,

$$\|\tilde{S}_k E_k\|_a \leq C\theta^{a-b-1}\|E_k\|_b \leq C_\epsilon \theta^{\epsilon+a-b-1}.$$

Now, in order to give an estimate for g_{k+1}, we finally need an estimate for $\tilde{S}_k f$. With $f \in \mathscr{H}^{\alpha+\lambda_1}$ by using again (iv) in Theorem A.10 we obtain:

$$\|\tilde{S}_k f\|_a \leq C\theta_k^{a-\alpha-\lambda_1-1}\|f\|_{\alpha+\lambda_1}.$$

Using all these estimates, we deduce

$$\|g_{k+1}\|_a \leq C_\epsilon(\theta^{L(a)-1} + \theta^{\epsilon+a-b-1} + \theta_k^{a-\alpha-\lambda_1-1}\|f\|_{\alpha+\lambda_1}) \tag{A.17}$$

for $\epsilon > 0$ and $b-\lambda_0$ the largest value of a for which (A.8) is satisfied.

With all this preliminary work done we are now ready to give an estimate for $\dot{u}_{k+1}$.

Estimate of $\dot{u}_{k+1}$

Recalling the definition of $\dot{u}_{k+1}$ i.e.

$$\dot{u}_{k+1} = \Psi(v_{k+1})g_{k+1}$$

by using (2.10) and (A.4), we deduce when $a \in [\alpha_-, \alpha_+]$

$$\begin{aligned}\|\dot{u}_{k+1}\|_{\mu_1+a} &= \|\Psi(v_{k+1})g_{k+1}\|_{\mu_1+a}\\ &\leq C(\|g_{k+1}\|_{\lambda_1+a} + \|g_{k+1}\|_{\lambda_2}\|v_{k+1}\|_{\mu_2+a}) \qquad \text{(A.18)}\\ &\leq C(\|g_{k+1}\|_{\lambda_1+a} + \|g_{k+1}\|_{\lambda_2}\theta_{k+1}^{(\mu_2+a-\alpha-\mu_1)^+})\end{aligned}$$

if $\alpha_- \geq 0$ and $\alpha_+ \leq a_\Psi$. Now returning to Hörmander's induction proof, we want to show that (A.18) implies (A.1) with $j = k+1$. Using (A.17) and setting $a = \lambda_1 + a$ we deduce, if $\|f\|_{\alpha+\lambda_1} < \delta/2$ is small enough, θ_0 is large enough that

$$\|g_{k+1}\|_{\lambda_1+a} \leq C_\epsilon(\theta_{k+1}^{L(\lambda_1+a)-1} + \theta_{k+1}^{\epsilon+a+\lambda_1-b-1} + (\delta/2)\theta_{k+1}^{a-\alpha-1})$$

and provided that

$$L(\lambda_1 + a) < a - \alpha, \quad \lambda_1 + a - b < a - \alpha \quad \text{when} \quad a \in [\alpha_-, \alpha_+]$$

holds, we obtain by noting that

$$\theta_{k+1}^{\epsilon+\lambda_1+a-b-1} \leq \theta_{k+1}^{a-\alpha-1}\theta_{k+1}^{-\epsilon} \leq (\delta/2C)\theta_{k+1}^{a-\alpha-1}$$

the following estimate stated by Hörmander

$$C\|g_{k+1}\|_{\lambda_1+a} \leq (\delta/2)\theta_{k+1}^{a-\alpha-1}. \tag{A.19}$$

Now, by using (A.17) again and setting $a = \lambda_2$, $\|f\|_{\alpha+\lambda_1} < \delta/2$, θ_0 large enough for $a \in [\alpha_-, \alpha_+]$, we obtain

$$\|g_{k+1}\|_{\lambda_2} \leq C_\epsilon(\theta_{k+1}^{L(\lambda_2)-1} + \theta_{k+1}^{\epsilon+\lambda_2-b-1} + (\delta/2)\theta_{k+1}^{\lambda_2-\alpha-\lambda_1-1})$$

and we notice that if $b > \lambda_1 + \alpha$ and the following conditions are fulfilled

$$\lambda_2 - \alpha - \lambda_1 + (\mu_2 + a - \alpha - \mu_1)^+ \leq a - \alpha$$
$$L(\lambda_2) + (\mu_2 + a - \alpha - \mu_1)^+ < a - \alpha$$

we have

$$C\|g_{k+1}\|_{\lambda_2}\theta_{k+1}^{(\mu_2+a-\alpha-\mu_1)^+} \leq (\delta/2)\theta_{k+1}^{a-\alpha-1}. \tag{A.20}$$

Combining (A.19) and (A.20) and using (A.18) we have just proved

$$\|\dot{u}_{k+1}\|_{\mu_1+a} \leq \delta\theta_{k+1}^{a-\alpha-1} \tag{A.21}$$

which is (A.1) for $j = k + 1$. Finally, if all the preceding conditions are fulfilled, κ and θ_0 being fixed, we note that (A.1) is fulfilled for $k = 0$ if $\|f\|_{\alpha+\lambda_1}$ is sufficiently small. This completes the induction proof. A detailed, very technical analysis of all the necessary conditions that have to be imposed for the induction proof can be found in [19, pages 23 - 24] .
Now, returning to Theorem 2.1, by Lemma A.1 and the proof of (A.1) noting that $\dot{u}_k \in C^\infty$ and defining $u(f) := \lim_{k\to\infty} u_k$, we have already proved the assertions (i), (ii) and (iv). Next, we want to give a proof for the remaining assertions.

Proof. In order to prove (iii) we first recall that

$$\Phi(u_{k+1}) - \Phi(u_0) = \sum_{j=0}^{k} \triangle_j(g_j + e_j)$$

and

$$\sum_{j=0}^{k} \triangle_j g_j + S_{\theta_k}E_k = S_{\theta_k}f.$$

By combining these two equations and by using $E_k = \sum_{j=0}^{k-1} e_j$ we deduce

$$\Phi(u_{k+1}) - \Phi(u_0) = S_{\theta_k} f - S_{\theta_k} E_k + \sum_{j=0}^{k} e_j = S_{\theta_k} f - S_{\theta_k} E_k + E_{k+1}$$
$$= S_{\theta_k} f + \triangle_k e_k + (E_k - S_{\theta_k} E_k).$$

By using now (A.14) we deduce

$$\|e_k\|_{\alpha+\lambda_1} \leq C\theta_j^{L(\alpha+\lambda_1)-1}$$

and for $L(\alpha + \lambda_1) < 0$ we have

$$\|e_k\|_{\alpha+\lambda_1} \to 0.$$

Using the proof for the estimate of g_{k+1} we also obtain

$$\|E_k - S_{\theta_k} E_k\|_{\alpha+\lambda_1} \to 0.$$

Finally we deduce

$$\|\Phi(u_{k+1}) - \Phi(u_0) - S_{\theta_k} f\|_{\alpha+\lambda_1} \to 0$$

which means $S_{\theta_k} f \to f$ and gives(iii).
For the proof of (v), by recalling the estimate of $\dot{u}_{k+1}$, taking $f \in \mathscr{H}^{\beta+\lambda_1}$ and using (A.17) , we have for some $\eta > 0$ and $\alpha_+ = a_\Psi$

$$\|\dot{u}_{k+1}\|_{a+\mu_1} \leq C(\|f\|_{\beta+\lambda_1} \theta_{k+1}^{a-\beta-1} + \theta_{k+1}^{a-\alpha-1-\eta}), \quad a \in [\alpha_-, \alpha_+].$$

Now, Hörmander shows by using a set of necessary conditions (see [19, Equation 2.2.28]) that

$$\|\dot{u}_k\|_{a+\mu_1} \leq C\theta_k^{a-\beta-1}, \quad a \in [\alpha_-, \alpha_+]$$

and with the condition $\alpha_- < \beta < a_\Psi = \alpha_+$ which means $\beta \in [\alpha_-, \alpha_+]$ he obtains (v). □

A.2. Hörmander Appendix

Here we just list some theorems from Hörmander's appendix which are needed for our considerations.

Theorem A.5, [19] $\mathscr{H}^a$ is a Banach space which decreases when a increases. For $0 \leq a \leq b$ and b bounded, $0 < \lambda < 1$, there is a constant C such that

$$\|u\|_a \leq C\|u\|_b, \quad \|u\|_{\lambda a+(1-\lambda)b} \leq C\|u\|_a^\lambda \|u\|_b^{1-\lambda}. \tag{A.22}$$

Moreover, if $1 \leq p < \infty$

$$\|u\|_a \leq C\|u\|_{L^p}^{p(b-a)/(n+pb)} \|u\|_b^{(n+pa)/(n+pb)}. \tag{A.23}$$

Corollary A.6, [19] If $u \in \mathscr{H}^{a_j}, v \in \mathscr{H}^{b_j}, j = 1, \dots, J$ and if (a, b) is in the convex hull of $(a_j, b_j) \in \mathbb{R}^2, j = 1, \dots, J$, then $u \in \mathscr{H}^a, v \in \mathscr{H}^b$ and

$$\|u\|_a \|v\|_b \leq C \sum_1^J \|u\|_{a_j} \|v\|_{b_j}.$$

Theorem A.7, [19] $\mathscr{H}^a$ is a ring. When a is bounded there is a constant C such that

$$\|uv\|_a \leq C(\|u\|_a \|v\|_0 + \|u\|_0 \|v\|_a). \tag{A.24}$$

Theorem A.8, [19] If $a \geq 1$ and $f, g \in \mathscr{H}^a$, then $f \circ g \in \mathscr{H}^a$ and

$$\|f \circ g\|_a \leq C(\|f\|_a \|g\|_1^a + \|f\|_1 \|g\|_a + \|f\|_0). \tag{A.25}$$

When $0 \leq a \leq 1$, then

$$\|f \circ g\|_a \leq \min(\|f\|_1 \|g\|_a, \|f\|_a \|g\|_1^a) + \|f\|_0. \tag{A.26}$$

Theorem A.10, [19] The smoothing operators S_θ have the following properties for $\theta > 1$ and $u \in \mathcal{E}'(K) \cap \mathscr{H}^a$, when a, b are non-negative and bounded numbers,

(i) $\|S_\theta u\|_b \leq C \|u\|_a, \quad b \leq a;$

(ii) $\|S_\theta u\|_b \leq C \theta^{b-a} \|u\|_a, \quad a \leq b;$

(iii) $\|u - S_\theta u\|_b \leq C \theta^{b-a} \|u\|_a, \quad b \leq a;$

(iv) $\left\| \frac{d}{d\theta} S_\theta u \right\|_b \leq C \theta^{b-a-1} \|u\|_a.$

Theorem A.11, [19] Let u_θ for $\theta > \theta_0$ be a C^∞ function in B and assume that

$$\|u_\theta\|_{a_j} \leq M \theta^{b_j - 1}, \quad j = 0, 1,$$

where $b_0 < 0 < b_1$ and $a_0 < a_1$. Define λ by $\lambda b_0 + (1 - \lambda) b_1 = 0$ and set $a = \lambda a_0 + (1 - \lambda) a_1$, that is,

$$a = (a_0 b_1 - a_1 b_0)/(b_1 - b_0).$$

If a is not an integer, it follows then that

$$u = \int_{\theta_0}^\infty u_\theta d\theta$$

is in $\mathscr{H}^a$ and that $\|u\|_a \leq C_a M$.

Theorem A.14, [19] Let Ω be an open bounded set in $\mathbb{R}^n$ with C^∞ boundary $\partial\Omega = \Sigma_0 \cup \Sigma_1$ where Σ_0, Σ_1 are open and closed disjoint subsets (one of which may be empty). If $u \in \mathscr{H}^{a+1}(\overline{\Omega}), a > 0$ is not an integer, and

$$\sum \frac{\partial}{\partial x_j}\left(A_{jk}\frac{\partial u}{\partial x_k}\right) = 0 \quad \text{in} \quad \Omega, \quad u = g_0 \quad \text{on} \quad \Sigma_0,$$
$$Bu = \sum_1^n B_j \frac{\partial u}{\partial x_j} + B_0 u = g_1 \quad \text{on} \quad \Sigma_1,$$

it follows that

$$\begin{aligned} \|u\|_{1+a}^{\Omega} \leq & C_a\{\|g_0\|_{a+1}^{\Sigma_0} + \|g_1\|_a^{\Sigma_1} + \|u\|_0^{\Sigma_1} \\ & + \|g_0\|_{\epsilon+1}^{\Sigma_0} + \|g_1\|_\epsilon^{\Sigma_1} + \|u\|_0^{\Sigma_1}(\|B\|_a^{\Sigma_1} + \|A\|_a^{\Omega})\}, \end{aligned} \tag{A.27}$$

provided that for some fixed C

$$C|B_n| \geq 1; \quad C\sum A_{jk}\xi_j\xi_k \geq \sum \xi_j^2,\ \xi \in \mathbb{R}^n, \quad \|B\|_\epsilon^{\Sigma_1} \leq C; \quad \|A\|_\epsilon^{\Omega} \leq C. \tag{A.28}$$

Here

$$\|B\|_a^{\Sigma_1} = \sum_0^n \|B_j\|_a^{\Sigma_1}, \quad \|A\|_a^{\Omega} = \sum \|A_{jk}\|_a^{\Omega}.$$

A.3. Boundary Integral Operators

In boundary value problems, a differential operator acts on a function u in every point x of a domain. Once the fundamental solution is known, this operator can be replaced by a boundary integral operator. In Chapter 4 such boundary integral operators are used for an exterior Laplacian problem.

Let $\Omega \subset \mathbb{R}^3$ be a domain with piecewise Lipschitz boundary $\Gamma = \partial\Omega$ and let the solution u satisfy

$$-\Delta u(x) = 0 \qquad x \in \mathbb{R}^3 \setminus \overline{\Omega} \tag{A.29a}$$
$$u(x) = \frac{c}{|x|} + b + O(|x|^{-2}) \quad \text{for} \quad |x| \to \infty \tag{A.29b}$$

with b, c real constants. In the radiation condition (A.29b) $O(|x|^{-2})$ is the Landau symbol with $\lim_{|x|\to\infty} O(|x|^{-2}) = 0$. The fundamental solution $k(x, y)$ of the Laplace operator in three dimensions is given by

$$k(x, y) = -\frac{1}{4\pi}\frac{1}{\|x - y\|}.$$

The second Green's formula provides the *representation formula*

$$u(x) = -\int_\Omega k(x, y)\Delta u(y)\, dx_y + \int_\Gamma k(x, y)\partial_{n_y} u(y) - \partial_{n_y} k(x, y) u(y)\, ds_y, \quad x \in \mathbb{R}^3 \setminus \overline{\Omega} \tag{A.30}$$

and taking the limit $x \to \Gamma$ and denoting $\phi = \partial_n u$ we obtain the well-known system of boundary integral equations

$$\begin{pmatrix} u \\ \phi \end{pmatrix} = \begin{pmatrix} \frac{1}{2} + K & -V \\ -W & \frac{1}{2} - K' \end{pmatrix} \begin{pmatrix} u \\ \phi \end{pmatrix}$$

with the single layer potential V, the double layer potential K, its adjoint K' and the hypersingular integral operator W.

$$\begin{aligned} V\phi(x) &:= \int_\Gamma k(x,y)\phi(y)\, ds_y, & Wu(x) &:= -\frac{\partial}{\partial n_x}\int_\Gamma \frac{\partial}{\partial n_y} k(x,y)u(y)\, ds_y, \\ Ku(x) &:= \int_\Gamma \frac{\partial}{\partial n_y} k(x,y)u(y)\, ds_y, & K'\phi(x) &:= \frac{\partial}{\partial n_x}\int_\Gamma k(x,y)\phi(y)\, ds_y. \end{aligned}$$

Lemma A.2 (Costabel [5])**.** *Let Γ be the boundary of a Lipschitz domain. Then the integral operators*

$$\begin{aligned} V &: H^{-\frac{1}{2}+s}(\Gamma) \to H^{\frac{1}{2}+s}(\Gamma), & W &: H^{\frac{1}{2}+s}(\Gamma) \to H^{-\frac{1}{2}+s}(\Gamma) \\ K &: H^{\frac{1}{2}+s}(\Gamma) \to H^{\frac{1}{2}+s}(\Gamma), & K' &: H^{-\frac{1}{2}+s}(\Gamma) \to H^{-\frac{1}{2}+s}(\Gamma) \end{aligned}$$

are bounded for all $s \in [-\frac{1}{2}, \frac{1}{2}]$, i.e. there exist constants C_V, C_K, $C_{K'}$, $C_W > 0$ such that

$$\begin{aligned} \|V\phi\|_{H^{\frac{1}{2}+s}(\Gamma)} &\le C_V \|\phi\|_{H^{-\frac{1}{2}+s}(\Gamma)}, & \|Wu\|_{H^{-\frac{1}{2}+s}(\Gamma)} &\le C_W \|u\|_{H^{\frac{1}{2}+s}(\Gamma)}, \\ \|Ku\|_{H^{\frac{1}{2}+s}(\Gamma)} &\le C_K \|u\|_{H^{\frac{1}{2}+s}(\Gamma)}, & \|K'\phi\|_{H^{-\frac{1}{2}+s}(\Gamma)} &\le C_{K'} \|\phi\|_{H^{-\frac{1}{2}+s}(\Gamma)}. \end{aligned}$$

Lemma A.3. *Let $\Gamma \subset \mathbb{R}^3$ be the boundary of a Lipschitz domain Ω. Then V is $H^{-\frac{1}{2}}(\Gamma)$-elliptic, i.e. $\exists\, c_V > 0$ s.t.*

$$\langle V\phi, \phi\rangle_\Gamma \ge c_V \|\phi\|^2_{H^{-\frac{1}{2}}(\Gamma)} \quad \forall\, \phi \in H^{-\frac{1}{2}}(\Gamma).$$

It is well known [46] that for $\Omega \subset \mathbb{R}^3$ the mapping V has a bounded inverse $V^{-1} : H^{1/2}(\Gamma) \to H^{-1/2}(\Gamma)$ with

$$\|V^{-1}\xi\|_{H^{-1/2}(\Gamma)} \le \frac{1}{c_V}\|\xi\|_{H^{1/2}(\Gamma)} \quad \forall\, \xi \in H^{1/2}(\Gamma).$$

For our numerical computations in Section 5.1 we also need the following properties of the gradient of the single layer potential.
Following [40], the normal component of the gradient of the single layer potential jumps i.e

$$\frac{\partial}{\partial n}(V\phi)^{\pm}(x) = \mp\frac{1}{2}\phi(x) - \text{p.v}\int_\Gamma \phi(y)n(x)\cdot\frac{(x-y)}{|x-y|^3} ds_y$$

while its tangential component is continuous across Γ i.e

$$\frac{\partial}{\partial t}(V\phi)^{+}(x) = \frac{\partial}{\partial t}(V\phi)^{-}(x) = \frac{1}{4\pi}\text{p.v}\int_\Gamma \phi(y)t(x)\cdot\frac{(x-y)}{|x-y|^3} ds_y.$$

A.4. Proofs of Lemma 4.3 and Proposition 4.4

Lemma 4.3 The bilinear form B satisfies the inf-sup condition on $(H^{-1/2}(\mathbb{S}^m),\mathcal{N}) \times (H^{-1/2}(\mathbb{S}^m),\mathcal{N})$, i.e.

$$\exists \alpha_0 > 0 : \inf_{\substack{u\in H^{-1/2}(\mathbb{S}^m)\\ p\in\mathcal{N}}} \sup_{\substack{v\in H^{-1/2}(\mathbb{S}^m)\\ q\in\mathcal{N}}} \frac{|B(u,p;v,q)|}{|||(u,p)|||\,|||(v,q)|||} \geq \alpha_0. \tag{A.31}$$

Proof. Given $(u,p)\in H^{-1/2}(\mathbb{S}^m)\times\mathcal{N}$, $V=V^*$ due to the self adjointness of the single layer potential. Note that $Vp\in\mathcal{N}$ due to the orthogonality of spherical harmonics and $(H_{1,m'}|_{\mathbb{S}_R}) = R\cdot Y_{1,m'}(Y/R)$.
We choose

$$q = -2Vp \in \mathcal{N}, \quad v = (u+p)\in H^{-1/2}(\mathbb{S}^m). \tag{A.32}$$

Using the definition of the bilinear form B we have

$$\begin{aligned}
B(u,p;v,q) &= \langle V(u+p),v\rangle + \langle u,q\rangle \\
&= \langle V(u+p),u+p\rangle - 2\langle u,Vp\rangle \\
&= \langle Vu,u\rangle + 2\langle Vu,p\rangle + \langle Vp,p\rangle - 2\langle u,Vp\rangle \\
&\geq \alpha\|u\|^2_{H^{-1/2}(\mathbb{S}^m)} + \alpha\|p\|^2_{H^{-1/2}(\mathbb{S}^m)} + 2\langle Vu,p\rangle - 2\langle Vu,p\rangle \\
&= \alpha(\|u\|^2_{H^{-1/2}(\mathbb{S}^m)} + \|p\|^2_{H^{-1/2}(\mathbb{S}^m)}) = \alpha|||(u,p)|||^2_{H^{-1/2}(\mathbb{S}^m)}.
\end{aligned}$$

On the other hand, we have by using Young's inequality

$$\begin{aligned}
|||(v,q)||| &= (\|v\|^2_{H^{-1/2}(\mathbb{S}^m)} + \|q\|^2_{H^{-1/2}(\mathbb{S}^m)})^{1/2} \\
&= (\|u+p\|^2_{H^{-1/2}(\mathbb{S}^m)} + 4\|Vp\|^2_{H^{-1/2}(\mathbb{S}^m)})^{1/2} \\
&= (\|u\|^2_{H^{-1/2}(\mathbb{S}^m)} + \|p\|^2_{H^{-1/2}(\mathbb{S}^m)} + 2\langle Vu,p\rangle + 4\|Vp\|^2_{H^{-1/2}(\mathbb{S}^m)})^{1/2} \\
&\underset{\text{Young}}{\leq} C_1(\|u\|^2_{H^{-1/2}(\mathbb{S}^m)} + \|p\|^2_{H^{-1/2}(\mathbb{S}^m)} + \|Vp\|^2_{H^{1/2}(\mathbb{S}^m)})^{1/2} \\
&\leq C_1(\|u\|^2_{H^{-1/2}(\mathbb{S}^m)} + \|p\|^2_{H^{-1/2}(\mathbb{S}^m)} + \widetilde{C}^2\|p\|^2_{H^{-1/2}(\mathbb{S}^m)})^{1/2} \\
&\leq C(\|u\|^2_{H^{-1/2}(\mathbb{S}^m)} + \|p\|^2_{H^{-1/2}(\mathbb{S}^m)})^{1/2} = C|||(u,p)|||
\end{aligned}$$

and the assertion follows. □

Proposition 4.4 Let $\{Q_N\}_N$ be dense in $H^{-1/2}(\mathbb{S}^m)$ and $\mathcal{N}\subset H^{-1/2}(\mathbb{S}^m)$ be finite dimensional. We define

$$\eta(N) := \sup_{p\in\mathcal{N}} \inf_{p_N\in Q_N} \frac{\|p-p_N\|_{H^{-1/2}(\mathbb{S}^m)}}{\|p\|_{H^{-1/2}(\mathbb{S}^m)}}. \tag{A.33}$$

Then there holds for all $N\geq N_0$

$$\inf_{\substack{u_N\in Q_N\\ p\in\mathcal{N}}} \sup_{\substack{v_N\in Q_N\\ q\in\mathcal{N}}} \frac{|B(u_N,p;v_N,q)|}{|||(u_N,p)|||\,|||(v_N,p)|||} \geq \alpha_0 > 0, \tag{A.34}$$

provided that N_0 is such that $\eta(N_0)$ is sufficiently small.

Proof. Let $(u_N,p)\in(Q_N,\mathcal{N})$ be given and $\|u_N\|^2_{H^{-1/2}(\mathbb{S}^m)}+\|p\|^2_{H^{-1/2}(\mathbb{S}^m)}>0$.
We choose $q=-2Vp\in\mathcal{N}$ and $v_N\in Q_N$ to be the solution of

$$\forall\, w\in Q_N:\langle w,Vv_N\rangle=\langle w,V(u_N+p)\rangle. \tag{A.35}$$

Due to elliptical regularity of the single layer potential V and the fact that V is continuous we have

$$\begin{aligned}\|v_N\|_{H^{-1/2}(\mathbb{S}^m)}&\le\frac{1}{\alpha}\|V(u_N+p)\|_{H^{1/2}(\mathbb{S}^m)}\le\frac{C_V}{\alpha}\|u_N+p\|_{H^{-1/2}(\mathbb{S}^m)}\\&\le\frac{C_V}{\alpha}(\|u_N\|_{H^{-1/2}(\mathbb{S}^m)}+\|p\|_{H^{-1/2}(\mathbb{S}^m)})\end{aligned}$$

and we deduce

$$\begin{aligned}\|v_N\|_{H^{-1/2}(\mathbb{S}^m)}&\le\frac{C_V}{\alpha}(\|u_N\|_{H^{-1/2}(\mathbb{S}^m)}+\|p\|_{H^{-1/2}(\mathbb{S}^m)})\\&\le C(\|u_N\|^2_{H^{-1/2}(\mathbb{S}^m)}+\|p\|^2_{H^{-1/2}(\mathbb{S}^m)})^{1/2}\\&\le\widetilde{C}(\|u_N\|_{H^{-1/2}(\mathbb{S}^m)}+\|p\|_{H^{-1/2}(\mathbb{S}^m)}).\end{aligned}$$

More generally we can write

$$\|v_N\|_{H^{-1/2}(\mathbb{S}^m)}\le C|||(u_N,p)|||\le C(\|u_N\|_{H^{-1/2}(\mathbb{S}^m)}+\|p\|_{H^{-1/2}(\mathbb{S}^m)}). \tag{A.36}$$

Now we choose in (A.35) $w=u_N+P_Np\in Q_N$ and set $p_N=P_Np$.
This yields

$$\langle u_N+p_N,Vv_N\rangle=\langle u_N+p_N,V(u_N+p)\rangle. \tag{A.37}$$

Using again the definition of the bilinear form B we deduce

$$\begin{aligned}B(u_N,p;v_N,q)&=\langle Vu_N,v_N\rangle+\langle Vp,v_N\rangle+\langle u_N,q\rangle=\langle V(u_N+p),v_N\rangle+\langle u_N,q\rangle\\&=\langle V(u_N+p_N-p_N+p),v_N\rangle+\langle u_N,q\rangle\\&=\langle u_N+p_N,Vv_N\rangle+\langle V(p-p_N),v_N\rangle+\langle u_N,q\rangle\\&=\langle u_N+p_N,V(u_N+p)\rangle+\langle V(p-p_N),v_N\rangle+\langle u_N,q\rangle\\&\underset{(A.35)}{=}\langle u_N+p_N-p+p,V(u_N+p)\rangle+\langle V(p-p_N),v_N\rangle+\langle u_N,q\rangle\\&=\langle u_N+p,V(u_N+p)\rangle+\langle p_N-p,V(u_N+p)\rangle\\&\quad+\langle V(p-p_N),v_N\rangle+\langle u_N,q\rangle\\&=\|u_N+p\|^2_{H^{-1/2}(\mathbb{S}^m)}+\langle p_N-p,V(u_N+p)\rangle+\langle V(p-p_N),v_N\rangle+\langle u_N,q\rangle\\&=\|u_N\||^2_{H^{-1/2}(\mathbb{S}^m)}+\|p_N\||^2_{H^{-1/2}(\mathbb{S}^m)}+2\langle Vu_N,p\rangle-2\langle u_N,Vp\rangle\\&\quad+\langle p_N-p,V(u_N+p)\rangle+\langle V(p-p_N),v_N\rangle\\&=|||(u_N,p)|||^2+\langle p_N-p,V(u_N+p)\rangle+\langle V(p-p_N),v_N\rangle\\&\ge|||(u_N,p)|||^2-\|p-p_N\|_{H^{-1/2}(\mathbb{S}^m)}(C\|u_N+p\|_{H^{-1/2}(\mathbb{S}^m)}+C\|v_N\|_{H^{-1/2}(\mathbb{S}^m)})\\&\underset{(A.36)}{\ge}|||(u_N,p)|||^2-\|p-p_N\|_{H^{-1/2}(\mathbb{S}^m)}(C\cdot\widetilde{C}|||(u_N,p)|||+C\cdot\widehat{C}|||(u_N,p)|||)\\&=|||(u_N,p)|||^2-\frac{\|p-p_N\|_{H^{-1/2}(\mathbb{S}^m)}}{\|p\|_{H^{-1/2}(\mathbb{S}^m)}}\widehat{\widehat{C}}|||(u_N,p)|||\|p\|_{H^{-1/2}(\mathbb{S}^m)}\\&\ge(1-\eta(N)\widehat{\widehat{C}})|||(u_N,p)|||^2.\end{aligned}$$

On the other hand, we have with (A.32) and (A.36)

$$\begin{aligned}|||(v_N, q)||| &= (\|v_N\|^2_{H^{-1/2}(\mathbb{S}^m)} + \|q\|^2_{H^{-1/2}(\mathbb{S}^m)})^{1/2} \\ &\leq \{\widetilde{C}(\|u_N\|^2_{H^{-1/2}(\mathbb{S}^m)} + \|p\|^2_{H^{-1/2}(\mathbb{S}^m)}) + 4\|Vp\|^2_{H^{-1/2}(\mathbb{S}^m)})^{1/2} \\ &\leq \{\widetilde{C}(\|u_N\|^2_{H^{-1/2}(\mathbb{S}^m)} + \|p\|^2_{H^{-1/2}(\mathbb{S}^m)}) + 4\widehat{C}^2\|p\|^2_{H^{-1/2}(\mathbb{S}^m)})^{1/2} \\ &\leq \widehat{\widetilde{C}}(\|u_N\|^2_{H^{-1/2}(\mathbb{S}^m)} + \|p\|^2_{H^{-1/2}(\mathbb{S}^m)}) \\ &= C|||(u_N, p)|||\end{aligned}$$

and the assertion (A.34) follows. □

6. A Meshless Method for an Exterior Neumann Boundary Value Problem on an Oblate Spheroid

In order to get a first impression on the use of meshless methods in geophysical applications we consider in this chapter, as a simple model problem, the Neumann problem for the Laplacian exterior to an oblate spheroid, where the orbits of satellites are located. The satellite creates data which amount to boundary conditions in scattered points. A key tool of the approach is the use of the Dirichlet-to-Neumann map which directly converts the boundary value problem into a pseudodifferential operator on the spheroid. We handle the arising integral equation with Fourier techniques by expansion into appropriate spherical harmonics. This approach was originally taken by Huang and Yu [20] who solved this pseudodifferential equation numerically with standard boundary elements on a regular grid on the angular domain of the spherical coordinates. We use spherical radial basis functions instead, allowing for better handling of scattered data. As main result we prove that if the solution is smooth, then a high rate of convergence of the approximate solution can be achieved by choosing appropriate radial basis functions. The results of this chapter have been reported in our article [6] (with a slightly different conjecture).

6.1. Preliminary Results

Following [20], let $\Gamma_0 = \{(x_1, x_2, x_3) : \frac{x_1^2}{a^2} + \frac{x_2^2}{a^2} + \frac{x_3^2}{b^2} = 1,\ a > b > 0\}$ be an oblate spheroid and Ω^c be the unbounded domain outside the boundary Γ_0. Through coordinate transformation a point $\boldsymbol{x} = (x_1, x_2, x_3)$ can be represented in oblate spheroid coordinates as

$$\begin{cases} x_1 = f_0 \cosh \mu_0 \sin\theta \cos\varphi \\ x_2 = f_0 \cosh \mu_0 \sin\theta \sin\varphi \\ x_3 = f_0 \sinh \mu_0 \cos\theta \end{cases} \tag{6.1}$$

where $\mu_0 > 0, f_0 = \sqrt{a^2 - b^2}, a = f_0 \cosh \mu_0, b = f_0 \sinh \mu_0, \theta \in [0, \pi]$ and $\varphi \in [0, 2\pi)$.

We consider the following exterior Neumann problem: given $g \in L_2(\Gamma_0)$, find $U \in \Omega^c$

satisfying

$$\begin{cases} \Delta U = 0 & \text{in} \quad \Omega^c \\ \partial_\nu U = g & \text{on} \quad \Gamma_0 \\ U(\boldsymbol{x}) = O(||\boldsymbol{x}||^{-1}) & \text{as} \quad ||\boldsymbol{x}|| \to \infty \end{cases} \tag{6.2}$$

where $||\boldsymbol{x}||$ denotes the Euclidean norm of $\boldsymbol{x}$ and ν denotes the unit outward normal vector on Γ_0.
Using the oblate coordinate transformation we obtain for the Laplace operator

$$\begin{aligned} \Delta U &= \frac{1}{f_0^2(\cosh^2\mu - \sin^2\theta)} \left\{ \frac{1}{\cosh\mu} \frac{\partial}{\partial\mu} \left(\cosh\mu \frac{\partial U}{\partial \mu} \right) \right. \\ &+ \left. \frac{1}{\sin\theta} \frac{\partial}{\partial\theta} \left(\sin\theta \frac{\partial u}{\partial\theta} \right) + \left(\frac{1}{\sin^2\theta} - \frac{1}{\cosh^2\mu} \right) \frac{\partial^2 U}{\partial\varphi^2} \right\}. \end{aligned}$$

Let $\Psi(\mu, \theta, \varphi) = F(\mu)G(\theta)H(\varphi)$ be such that $\Delta\Psi = 0$. By using the technique of separation of variables we obtain

$$\begin{aligned} \frac{d^2}{d\varphi^2} H(\varphi) + m^2 H(\varphi) &= 0, \\ \frac{1}{\cos\theta} \frac{d}{d\theta} \left(\cos\theta \frac{dG(\theta)}{d\theta} \right) - \frac{m^2 G(\theta)}{\cos^2\theta} + n(n+1)G(\theta) &= 0, \\ \frac{1}{\cosh\mu} \frac{d}{d\mu} \left(\cosh\mu \frac{dF(\theta)}{d\mu} \right) + \frac{m^2 F(\theta)}{\cosh^2\mu} - n(n+1)F(\theta) &= 0 \end{aligned}$$

where m, n are integers.
A solution of the above system is

$$\Psi_n^m(\mu, \theta, \varphi) = T_n^m(\sinh\mu) Y_{nm}(\theta, \varphi), \quad m = -n, ..., n; \quad n = 0, 1, 2, ...$$

with T_n^m given by

$$T_n^m = i \exp(\frac{i\pi n}{2}) Q_n^m(ix), \quad i^2 = -1$$

where $Q_n^m(x)$ are the associated Legendre functions of the second kind (see [1], Chapter 8) and $Y_{nm}(\theta, \varphi)$ are spherical harmonics of degree n (see [32]). The set of spherical harmonics

$$\{Y_{nm} : m = -n, ..., n; \quad n = 0, 1, 2, ...\}$$

forms an orthonormal basis for $L^2(\mathbb{S}^2)$ where $\mathbb{S}^2$ is the unit sphere in $\mathbb{R}^3$.
We expand $u(\theta, \varphi) := U(\mu_0, \theta, \varphi)$ into an absolutely convergent series

$$u(\theta, \varphi) = \sum_{n=0}^{\infty} \sum_{m=-n}^{n} \widehat{u}_{nm} Y_{nm}(\theta, \varphi) \tag{6.3}$$

where

$$\widehat{u}_{nm} = \int_0^{\pi} \int_0^{2\pi} u(\theta, \varphi) Y_{nm}^*(\theta, \varphi) \sin\theta \, d\varphi \, d\theta \tag{6.4}$$

with Y_{nm}^* being the complex conjugate of Y_{nm}. The solution of the Laplace equation in the unbounded domain Ω^c outside Γ_0 is then given by the series

$$U(\mu,\theta,\varphi) = \sum_{n=0}^{\infty}\sum_{m=-n}^{n} \frac{T_n^m(\sinh\mu)}{T_n^m(\sinh\mu_0)}\widehat{u}_{nm}Y_{nm}(\theta,\varphi), \quad \mu \ge \mu_0 > 0.$$

We note that

$$\left\| \frac{\partial \boldsymbol{x}}{\partial \mu}(\mu,\theta,\varphi) \right\| = f_0\sqrt{\cosh^2\mu - \sin^2\theta}.$$

Hence, the outward normal derivative $\partial_\nu U$ on Γ_0 can be computed as

$$\partial_\nu U(\theta,\varphi) = -\frac{1}{f_0\sqrt{\cosh^2\mu_0 - \sin^2\theta}}\frac{\partial U}{\partial \mu}(\mu_0,\theta,\varphi).$$

Therefore, the normal derivative of the solution on Γ_0 is

$$\partial_\nu U(\theta,\varphi) = -\frac{1}{f_0\sqrt{\cosh^2\mu_0 - \sin^2\theta}}\sum_{n=0}^{\infty}\sum_{m=-n}^{n}\frac{\frac{dT_n^m}{d\mu}(\sinh\mu_0)}{T_n^m(\sinh\mu_0)}\widehat{u}_{nm}Y_{nm}(\theta,\varphi).$$

We denote by $\mathcal{K}$ the Dirichlet-to-Neumann map (Steklov-Poincaré operator) defined for any $v \in \mathcal{H}^{1/2}(\mathbb{S}^2)$ by

$$(\mathcal{K}v)(\theta,\varphi) := -\frac{1}{f_0\sqrt{\cosh^2\mu_0 - \sin^2\theta}}\sum_{n=0}^{\infty}\sum_{m=-n}^{n}\frac{\frac{dT_n^m}{d\mu}(\sinh\mu_0)}{T_n^m(\sinh\mu_0)}\widehat{v}_{nm}Y_{nm}(\theta,\varphi). \tag{6.5}$$

It is known that (see e.g. [37]) (6.2) is equivalent to

$$\mathcal{K}u = g \quad \text{on} \quad \Gamma_0. \tag{6.6}$$

6.2. Weak Boundary Integral Formulation

Let $\mathcal{D}'(\Gamma_0)$ be the set of all distributions defined on Γ_0. The Sobolev spaces $\mathcal{H}^s(\Gamma_0), s \in \mathbb{R}$, are defined by

$$\mathcal{H}^s(\Gamma_0) = \{f \in \mathcal{D}'(\Gamma_0) : \|f\|^2_{\mathcal{H}^s(\Gamma_0)} = \sum_{n=0}^{\infty}\sum_{m=-n}^{n}(1+n^2)^s|\widehat{f}_{nm}|^2 < \infty\}.$$

The weak formulation of the equation (6.6) is: Find $u \in \mathcal{H}^{1/2}(\Gamma_0)$ satisfying

$$D(u,v) = \int_{\Gamma_0} gv\,ds \quad \forall\, v \in \mathcal{H}^{1/2}(\Gamma_0) \tag{6.7}$$

where

$$D(u,v) := \int_{\Gamma_0}(\mathcal{K}u)v\,ds.$$

Since the measure of Γ_0 is $ds = f_0^2 \cosh\mu_0 \sqrt{\cosh^2\mu_0 - \sin\theta}\sin\theta\, d\theta\, d\varphi$ and the measure on the unit sphere $\mathbb{S}^2$ is $d\sigma = \sin\theta\, d\theta\, d\varphi$ we deduce from the definition of $D(u,v)$

$$\begin{aligned} D(u,v) &= f_0^2 \cosh\mu_0 \int_0^{2\pi}\int_0^{\pi} (\mathcal{K}u)v\sqrt{\cosh^2\mu_0 - \sin^2\theta}\sin\theta\, d\theta\, d\varphi \\ &= f_0^2 \cosh\mu_0 \int_{\mathbb{S}^2} (\mathcal{K}u)v\sqrt{\cosh^2\mu_0 - \sin^2\theta}\, d\sigma. \end{aligned}$$

Using (6.5), we have

$$D(u,v) = -f_0 \sum_{n=0}^{\infty}\sum_{m=-n}^{n} \frac{dT_n^m(\sinh\mu_0)/d\mu}{T_n^m(\sinh\mu_0)} \cosh(\mu_0)\, \widehat{u}_{nm}\widehat{v}_{nm}^*.$$

By defining

$$G_n^m(x) := -\frac{(1+x^2)\frac{d}{dx}T_n^m(x)}{T_n^m(x)} \tag{6.8}$$

we have

$$G_n^m(\sinh\mu) = -\frac{\frac{d}{d\mu}T_n^m(\sinh\mu)}{T_n^m(\sinh\mu)}\cosh\mu.$$

Now we can rewrite $D(u,v)$ as

$$D(u,v) = f_0 \sum_{n=0}^{\infty}\sum_{m=-n}^{n} G_n^m(\sinh\mu_0)\widehat{u}_{nm}\widehat{v}_{nm}^*. \tag{6.9}$$

The following result is proved in [20]:

Theorem 6.1. *The bilinear form $D(\cdot,\cdot)$ is continuous and coercive on $\mathcal{H}^{1/2}(\Gamma_0)$, i.e., there exists constants C_1 and C_2 such that*

$$|D(u,v)| \le C_1\|u\|_{\mathcal{H}^{1/2}(\Gamma)}\|v\|_{\mathcal{H}^{1/2}(\Gamma)} \quad \forall\, u,v \in \mathcal{H}^{1/2}(\Gamma_0)$$

and

$$C_2\|v\|^2_{\mathcal{H}^{1/2}(\Gamma_0)} \le |D(v,v)| \quad \forall\, v \in \mathcal{H}^{1/2}(\Gamma_0)$$

So, by using Lax–Milgram theorem, there exists a unique solution for the variational problem (6.7).

In the next section we will approximate u by spherical radial basis functions (SRBFs).

6.3. Galerkin Approximation Using SRBFs

The finite dimensional subspaces that we use in our approximation are defined by positive definite kernels on $\mathbb{S}^2$ and spherical radial basis functions (see Appendix B).

The positive definite kernels are defined as in Section B.1.2. We define the kernel Φ by a shape function ϕ as in (B.6). Due to the addition formula for spherical harmonics, the kernel Φ can be represented as

$$\Phi(\boldsymbol{y},\boldsymbol{z}) = \sum_{n=0}^{\infty}\sum_{m=-n}^{n} \widehat{\phi}(n) Y_{nm}(\boldsymbol{y}) Y_{nm}^{*}(\boldsymbol{z}). \tag{6.10}$$

The native space $\mathcal{N}_\phi$ defined by (B.10) with the kernel Φ is a reproducing kernel Hilbert space. In Section B.1.2 we have shown that when

$$\widehat{\phi}(n) \simeq (1+n^2)^{-\tau}, \tag{6.11}$$

then the native space $\mathcal{N}_\phi$ can be identified with the Sobolev space $\mathcal{H}^\tau(\mathbb{S}^2)$ defined as

$$\mathcal{H}^\tau(\mathbb{S}^2) := \{v \in \mathcal{D}'(\mathbb{S}^2) : \sum_{n=0}^{\infty}\sum_{m=-n}^{n} |\widehat{v}_{nm}|^2 (1+n^2)^\tau < \infty\}.$$

Since the approximate solution to (6.7) is sought in a finite dimensional subspace of $\mathcal{H}^{1/2}(\Gamma_0)$, in order to make use of the SRBFs we introduce the following bijection $\omega : \Gamma_0 \to \mathbb{S}^2$ (where $\mathbb{S}^2$ is the unit sphere in $\mathbb{R}^3$),

$$\omega(\boldsymbol{x}) = (\sin\theta\cos\varphi, \sin\theta\sin\varphi, \cos\theta) \tag{6.12}$$

where $\boldsymbol{x}$ is an arbitrary point on Γ_0 with oblate spheroidal coordinates

$$\boldsymbol{x}(\theta,\varphi)=(f_0 \cosh\mu_0 \sin\theta\, \cos\varphi, f_0\, \cosh\mu_0\, \sin\theta\, \sin\varphi, f_0\, \sinh\mu_0\, \cos\theta)\, \in \Gamma_0. \tag{6.13}$$

Using this map, we define a reproducing kernel on Γ_0 as

$$\Psi(\boldsymbol{x},\boldsymbol{x}') = \Phi(\omega(\boldsymbol{x}), \omega(\boldsymbol{x}')), \quad \boldsymbol{x},\boldsymbol{x}' \in \Gamma_0 \tag{6.14}$$

where Φ is the kernel defined on $\mathbb{S}^2$; see (B.6).
The kernel Ψ can be expanded into a series of spherical harmonics as

$$\Psi(\boldsymbol{x},\boldsymbol{x}') = \sum_{n=0}^{\infty}\sum_{m=-n}^{n} \widehat{\phi}(n) Y_{nm}(\omega(\boldsymbol{x})) Y_{nm}^{*}(\omega(\boldsymbol{x}')) \tag{6.15}$$

where we choose ϕ such that $\widehat{\phi} \simeq (1+n^2)^{-\tau}$ for some $\tau > 0$. Given a set of scattered data points $X = \{\boldsymbol{x}_1, ..., \boldsymbol{x}_M\} \subset \Gamma_0$. We define V^τ by

$$V^\tau := \text{span}\{\Psi_1, \cdots, \Psi_M\} \tag{6.16}$$

where $\Psi_j := \Psi(x_j, \cdot)$, $j = 1, \cdots, M$.
The solution of (6.7) is approximated by $u_X \in V^\tau$ satisfying

$$D(u_X, v) = \int_{\Gamma_0} gv\, ds \quad \forall\, v \in V^\tau. \tag{6.17}$$

To this end we have to solve a linear system

$$A\boldsymbol{c} = \boldsymbol{g} \tag{6.18}$$

where A is a matrix with entries

$$A_{i,j} = D(\Psi_i, \Psi_j), \quad i, j = 1, ..., M,$$

and $\boldsymbol{g}$ is a vector with entries

$$g_j = \int_{\Gamma_0} g\Psi_j \, ds, \quad j = 1, .., M.$$

Using (6.9) and (6.15) we can write

$$A_{i,j} = f_0 \sum_{n=0}^{\infty} \sum_{m=-n}^{n} [\widehat{\phi}(n)]^2 G_n^m(\sinh \mu_0) Y_{nm}(\omega(\boldsymbol{x}_i)) Y_{nm}^*(\omega(\boldsymbol{x}_j)). \tag{6.19}$$

The positive definiteness of the matrix A is a direct consequence of coercivity of the bilinear form $D(\cdot, \cdot)$ established in Theorem 6.1. In our computations we use the truncated version of $D(\cdot, \cdot)$ defined by

$$D_N(u, v) = f_0 \sum_{n=0}^{N} \sum_{m=-n}^{n} G_n^m(\sinh \mu_0) \widehat{u}_{nm} \widehat{v}_{nm}^*. \tag{6.20}$$

The matrix A is approximated by $A^{(N)}$ with entries

$$A_{i,j}^{(N)} = f_0 \sum_{n=0}^{N} \sum_{m=-n}^{n} [\widehat{\phi}(n)]^2 G_n^m(\sinh \mu_0) Y_{nm}(\omega(\boldsymbol{x}_i)) Y_{nm}^*(\omega(\boldsymbol{x}_j))$$

where N denotes the number of series terms of the truncated matrix element $A_{i,j}^{(N)}$. We compute the actual Galerkin approximation u_X by solving (6.18) with the Galerkin matrix A^N obtained via the truncated entries $A_{i,j}^{(N)}$. We have to choose a sufficient large N (N=100 is used in our numerical experiments) to guarantee the positive definiteness of the matrix $A^{(N)}$. This is termed a "variational" crime by Strang and Fix [49] and will be discussed later in the error analysis. The integral

$$\int_{\Gamma_0} g\Psi_j \, ds = f_0^2 \cosh \mu_0 \int_0^{\pi} \int_0^{2\pi} g(\theta, \varphi) \sqrt{\cosh^2 \mu_0 - \sin^2 \theta} \, \Psi_j(\theta, \varphi) \, \sin \theta \, d\varphi \, d\theta$$

can be evaluated by an appropriate cubature on the sphere $\mathbb{S}^2$ (e.g. [8]) or by using the Fourier expansion of g and Ψ_j.

Let $Y = \{\boldsymbol{y}_1, ..., \boldsymbol{y}_M\}$ be the image of X under the map ω, i.e. $\boldsymbol{y}_j = \omega(\boldsymbol{x}_j)$ for $j = 1, ..., M$. As Y is a set of scattered points on $\mathbb{S}^2$, we define the mesh norm h_Y of Y as usual

$$h_Y = \sup_{\boldsymbol{y} \in \mathbb{S}^2} \min_{\boldsymbol{y}_j \in Y} \cos^{-1}(\boldsymbol{y} \cdot \boldsymbol{y}_j).$$

We have the following approximation property:

Theorem 6.2. *Assume that (6.11) holds for* $\tau > 1$*. If* $f \in \mathcal{H}^\tau(\Gamma_0)$*, then for* $t \leq \tau$*,* $t \leq s \leq 2\tau$ *there exists* $\eta \in V^\tau$ *so that*

$$\|f - \eta\|_{\mathcal{H}^t(\Gamma_0)} \leq c h_Y^{s-t} \|f\|_{\mathcal{H}^s(\Gamma_0)}$$

where c *is a positive constant independent of* Y*.*

Proof. For any function $f \in \mathcal{H}^\tau(\Gamma_0)$, if $F(\boldsymbol{y}) = f(\omega^{-1}(\boldsymbol{y}))$ then F is a function in $\mathcal{H}^\tau(\mathbb{S}^2)$ and

$$\widehat{F}_{nm} = \widehat{f}_{nm} = \int_0^\pi \int_0^{2\pi} f(\theta, \varphi) \sin\theta d\varphi d\theta.$$

Hence,

$$\|f\|^s_{\mathcal{H}^s(\Gamma_0)} = \sum_{n=0}^{\infty} \sum_{m=-n}^{n} (1+n^2)^s |\widehat{F}_{nm}|^2 = \|F\|^2_{\mathcal{H}^s(\mathbb{S}^2)}. \tag{6.21}$$

Using the result in Theorem 3.7 [51] (see also Remark 5.1 therein) there exists $\tilde{\eta} \in \operatorname{span}\{\Phi(\boldsymbol{y}_j, \cdot) : j = 1, ..., M\}$ so that

$$\|F - \tilde{\eta}\|_{\mathcal{H}^t(\mathbb{S}^2)} \leq c h_Y^{s-t} \|F\|_{\mathcal{H}^s(\mathbb{S}^2)}.$$

Defining $\eta(\boldsymbol{x}) := \tilde{\eta}(\omega(\boldsymbol{x}))$ and using (6.21) we deduce the required result noting that $\eta \in V^\tau$. □

6.4. A Priori Estimate for the Galerkin Approximation of the Exact Solution

Using Theorem 6.2 we will derive an error estimate for the approximation of the solution u of (6.7) by the solutions u_X of (6.17). To obtain this estimate we need the following inequality which we are not able to prove. However, our numerical experiments support our claim.

For any $\epsilon > 0$ *and* $N_0 > 0$*, there exists* $c > 0$ *such that for any* $M > 0$*,* $N \geq N_0$ *and* $\boldsymbol{\beta} = (\beta_1, \cdots, \beta_M) \in \mathbb{R}^M$*, there holds*

$$\sum_{n \geq N+1} n^{-1-\epsilon} \sum_{i,j=1}^{M} \beta_i \beta_j P_n(\boldsymbol{x}_i \cdot \boldsymbol{x}_j) \leq c \sum_{n=0}^{N} n^{-1-\epsilon} \sum_{i,j=1}^{M} \beta_i \beta_j P_n(\boldsymbol{x}_i \cdot \boldsymbol{x}_j). \tag{6.22}$$

We have carried out an extensive experiment to check (6.22), namely we computed

$$F(N) = \max_{\beta \in B} \max_{1 \leq M \leq 100} \frac{\sum_{n \geq N+1} n^{-1-\epsilon} \sum_{i,j=1}^{M} \beta_i \beta_j P_n(\boldsymbol{x}_i \cdot \boldsymbol{x}_j)}{\sum_{n \leq N} n^{-1-\epsilon} \sum_{i,j=1}^{M} \beta_i \beta_j P_n(\boldsymbol{x}_i \cdot \boldsymbol{x}_j)}$$

with $\epsilon = 0.01$ and with $\boldsymbol{\beta}$ in a set B random chosen which turns out to have l_2-norm varying from 2.367 to $2.966 \cdot 10^4$. The infinite sum in the numerator of the fraction defining $F(N)$ was computed by a truncated series $\sum_{n=N+1}^{N^*}$ with different values of N^*. We present in Figures (6.1) -(6.3) the graphs of $F(N)$ in these different cases. They support our claim (6.22).

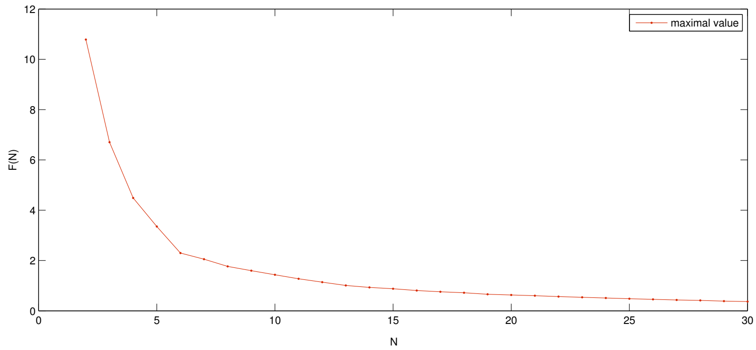

Figure 6.1.: $F(N)$ computed for $N^* = 80$

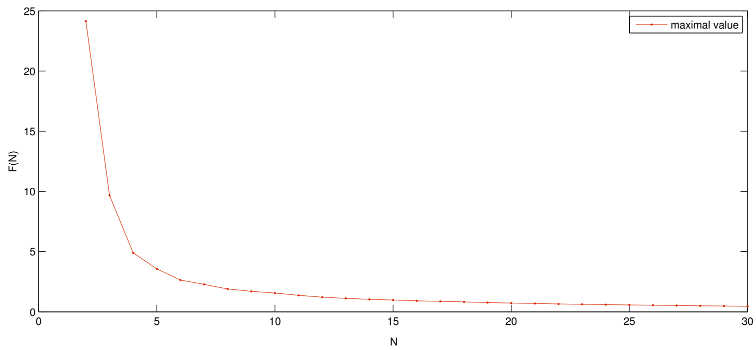

Figure 6.2.: $F(N)$ computed for $N^* = 100$

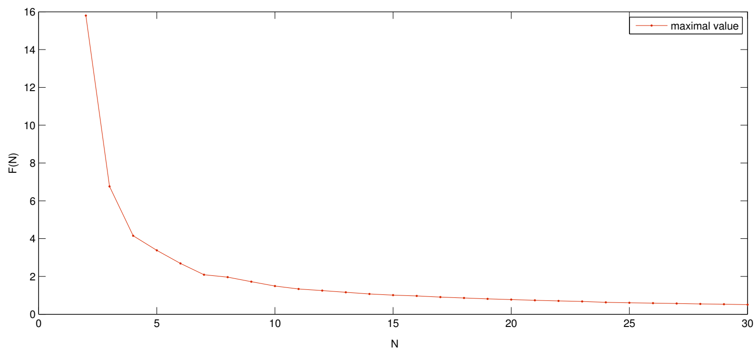

Figure 6.3.: $F(N)$ computed for $N^* = 120$

Theorem 6.3. *Let V^τ be defined by (6.16) with Ψ satisfying (6.11) where $\tau > 1$. Assume that the solution u to (6.7) belongs to $\mathcal{H}^s(\Gamma_0)$ for some s satisfying $1/2 < s < 2\tau - 1$. Then for any $N_0 > 0$, there exists a positive constant C independent of the set X such that for all $N \geq N_0$ there holds*

$$\|u - u_X\|_{\mathcal{H}^{1/2}(\Gamma_0)} \leq C(h_Y^{s-1/2} + N^{-s+1/2})\|u\|_{\mathcal{H}^s(\Gamma_0)}.$$

Proof. By using Strang Lemma [49], we have the following estimate

$$\|u - u_X\|_{\mathcal{H}^{1/2}(\Gamma_0)} \leq \inf_{v\in V^\tau} \|u - v\|_{\mathcal{H}^{1/2}(\Gamma_0)} + \max_{v\in V^\tau} \frac{|D_N(u,v) - D(u,v)|}{[D_N(v,v)]^{1/2}}. \tag{6.23}$$

The first term on the right-hand side can be estimated using Theorem 6.2

$$\inf_{v\in V^\tau} \|u - v\|_{\mathcal{H}^{1/2}(\Gamma_0)} \leq ch_Y^{s-1/2}\|u\|_{\mathcal{H}^s(\Gamma_0)}. \tag{6.24}$$

To estimate the second term on the right-hand side, firstly we note that it is shown in [20, Lemma 3.1]

$$c(\mu_0)(n^2 + 1)^{1/2} < G_n^m(\sinh \mu_0) < C(\mu_0)(n^2 + 1)^{1/2}, \tag{6.25}$$

and that $G_n^{-m}(\sinh \mu_0) = G_n^m(\sinh \mu_0)$ for $0 \leq m \leq n$ and $n = 0, 1, 2 \ldots.$
By using the Cauchy-Schwarz inequality and (6.25) we have

$$\begin{aligned}|D_N(u,v) - D(u,v)| &= \left| f_0 \sum_{n=N+1}^{\infty} \sum_{m=-n}^{n} G_n^m(\sinh \mu_0)\widehat{u}_{nm}\widehat{v}_{nm}^* \right| \\ &\leq C \left(\sum_{n=N+1}^{\infty} (n^2+1)^{\frac{1}{2}} |\widehat{u}_{nm}|^2 \right)^{\frac{1}{2}} \left(\sum_{n=N+1}^{\infty} (n^2+1)^{\frac{1}{2}} |\widehat{v}_{nm}|^2 \right)^{\frac{1}{2}}.\end{aligned}$$

It follows from

$$\sum_{n=N+1}^{\infty} (n^2+1)^{\frac{1}{2}} |\widehat{v}_{nm}|^2 \leq (1 + N^2)^{-s+1/2}\|v\|^2_{\mathcal{H}^s(\Gamma_0)} \quad \forall\, v \in \mathcal{H}^s(\Gamma_0),\ s > 1/2$$

that

$$|D_N(u,v) - D(u,v)| \leq C\,(1 + N^2)^{-s+1/2}\|u\|_{\mathcal{H}^s(\Gamma_0)}\|v\|_{\mathcal{H}^s(\Gamma_0)}. \tag{6.26}$$

Using (6.25) again we have

$$D_N(v,v) = f_0 \sum_{n=0}^{N} \sum_{m=-n}^{n} G_n^m(\sinh \mu_0)|\widehat{v}_{nm}|^2 > c(\mu_0) \sum_{n=0}^{N} \sum_{m=-n}^{n} (n^2+1)^{1/2}|\widehat{v}_{nm}|^2.$$

Hence,

$$\begin{aligned}D_N(v,v) &> c(\mu_0) \sum_{n=0}^{N} \sum_{m=-n}^{n} (n^2+1)^s(n^2+1)^{1/2-s}|\widehat{v}_{nm}|^2 \\ &\geq c(N^2+1)^{1/2-s} \sum_{n=0}^{N} \sum_{|m|\leq n} (n^2+1)^s|\widehat{v}_{nm}|^2 \quad \text{for} \quad s > 1/2. \end{aligned}\tag{6.27}$$

Let

$$A := \sum_{n=0}^{N} \sum_{|m| \le n} (n^2+1)^s |\widehat{v}_{nm}|^2.$$

Since $v \in V^\tau$ we write v as $v = \sum_{i=1}^{M} \beta_i \Psi_i$. Hence, $\widehat{v}_{nm} = \sum_{i=1}^{M} \beta_i (\widehat{\Psi}_i)_{nm}$. Note that

$$(\widehat{\Psi}_i)_{n,m} = |\widehat{\phi}(n)| Y_{nm}(\boldsymbol{x}_i). \tag{6.28}$$

Therefore,

$$A = \sum_{n=0}^{N} (n^2+1)^s \sum_{i,j=1}^{M} \beta_i \beta_j |\widehat{\phi}(n)|^2 \sum_{m=-n}^{n} Y_{nm}(\boldsymbol{x}_i) Y_{nm}^*(\boldsymbol{x}_j).$$

By using the addition formula (B.7) and (6.11) we deduce

$$A = \sum_{n=0}^{N} (2n+1)(n^2+1)^{s-2\tau} \sum_{i,j=1}^{M} \beta_i \beta_j P_n(\boldsymbol{x}_i \cdot \boldsymbol{x}_j). \tag{6.29}$$

By using (6.22) we deduce

$$A \ge c \sum_{n=N+1}^{\infty} (2n+1)(n^2+1)^{s-2\tau} \sum_{i,j=1}^{M} \beta_i \beta_j P_n(\boldsymbol{x}_i \cdot \boldsymbol{x}_j). \tag{6.30}$$

It is then clear that

$$A \ge c ||v||^2_{\mathcal{H}^s(\Gamma_0)}. \tag{6.31}$$

This together with (6.27) gives

$$D_N(v,v) = c(N^2+1)^{1/2-s} ||v||^2_{\mathcal{H}^s(\Gamma_0)}. \tag{6.32}$$

Combining all the estimates in (6.26) and (6.32), we obtain

$$\max_{v \in V^\tau} \frac{|D_N(u,v) - D(u,v)|}{[D_N(v,v)]^{1/2}} \le c N^{-s+1/2} ||u||_{\mathcal{H}^s(\Gamma_0)}.$$

This together with (6.24) proves the assertion.

□

6.5. Implementation of the Approximation Method

In order to compute the entries A_{ij} of the stiffness matrix given in (6.18), we need to compute the spherical harmonics Y_{nm} and the functions G_n^m; see (6.19).
The spherical harmonics are computed by using the formula (see [1])

$$Y_{nm}(\theta, \varphi) := \sqrt{\frac{2n+1}{4\pi}} P_n^{|m|}(\cos\theta) e^{im\varphi} \tag{6.33}$$

where $P_n^m(x)$ are associated Legendre functions of the first kind which can be computed using the following recurrence relations for $m = 0, 1, 2, \ldots, n$ and $n = 0, 1, 2, \ldots$

$$\begin{aligned} P_n^n(x) &= \frac{\sqrt{(2n)!}}{2^n n!}(1-x^2)^{n/2}, \\ P_{n-1}^n(x) &= 0, \\ P_{n+1}^m(x) &= v_n^m x P_n^m(x) + w_n^m P_{n-1}^m(x), \end{aligned}$$

where

$$v_n^m = \frac{(2n+1)}{\sqrt{(n-m+1)(n+m+1)}} \quad \text{and} \quad w_n^m = \frac{\sqrt{(n-m)(n+m)}}{\sqrt{(n-m+1)(n+m+1)}}.$$

The functions T_n^m given by

$$T_n^m(x) = i \exp\left(\frac{i\pi n}{2}\right) Q_n^m(ix) \tag{6.34}$$

are calculated using the algorithm for oblate spheroidal harmonics presented in Gil and Segura [13].

In order to calculate $\frac{d}{dx}T_n^m$ we use (6.34).
We have

$$Q_{n+1}^m(ix) = -i \exp(-\frac{i\pi(n+1)}{2})T_{n+1}^m(x) \text{ and } Q_n^m(ix) = -i\exp(-\frac{i\pi n}{2})T_n^m(x).$$

Thus,

$$\frac{Q_{n+1}^m(ix)}{Q_n^m(ix)} = -i\frac{T_{n+1}^m(x)}{T_n^m(x)} \tag{6.35}$$

and with

$$\frac{d}{dx}T_n^m(x) = -\exp\big(\frac{i\pi n}{2}\big)\frac{d}{dz}Q_n^m(ix) \quad (z = ix)$$

we finally obtain

$$\frac{\frac{d}{dx}T_n^m(x)}{T_n^m(x)} = \frac{-\exp\left(\frac{i\pi n}{2}\right)\frac{d}{dz}Q_n^m(ix)}{i\exp\left(\frac{i\pi n}{2}\right)Q_n^m(ix)} = i\frac{\frac{d}{dz}Q_n^m(ix)}{Q_n^m(ix)}. \tag{6.36}$$

Furthermore, it is known that (see [20])

$$-i\frac{\frac{d}{dz}Q_n^m(z)}{Q_n^m(z)}(1-z^2) = (n+1)(-iz) + (n-m+1)\frac{iQ_{n+1}^m(z)}{Q_n^m(z)} \tag{6.37}$$

and comparing (6.36) and (6.37) (with $z = ix \Longrightarrow (1-z^2) = (1+x^2)$) we have

$$\begin{aligned} -(1+x^2)\frac{\frac{d}{dx}T_n^m(x)}{T_n^m(x)} &= -i\frac{\frac{d}{dz}Q_n^m(z)}{Q_n^m(z)}(1-z^2) \\ &= (n+1)(-iz) + (n-m+1)\frac{iQ_{n+1}^m(z)}{Q_n^m(z)}. \end{aligned}$$

Therefore, the recurrence relation (with $iz = x$ and (6.35)) for $\frac{d}{dx}T_n^m$ can be expressed as

$$-(1+x^2)\frac{\frac{d}{dx}T_n^m(x)}{T_n^m(x)} = (n+1)x + (n-m+1)\frac{T_{n+1}^m(x)}{T_n^m(x)}. \tag{6.38}$$

With this relation the term $G_n^m(\sinh\mu_0)$ in the entry A_{ij} of the stiffness matrix (see (6.19) and (6.8)) can be computed by using the relation

$$G_n^m(x) = (n+1)x + (n-m+1)\frac{T_{n+1}^m(x)}{T_n^m(x)}, \quad m = 0, 1, \dots, n; \quad n = 0, 1, 2, \dots.$$

For negative values of m we use the relation $G_n^m(x) = G_n^{-m}(x)$.
The right hand side terms g_j are computed by using the Fourier coefficients of g and Φ_j and Parseval's identity.
We use different kernels $\Psi(\boldsymbol{x}, \boldsymbol{x}') = \Phi(\omega(\boldsymbol{x}), \omega(\boldsymbol{x}'))$ in our numerical experiments, where the functions Φ are restrictions to the sphere of two different classes of positive definite RBFs defined by Matérn and Wendland functions. The Matérn functions (or Sobolev splines) were introduced for statistical applications in [27]. They are defined by

$$\phi_\nu(r) = \frac{2^{\nu-1}}{\Gamma(\beta)} r^{\nu-3/2} K_{\nu-3/2}(r), \quad \nu > 3/2,$$

where K_ν is the K-Bessel function of order ν. In $\mathbb{R}^3$, the Fourier transform of ϕ decays like

$$\widehat{\phi}(\xi) \sim (1 + \|\xi\|_2^2)^{-\nu}.$$

The Matérn kernels used in our experiments are listed in Table 6.1. When restricting to the sphere, the native space associated with the kernel $\Phi(\boldsymbol{y}, \boldsymbol{z}) := \phi_\nu(\sqrt{2 - 2\boldsymbol{y} \cdot \boldsymbol{z}})$ is the Sobolev space $\mathcal{H}^{\nu-1/2}(\mathbb{S}^2)$ ([33]).

ν	$\phi_\nu(r)$	τ
2	e^{-r}	1.5
3	$e^{-r}(1+r)$	2.5

Table 6.1.: Matérn's RBFs

The Wendland functions [55] are positive definite functions with compact support. For any non-negative integer m, let

$$\widetilde{\rho}_m(r) = \begin{cases} (1-r)^{m+2}, & 0 < r \le 1, \\ 0, & r > 1, \end{cases}$$

and

$$\rho_m(r) = I^m \widetilde{\rho}_m(r), \quad r \ge 0$$

where I is a smoothing operator on the space $C_K[0,\infty)$ of continuous functions in $[0,\infty)$ with compact supports defined by

$$I : C_K[0,\infty) \to C_K[0,\infty), \quad Iv(r) = \int_r^\infty sv(s)ds, \quad r \ge 0.$$

For arbitrary $\boldsymbol{y}, \boldsymbol{z} \in \mathbb{S}^2$,

$$\Phi(\boldsymbol{y}, \boldsymbol{z}) = \rho_m(\sqrt{2 - 2\boldsymbol{y} \cdot \boldsymbol{z}}),$$

with ρ_m being defined as above. It is shown by Narcowich and Ward [34] that in this case, (6.11) holds for $\tau = m + 3/2$. The Wendland functions used in our experiments are listed in Table 6.2.

m	$\rho_m(r)$	τ
0	$(1-r)_+^2$	1.5
1	$(1-r)_+^4(4r+1)$	2.5
2	$(1-r)_+^6(35r^2+18r+3)$	3.5

Table 6.2.: Wendland's RBFs

6.6. Numerical Experiments

In our experiment we choose the oblate spheroid Γ_0 such that $f_0 = 4$ and $\mu_0 = 1$. Let the Neumann condition be

$$g = -\frac{\sinh\mu \sin\theta \cos\varphi(2\cosh^2\mu + \cos^2\theta)}{f_0^2(\cosh^2\mu - \cos^2\theta)^{\frac{5}{2}}}$$

so that the exact solution to (6.2) is

$$u = \frac{\cosh\mu \sin\theta \cos\varphi}{f_0^2(\cosh^2\mu - \cos^2\theta)^{\frac{3}{2}}}. \tag{6.39}$$

This example is taken from [20] where the authors solve (6.7) using piecewise bilinear functions on grids of $\Lambda = \{(\theta, \varphi) : 0 \le \theta \le \pi, 0 \le \varphi \le 2\pi\}$.

We solved (6.17) in the space V^τ defined in (6.16) with three different types of sets of points X.

Points of type 1. As in [20], we divide the intervals $[0, \pi]$ and $[0, 2\pi]$ into N_1 and N_2 subintervals, respectively by

$$\theta_s = s\pi/N_1, \quad s = 0, 1, 2, ..., N_1$$

and

$$\varphi_t = 2t\pi/N_2, \quad t = 0, 1, 2, ..., N_2.$$

Then we use $M := N_2(N_1 - 1)$ points on Γ_0,

$$\boldsymbol{x}_{(N_2-1)s+t} = (f_0 \cosh\mu_0 \sin\theta_s \cos\varphi_t, f_0 \cosh\mu_0 \sin\theta_s \sin\varphi_t, f_0 \sinh\mu_0 \cos\theta_s),$$

where $1 \le s \le N_1 - 1$ and $1 \le t \le N_2$ to construct the basis functions.

Points of type 2. Next, we generate sets of points X on Γ_0 as images under the mapping ω, see (6.12), of sets of points $Y = \{\boldsymbol{y}_1, ..., \boldsymbol{y}_M\}$ on $\mathbb{S}^2$ which are defined by using Saff's algorithm [39]. This algorithm partitions $\mathbb{S}^2$ into M equal-area regions whose centre are $\boldsymbol{y}_1, ..., \boldsymbol{y}_M$; see Figure 1.

Points of type 3. Finally, we use sets of scattered points on the oblate spheroid which are obtained by mapping to the oblate spheroid the geocentric coordinates of data points taken from MAGSAT satellite data; see Figure 2. These sets are extracted from a full data set about 26 million points in such a way that the separation radius of each set

$$q_Y = \frac{1}{2} \min_{\boldsymbol{y} \neq \boldsymbol{y}'} \cos^{-1}(\boldsymbol{y} \cdot \boldsymbol{y}')$$

is not too small; see Table 6.8.
We solved the matrix equation (6.18) by the conjugate gradient method with relative tolerance 10^{-10}, i.e. the stopping criteria is

$$\frac{\|A\boldsymbol{c}^{(m)} - \boldsymbol{g}\|_{l^2}}{\|\boldsymbol{g}\|_{l^2}} \leq 10^{-10}. \tag{6.40}$$

Here $\boldsymbol{c}^{(m)}$ is the m-th iterate.
Let $e := u - u_X$ where $u(\theta, \varphi) = U(\mu_0, \theta, \varphi)$ is the solution to (6.7) and u_X is the solution to (6.17).
We compute $\|e\|_{\mathcal{L}^2(\Gamma_0)}$ and $\|e\|_{\mathcal{H}^{1/2}(\Gamma_0)}$ approximately by

$$\|e\|_{\mathcal{L}^2(\Gamma_0)} \approx \left(\sum_{n=0}^{120} \sum_{m=-n}^{n} |(\widehat{u}_X)_{nm} - \widehat{u}_{nm}|^2 \right)^{1/2}$$

and

$$\|e\|_{\mathcal{H}^{1/2}(\Gamma_0)} \approx \left(\sum_{n=0}^{120} (1+n^2)^{1/2} \sum_{m=-n}^{n} |(\widehat{u}_X)_{nm} - \widehat{u}_{nm}|^2 \right)^{1/2}$$

in which

$$(\widehat{u}_X)_{nm} = \sum_{i=1}^{M} \widehat{\phi}(n) c_i Y_{nm}(\omega(\boldsymbol{x}_i))$$

and $\widehat{u}_{nm}$ is computed by using a quadrature [8] for formula (6.3).
We also compute l_2 and l_∞ errors for point sets of type 1. Let $\mathcal{G}$ be points of the grid of size $(N_1, N_2) = (160, 320)$, then

$$\|e\|_{l^\infty(\Gamma_0)} = \max_{y \in \mathcal{G}} |u_X(y) - u(y)|$$

and

$$\|e\|_{l^2(\Gamma_0)} = \left(\frac{1}{|\mathcal{G}|} \sum_{y \in \mathcal{G}} |u_X(y) - u(y)|^2 \right)^{1/2}$$

where $|\mathcal{G}| = 50880$ is cardinality of $\mathcal{G}$ and $|\mathcal{G}| := N_2(N_1 - 1)$.
Table 6.3 and Figure 6.4 show the experimental orders of convergence (EOC) for the errors in the $\mathcal{H}^{-1/2}(\Gamma_0)$-norm (energy norm) when Saff points (points of type 2) and Wendland's kernels are used. Table 6.4 and Figure 6.5 show the corresponding results when Matérn kernels are used.

The numbers in the Tables 6.5, 6.6 and 6.7 show fast convergence of our RBF Galerkin method applied to the Poincaré-Steklov operator with different values of N on different grids of size (N_1, N_2), when Wendland's kernels are used .

Table 6.8 gives the errors in the $L^2(\Gamma_0)$ and $\mathcal{H}^2(\Gamma_0)$ norms for scattered points (points of type 3). In this case, the matrix is ill conditioned and hence a preconditioner is required.

Therefore, by noting (6.8), the symbol of the operator $\mathcal{K}$ defined in (6.5) behaves like $(n^2 + 1)^{1/2}$, i.e. $\mathcal{K}$ is a pseudodifferential operator of order 1. This allows us to extend the analysis [52] for the overlapping Schwarz preconditioner on the sphere to the oblate spheroid. The preconditioner is defined by the additive Schwarz operator, using a subspace decomposition of V^τ as

$$V^\tau = V_0 + ... + V_J.$$

These subspaces $V_j, j = 0, ..., J$ are defined from a decomposition of the set Y into overlapping subsets $Y_j, j = 0, ..., J$. These subsets are generated by the following algorithm:

Select $\alpha \in (0, \pi/3)$, $\beta \in (0, \pi]$;
$\boldsymbol{p}_1 = \boldsymbol{y}_1 \in Y$;
$Y_0 := \{\boldsymbol{p}_1\}$;
$Y_1 := \{\boldsymbol{y} \in Y : \cos^{-1}(\boldsymbol{y} \cdot \boldsymbol{p}_1) \leq \alpha\}$;
$J = 1, k = 1$;
while $Y_1 \cup ... \cup Y_k \neq Y$ **do**
  $k = k + 1$;
  $\boldsymbol{p}_k$ is chosen from $Y \backslash Y_0$ such that $\cos^{-1}(\boldsymbol{p}_{k-1} \cdot \boldsymbol{p}_k) \geq \beta$;
  $Y_0 := Y_0 \cup \{\boldsymbol{p}_k\}$;
  $Y_k := \boldsymbol{y} \in Y : \cos^{-1}(\boldsymbol{y} \cdot \boldsymbol{p}_k) \leq \alpha$;
end while
$J = k$

Each set Y_k is a collection of points inside a spherical cap of radius α centered at $\boldsymbol{p}_k$. The centers $\boldsymbol{p}_k$ are chosen so that the geodesic distance between two successive centers is no less than β.

Table 6.9 shows the corresponding numbers of iteration of the preconditioned conjugate gradient using the same stopping criteria as before, i.e. with the relative tolerance $\leq 10^{-10}$. Errors of the same order as in the non-preconditioned case are obtained. The advantage of the preconditioner can be observed.

m	M	h_X	$\mathcal{H}^{1/2}err$	EOC
0	100	0.2672	3.1112E-03	
	200	0.1942	1.3158E-03	2.70
	500	0.1237	3.9392E-04	2.67
	1000	0.0849	1.6113E-04	2.38
	2000	0.0609	6.7877E-05	2.60
	4000	0.0426	2.4877E-05	2.81
1	100	0.2672	1.0988E-03	
	200	0.1942	1.9053E-04	5.49
	500	0.1237	2.4204E-05	4.57
	1000	0.0849	4.7746E-06	4.31
	2000	0.0609	9.9207E-07	4.73
	4000	0.0426	1.9228E-07	4.59
2	100	0.2672	1.1860E-03	
	200	0.1942	8.0785E-05	8.42
	500	0.1237	3.6622E-06	6.86
	1000	0.0849	3.3840E-07	6.33
	2000	0.0609	3.6577E-08	6.70
	4000	0.0426	3.5598E-09	6.52

Table 6.3.: Errors with Saff points and $\rho_m(r)$

ν	M	h_X	$\mathcal{H}^{1/2}err$	EOC
2	100	0.2672	1.3063E-03	
	200	0.1942	5.3882E-04	2.78
	500	0.1237	1.6489E-04	2.63
	1000	0.0849	6.7086E-05	2.39
	2000	0.0609	2.7266E-05	2.71
	4000	0.0426	1.0090E-05	2.78
3	100	0.2672	1.7780E-04	
	200	0.1942	2.3464E-05	6.35
	500	0.1237	2.3542E-06	5.10
	1000	0.0849	3.7971E-07	4.85
	2000	0.0609	7.6692E-08	4.81
	4000	0.0426	1.4582E-08	4.65

Table 6.4.: Errors with Saff points and $\nu_m(r)$

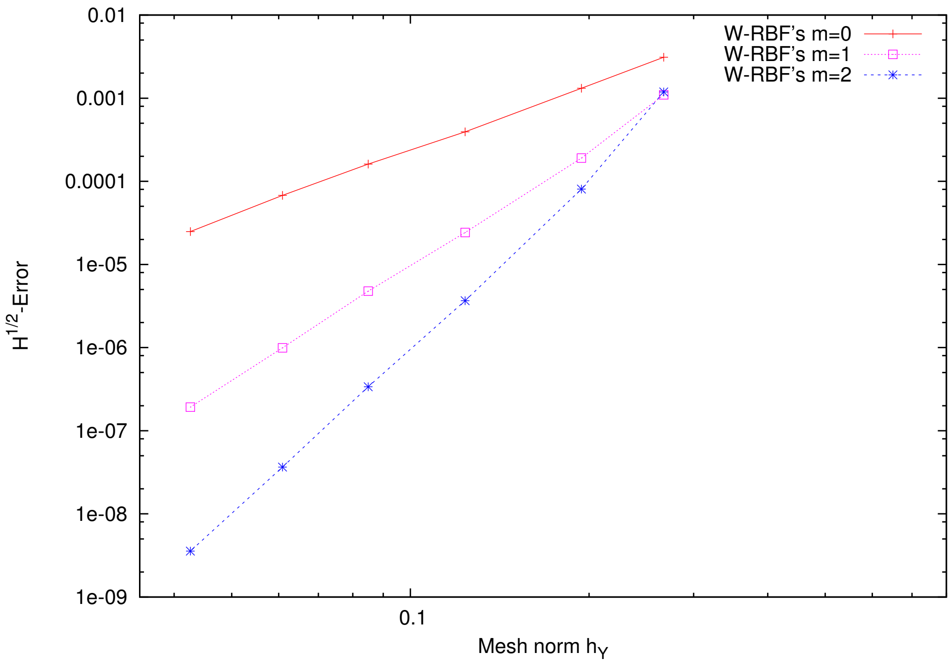

Figure 6.4.: Log-log plot for $\mathcal{H}^{1/2}(\Gamma_0)$ errors using Wendland RBFs $\rho_m(r)$

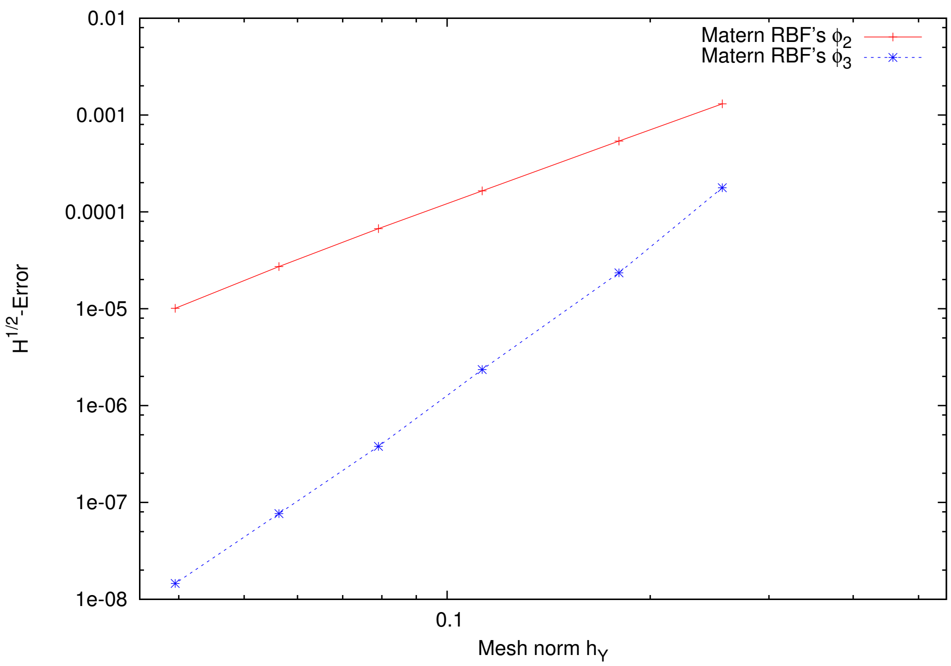

Figure 6.5.: Log-log plot for $\mathcal{H}^{1/2}(\Gamma_0)$ errors using Matern RBFs $\nu_m(r)$

m	N_1	N_2	$\|e\|_{\mathcal{L}^2(\Gamma_0)}$	$\|e\|_{\mathcal{H}^{1/2}(\Gamma_0)}$	$\|e\|_{l^2(\Gamma_0)}$	$\|e\|_{l^\infty(\Gamma_0)}$
0	10	20	0.3854E-03	0.1779E-02	0.1028E-03	0.6957E-03
0	20	40	0.4949E-04	0.3248E-03	0.1343E-04	0.9091E-04
0	40	80	0.5814E-05	0.5303E-04	0.1888E-05	0.1116E-04
0	80	160	0.2402E-08	0.2470E-07	0.4065E-06	0.1425E-05
1	10	20	0.1033E-03	0.4509E-03	0.2828E-04	0.1099E-03
1	20	40	0.2922E-05	0.1848E-04	0.7933E-06	0.3357E-05
1	40	80	0.9079E-07	0.8163E-06	0.2402E-07	0.1068E-06
1	80	160	0.8770E-09	0.5410E-08	0.1235E-08	0.4930E-08
2	10	20	0.6982E-04	0.2818E-03	0.2356E-04	0.6829E-04
2	20	40	0.4338E-06	0.2695E-05	0.1310E-06	0.4398E-06
2	40	80	0.3392E-08	0.2924E-07	0.1089E-08	0.4647E-08
2	80	160	0.1155E-08	0.6304E-08	0.6819E-09	0.4083E-08

Table 6.5.: Errors on grided points, with $\rho_m(r)$, using conjugate gradient method for $N_{max} = 120, N_{truncate} = 80$

m	N_1	N_2	$\|e\|_{\mathcal{L}^2(\Gamma_0)}$	$\|e\|_{\mathcal{H}^{1/2}(\Gamma_0)}$	$\|e\|_{l^2(\Gamma_0)}$	$\|e\|_{l^\infty(\Gamma_0)}$
0	10	20	0.3854E-03	0.1779E-02	0.1028E-03	0.6957E-03
0	20	40	0.4949E-04	0.3248E-03	0.1343E-04	0.9092E-04
0	40	80	0.5814E-05	0.5303E-04	0.1889E-05	0.1114E-04
0	80	160	0.2407E-08	0.2463E-07	0.4065E-06	0.1425E-05
1	10	20	0.1033E-03	0.4509E-03	0.2828E-04	0.1099E-03
1	20	40	0.2922E-05	0.1848E-04	0.7933E-06	0.3357E-05
1	40	80	0.9079E-07	0.8163E-06	0.2402E-07	0.1068E-06
1	80	160	0.8768E-09	0.5410E-08	0.1235E-08	0.4936E-08
2	10	20	0.6982E-04	0.2818E-03	0.2356E-04	0.6829E-04
2	20	40	0.4338E-06	0.2695E-05	0.1310E-06	0.4398E-06
2	40	80	0.3393E-08	0.2924E-07	0.1090E-08	0.4659E-08
2	80	160	0.1153E-08	0.6296E-08	0.6811E-09	0.4094E-08

Table 6.6.: Errors on grided points, with $\rho_m(r)$, using conjugate gradient method for $N_{max} = 120, N_{truncate} = 100$

m	N_1	N_2	$\|e\|_{\mathcal{L}^2(\Gamma_0)}$	$\|e\|_{\mathcal{H}^{1/2}(\Gamma_0)}$	$\|e\|_{l^2(\Gamma_0)}$	$\|e\|_{l^\infty(\Gamma_0)}$
0	10	20	0.3854E-03	0.1779E-02	0.1028E-03	0.6957E-03
0	20	40	0.4949E-04	0.3248E-03	0.1343E-04	0.9093E-04
0	40	80	0.5814E-05	0.5303E-04	0.1889E-05	0.1114E-04
0	80	160	0.2391E-08	0.2437E-07	0.4065E-06	0.1425E-05
1	10	20	0.1033E-03	0.4509E-03	0.2828E-04	0.1099E-03
1	20	40	0.2922E-05	0.1848E-04	0.7933E-06	0.3357E-05
1	40	80	0.9079E-07	0.8163E-06	0.2402E-07	0.1068E-06
1	80	160	0.8743E-09	0.5401E-08	0.1234E-08	0.4908E-08
2	10	20	0.6982E-04	0.2818E-03	0.2356E-04	0.6829E-04
2	20	40	0.4338E-06	0.2695E-05	0.1310E-06	0.4397E-06
2	40	80	0.3392E-08	0.2924E-07	0.1090E-08	0.4640E-08
2	80	160	0.1155E-08	0.6304E-08	0.6818E-09	0.4100E-08

Table 6.7.: Errors on grided points, with $\rho_m(r)$, using conjugate gradient method for $N_{max} = 120, N_{truncate} = 120$

M	q_Y	$\|e\|_{\mathcal{L}^2(\Gamma_0)}$	$\|e\|_{\mathcal{H}^{1/2}(\Gamma_0)}$	ITER	CPU
3470	$\pi/140$	6.25503E-006	5.01114E-005	2809	234.6
7763	$\pi/200$	2.41695E-006	2.13257E-005	27064	13323.7
10443	$\pi/240$	1.87142E-006	1.62031E-005	30931	17361.9

Table 6.8.: Errors with scattered points from MAGSAT, using conjugate gradient method for $N_{max} = 120, N_{truncate} = 100$ and $\rho_0(r)$

M	$\cos\alpha$	$\cos\beta$	$\|e\|_{\mathcal{L}^2(\Gamma_0)}$	$\|e\|_{\mathcal{H}^{1/2}(\Gamma_0)}$	ITER	CPU
3470	0.9	-0.15500000	6.24283E-006	5.02580E-005	73	4.3
7763	0.97	0.99999996	2.41695E-006	2.13257E-005	939	294.1
10443	0.98	0.99999996	1.87142E-006	1.62031E-005	1602	1085.8

Table 6.9.: Errors with scattered points from MAGSAT, for overlapping additive Schwarz preconditioner for $N_{max} = 120, N_{truncate} = 100$ and $\rho_0(r)$

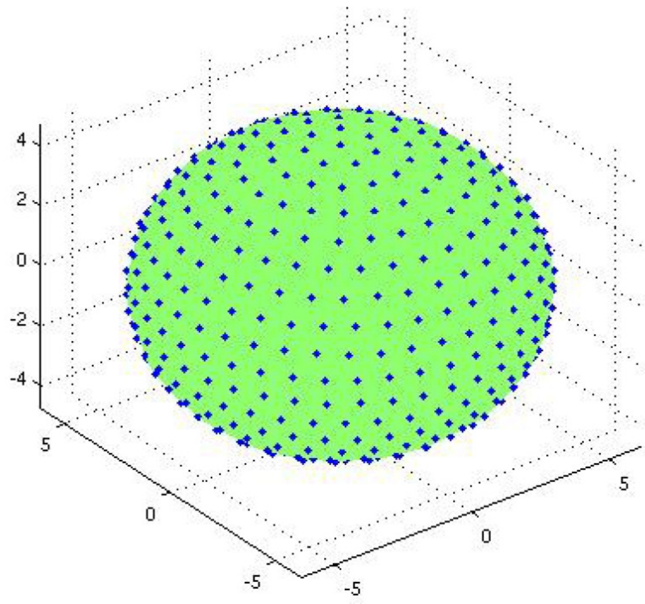

Figure 6.6.: Image of Saff points on the oblate spheroid

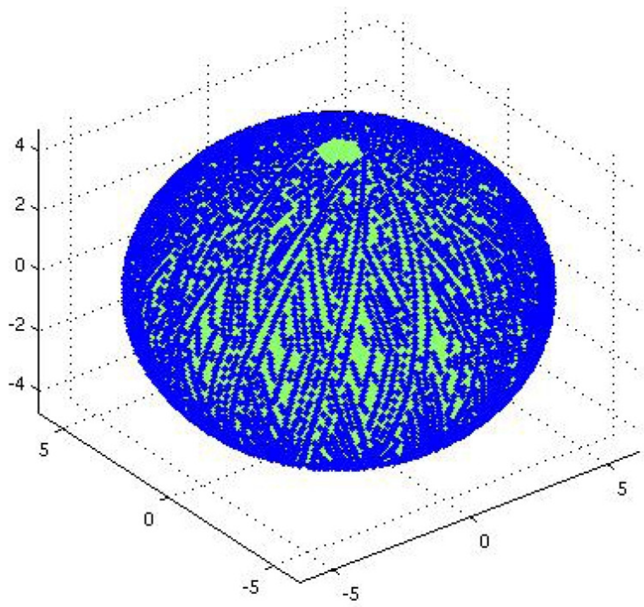

Figure 6.7.: Image of satellite points on the oblate spheroid

7. A First Application of Meshless Methods to the Linearized Molodensky Problem

In this chapter we use spherical radial basis functions to approximate the solution of the linearized Molodensky problem on the unit sphere. The approximate solution is computed with a corresponding meshless Galerkin scheme using scattered data from satellites. Our numerical experiments show that this meshless method is superior to standard boundary element computations with piecewise constants. The results in this chapter are published in [48].

7.1. Boundary Integral Equation

We reconsider the linearized Molodensky problem in geodesy for the disturbing gravity potential u.
For a given right hand side g find u satisfying:

$$\begin{aligned} \Delta u &= 0 && \text{in} \quad \Omega = \mathbb{R}^3 \backslash \overline{\Omega} \\ -\frac{2}{r}u - \frac{\partial u}{\partial r} &= g && \text{on} \quad \partial\overline{\Omega} \qquad (7.1) \\ u &= \frac{1}{r} + O(r^{-3}) && \text{for} \quad r \to \infty \qquad (7.2) \end{aligned}$$

where $\partial\overline{\Omega}$ denotes the telluroid and r denotes the radius of $\boldsymbol{x} \in \mathbb{R}^3$. In the following, we consider the model where the surface of the earth is given by $\mathbb{S}^2$ the boundary of the unit ball $\overline{\Omega} = \overline{B}_1(0)$. As described in the paper by Heck [16] a single layer potential ansatz leads to pseudodifferential equation (a second kind Fredholm integral equation) on $\mathbb{S}^2$ which will be solved numerically in the following by use of radial basis functions. By inserting the approximation of the density back into the single layer potential we thus obtain an approximation for the gravity potential u, the solution of the above geodetic boundary value problem GBVP(7.1).
In detail we proceed as follows: We write u as single layer potential V with unknown density μ for $\boldsymbol{X} \notin \mathbb{S}^2$

$$u(\boldsymbol{X}) = V\mu(\boldsymbol{X}) = \frac{1}{4\pi} \int_{\mathbb{S}^2} \frac{\mu(\boldsymbol{y})}{|\boldsymbol{X} - \boldsymbol{y}|} ds(\boldsymbol{y}) \qquad (7.3)$$

and compute

$$(\operatorname{grad} V\mu(\boldsymbol{x}))_+ = -\frac{1}{2}\mu(\boldsymbol{x})\boldsymbol{n}_{\boldsymbol{x}} - \frac{1}{4\pi}\text{p.v.}\int_{\mathbb{S}^2} \frac{\boldsymbol{x}-\boldsymbol{y}}{|\boldsymbol{x}-\boldsymbol{y}|^3}\mu(\boldsymbol{y})ds(\boldsymbol{y})$$

where $+$ denotes the limit on the surface $\mathbb{S}^2$ from the exterior domain Ω and $\boldsymbol{n}$ is the normal on $\mathbb{S}^2$ pointing into Ω.
Furthermore

$$\frac{\partial(V\mu)}{\partial r}(\boldsymbol{x}) = \operatorname{grad} V\mu(\boldsymbol{x})\cdot\frac{\boldsymbol{x}}{|\boldsymbol{x}|} = -\frac{1}{2}\mu(\boldsymbol{x})\cos(\boldsymbol{n}_{\boldsymbol{x}},\boldsymbol{x}) - \frac{1}{4\pi}\text{p.v.}\int_{\mathbb{S}^2}\frac{(\boldsymbol{x}-\boldsymbol{y})\cdot\boldsymbol{x}}{|\boldsymbol{x}||\boldsymbol{x}-\boldsymbol{y}|^3}\mu(\boldsymbol{y})ds(\boldsymbol{y})$$

and

$$\frac{2}{r}V\mu = \frac{2}{|\boldsymbol{x}|}\frac{1}{4\pi}\int_{\mathbb{S}^2}\frac{\mu(\boldsymbol{y})}{|\boldsymbol{x}-\boldsymbol{y}|}ds(\boldsymbol{y}).$$

Inserting these expressions into the boundary condition (GBVP) yields (see [16])

$$\begin{aligned}
-\frac{2}{r}V\mu(\boldsymbol{x}) - \frac{\partial V\mu}{\partial r}(\boldsymbol{x}) &= \frac{1}{2}\mu(\boldsymbol{x})\cos(\boldsymbol{n}_{\boldsymbol{x}},\boldsymbol{x}) \\
&\quad + \frac{1}{4\pi}\text{p.v.}\int_{\mathbb{S}^2}\left[\frac{(\boldsymbol{x}-\boldsymbol{y})\cdot\boldsymbol{x}}{|\boldsymbol{x}||\boldsymbol{x}-\boldsymbol{y}|^3} - \frac{2}{|\boldsymbol{x}||\boldsymbol{x}-\boldsymbol{y}|}\right]\mu(\boldsymbol{y})ds(\boldsymbol{y}) \\
&= \frac{1}{2}\mu(\boldsymbol{x})\cos(\boldsymbol{n}_{\boldsymbol{x}},\boldsymbol{x}) + \frac{1}{4\pi}\text{p.v.}\int_{\mathbb{S}^2}\frac{|\boldsymbol{x}|^2-|\boldsymbol{y}|^2-3|\boldsymbol{x}-\boldsymbol{y}|^2}{2|\boldsymbol{x}||\boldsymbol{x}-\boldsymbol{y}|^3}\mu(\boldsymbol{y})ds(\boldsymbol{y}) \\
&= g(\boldsymbol{x}).
\end{aligned}$$

This becomes

$$\begin{aligned}
S\mu(\boldsymbol{x}) :&= 2\left(-\frac{1}{4\pi}\int_{\mathbb{S}^2}\frac{\mu(\boldsymbol{y})}{||\boldsymbol{x}-\boldsymbol{y}||}do_y\right) + \frac{1}{2}\mu(\boldsymbol{x}) + \frac{1}{4\pi}\int_{\mathbb{S}^2}\frac{(\boldsymbol{x}-\boldsymbol{y})\cdot\boldsymbol{x}}{||\boldsymbol{x}-\boldsymbol{y}||^3}\mu(\boldsymbol{y})do_y \\
&= \frac{1}{2}\mu(\boldsymbol{x}) + \frac{1}{4\pi}\text{p.v.}\int_{\mathbb{S}^2}\frac{-3\mu(\boldsymbol{y})}{2||\boldsymbol{x}-\boldsymbol{y}||}do_y \qquad (7.4) \\
&= g(\boldsymbol{x}).
\end{aligned}$$

Now we observe that the action of the above pseudodifferential operator S can be rewritten via its discrete symbol $\widehat{S}$ and the Fourier coefficients $\widehat{\mu}_{l,m}$ of μ with respect to spherical harmonics $Y_{l,m}$ of degree l as

$$S\mu = \sum_{l=0}^{\infty}\sum_{m=-l}^{l}\widehat{S}(l)\widehat{\mu}_{l,m}Y_{l,m}$$

with symbol

$$\widehat{S}(l) = \frac{l-1}{2l+1} \quad \text{and} \quad \widehat{\mu}_{l,m} = \langle\mu,\overline{Y_{l,m}}\rangle_{L_2(\mathbb{S}^2)},$$

compare (7.14) below. As pseudodifferential operator of order zero S maps $\mathcal{H}^s$ into itself for any $s\in\mathbb{R}$ where the Sobolev space $\mathcal{H}^s$ is defined by

$$\mathcal{H}^s = \left\{v:\mathbb{S}^2\to\mathbb{R} \mid \sum_{l=0}^{\infty}\sum_{m=-l}^{l}(l+1)^{2s}|\widehat{v}_{l,m}|^2 < \infty\right\}.$$

Let us abbreviate the pseudodifferential equation (7.4) as

$$S\mu = g \quad \text{on} \quad \mathbb{S}^2. \tag{7.5}$$

We observe that

$$\widehat{S}(l) = \frac{l-1}{2l+1} = 0 \quad \text{for} \quad l = 1.$$

So $\ker S = \operatorname{span}\{Y_{1,m},\ m = -1, 0, 1\}$. Therefore, to ensure solvability of (7.5) we must impose side conditions :

$$\gamma^j \mu = a_j \quad (j = 1, 2, 3) \tag{7.6}$$

with given $a_j \in \mathbb{R}$ and a unisolvent set of linear functionals $\{\gamma^j\}$, i.e. for any $\nu \in \ker S$, if $\gamma^j \nu = 0, j = 1, 2, 3$, then $\nu = 0$.
Application of classical Riesz-Schauder theory gives the following theorem.

Theorem 7.1. *Equations (7.5) and (7.6) have a unique solution if*

$$\langle g, \Phi \rangle = 0 \quad \forall \Phi \in ker S.$$

Now, we analyse the above side conditions. First let us rewrite the single layer potential as

$$V\mu(\boldsymbol{X}) = \frac{1}{4\pi} \int_{\mathbb{S}^2} \frac{\mu(\boldsymbol{y})}{2 \sin \frac{\psi}{2}} ds(\boldsymbol{y}) \tag{7.7}$$

where ψ is the angle between $\boldsymbol{X}$ and $\boldsymbol{y}$ (c.f. [16]).
We expand the disturbing potential outside the boundary sphere $\mathbb{S}^2$ into solid spherical harmonics

$$u(\boldsymbol{X}) = \sum_{n=0}^{\infty} \left(\frac{1}{r}\right)^{n+1} u_n(\boldsymbol{x}), \quad \boldsymbol{X} = r \cdot \boldsymbol{x}, \quad r > 1 \tag{7.8}$$

where

$$u_n(\boldsymbol{x}) = \sum_{m=-n}^{n} \widehat{u}_{n,m} Y_{n,m}(\boldsymbol{x}).$$

Correspondingly, we expand the functions $g(\boldsymbol{x})$ and $\mu(\boldsymbol{x})$ in surface spherical harmonics

$$g(\boldsymbol{x}) = \sum_{n=0}^{\infty} g_n(\boldsymbol{x}), \quad \mu(\boldsymbol{x}) = \sum_{n=0}^{\infty} \mu_n(\boldsymbol{x}) \tag{7.9}$$

where

$$g_n(\boldsymbol{x}) = \sum_{m=-n}^{n} \widehat{g}_{n,m} Y_{n,m}(\boldsymbol{x}) \quad \text{and} \quad \mu_n(\boldsymbol{x}) = \sum_{m=-n}^{n} \widehat{\mu}_{n,m} Y_{n,m}(\boldsymbol{x}).$$

Note that due to (7.3) we have

$$\frac{1}{4\pi} \int_{\mathbb{S}^2} \frac{\mu_n(\boldsymbol{y})}{2 \sin \frac{\psi}{2}} ds(\boldsymbol{y}) = \left(\frac{1}{r}\right)^{n+1} u_n(\boldsymbol{x}). \tag{7.10}$$

Furthermore, with (7.7) the integral equation (7.4) becomes

$$\frac{1}{2}\mu(\boldsymbol{x}) + \frac{1}{4\pi} \int_{\mathbb{S}^2} \frac{-3\mu(\boldsymbol{y})}{4 \sin \frac{\psi}{2}} d\sigma(\boldsymbol{y}) = g(\boldsymbol{x}). \tag{7.11}$$

Then inserting (7.9), (7.10) and (7.8) and equating the coefficients we obtain

$$\mu_n(\boldsymbol{x}) - 3r^{-n-1}u_n(\boldsymbol{x}) = 2g_n(\boldsymbol{x}). \tag{7.12}$$

Setting $r = 1$ we have

$$\begin{aligned} \mu_0(\boldsymbol{x}) - 3u_0(\boldsymbol{x}) &= 2g_0(\boldsymbol{x}) \quad \text{for} \quad n = 0, \\ \mu_1(\boldsymbol{x}) - 3u_1(\boldsymbol{x}) &= 2g_1(\boldsymbol{x}) \quad \text{for} \quad n = 1. \end{aligned}$$

Therefore with

$$u_1(\boldsymbol{x}) = \sum_{m=-1}^{1} \widehat{u}_{1,m} Y_{1,m}(\boldsymbol{x}),\; g_1(\boldsymbol{x}) = \sum_{m=-1}^{1} \widehat{g}_{1,m} Y_{1,m}(\boldsymbol{x}) \quad \text{and} \quad \mu_1(\boldsymbol{x}) = \sum_{m=-1}^{1} \widehat{\mu}_{1,m} Y_{1,m}(\boldsymbol{x})$$

we obtain

$$\widehat{\mu}_{1,m} - 3\widehat{u}_{1,m} = 2\widehat{g}_{1,m}, \qquad m = -1, 0, 1. \tag{7.13}$$

Now let us analyse the discrete symbol $\widehat{S}(l)$ of the pseudodifferential operator S. This can be computed by simply inserting the expansion for u and g into the boundary condition of the GBVP(7.1).
Using

$$\left(-\frac{2}{r}u - \frac{\partial u}{\partial r}\right)_{\mathbb{S}^2} = g$$

we have

$$-\frac{2}{r}\sum_{n=0}^{\infty}\left(\frac{1}{r}\right)^{n+1} u_n(\boldsymbol{x}) + \sum_{n=0}^{\infty}(n+1)\frac{1}{r^{n+2}}u_n(\boldsymbol{x}) = \sum_{n=0}^{\infty} g_n(\boldsymbol{x})$$

or

$$\sum_{n=0}^{\infty} \frac{(n-1)}{r^{n+2}} u_n(\boldsymbol{x}) = \sum_{n=0}^{\infty} g_n(\boldsymbol{x}).$$

Equating the coefficients and then inserting in (7.12) gives with $r = 1$

$$\mu_n(\boldsymbol{x}) - \frac{3}{n-1} g_n(\boldsymbol{x}) = 2g_n(\boldsymbol{x})$$

hence,

$$\mu_n(\boldsymbol{x}) = \left(2 + \frac{3}{n-1}\right) g_n(\boldsymbol{x}) = \frac{2n+1}{n-1} g_n(\boldsymbol{x}) \tag{7.14}$$

from which we deduce the result on the discrete symbol $\widehat{S}$ of the pseudodifferential operator S (compare Heck [16]).

7.2. Meshless Galerkin Method with Boundary Integral Equations

The solutions of (7.5), (7.6) are approximated by spherical radial basis functions. Let

$$\rho_m(r) = \begin{cases} (1-r)^{m+2}, & 0 < r \le 1, \\ 0, & r > 1. \end{cases}, \qquad m = 0, 1, 2.$$

We define $\phi : [-1, 1] \to \mathbb{R}$ by $\phi(t) = \rho_m(\sqrt{2-2t})$. This is called the Wendland function. For a set of data points $\{\mathbf{x}_1, \mathbf{x}_2, \ldots, \mathbf{x}_N\}$ on the sphere we define a set of spherical radial basis functions as:

$$\Phi_i(\boldsymbol{x}) := \sum_{n=0}^{\infty} \sum_{m=-n}^{n} \widehat{\phi}(n)\overline{Y_{n,m}(\boldsymbol{x}_i)}Y_{n,m}(\boldsymbol{x}) = \phi(\boldsymbol{x} \cdot \boldsymbol{x}_i)$$

with Fourier-Legendre coefficients

$$\widehat{\phi}(n) = 2\pi \int_{-1}^{1} \phi(t)P_n(t)dt$$

and Legendre polynomials P_n of degree n.
It is shown in [34, Proposition 4.6] that for $m = 0, 1, 2$

$$c_1(1+n^2)^{-m-3/2} \leq \widehat{\phi}(n) \leq c_2(1+n^2)^{-m-3/2}$$

for all $n = 0, 1, 2, \ldots$, where c_1 and c_2 are positive constants.
Now, the numerical scheme under consideration is the Galerkin method (G):
Find $\tilde{\mu}_N = \tilde{\mu}_1 + \tilde{\mu}_0$ with $\tilde{\mu}_1 = \sum_{i=1}^{N} c_i\Phi_i^*$

$$\langle S\tilde{\mu}_1, \Phi_k^* \rangle_{L_2(\mathbb{S}^2)} = \langle g, \Phi_k^* \rangle_{L_2(\mathbb{S}^2)}, \qquad 1 \leq k \leq N$$

where Φ_i^* is obtained from Φ_i by deleting the Fourier terms for $n = 0$ and $n = 1$.
The part $\tilde{\mu}_0$ of the Galerkin solution $\tilde{\mu}_N$ must satisfy the side conditions

$$\begin{aligned} \gamma^0\tilde{\mu}_0 &= \int_{\mathbb{S}^2} \tilde{\mu}_0 Y_{0,0} = a_0, & \gamma^1\tilde{\mu}_0 &= \int_{\mathbb{S}^2} \tilde{\mu}_0 Y_{1,-1} = b_{-1}, \\ \gamma^2\tilde{\mu}_0 &= \int_{\mathbb{S}^2} \tilde{\mu}_0 Y_{1,0} = b_0, & \gamma^3\tilde{\mu}_0 &= \int_{\mathbb{S}^2} \tilde{\mu}_0 Y_{1,1} = b_1. \end{aligned} \tag{7.15}$$

Note that the term for $n = 0$ in the expansion for Φ_i is dropped to make all Fourier modes in the entries of the Galerkin stiffness matrix positive. The side conditions $\gamma^1, \gamma^2, \gamma^3$ are just the side conditions (7.6), whereas the side condition γ^0 is needed since we dropped the expansion term for $n = 0$ in Φ_i.

Theorem 7.2. *For N sufficiently large the Galerkin scheme (G) is uniquely solvable and the Galerkin solution $\tilde{\mu}_N = \tilde{\mu}_1 + \tilde{\mu}_0$ converges to the exact solution $\mu \in \mathcal{H}^s$, $0 \leq s \leq m+3$,*

$$||\mu - \tilde{\mu}_N||_{\mathcal{H}^0} = O(h^s),$$

where $\mathcal{H}^0 := L^2(\mathbb{S}^2)$.

Proof. The convergence of the Galerkin scheme follows due to the fact that the pseudodifferential operator S can be written as identity plus a compact operator. Therefore, it is a strongly elliptic operator in the sense of Wendland [56]. Due to the general convergence results in Stephan and Wendland [47], strong ellipticity together with the side conditions guarantee convergence of general Galerkin schemes including the case of radial basis functions considered here. The convergence estimate follows by applying a corresponding approximation result of functions in the Sobolev space $\mathcal{H}^s$ by radial basis functions from [51] together with the quasi optimality of the Galerkin error. The latter quasi optimality follows from the analysis in [47]. □

Next we comment on the computation of the Galerkin stiffness matrix and the right hand side. Note that

$$\begin{aligned}\langle S\Phi_i^*, \Phi_j^* \rangle_{L^2(\mathbb{S}^2)} &= \sum_{n=2}^{\infty} \sum_{m=-n}^{n} \frac{n-1}{2n+1} |\widehat{\phi}(n)|^2 \overline{Y_{n,m}(\boldsymbol{x}_i)} Y_{n,m}(\boldsymbol{x}_j) \\ &= \sum_{n \neq 1, n \neq 2} \frac{n-1}{4\pi} |\widehat{\phi}(n)|^2 P_n(\boldsymbol{x}_i \cdot \boldsymbol{x}_j)\end{aligned}$$

where we have used

$$(\widehat{\Phi}_i^*)_{n,m} = \widehat{\phi}(n) \overline{Y_{n,m}(\boldsymbol{x}_i)} \tag{7.16}$$

and the addition theorem

$$P_n(\mathbf{x} \cdot \mathbf{y}) = \frac{4\pi}{2n+1} \sum_{m=-n}^{n} \overline{Y_{n,m}(\boldsymbol{x})} Y_{n,m}(\boldsymbol{y}).$$

For the right hand side we have

$$\langle g, \Phi_k^* \rangle_{L^2(\mathbb{S}^2)} = \sum_{n=0}^{\infty} \sum_{m=-n}^{n} (\widehat{g})_{n,m} \widehat{\phi}(n) \overline{Y_{n,m}(\boldsymbol{x}_k)}. \tag{7.17}$$

7.3. Numerical Example

In the following we compute approximations of the Galerkin solution $\tilde{\mu}_N$ of (G) by truncating the series expansion of Φ_i^* at $n = 500$.
We consider

$$u(\mathbf{X}) = \frac{1}{||\boldsymbol{X} - \boldsymbol{p}||}, \quad \boldsymbol{p} = (0, 0, 0.5)$$

and compute the right hand side via

$$g = -2u - \frac{\partial u}{\partial n} \quad \text{on} \quad \mathbb{S}^2.$$

In the side conditions (7.15) we choose

$$a_0 = 2\sqrt{\pi},\ b_1 = b_{-1} = 0,\ b_0 = \sqrt{3\pi}.$$

This gives

$$\begin{aligned}\tilde{\mu}_0 &= a_0 Y_{0,0} + b_{-1} Y_{1,-1} + b_0 Y_{1,0} + b_1 Y_{1,1} \\ &= 2\sqrt{\pi}\sqrt{\frac{1}{4\pi}} + \sqrt{3\pi}\sqrt{\frac{3}{4\pi}}\cos\theta = 1 + \frac{3}{2}\cos\theta.\end{aligned}$$

In Table 7.1 we have listed $|(u_N(\boldsymbol{q}) - u(\boldsymbol{q}))|$ for $\boldsymbol{q} = (1.10227, 1.10227, 0.9)$ with

$$u_N(\boldsymbol{q}) := \frac{1}{4\pi}\int_{\mathbb{S}^2} \frac{\tilde{\mu}_N(\boldsymbol{y})}{||\boldsymbol{q} - \boldsymbol{y}||} ds(y)$$

where $\tilde{\mu}_N$ is the Galerkin solution of our Galerkin system (G) computed with the Wendland radial basis functions [54] mentioned in Section 7.2, namely

$$\phi(t) = (1 - \sqrt{2 - 2t})^{m+2}.$$

We denote this Galerkin approximation "meshless" in Table 7.1 to distinguish from the standard boundary element solution computed with piecewise constants on the uniform mesh of Figure 7.2.

In the tables below we list the respective experimental orders of convergence for the pointwise error of the gravity potential at the point $\boldsymbol{q}$ outside of the unit sphere $\mathbb{S}^2$. The numerical experiments are performed on a uniform grid of Saff points c.f. Figure 7.1. The errors are plotted in Figure 7.3.

For comparison we present here also the numerical experiments when solving approximately the integral equation (7.4) with standard BEM when using piecewise constant basis functions on triangles which approximate the surface c.f. Figure 7.2.
Table 7.2 shows the corresponding results (again $\vec{q} = (1.10227, 1.10227, 0.9)$). In Figure 7.3 we see that radial basis functions give better convergence than standard BEM.

Since data are not available at the poles we must use for the standard BEM with piecewise constants the grid shown in Figure 7.4 with holes at the poles. Table 7.3 and Table 7.4 and Figure 7.4 show clearly that scaled radial basis functions give much better results than standard boundary elements.

Concluding, we have shown that for geodetic boundary value problems the reduction to boundary integral equations leads to a fast numerical method when the Galerkin scheme is performed with spherical radial basis functions.

m	N	Value	$\lvert(u_N(\boldsymbol{q}) - u(\boldsymbol{q}))\rvert$	EOC
0	200	0.69442	0.07305	
	500	0.67349	0.05212	0.37
	1000	0.65323	0.03186	0.71
	2000	0.62413	0.00276	3.53
	4000	0.62213	0.00076	1.86
	8000	0.62198	0.00061	0.32
1	200	0.79285	0.17148	
	500	0.62781	0.00644	3.58
	1000	0.62731	0.00594	0.17
	2000	0.62326	0.00189	1.65
	4000	0.62228	0.00091	1.05
	8000	0.62197	0.00059	0.61
2	200	0.71406	0.09269	
	500	0.62638	0.00501	3.18
	1000	0.62603	0.00466	0.10
	2000	0.62283	0.00146	1.67
	4000	0.62192	0.00055	1.41
	8000	0.62156	0.00019	1.53

Table 7.1.: Meshless Galerkin approximation u_N of gravity potential u; single layer density computed by spherical radial basis functions centered at N Saff points

N	Value	$\lvert(u_N(\boldsymbol{q}) - u(\boldsymbol{q}))\rvert$	EOC
500	0.61808	0.00329	
1000	0.61932	0.00205	0.68
2000	0.62010	0.00127	0.69
4000	0.62028	0.00109	0.22
8000	0.62051	0.00086	0.34

Table 7.2.: Standard BEM Galerkin approximation u_N of gravity potential u; single layer density computed by pw. constants on triangles with N Saff points

	N	Value	$\lvert(u_N(\boldsymbol{q}) - u(\boldsymbol{q}))\rvert$	EOC
m=0	2133	0.62932	0.00795	
scale=20.5	3458	0.62507	0.00369	1.75
	4108	0.62288	0.00151	6.75
	7663	0.62254	0.00117	0.41
	10443	0.62167	0.00030	1.40
m=0	2133	0.62915	0.00778	
scale=20	3458	0.62471	0.00334	1.58
	4108	0.62241	0.00104	5.19
	7663	0.62203	0.00066	0.75
	10433	0.62112	0.00024	3.21

Table 7.3.: Meshless Galerkin approximation with spherical radial basis functions at scattered points on $\mathbb{S}^2$

N	Value	$\lvert(u_N(\boldsymbol{q}) - u(\boldsymbol{q}))\rvert$	EOC
2133	0.67059	0.04922	
7699	0.64751	0.02614	0.49
10643	0.63797	0.01660	1.40

Table 7.4.: BEM Galerkin approximation with pw. constants on triangles with vertices at scattered points

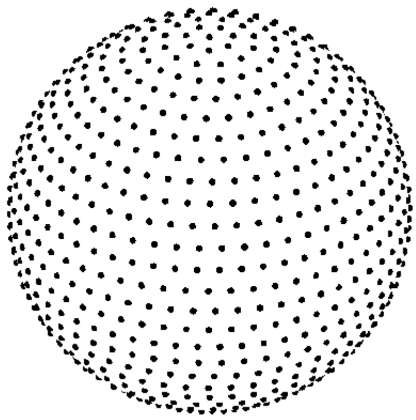

Figure 7.1.: Uniformly distributed Saff points on $\mathbb{S}^2$ ($N = 1000$ Saff points), c.f. [15]

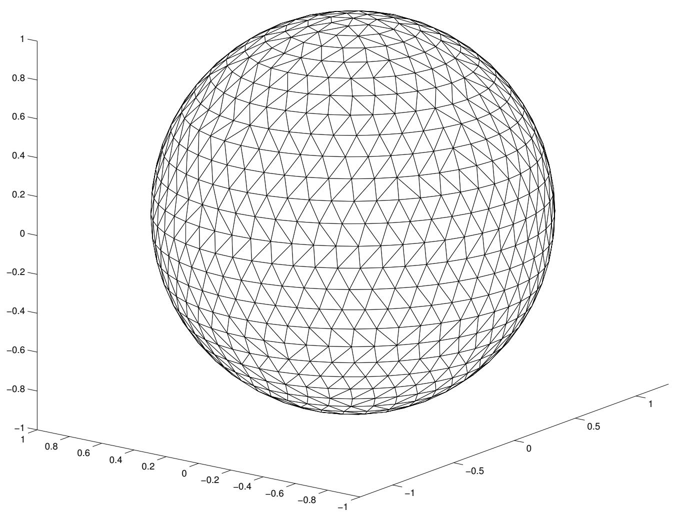

Figure 7.2.: Boundary element mesh consisting of triangles with vertices at $N = 1000$ Saff points

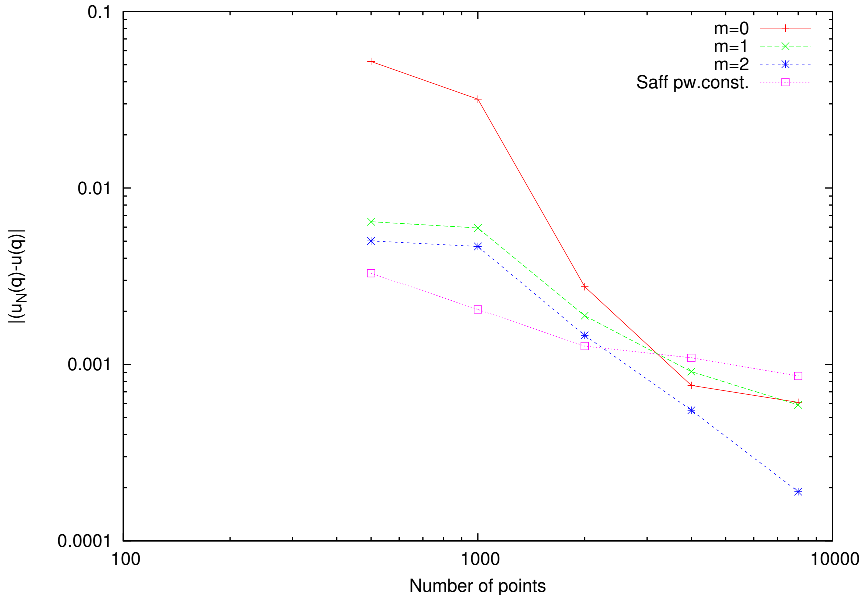

Figure 7.3.: Pointwise error $|(u_N(\boldsymbol{q}) - u(\boldsymbol{q}))|$ with $\tilde{\mu}_N$ computed with radial basis functions $(m = 0, 1, 2)$ and piecewise constants in the Saff points in Fig 7.1 and Fig 7.2.

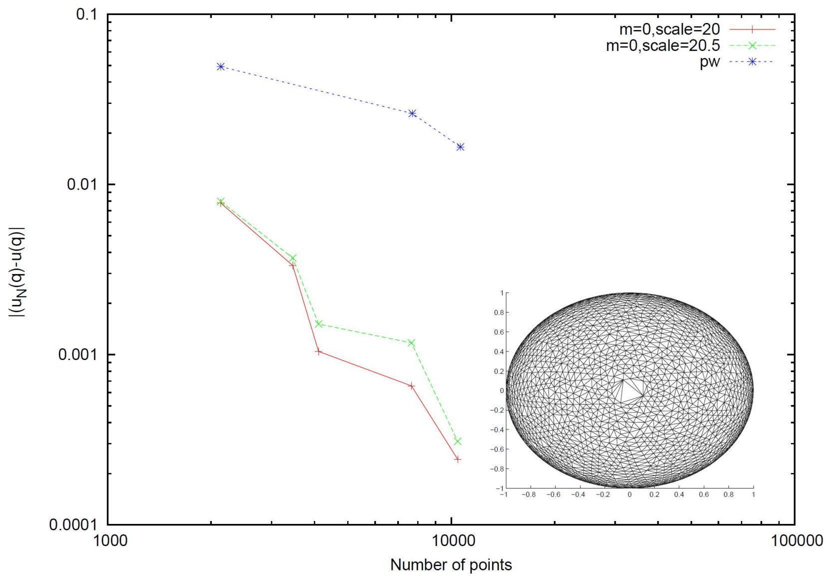

Figure 7.4.: Pointwise error $|(u_N(\boldsymbol{q}) - u(\boldsymbol{q}))|$ for $\tilde{\mu}_N$ computed on N=3458 scattered points with scaled radial basis functions or piecewise constants

B.

B.1. A Short Introduction to Spherical Radial Basis Functions

B.1.1. Basic Definitions and Notations

Spherical harmonics are defined as the restrictions of homogeneous polynomials that satisfy the Laplace equation [11]. Suppose that $H_n : \mathbb{R}^3 \to \mathbb{R}$ is a homogeneous polynomial of degree n such that $\Delta_x H_n(x) = 0$ for all $x \in \mathbb{R}^3$; then the restriction $Y_n = H_n|_\Omega$ is called *spherical harmonic* of degree n. For our purpose we identify $\Omega = \mathbb{S}^2$, where $\mathbb{S}^2$ is the unit sphere in $\mathbb{R}^3$. We denote the space of all spherical harmonics of degree n by $\mathbb{H}_n$. The dimension of this space being $2n+1$, we may choose for it an orthonormal basis $\{Y_{nm}\}_{m=-n}^{n}$. The collection of all the spherical harmonics

$$\{Y_{nm} : m = -n, \ldots, n, \quad n \geq 0\}$$

forms an orthonormal basis for $L^2(\mathbb{S}^2)$.
For $s \in \mathbb{R}$, the Sobolev space $\mathcal{H}^s(\mathbb{S}^2)$ is defined by

$$\mathcal{H}^s(\mathbb{S}^2) := \big\{ v \in \mathcal{D}'(\mathbb{S}^2) : \sum_{n=0}^{\infty} \sum_{m=-n}^{n} |\widehat{v}_{nm}|^2 (1+n^2)^s < \infty \big\} \tag{B.1}$$

where $\mathcal{D}(\mathbb{S}^2)$ is the space of distributions on $\mathbb{S}^2$ and $\widehat{v}_{nm}$ are the Fourrier coefficients of v,

$$\widehat{v}_{nm} = \langle v, Y_{nm} \rangle_{L^2(\mathbb{S}^2)}.$$

The space $\mathcal{H}^s(\mathbb{S}^2)$ is equipped with the following norm and inner product

$$\|v\|_{\mathcal{H}^s(\mathbb{S}^2)} := \big(\sum_{n=0}^{\infty} \sum_{m=-n}^{n} (1+n^2)^s |\widehat{v}_{nm}|^2 \big)^{1/2} \tag{B.2}$$

and

$$\langle v, w \rangle_{\mathcal{H}^s(\mathbb{S}^2)} := \sum_{n=0}^{\infty} \sum_{m=-n}^{n} (1+n^2)^s \widehat{v}_{nm} \widehat{w}_{nm}.$$

In Chapter 6 we will also use the Cauchy-Schwarz inequality given by

$$|\langle v, w \rangle_s| \leq \|v\|_s \|w\|_s \quad \forall\, v, w \in \mathcal{H}^s(\mathbb{S}^2), \quad \forall\, s \in \mathbb{R}. \tag{B.3}$$

Let $\{\widehat{L}(n)\}_{n\geq 0}$ be a sequence of real numbers. A pseudodifferential operator L is a linear operator that assigns to any $v \in \mathcal{D}'(\mathbb{S}^2)$ a distribution

$$Lv := \sum_{n=0}^{\infty} \sum_{m=-n}^{n} \widehat{L}(n)\widehat{v}_{nm} Y_{nm}.$$

The sequence $\{\widehat{L}(n)\}_{n\geq 0}$ is called the *spherical symbol* of L.
Let $\mathcal{K}(L) := \{n \in \mathbb{N} : \widehat{L}(n) = 0\}$. Then

$$\ker L = \text{span}\,\{Y_{nm} : n \in \mathcal{K}(L), \quad m = -n, \dots n\}.$$

B.1.2. Spherical Radial Basis Functions

Positive-Definite Kernels

A continuous function $\Phi : \mathbb{S}^2 \times \mathbb{S}^2$ is called a *positive definite kernel* on $\mathbb{S}^2$ if it satisfies

(i) $\Phi(\boldsymbol{x}, \boldsymbol{y}) = \Phi(\boldsymbol{y}, \boldsymbol{x}) \quad \forall\, \boldsymbol{y}, \boldsymbol{z} \in \mathbb{S}^2$

(ii) for any positive integer K and any set of distinct scattered points $\{\boldsymbol{y}_1, ..., \boldsymbol{y}_K\} \subset \mathbb{S}^2$, the $N \times N$ matrix A with entries $A_{i,j} = \Phi(\boldsymbol{y}_i, \boldsymbol{y}_j)$ is positive semi-definite.

If the matrix A is positive definite then Φ is called a *strictly positive definite* kernel; see [41, 57].
We define the kernel Φ by a shape function ϕ as follows. Let $\phi : [-1, 1] \to \mathbb{R}$ be an univariate function having a series expansion in term of Legendre polynomials

$$\phi(t) = \frac{1}{4\pi} \sum_{n=0}^{\infty} (2n+1)\widehat{\phi}(n) P_n(t) \tag{B.4}$$

where $\widehat{\phi}(n)$ is the *Fourier-Legendre coefficient*,

$$\widehat{\phi}(n) = 2\pi \int_{-1}^{1} \phi(t) P_n(t) dt. \tag{B.5}$$

Here, we denoted by $P_n(t)$ the degree n normalised Legendre polynomial in n variables so that $P_n(1) = 1$. Now, by using this shape function ϕ, we define

$$\Phi(\boldsymbol{x}, \boldsymbol{y}) := \phi(\boldsymbol{x} \cdot \boldsymbol{y}), \quad \forall\, \boldsymbol{x}, \boldsymbol{y} \in \mathbb{S}^2 \tag{B.6}$$

where we denoted by $\boldsymbol{x} \cdot \boldsymbol{y}$ the scalar product between $\boldsymbol{x}$ and $\boldsymbol{y}$. Noting that $\boldsymbol{x} \cdot \boldsymbol{y}$ is the cosine of the angle between $\boldsymbol{x}$ and $\boldsymbol{y}$, called the geodesic distance between the two points, we deduce that the kernel Φ is a zonal kernel. Due to the addition formula for spherical harmonics

$$\sum_{m=-n}^{n} Y_{nm}(\boldsymbol{x}) Y^*_{nm}(\boldsymbol{y}) = \frac{2n+1}{4\pi} P_n(\boldsymbol{x} \cdot \boldsymbol{y}) \quad \forall\, \boldsymbol{x}, \boldsymbol{y} \in \mathbb{S}^2 \tag{B.7}$$

the kernel Φ can be represented as

$$\Phi(\boldsymbol{x}, \boldsymbol{y}) = \sum_{n=0}^{\infty} \sum_{m=-n}^{n} \widehat{\phi}(n) Y_{nm}(\boldsymbol{x}) Y_{nm}^{*}(\boldsymbol{y}). \tag{B.8}$$

A complete characterisation of strictly positive definite kernels is established in [4]: the kernel Φ is strictly positive definite if and only if $\widehat{\phi}(n) \geq 0$ for all $n \geq 0$ and $\widehat{\phi}(n) > 0$ for infinitely many even values of n and infinitely many odd values of n; see [41] and [57].

Spherical Radial Basis Functions

For a given shape function ϕ satisfying

$$\widehat{\phi}(n) \simeq (1+n^2)^{-\tau} \quad \forall\, n \geq 0 \tag{B.9}$$

for some $\tau \in \mathbb{R}$, the corresponding kernel Φ given by (B.6) is strictly positive definite. The *native space* associated with the kernel Φ which is defined by

$$\mathcal{N}_{\phi} = \Big\{ v \in \mathcal{D}'(\mathbb{S}^2) : \sum_{n=0}^{\infty} \sum_{m=-n}^{n} \frac{|\widehat{v}_{nm}|^2}{\widehat{\phi}(n)} < \infty \Big\} \tag{B.10}$$

is equipped with an inner product and a norm defined by

$$\langle v, w \rangle_{\phi} = \sum_{n=0}^{\infty} \sum_{m=-n}^{n} \frac{\widehat{v}_{nm} \widehat{w}_{nm}}{\widehat{\phi}(n)} \quad \text{and} \quad \|v\|_{\phi} = \left(\sum_{n=0}^{\infty} \sum_{m=-n}^{n} \frac{|\widehat{v}_{nm}|^2}{\widehat{\phi}(n)} \right)^{1/2}.$$

If the coefficients $\widehat{\phi}(n)$ for $n = 0, 1, \ldots$ satisfy

$$c_1 (1+n^2)^{-\tau} \leq \widehat{\phi}(n) \leq c_2 (1+n^2)^{-\tau}$$

for some positive constants c_1 and c_2, and some $\tau \in \mathbb{R}$, then the native space $\mathcal{N}_{\phi}$ can be identified with the Sobolev space $\mathcal{H}^{\tau}(\mathbb{S})$, and the corresponding norms are equivalent. Let $Y = \{\boldsymbol{y}_1, \ldots, \boldsymbol{y}_n\}$ be a set of data points on the sphere. Two important parameters characterising the set Y are the *mesh norm* h_Y and the separation radius q_Y defined by

$$h_Y := \sup_{\boldsymbol{y} \in \mathbb{S}^2} \min_{1 \leq i \leq N} \cos^{-1}(\boldsymbol{y} \cdot \boldsymbol{y}_i) \quad \text{and} \quad q_Y := \frac{1}{2} \min_{\substack{i \neq j \\ 1 \leq i,j \leq N}} \cos^{-1}(\boldsymbol{y}_i \cdot \boldsymbol{y}_j). \tag{B.11}$$

The *spherical basis functions* Φ_i, $i = 1, \ldots, N$, associated with Y and the kernel Φ are defined by

$$\Phi_i(\boldsymbol{y}) := \Phi(\boldsymbol{y}, \boldsymbol{y}_i) = \sum_{n=0}^{\infty} \sum_{m=-n}^{n} \widehat{\phi}(n) Y_{nm}^{*}(\boldsymbol{y}_i) Y_{nm}(\boldsymbol{y}). \tag{B.12}$$

8. Conclusion

In this dissertation three different algorithms based on the abstract Nash-Hörmander method are presented. As far as we know from the literature, there are no numerical experiments for the full nonlinear Molodensky problem with surface update until now. Thus, the first difficulty was to develop an implementable algorithm based on the Nash-Hörmander method. We considered a model problem for a given initial surface, the unit sphere $\mathbb{S}^2$, with given gravity potential W_0 and gravity vector G_0. Furthermore, there are given values for gravity potential W_{meas} and gravity vector G_{meas} and the corresponding surface has to be determined via the Nash-Hörmander algorithm. In our model problem for the numerical experiments the given values W_{meas}, G_{meas} belong to a sphere with radius 1.1. Therefore, our algorithm should converge to the final surface which is here the sphere of radius 1.1.

In general, our algorithm based on the boundary element method should work for any given initial surfaces with explicitly given W_0 and G_0. In particular, we have seen that the smoother is very useful in our numerical experiments. We strongly believe that a very fine mesh on the initial surfaces will give suitable approximations by implying better Galerkin approximations of the potentials and the Hessians and the surface updates. However, this implies a high complexity of our algorithms (Algorithm 4.1, Algorithm 4.2, Algorithm 4.3), due to the large amount of unknowns.

A key point in the Nash-Hörmander algorithm in all its versions is the computation of the Hessian matrix needed for the update $\dot{\varphi}_m$ of the surface. Unfortunately the Nash-Hörmander algorithm is very vulnerable due to the computation of this Hessian matrix. While the numerical experiments clearly show that for the cube, where we have no domain approximation, we can compute the Hessian very accurately, in the case of the sphere the domain approximation error is dominating. Therefore, the accurate computation of the surface update is very difficult. An other consequence of the inaccurate computation of the Hessian is that the computation of the directional vector h is inexact. This is an additional difficulty for the Nash-Hörmander algorithm. Thus, further research on the computation of the 3d Hessian on sphere like surfaces is necessary.

Also a better approximation of the surface is needed. If enough memory is available, we could further decrease the mesh size and thus improve the accuracy in the computation of the Hessian and obtain better results. By using Matlab's Parallel Computing Toolbox and some optimizations of the code, the computation time was reduced at the cost of increased memory use. Further improvement of the computation time can be achieved by constructing suitable preconditioners.

It is conceivable to implement the Nash-Hörmander algorithm with spherical radial basis functions instead of standard boundary elements (we took piecewise polynomials of degree 2 on triangles). As shown in Chapter 7 and in our paper [48] we applied successfully the spherical radial basis functions to the boundary integral equation on the unit sphere for the linearized Molodensky problem. However, the generalization to the full nonlinear Molodensky problem remains to be studied. Also, it remains to be studied to which extent truncation of the series expansion (which gives the radial basis functions in terms of spherical harmonics) limits the accuracy and practical relevance for the nonlinear Molodensky problem. On the other hand, an advantage of this method is that theoretically optimal smoothing operators are easily implemented by truncating the series expansion. Note that using the method presented in Chapter 6, the nonlinear Molodensky problem could be also computed on the oblate spheroid, which approximates the Earth's shape better than the sphere. The approaches in Chapter 6 and 7 are suitable for handling scattered data from satellite measurements. In this way, further research can be done with real satellite data to get an approximation of the real earth's shape.

There are further ways conceivable to implement the Nash-Hörmander algorithm. Spherical splines might lead to a better surface approximation [2, 38]. However, if we use the method proposed in [2] to compute the integrals by mapping a surface triangle T to a planar triangle, which has the same vertices as those of T and then use a standard technique of numerical integration for planar triangles, this could lead to the same difficulties that we encountered in our approach. Here one has to find explicit formulas for integrals of spherical Bernstein-Bézier polynomials to compute the arising integrals more accurately.

Bibliography

[1] M. Abramowitz and I. A. Stegun, *Handbook of Mathematical Functions with Formulas, Graphs, and Mathematical Tables*, Denver, New York, 1965.

[2] P. Alfeld, M. Neamtu, and L. Schumaker, *Fitting scattered data on sphere-like surfaces using spherical splines*, J. Comput. Appl. Math, 73 (1996), pp. 5–43.

[3] P. L. Butzer and H. Berens, *Semi-groups of operators and approximation*, Die Grundlehren der mathematischen Wissenschaften, Band 145, Springer-Verlag New York Inc., New York, 1967.

[4] D. Chen, V. A. Menegatto, and X. Sun, *A necessary and sufficient condition for strictly positive definite functions on spheres*, Proc. Amer. Math. Soc., 131 (2003), pp. 2733–2740 (electronic).

[5] M. Costabel, *Boundary integral operators on Lipschitz domains: elementary results*, SIAM J. Math. Anal., 19 (1988), pp. 613–626.

[6] A. Costea, Q. T. Le Gia, D. Pham, E. Stephan, and T. Tran, *Solving the Dirichlet-to-Neumann map on an oblate spheroid by a mesh-free method*, Computers and Mathematics with Applications, (2012). Submitted.

[7] A. Costea, Q. T. Le Gia, E. Stephan, and T. Tran, *Meshless BEM and overlapping Schwarz preconditioners for exterior problems on spheroids*, Studia Geophysica et Geodaetica, 55 (2011), pp. 465–477.

[8] J. R. Driscoll and D. M. Healy, Jr., *Computing Fourier transforms and convolutions on the 2-sphere*, Adv. in Appl. Math., 15 (1994), pp. 202–250.

[9] S. Erichsen and S. A. Sauter, *Efficient automatic quadrature in 3-d Galerkin BEM*, Comput. Methods Appl. Mech. Engrg., 157 (1998), pp. 215–224. Seventh Conference on Numerical Methods and Computational Mechanics in Science and Engineering (NMCM 96) (Miskolc).

[10] G. Fasshauer and J. Jerome, *Multistep approximation algorithms: Improved convergence rates through postconditioning with smoothing kernels*, Advances in Computational Mathematics, 10 (1999), pp. 1–27. 10.1023/A:1018962112170.

[11] W. Freeden, *Multiscale modelling of spaceborne geodata*, European Consortium for Mathematics in Industry, B. G. Teubner, Stuttgart, 1999.

[12] W. Freeden and C. Mayer, *Multiscale solution for the Molodensky problem on regular telluroidal surfaces*, Acta Geodaetica et Geophysica Hungarica, 41 (2006), pp. 55–86.

[13] A. Gil and J. Segura, *A code to evaluate prolate and oblate spheroidal harmonics*, Computer Physics Communications., 108 (1998), pp. 267–278.

[14] J. Hadamard, *Lectures on Cauchy's problem in linear partial differential equations*, Dover Publications, New York, 1953.

[15] D. P. Hardin and E. B. Saff, *Discretizing manifolds via minimum energy points*, Notices Amer. Math. Soc., 51 (2004), pp. 1186–1194.

[16] B. Heck, *Integral equation methods in physical geodesy*, in Grafarend, E.W./Krumm, F.W./Schwarze,V.S. (Eds.):Geodesy - The Challenge of the 3rd Millenium, Springer, 2002, pp. 197–206.

[17] W. A. Heiskanen and H. Moritz, *Physical Geodesy*, W. H. Freeman, San Francisco, 1993 reprint ed., 1967.

[18] L. Hörmander, *Linear partial differential operators*, Third revised printing. Die Grundlehren der mathematischen Wissenschaften, Band 116, Springer-Verlag New York Inc., New York, 1969.

[19] ——, *The boundary problems of physical geodesy*, Arch. Rational Mech. Anal., 62 (1976), pp. 1–52.

[20] H. Huang and D. Yu, *The ellipsoid artificial boundary method for three-dimensional unbounded domains*, J. Comput. Math., 27 (2009), pp. 196–214.

[21] R. Klees, M. van Gelderen, C. Lage, and C. Schwab, *Fast numerical solution of the linearized Molodensky problem*, Journal of Geodesy, 75 (2001), pp. 349–362. 10.1007/s001900100183.

[22] T. Krarup, *Letters on Molodensky's problem, iii*, Unpublished manuscript, Geodaetisk Institut, (1973).

[23] A. Lunardi, *Analytic semigroups and optimal regularity in parabolic problems*, Progress in Nonlinear Differential Equations and their Applications, 16, Birkhäuser Verlag, Basel, 1995.

[24] M. Maischak, *Analytical evaluation of potentials and computation of galerkin integrals on triangles and parallelograms.*, tech. rep., ifam50, 2001.

[25] ——, *Technical manual of the program system maiprogs*, 2001.

[26] P. A. Martin, *Addendum: "Exact solution of a simple hypersingular integral equation" [J. Integral Equations Appl.* **4** *(1992), no. 2, 197–204; MR1172889 (93c:45005)]*, J. Integral Equations Appl., 5 (1993), p. 297.

[27] B. Matérn, *Spatial variation*, vol. 36 of Lecture Notes in Statistics, Springer-Verlag, Berlin, second ed., 1986.

[28] S. G. Mikhlin and S. Prössdorf, *Singular integral operators*, vol. 68 of Mathematische Lehrbücher und Monographien, II. Abteilung: Mathematische Monographien [Mathematical Textbooks and Monographs, Part II: Mathematical Monographs], Akademie-Verlag, Berlin, 1986. Translated from the German by Albrecht Böttcher and Reinhard Lehmann.

[29] M. Molodenski, *Grundbegriffe der geodätischen Gravimetrie*, VEB Verlag Technik, Berlin, 1958.

[30] M. S. Molodenskii, *Methods for study of the external gravitational field and figure of the earth*, Jerusalem, Israel Program for Scientific Translations; [available from the Office of Technical Services, U.S. Dept. of Commerce, Washington], 1962.

[31] H. Moritz, *Advanced physical geodesy*, Karlsruhe : Wichmann ; Tunbridge, Eng. : Abacus Press, 1980.

[32] C. Müller, *Spherical harmonics*, vol. 17 of Lecture Notes in Mathematics, Springer-Verlag, Berlin, 1966.

[33] F. J. Narcowich, X. Sun, and J. D. Ward, *Approximation power of RBFs and their associated SBFs: a connection*, Adv. Comput. Math., 27 (2007), pp. 107–124.

[34] F. J. Narcowich and J. D. Ward, *Scattered data interpolation on spheres: error estimates and locally supported basis functions*, SIAM J. Math. Anal., 33 (2002), pp. 1393–1410 (electronic).

[35] J. Nash, *The imbedding problem for Riemannian manifolds*, Ann. of Math. (2), 63 (1956), pp. 20–63.

[36] J.-C. Nédélec, *Curved finite element methods for the solution of singular integral equations on surfaces in* R^3, Comput. Methods Appl. Mech. Engrg., 8 (1976), pp. 61–80.

[37] ——, *Acoustic and Electromagnetic Equations*, Springer-Verlag, New York, 2000.

[38] D. T. Pham, *Pseudodifferential equations on spheres with spherical radial basis functions and spherical splines*, dissertation, The School of Mathematics and Statistics, The University of New South Wales, 2011.

[39] E. B. Saff and A. B. J. Kuijlaars, *Distributing many points on a sphere*, Math. Intelligencer, 19 (1997), pp. 5–11.

[40] A. Schlömerkemper, *About solutions of Poisson's equation with transition condition in non-smooth domains*, Z. Anal. Anwend., 27 (2008), pp. 253–281.

[41] I. J. Schoenberg, *Positive definite functions on spheres*, Duke Math. J., 9 (1942), pp. 96–108.

[42] C. Schwab, *Variable order composite quadrature of singular and nearly singular integrals*, Computing, 53 (1994), pp. 173–194.

[43] J. Schwartz, *On Nash's implicit functional theorem*, Comm. Pure Appl. Math., 13 (1960), pp. 509–530.

[44] S. Seo, M. K. Chung, and H. K. Vorperian, *Heat kernel smoothing using Laplace-Beltrami eigenfunctions*, in Proceedings of the 13th international conference on Medical image computing and computer-assisted intervention: Part III, MICCAI'10, Berlin, Heidelberg, 2010, Springer-Verlag, pp. 505–512.

[45] M. A. Shubin, *Pseudodifferential operators and spectral theory*, Springer-Verlag, Berlin, second ed., 2001. Translated from the 1978 Russian original by Stig I. Andersson.

[46] O. Steinbach, *Numerische Näherungsverfahren für elliptische Randwertprobleme. Finite Elemente und Randelemente.*, Teubner, Stuttgart, 2003.

[47] E. Stephan and W. Wendland, *Remarks to Galerkin and least squares methods with finite elements for general elliptic problems*, in Ordinary and partial differential equations (Proc. Fourth Conf., Univ. Dundee, Dundee, 1976), Springer, Berlin, 1976, pp. 461–471. Lecture Notes in Math., Vol. 564.

[48] E. P. Stephan, T. Tran, and A. Costea, *A boundary integral equation on the sphere for high-precision geodesy*, in Computer Methods in Mechanics, M. Kuczma and K. Wilmanski, eds., vol. 1 of Advanced Structured Materials, Springer Berlin Heidelberg, 2010, pp. 99–110.

[49] G. Strang and G. J. Fix, *An analysis of the finite element method*, Prentice-Hall Inc., Englewood Cliffs, N. J., 1973. Prentice-Hall Series in Automatic Computation.

[50] M. E. Taylor, *Partial differential equations III. Nonlinear equations*, vol. 117 of Applied Mathematical Sciences, Springer, New York, second ed., 2011.

[51] T. Tran, Q. T. Le Gia, I. H. Sloan, and E. P. Stephan, *Boundary integral equations on the sphere with radial basis functions: error analysis*, Appl. Numer. Math., 59 (2009), pp. 2857–2871.

[52] ——, *Preconditioners for pseudodifferential equations on the sphere with radial basis functions*, Numer. Math., 115 (2010), pp. 141–163.

[53] W. Trebels and U. Westphal, *K-functionals related to semigroups of operators*, Rend. Circ. Mat. Palermo (2) Suppl., (2005), pp. 603–620.

[54] H. Wendland, *Piecewise polynomial, positive definite and compactly supported radial functions of minimal degree*, Advances in Computational Mathematics, 4 (1995), pp. 389–396. 10.1007/BF02123482.

[55] ——, *Scattered data approximation*, vol. 17 of Cambridge Monographs on Applied and Computational Mathematics, Cambridge University Press, Cambridge, 2005.

[56] W. L. Wendland, *Asymptotic accuracy and convergence for point collocation methods*, in Topics in boundary element research, Vol. 2, Springer, Berlin, 1985, pp. 230–257.

[57] Y. Xu and E. W. Cheney, *Strictly positive definite functions on spheres*, Proc. Amer. Math. Soc., 116 (1992), pp. 977–981.

Curriculum Vitae

Personal Data:

Name:	Adrian Costea
Born:	29/06/1980, Brasov, Romania
Citizenship:	Romanian, German

Education:

07/2012	Scheduled Ph.D. graduation
05/2008	Start of Ph.D. Program at the Institute of Applied Mathematics, Leibniz Universität Hannover, Germany
04/2008	Completion of studies of mathematics - field Computational Sciences (Studienrichtung Rechnergestützte Wissenschaften) Diploma degree: Dipl.-Math.
11/2007	Diploma thesis with title: *Finite Elemente und Randelemte bei Deformationsprozessen* at Leibniz Universität Hannover, Germany
10/2005	Intermediate diploma in mathematics (Vordiplom)
04/2004	Start of studies of mathematics with minor subject physics at Leibniz Universität Hannover, Germany
10/2000	Start of studies of physics at Leibniz Universität Hannover, Germany (change of field of studies in 2004)
10/1998	Start of studies of physics at Universitatea Babes-Bolyai, Cluj, Romania (2 years as precondition for studying abroad)
07/1998	University-entrance diploma (Abiturzeugnis)
1994-1998	School attendance at Joseph Haltrich, Sighisoara, Romania
1986-1994	Primary School Rupea, Romania (German-language department)

Employment:

since 05/2008	Research assistant at the Institute of Applied Mathematics, Leibniz Universität Hannover, Germany (financially supported by the Cluster of Excellence QUEST)
06/2007-11/2007	Student assistant at the Institute of Applied Mathematics, Leibniz Universität Hannover, Germany